

GEOLOGICA ULTRAIECTINA

Mededelingen van de  
Faculteit Geowetenschappen  
Universiteit Utrecht

No. 227

Holocene environmental changes disclosed  
from anoxic fjord sediments by biomarkers  
and their radiocarbon content

Rienk H. Smittenberg



# **Holocene environmental changes disclosed from anoxic fjord sediments by biomarkers and their radiocarbon content**

Holocene milieuveranderingen gereconstrueerd uit anoxische fjord sedimenten middels biomarkers en hun radio-actief koolstof gehalte

(met een samenvatting in het Nederlands)

## **Proefschrift**

ter verkrijging van de graad van doctor  
aan de Universiteit Utrecht  
op gezag van de Rector Magnificus, Prof. Dr. W.H. Gispen,  
ingevolge het besluit van het College voor Promoties  
in het openbaar te verdedigen  
op maandag 15 september 2003 des middags te 4.15 uur

door

**Rienk Hajo Smittenberg**

geboren op 23 maart 1973 te Eck en Wiel

Promotor: Prof. Dr. J.W. de Leeuw  
Department of Geochemistry  
Utrecht University  
Utrecht, The Netherlands

Copromotores: Dr. Ir. J.S. Sinninghe Damsté  
Department of Geochemistry  
Utrecht University  
Utrecht, The Netherlands

Dr. S. Schouten  
Department of Marine Biogeochemistry and Toxicology  
Royal Netherlands Institute of Sea Research  
Texel, The Netherlands

The research described in this thesis was carried out at the Department of Biogeochemistry and Toxicology of the Royal Netherlands Institute of Sea Research, P.O. Box 59, 1790 AB Den Burg, The Netherlands. The investigations were supported by the Research Council for Earth and Life Science (ALW) with the financial support from the Netherlands Organization for Scientific Research (NWO).

ISBN 90-5744-086-5

Aan mijn ouders



## Contents

	Page
Voorwoord	1
<b>Chapter 1</b> Introduction	3
<b>Chapter 2</b> Rapid isolation of biomarkers for compound specific radiocarbon dating using high-performance liquid chromatography and flow injection analysis - atmospheric pressure chemical ionisation - mass spectrometry	13
<b>Chapter 3</b> Compound-specific radiocarbon dating of the varved Holocene sedimentary record of Saanich Inlet, Canada	29
<b>Chapter 4</b> Radiocarbon ages of terrestrial <i>n</i> -alkanes from Holocene sediments of a Canadian fjord reveal an increasing 'soil reservoir effect'	55
<b>Chapter 5</b> Late Holocene environmental changes in an euxinic fjord as revealed by the sedimentary biomarker record	67
<b>Chapter 6</b> Pre- and post-industrial environmental changes as revealed by the biogeochemical sedimentary record of Drammensfjord, Norway	91
<b>Chapter 7</b> The demise of the alga <i>Botryococcus braunii</i> from a Norwegian fjord is due to early eutrophication	115
References	127
Summary	137
Samenvatting	139
Dankwoord	141
Curriculum Vitae	143





## Voorwoord

*In september 1998 betrad ik, na mij 6 jaar lang in het water, de atmosfeer, en vooral de bodem gestort te hebben, de wereld binnen die organische geochemie heet. Dat leek me wel wat: klimaatsveranderingen reconstrueren met behulp van moleculaire fossielen. En nog nuttig ook, in het licht bezien van alle bezorgdheid die er heerst over de klimaatsveranderingen veroorzaakt door het verstoken van fossiele brandstoffen. Werken op Texel op het NIOZ was ook leuk: lekker aan zee. En zowel de beloofde vaartocht naar Noorwegen om monsters te nemen als metingen doen in de VS zouden vast ook mooie ervaringen worden.*

*In het begin zie je door de bomen het bos niet. Of eigenlijk, je ziet erg weinig. Nadat je met organische oplosmiddelen een soort van koffie-extract hebt gemaakt van een beetje prut uit de bodem van een fjord, spuit je daarvan 1 microliter met een injectienaald in een duur apparaat, wat daarna piekjes en getalletjes produceert. Tja, zie daar maar eens wijs uit te worden. Gelukkig zijn er dan bibliotheken, ook wandelende, waarin je kan opzoeken (of vragen) wat het betekent: een piekje betekent detectie van een biomarker. De getalletjes hoeveel, of wat voor soort. De afgelopen jaren heb ik mij dus bekwaamd in het herkennen van specifieke vetachtige organische verbindingen die door planten, algen, bacteriën, archaea (oerbacteriën) worden gemaakt, zogenaamde biomarkers, die (deels) bewaard blijven in mariene sedimenten, en in het meten van hun koolstof-isotopen samenstelling.*

*Na verloop van tijd begint in je eigen hoofd ook een bibliotheekje te ontstaan, begin je ook patronen te herkennen: kan je de verschillende 'bomen' in het bos benoemen, en kan je bij een stevige wandeltocht het 'bos' zien veranderen door de tijd heen: op een of andere manier (en dat is het grootste stuk van de puzzel) veroorzaakt door veranderingen in milieu en klimaat! En als je dan ook nog de leeftijd kan meten van de 'bomen', weet je ook nog eens hoe oud het bos is, en of er hele oude bomen staan of niet.*

*De resultaten van mijn 'wandeltochten' staan in dit proefschrift: 'Holocene milieuveranderingen gereconstrueerd uit anoxische fjord sedimenten middels biomarkers en hun radio-actief koolstof gehalte'. Ik wens u veel leesplezier. Ik geef toe, het is enigszins specialistisch. Als u het niet helemaal begrijpt, vraag gerust, dan zal ik het proberen uit te leggen.*

*Before you lies the thesis 'Holocene environmental changes disclosed from anoxic fjord sediments by biomarkers and their radiocarbon content'. Enjoy your reading.*

*Rienk Smittenberg,  
Texel / Den Helder, juni 2003*



## Chapter 1

### Introduction

#### 1.1. Human-induced environmental change and natural ecosystem variability

Although only the far future will learn whether the accreditation 'Anthropocene', to the current timeframe [Crutzen, 2002] is a valid one, or that we are now causing an 'anthropogenic event' within geological history, it is evident that the behaviour of humankind has measurable effects on the earth's bio- and geosphere [<http://www.igbp.kva.se>], causing ecological, agricultural, economical and social damage. However, the observed changes, like the global temperature rise [e.g. Mann *et al.*, 1998; Petit *et al.*, 2000; Levitus *et al.*, 2000] the desertification of the Sahel region [Prince *et al.*, 1998 and references therein] or the eutrophication of coastal regions [e.g. Nixon, 1990], may also be partly the result of random natural oscillations that occur on a decadal to centennial time scale [Broecker, 1995]. For instance, variations in the solar irradiance, of which the 11-year sunspot cycle is the most known one, may be a governing factor in the global temperature [Geel *et al.*, 1999], while the North Atlantic Oscillation (NAO) and El Niño also have substantial impacts on regional scales [e.g. Cullen *et al.*, 2001; Moy *et al.*, 2002]. To gain insight into the causes and mechanisms that lie behind both natural variability and human-induced changes, reliable knowledge of the past is necessary. However, instrumental records of the climate are only available for the last century, together with some scattered historical data from before that time [Bradley and Jones, 1992], so that the scientific community has to rely for a large extent on proxy data [Wefer *et al.*, 1999; <http://www.ngdc.noaa.gov/paleo/recons.html>]. Even less information is available for the natural state of marine, coastal and terrigenous ecosystems, as environmental monitoring started only in the second half of the last century. Thus, to assess the natural 'background' and its variability against anthropogenic effects on a decadal to centennial time scale, paleoclimatic and paleoenvironmental proxies need to be recovered from natural records like annually deposited layers of ice [e.g. Petit *et al.*, 2000], tree rings [e.g. Cook *et al.*, 1998], corals [e.g. Beck *et al.*, 1997] or laminated sediments [e.g. Kemp, 1996; Hughen *et al.*, 2000]. Coastal sediments contain an integrated signal of terrigenous vegetation and marine biota, which are closely linked with climatic parameters and oceanographic processes, as well as with anthropogenic influences. Deconvolution of all these signals may be performed by analysis of molecular fossils, so-called biomarkers, preserved in the sedimentary record, in alliance with other geochemical and sedimentological techniques.

## 1.2. Anoxic fjords

Enclosed, anoxic fjords have since long been recognised as good locations for sedimentological, biological, ecological and (bio)geochemical studies [Degens and Stoffers, 1976]. Due to the anoxic conditions in the water column, organic matter is well preserved, while the sediments are not mixed by bioturbation due to the absence of infauna, which results in the preservation of annually deposited sediment layers, or varves [Richards, 1965; Anderson and Devol, 1973; 1987]. Together with generally high sedimentation rates, this allows sampling with a high, sometimes even sub-annual, resolution. Furthermore, the isolated setting of these fjords makes them 'natural laboratories' where many processes that take place or have taken place on a global scale may be observed on a small scale. For instance, the anoxic conditions that prevail in these fjords have been prevalent in the geological past on an oceanic scale [Kuypers *et al.*, 2002]. On another note, the physicochemistry and ecology of such relatively small and enclosed basins are in general much more sensitive to e.g. increasing nutrient loads or summer temperatures than the open coastal environment [Skei *et al.*, 2000]. This makes them very suitable as early indicators for environmental and climatic change [Gustafsson, 2000]. In general, anoxic fjords are characterised by the following features (Fig. 1.1):

- A shallow sill at the mouth of the fjord, often being the endmoraine of the glacier that shaped the fjord. This sill prevents the exchange of the fjord's bottom water below sill depth with oceanic water. In general the sill depth's have become shallower over the last millennia due to the isostatic uplift of formerly ice-covered land.

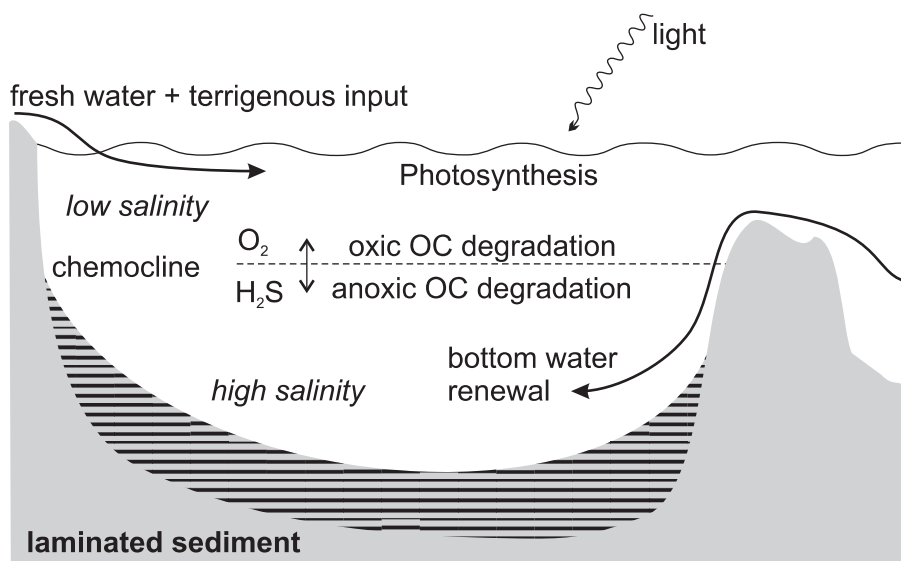


**Figure 1.1** Cartoon of an anoxic fjord with laminated sediment

- A positive water balance due to the runoff of fresh water from the surrounding areas, often via rivers that enter at the head of the fjord. This results in a strong pycnocline that causes distinct stratification of the water column. This stratification is enhanced in summer through warmer surface waters with a lower density, and weakened in winter by a reverse effect.
- More or less regularly occurring bottom water renewals, depending on the sill depth and on density variations of the surface or sub-surface water outside the fjord compared with that in the fjord. During these renewals, bottom water is displaced upwards.
- Anoxic conditions below the mixing zone caused by organic matter degradation, supporting the formation of free sulphide by sulphate reducers. These euxinic circumstances sometimes extend into the photic zone.
- A sometimes high primary production due to the supply of nutrients by either fluvial input or runoff from the surrounding land, which are contained within the fjord caused by the reduced water exchange with open sea. This also results in high heterotrophic activity and an enhancement of anoxic conditions. Nutrients may be recycled from below the pycnocline during winter mixing and bottom water renewals, resulting in a positive feedback mechanism.
- Relatively high sedimentation rates of 1-10 mm / yr.
- A yearly sedimentation cycle causing annual varves, roughly consisting of: a) terrigenous clastic material including mineral grains and terrigenous organic matter, introduced by periods of high fluvial input occurring mainly in spring; b) biogenic material consisting of diatoms, other microfossils and organic matter, produced during periods of high primary productivity; c) fine grained sediment derived from settling of suspended clay and organic matter in periods of low 'allochthonous' material. Furthermore, authigenic minerals like iron sulfides (e.g. pyrite, hydrotroillite) may become part of the mineral matrix.
- The absence of infauna due to the anoxic circumstances, resulting in the preservation of the annual varves.

For the studies described in this thesis, sediments of three anoxic fjords were used (Table 1.1, Fig. 1.2):

- a. The Kyllaren fjord, located in Western Norway. This is a small fjord with a maximum depth of 25 m and no freshwater input other than from runoff of the surrounding land. In the natural situation, it already had little exchange with open sea, but this was further decreased in the last century by the building of two dams. In the last decade  $H_2S(g)$  escaped from the fjord waters on multiple occasions, indicating the presence of a very shallow chemocline that sometimes reaches the surface. Besides the building of the dams, the fjord did not suffer from anthropogenic influences, and it may therefore be regarded as a natural very enclosed marine basin.

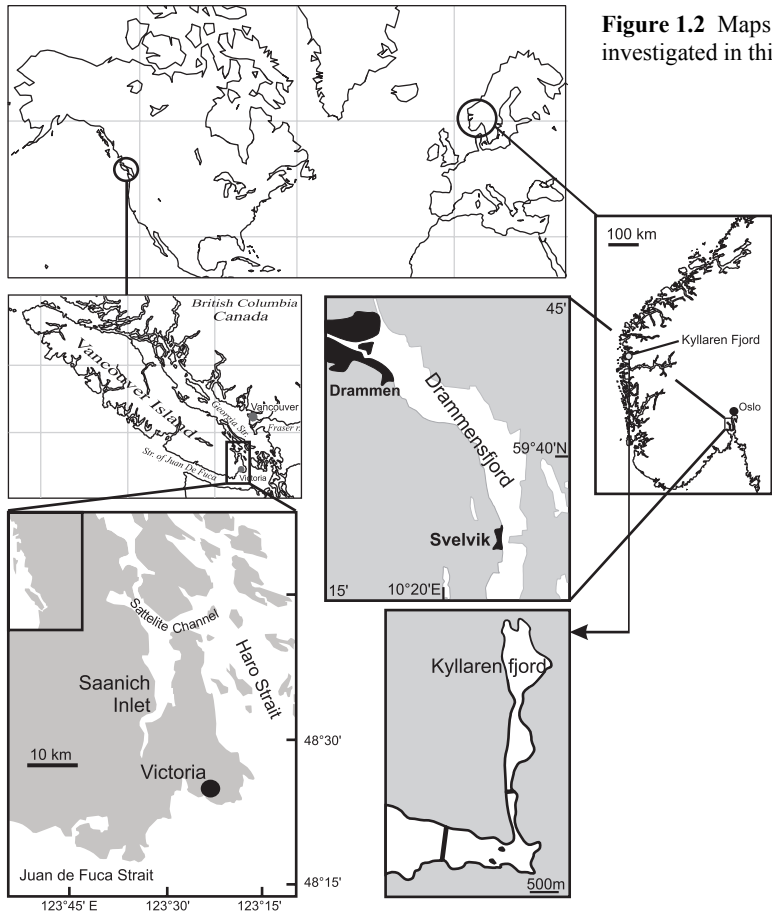


**Figure 1.2** Maps of the three fjords investigated in this thesis

**Table 1.1** Some environmental information on the three investigated fjords

<b>Fjord</b>	<b>Kyllaren fjord</b>	<b>Drammensfjord</b>	<b>Saanich Inlet</b>
Location	West Norway	South Norway	Vancouver Island, Canada
proximate co-ordinates	61°25'N 5°10'E	59°40'N 10°20'E	48°40'N 123°30'W
Surface (km <sup>2</sup> )	0.35	50	70
Depocentre depth (m)	29	124	237
Sill depth (m)	1-2	10%	65
Chemocline depth (m)	5-10*	60	120
Bottom water salinity (‰)	21-25	30.5	31
Surface water salinity (‰)	5-16	1-10	25-29
Sedimentation rate mm/yr	1-3	1-2	4-12 <sup>&amp;</sup>

% dredged from 6m in the 20<sup>th</sup> century  
 \* Occasional <0.5m  
 & Measured over a 6000 year period

- b. The South Norwegian Drammensfjord. This fjord has a maximum depth of 120 m and is influenced strongly by fresh water from the river Drammen that enters at the head of the fjord. Here the industrial town Drammen is located, and the fjord is known to have suffered from pollution in the last century, and likely even before that time.
- c. The Canadian Saanich Inlet, Vancouver Island. This fjord has a size comparable to that of the Drammensfjord, but has a maximum depth of 230m. Human activities seem to have been relatively limited. The influence of fresh surface water is less pronounced as in the investigated Norwegian fjords, while the marine primary productivity is much higher.

### 1.3. Lipid biomarkers

Sedimentary organic matter mainly consists of insoluble macromolecular material, which is either derived directly from organisms (e.g. algaenane, lignins, cutans) [De Leeuw and Largeau, 1993] or stems from polymerisation, condensation or vulcanisation of smaller organic molecules [Sinninghe Damsté and De Leeuw, 1990; Brassell, 1993; Tyson, 1995d]. A much smaller fraction (<10%) of sedimentary total organic carbon (TOC) is made up by solvent-extractable lipids. In general, these compounds functioned as membrane lipids, as storage products or as pigments, and they may be specific for certain groups of organisms or even specific genera [De Leeuw *et al.*, 1995]. They can thus be used as 'molecular fossils' or biomarkers, and their occurrence and distribution in sedimentary records contains environmental information from the time of their deposition. Examples of biomarkers are the long-chain *n*-alkanes, fatty acids and alcohols that are derived from vascular plants [Kolattukudy, 1980]. Dinosterol (4,23,24-trimethylcholest-22-ene-3 $\beta$ -ol) is produced by a number of dinoflagellates [e.g. Boon *et al.*, 1979], while other organisms do not appear to biosynthesise this sterol [Volkman, 1986]. Another example is crenarchaeol, a glycerol dialkyl glycerol tetraether that has, so far, only been found to be produced by ubiquitously occurring marine crenarchaeota, and this biomarker is therefore indicative for marine environments [Sinninghe Damsté *et al.*, 2002c]. Furthermore, the stable carbon composition of organic carbon and biomarkers, generally expressed as  $\delta^{13}\text{C}$  and reported against the Vienna Pee Dee Belemnite standard [Coplen, 1996] can reveal additional information concerning growth conditions of organisms and the environments they live in [Deines, 1980; Freeman *et al.*, 1990]. The  $\delta^{13}\text{C}$  value of organic compounds of autotrophic organisms is determined by both the  $\delta^{13}\text{C}$  value of the initial carbon source (i.e.  $\text{CO}_2$  or DIC), as well as by the enzymatically mediated carbon fractionation during biosynthesis, which is governed by various physical and biochemical parameters [Hayes, 2001]. Finally, the radiocarbon content of biomarkers may also reveal information on the source of certain biomarkers, as described below. Although the occurrence of a single specific biomarker in a sediment may already reveal important information, it is often the combination of a whole suite of biomarkers, their distributions and their respective isotopic compositions, together

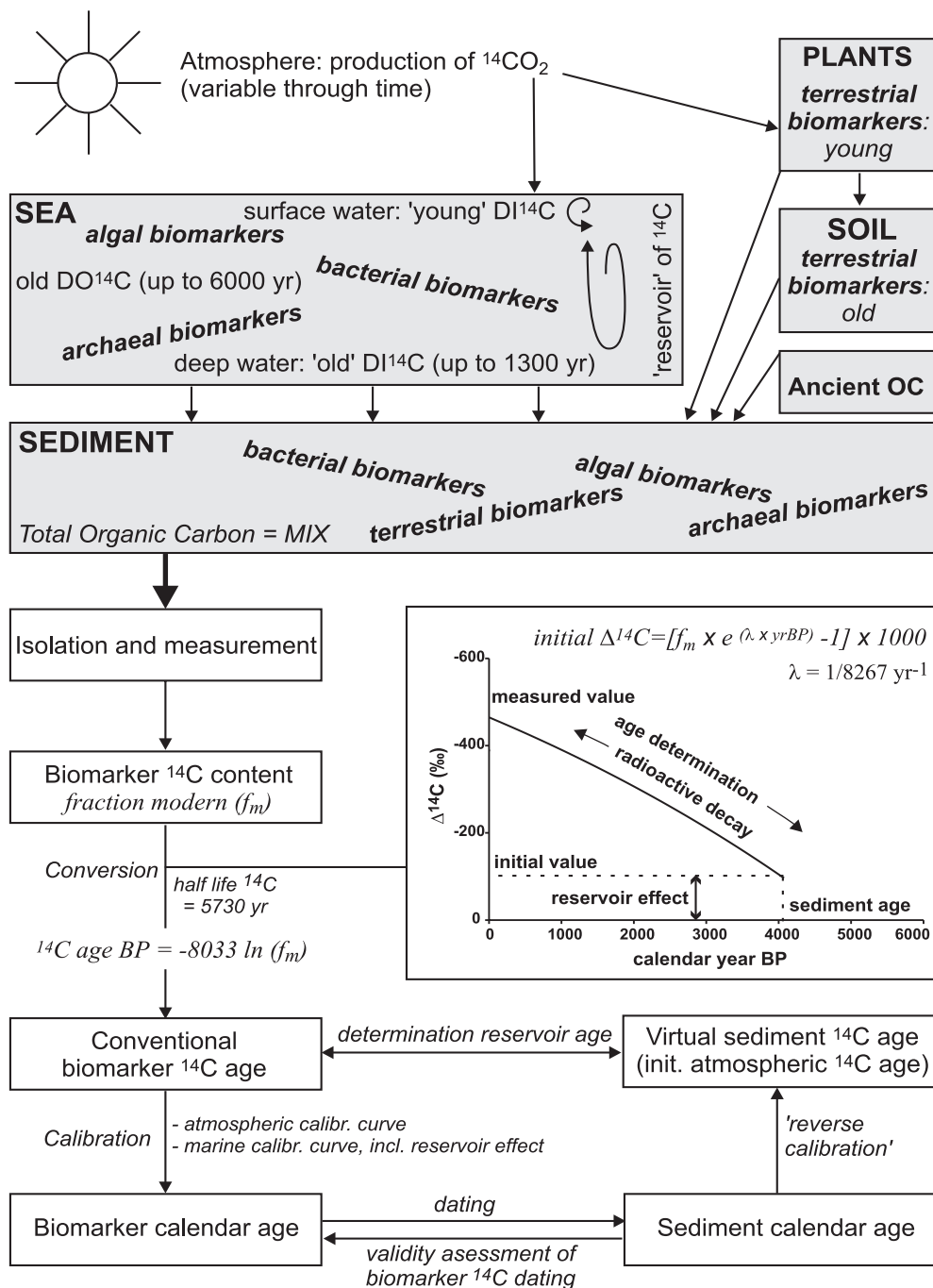


**Figure 1.3** Schematic overview of the systematics of compound-specific radiocarbon dating. For exhaustive  $^{14}\text{C}$  systematics and calculations see *Stuiver and Polach [1977]* or *Mook and Van der Plicht [1999]*.



with bulk sedimentary parameters like the total organic carbon content and sedimentological information that allows an integrated reconstruction of a past environment.

#### 1.4. Dating of laminated sediments: varve counting and compound specific $^{14}\text{C}$ analysis

To assess climatic or environmental variability using sedimentary records, including those of biomarkers, a good age model is of key importance. In order to produce a good age model, various dating methods are available. Dating of sediments from the last century is possible with the radioactive isotopes  $^{210}\text{Pb}$  and  $^{137}\text{Cs}$  [e.g. <http://climchange.cr.usgs.gov/info/lacs/dating>]. For laminated sediments, varve counting is also a good dating tool, which may result in very accurate age models [e.g. *Nederbragt and Thurow, 2001*]. This method works in essence the same as tree-ring counting, and results in a floating age scale that needs to be correlated to a real age, which may be available from the top sediment. However, in order for this method to be successful, the varves need to be annually deposited and thick enough to be recognisable, while also not too many disturbances like turbidites need to be present. To assess whether no errors are made because of missing varves or the presence of sub-annual varves, some independent dates are required. This may be provided by recognition of occasional events in the sediment, e.g. ash layers from historically known volcanic eruptions. The most widely dating method for Holocene sediments is, however, radiocarbon dating. This is generally performed on carbonaceous (e.g. shells or foraminifers) or organic macrofossils (e.g. seeds, twigs). The absence or scarcity of organic and carbonaceous macrofossils sometimes causes severe dating problems. Dating based on total organic matter is in general not possible since this is a complex mixture derived from a multitude of sources varying in radiocarbon age (Fig. 1.3) [*Eglinton et al., 1997*]. A possible solution for this problem was recently provided by the development of compound-specific radiocarbon analysis (CSRA) [*Eglinton et al., 1996*]. This novel method uses the advantage of accelerator mass spectrometry (AMS) to perform radiocarbon analysis on samples as small as 30  $\mu\text{g C}$ , allowing biomarkers isolated out of sedimentary lipid extracts to be analysed (Fig. 1.3) [*Pearson et al., 1998*]. To date, however, CSRA has almost exclusively been used to address carbon source related questions, by investigating the spread in radiocarbon age between biomarkers of different origin [*Pearson et al., 2001; Petsch et al., 2001; Ohkouchi et al., 2002*] in a manner that is comparable to radiocarbon analysis of fractions from the total organic carbon present in soils and sediments [e.g. *Druffel et al., 1996; Wang et al., 1998; Megens et al., 1998; Trumbore, 2000; Raymond and Bauer, 2001*]. For instance, the  $^{14}\text{C}$  content of a biomarker may reveal whether it is of terrigenous or marine origin: terrigenous biomarkers transported to marine sediments have generally been subject to pre-ageing on the continent, which distinguishes them from marine biomarkers that are readily deposited after production (Fig.

1.3). The latter is a prerequisite for dating purposes, which thus disqualifies CSRA of terrigenous biomarkers for this application. However, marine biomarkers not automatically meet the criterion of quick and definite deposition. *Ohkouchi et al.* [2002] found that lateral transport of fine-grained particles greatly affected the radiocarbon ages of haptophyte-derived alkenones, when compared with the ages obtained from planktonic foraminifera that were not displaced after their initial sedimentation. In quiet conditions like those prevalent in anoxic fjords, it is anticipated that such effects are insignificant, and that CSRA of marine biomarkers may be a valid means of dating. An additional step that needs to be performed for accurate radiocarbon dating, compared to the use of CSRA for carbon source-related studies, is the calibration to calendar ages. Because the radiocarbon production in the atmosphere has not been constant through time, radiocarbon ages differ in a variable way from calendar ages, which raises the need of a calibration curve when calendar ages are desired [*Stuiver and Braziunas*, 1993]. For atmospheric derived compounds, calibration is straightforward via well-documented archives of the atmospheric  $^{14}\text{C}$  content, mainly recovered from tree rings [*Stuiver et al.*, 1998b]. Next to natural variations in atmospheric  $^{14}\text{C}$  production, marine derived biomarker ages need to be corrected for a 'reservoir age' (Fig. 1.3). This is the average radiocarbon age of dissolved inorganic carbon (DIC), which varies for different geographical regions depending on ocean currents and seasonal upwelling [*Stuiver et al.*, 1998a]. Although disqualified for dating purposes, the  $^{14}\text{C}$  ages of terrigenous biomarkers in marine sediment may still reveal useful information. For instance, a record of the extent of pre-ageing of sedimentary terrigenous biomarkers may provide information on the development of the terrigenous (soil) organic carbon pool of the surrounding area. Furthermore, it may provide extra information about the relative contributions of terrigenous and marine derived organic carbon to the total organic carbon content of sediments.

## 1.5. Scope and framework of this thesis

The investigations described in this thesis were conducted to gain more knowledge about the natural environmental and climatic variability in the Holocene on a decadal to centennial time scale, and to assess the impact of mankind in the last centuries. To this end, sedimentary biomarker records of three different anoxic fjords were investigated. The laminated structure and the biogeochemical record of these fjord sediments were well preserved due to high sedimentation rates of 1-10 mm/yr and anoxic bottom water conditions causing low organic matter degradation rates and inhibition of infauna. Records of molecular fossils, or biomarkers, contain in principle signals of terrigenous vegetation and marine biota, which are closely linked with climatic and oceanographic parameters, and with anthropogenic influences. A large part of this thesis is also dedicated to compound-specific radiocarbon analysis. This relatively new technique added a new dimension to the use of biomarkers in paleoceanographic and -environmental research, as it may reveal

additional information on the source of organic compounds, as well as the timing and transport of various organic matter sources. It also opened the possibility to perform dating of sediments using molecular fossils in cases where carbonaceous or organic microfossils are absent or scarce.

This thesis is divided into two parts: in the first part (chapters 2-4) the technique and results of compound-specific radiocarbon dating are described and discussed. The second part of the thesis (Chapters 5-7) focuses on the reconstruction of environmental changes in the Holocene, primarily based on the distribution, accumulation rates and carbon isotopic composition of biomarkers.

**Chapter 2** describes a newly developed method to isolate glycerol dialkyl glycerol tetraethers (GDGTs), sterols and chlorophyll-derived phytol from complex lipid extracts by preparative high-performance liquid chromatography (HPLC), in order to determine the radiocarbon content of these biomarkers. This method makes use of rapid scanning of collected fractions with flow injection analysis - mass spectrometry (FIA-MS) in order to evaluate the separation procedure, requiring a time of analysis of only one minute per fraction.

**Chapter 3** describes the assessment of various biomarkers for their applicability for dating purposes. The biomarkers were extracted from sediments recovered from Saanich Inlet, Canada (Fig. 1.2), because this sediment was already varve-dated with an annual resolution, and exhibits high accumulation rates, thereby providing an ideal setting for this study. The results indicate that especially crenarchaeol, a biomarker derived from ubiquitously occurring crenarchaeota, is very suitable for dating purposes, due to its relatively easy isolation and high abundance in virtual all marine sediments. The  $^{14}\text{C}$  contents of the various biomarkers are also discussed in an oceanographic perspective, using the implied reservoir ages of their carbon source, DIC.

In **Chapter 4** the extent of pre-ageing of terrigenous *n*-alkanes present in the varve-dated Saanich Inlet sediments is discussed. It is observed that the *n*-alkane ages, compared with the varve ages, increase linearly with time. This is attributed to an increasing 'soil reservoir effect' caused by the build up and ageing of the (refractory) soil organic carbon pool since deglaciation of the area, including *n*-alkanes. This study shows how marine sedimentary records may be used to reconstruct the development of the terrigenous carbon pool.

In **Chapter 5** a combined organic biogeochemical, geochemical and sedimentological investigation is described that was conducted on the laminated sedimentary record of the small euxinic Kyllaren fjord (Fig. 1.2), spanning the last 400 years. The stable carbon isotopic composition of especially the biomarkers derived from photosynthetic sulphur bacteria revealed carbon recycling within the fjord. Three different groups of biomarkers were used to deconvolute changes in the accumulation rates of terrigenous and marine derived organic matter. The terrigenous biomarker group was influenced by a change in vegetation or in the precipitation regime of the area, possibly related with the last cold spell

of the 'little ice age'. The marine biomarkers could be used to reconstruct the eutrophication effects caused by the confinement of the fjord by the building of a partially open dam in 1954.

In **Chapter 6**, a study of the sedimentary record of the currently anoxic Drammensfjord (Fig. 1.2) is described. The sediments were obtained during a cruise of the R.V. 'Pelagia' in October 1999. After a basic sedimentological assessment, the biomarker distribution and accumulation rates within the laminated upper part of the sediments, representing approximately the last millennium, were investigated. This revealed that the fjord's ecosystem, dominated by the freshwater input from the river Drammen, remained virtually invariable until the 18<sup>th</sup> century. At that time, an additional input of resinous biomarkers derived from coniferous trees becomes apparent, marking the onset of sawmill activities in the area. This input increases substantially after the industrial revolution, while increasing accumulation rates of marine biomarkers reveal that this also caused eutrophication of the fjord.

The final **Chapter 7** discusses the effect of eutrophication of Drammensfjord, as this caused the demise of the alga *Botryococcus braunii*. This alga produces very specific biomarkers called botryococenes, of which mono- and bicyclic isomers are abundant lipids within the extracts of the Drammensfjord sediments. Because *B. braunii* generally thrives well under somewhat brackish and oligotrophic conditions, it appears that this species was outcompeted by faster growing phytoplankton, mainly diatoms. It is therefore concluded that this biomarker may in the future not only be used as a proxy for fresh water input, but moreover also as a marker for nutrient-poor environments.

## Chapter 2

### Rapid isolation of biomarkers for compound specific radiocarbon dating using high-performance liquid chromatography and flow injection analysis - atmospheric pressure chemical ionisation - mass spectrometry

*Rienk H. Smittenberg, Ellen C. Hopmans, Stefan Schouten and Jaap S. Sinninghe Damsté*

Published in Journal of Chromatography 978 (2002), 129-140

**Abstract** Repeated semi-preparative normal phase HPLC was performed to isolate selected biomarkers from sediment extracts for radiocarbon analysis. Flow injection analysis - mass spectrometry (FIA-MS) was used for rapid analysis of collected fractions to evaluate the separation procedure, taking only one minute per fraction. In this way glycerol dialkyl glycerol tetraethers, sterol fractions, and chlorophyll-derived phytol were isolated in sufficient quantities from typically 100 gram of marine sediment for radiocarbon analysis, without significant carbon isotopic fractionation or contamination.

#### 2.1. Introduction

Radiocarbon analysis has been used since the 1950s for dating purposes, but only since the development of accelerated mass spectrometry (AMS) in the 1990s, the required sample size has been reduced to such an extent that compound-specific radiocarbon analysis has become possible [Eglinton *et al.*, 1996]. Several scientific disciplines could potentially benefit from this development, ranging from earth sciences to archaeology and environmental research. For instance, radiocarbon analysis of specific sedimentary organic compounds of known origin (so-called biomarkers) can be used as an alternative dating method for carbonate-poor, but organic carbon-rich sediments. Dating based on total organic matter is not possible since this organic matter is a complex mixture derived from different sources with different radiocarbon ages [Eglinton *et al.*, 1997; Pearson *et al.*, 2000; Smittenberg *et al.*, 2003]. In addition, a greater insight in carbon cycling processes can be gained by measuring the age range of different organic matter fractions or organic compounds in sediments or soils [Pearson *et al.*, 2000; Trumbore, 2000; Petsch *et al.*, 2001]. Compound specific radiocarbon analysis mainly focuses on lipids because other compounds like proteins and carbohydrates generally degrade much faster and are in general virtually absent in the sedimentary record [Tyson, 1995d].

To measure the radiocarbon contents of individual lipids, substantial amounts (>30µg) are needed [Eglinton *et al.*, 1996]. Furthermore, carbon isotopic fractionation effects during

the isolation procedure should be avoided as much as possible as this will influence the  $^{14}\text{C}$  content of the compounds, although the final determination of the radiocarbon age is corrected for fractionation using the  $\delta^{13}\text{C}$  value of the measured compound [Stuiver and Polach, 1977]. Measuring original  $^{14}\text{C}$  contents is, however, always better than measuring  $^{14}\text{C}$  contents which are heavily influenced by method induced fractionation effects.

So far, isolation of specific lipids for radiocarbon dating from complex mixtures of organic compounds has only been done successfully using preparative capillary gas chromatography [Eglinton *et al.*, 1996; Pearson *et al.*, 2001]. However, this method is time consuming and can only be used for relatively apolar, low-molecular-mass compounds, typically hydrocarbons and derivitized alcohols or alkanolates with less than 30 carbon atoms. Furthermore, if derivitized compounds are measured, an additional measurement error is introduced by the added carbon atoms of the derivitizing agent, for which has to be corrected.

Here we present a relatively fast method to isolate higher molecular mass ( $>\text{C}_{30}$ ) and more polar lipid biomarkers out of sedimentary lipid extracts using semi-preparative high performance liquid chromatography (HPLC) and flow injection analysis - mass spectrometry (FIA-MS). The method enables the isolation of glycerol dialkyl glycerol tetraethers (GTGTs), specifically GDGT-0 and crenarchaeol (Fig. 2.1, I and II respectively), which are produced by archaea, two sterol fractions (Fig. 2.1, III and IV respectively), derived from eukaryotes, and chlorophyll-derived phytol (Fig. 2.1, V) derived from photosynthetic organisms, without fractionation and without detectable contamination in quantities sufficient for radiocarbon dating.

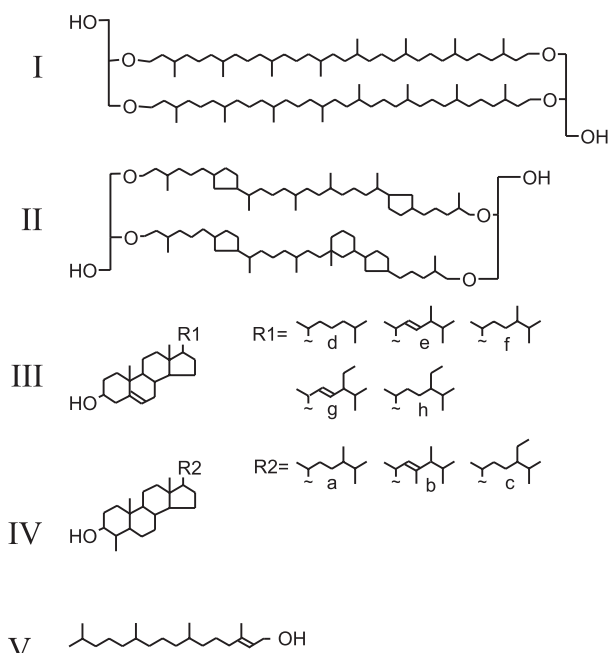


**Figure 2.1** Structures of isolated compounds. I. GDGT-0. II. Crenarchaeol. III.  $\Delta^5$ -sterols. IV. 4-methylsterols. V. Phytol. Different sterols are defined by different groups R1 and R2: *a.* 4,24-dimethyl-5 $\alpha$ (H)-cholest-3 $\beta$ -ol. *b.* 4,23,24-trimethyl-5 $\alpha$ (H)-cholest-22-en-3 $\beta$ -ol (dinosterol). *c.* 4-methyl, 24-ethyl-5 $\alpha$ (H)-cholest-3 $\beta$ -ol. The fraction collected between 24 and 25 min contained  $\Delta^5$  sterols. Indicated peaks: *d.* cholest-5-ene-3 $\beta$ -ol. *e.* 24-methyl-cholest-5,22-diene-3 $\beta$ -ol. *f.* 24-methyl-cholest-5-ene-3 $\beta$ -ol. *g.* 24-ethyl-cholest-5,22-diene-3 $\beta$ -ol. *h.* 24-ethyl-cholest-5-ene-3 $\beta$ -ol.

## 2.2. Experimental

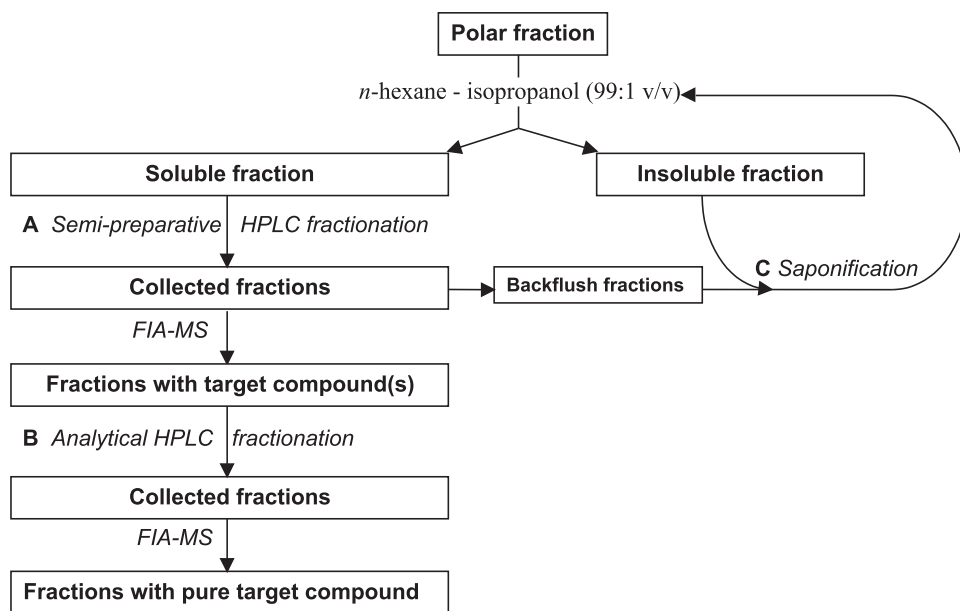
### 2.2.1. Sediment samples, controls and reference compounds

Sediment sub-samples of different age were obtained from piston cores taken in 1996 at Hole 1034C of Ocean Drilling Project leg 169S, Saanich Inlet, Canada [Bornhold *et al.*, 1998]. In addition, a freeze core was taken in the Saanich Inlet in 1998, from which two subsamples were taken.

To ensure that no contamination of allochthonous carbon was introduced during the isolation procedure, both a radiocarbon dead sample and a modern sample were subjected to the isolation procedure. Radiocarbon dead GDGTs were isolated from a 6 million year old Miocene marl from Vena del Gesso basin, Italy (for further information, see *Sinninghe Damsté et al.* [1995]). A cholesterol standard (99+ %; Sigma-Aldrich, Steinheim, Germany) with a modern radiocarbon signature served as the modern carbon control, as well as a control on carbon isotopic fractionation. The cholesterol standard also served as a testing and reference compound for HPLC-MS. A phytol standard (90-95 %; Fluka Chemie, Buchs, Switzerland) was also used as a reference compound.

### 2.2.2. Lipid extraction and pre-treatment

Sediment samples (100-150 g dry wt.) were freeze dried before lipid extraction. Extraction was performed with a dichloromethane-methanol (DCM-MeOH, 9:1 v/v) mixture using an Automated Solvent Extractor (Dionex Corp., Sunnyvale, CA, USA), deployed over three static cycles of 5 min of 100°C and 1000 psi, totalling on average 200 ml of solvent. To remove salt, the extracts were washed with 100 ml double distilled water against DCM in a separatory funnel, and dried over Na<sub>2</sub>SO<sub>4</sub>. The bulk of the solvent was removed by rotary evaporation and the remaining solvent under a stream of nitrogen. The extracts were subsequently separated into two fractions by column chromatography over activated Al<sub>2</sub>O<sub>3</sub> with *n*-hexane (hydrocarbon fractions, 4 column volumes) and DCM-MeOH (1:1 v/v; polar fractions, 3 column volumes) as eluents. Column volumes were 25-30 ml and column height was 13-15 cm. The polar fractions were used for the HPLC isolation procedure (Fig. 2.2). The solvents of the polar fractions were removed as described above, and the residues dissolved by sonication (10 min) in ca. 2 ml of *n*-hexane-isopropanol (99:1; v/v). The resulting suspensions were centrifuged (1 min, 2300 x g) and the supernatants were filtered through a 4-mm-diameter PTFE filter (0.45 µm pore size) to produce fractions suitable for injection on HPLC. The residues after filtration were recovered by rinsing the filter with DCM, and combined with the pellets that remained after centrifugation. These residues were combined with the backflush fractions collected from the semi-preparative HPLC step (see §2.2.3). The solvents of the combined fractions were removed as described above, and the residues saponified by reflux (1 h) in 10 ml 1M KOH-MeOH (96%) solution. The



GC, HPLC-MS, GC-MS, irm GC-MS, AMS <sup>14</sup>C

**Figure 2.2** Flow diagram of the followed isolation procedure. The polar fraction of a total lipid extract is dissolved in *n*-hexane-isopropanol (99:1 v/v) by sonication (10 min). The soluble part of the fraction is subjected to semi-preparative HPLC (step A) to yield 1-min fractions. Identification of target compound containing fractions is performed by flow injection analysis - mass spectrometry (FIA-MS). Fractions containing the same compound are combined and these combined fractions are then each subjected to a second preparative HPLC fractionation step (B) to yield 0.5-min fractions. Again FIA-MS is performed to identify which fractions contain the target compound. These are combined and dried to yield isolated compounds. The part not amenable by the followed HPLC technique (step C), i.e. the backflush fraction combined with the fraction insoluble in *n*-hexane-isopropanol (99:1, v/v), is saponified by basic hydrolysis. The resulting in *n*-hexane-isopropanol (99:1, v/v) soluble fraction is then subjected to steps A and B. irm: isotope ratio monitoring. AMS: accelerator mass spectrometry

fractions were acidified to pH 3 with 2M HCl in water-MeOH (1:1 v/v) and washed with DCM and double distilled water in a separatory funnel. The DCM fractions, containing the saponified polar lipids, were dried over Na<sub>2</sub>SO<sub>4</sub>. Further preparation for HPLC was performed as described above.

### 2.2.3. Isolation of compounds by semi-preparative HPLC

For semi-preparative HPLC, a Hewlett-Packard (Palo-Alto, CA, USA) 1100 series HPLC equipped with an autoinjector and Chemstation chromatography manager software was used, coupled to an Isco (Lincoln, NE, USA) Foxy Jr. fraction collector. Fractions soluble in *n*-hexane-isopropanol (99:1 v/v) (see §2.2.2) were first separated using a semi-



preparative NH<sub>2</sub> column (Econosphere, 10x250 mm, 10µm; Alltech Associates), maintained at 30°C. Injection volumes were typically 100 µl, containing up to 1 mg of material. Compounds were eluted isocratically with 99% *n*-hexane and 1% isopropanol for 5 min, followed by a linear gradient to 1.8% isopropanol in 44 min. Flow rate was 2.5 ml/min. After each run, the column was cleaned by back-flushing *n*-hexane-isopropanol (90:10 v/v) for 10 min. All eluents, including the backflush fraction, was collected in 1 min fractions in pre-combusted (480°C; 8 hrs) glass tubes. A second HPLC purification was performed on an analytical NH<sub>2</sub> column (Econosphere, 4.6 x 250 mm, 5 µm; Alltech Associates) using injection volumes of typically 25 µl out of 200 µl in which the fractions were concentrated. The same conditions as described above were used, except that the flow rate was reduced to 1 ml/min and that back flushing was performed with *n*-hexane-isopropanol (95:5 v/v). Fractions of 30 sec were collected during time windows where target compounds were expected to elute.

After isolation, the fractions containing 4-methylsterols were eluted over a pipette column partly filled with pre-combusted silicalite (PQ Zeolites, The Netherlands) with ethyl acetate, a method similar as described by *West et al.* [1990], to remove *n*-alkanols which were also present in these fractions.

As a reference compound for recovery, purity (contamination) and carbon isotopic effects a known amount (~1 mg) of the cholesterol standard was also subjected to the isolation procedure.

#### 2.2.4. Flow injection analysis – atmospheric pressure chemical ionisation mass spectrometry

Small aliquots of collected fractions (10-30 µl; 0.02-0.1% of the total, 1% in case of phytol) were analyzed by flow injection analysis - atmospheric pressure chemical ionization mass spectrometry (FIA-APCI-MS) using the same HPLC system as described above, coupled to an HP 1100 MSD mass spectrometer using atmospheric pressure chemical ionization (APCI-MS), operated in positive ion mode. Conditions for APCI-MS were as follows: nebulizer pressure 50 psi, vaporizer temperature 400°C, capillary voltage -4kV, corona current 4µA (≈1.8 kV). Injections were made at 1 min intervals into a stream of *n*-hexane-isopropanol (99:1 v/v) with a flow rate of 1 ml/min. Positive ion spectra were in general generated by scanning *m/z* 300-1450 (stepsize 0.1, 2.04 s/cycle) and in some cases by scanning *m/z* 150-1450 for tetraethers (Fig. 2.1, I and II), Δ<sup>5</sup> sterols (Fig. 2.1, III) and 4-methylsterols (Fig. 2.1, IV) and by scanning *m/z* 200-450 (stepsize 0.1, 1.92 s/cycle) for phytol (Fig. 2.1, V).

### 2.2.5. High Performance Liquid Chromatography - Mass Spectrometry

HPLC-MS analysis of individual tetraethers was performed on 1% aliquots of the obtained tetraether fractions using the same system as described above, following the method as described by *Hopmans et al.* [2000]. Quantification was performed by integration of peaks in the summed mass chromatograms of  $[M+H]^+$  and  $[M+H]^++1$  ions and comparison with a standard curve obtained using a dilution series of a known amount of a GDGT-0 standard.

### 2.2.6. Gas Chromatography and Gas Chromatography - Mass Spectrometry

To quantify amounts of sterols and chlorophyll-derived phytol, GC analyses were performed on 1 or 2% aliquots of total fractions, using a Fisons 8000 series instrument equipped with an on-column injector and a flame ionisation detector (FID). A fused silica capillary column (25 m x 0.32 mm) coated with CP Sil 5 (film thickness 0.12  $\mu\text{m}$ ) was used with helium as carrier gas. Known amounts of deuterated ante-iso  $C_{22}$ -alkane standard were added to the aliquots for quantification. The fractions were subsequently dissolved in 10  $\mu\text{l}$  pyridine together with 10  $\mu\text{l}$  bis(trimethylsilyl)trifluoroacetamide (BSTFA). This mixture was heated (60°C; 20 min) to convert alcohols into their corresponding trimethylsilyl ethers. The derivitized fractions were diluted with 75  $\mu\text{l}$  ethyl acetate and injected at 70°C. The oven was programmed to 130°C at 20°C / min and then at 4°C / min to 320°C at which it was held for 10 min. Quantification of the amounts of sterols and phytol was performed by comparing their integrated peak areas with that of the added standard.

GC-MS was performed using a Hewlett-Packard 5890 gas chromatograph interfaced to a VG Autospec Ultima mass spectrometer operated at 70 eV with a mass range of  $m/z$  50-800 and a cycle time of 1.7 s (resolution 1000). Gas chromatography was performed as described above. Compounds were identified by comparison of mass spectra and retention times with those reported in literature.

### 2.2.7. Stable carbon and radiocarbon isotopic measurements

To check for unwanted fractionation effects, compound specific stable carbon isotopic compositions of some phytol fractions and of the cholesterol standard were measured before and after isolation. Analyses were performed on a DELTA-C or a DELTA<sup>plus</sup> XL irm-GC/MS-system, both in principal similar to the DELTA-S system as described previously by *Merrit et al.* [1995]. The gas chromatograph was set up as described above. The carbon isotopic compositions of the compounds were corrected for added carbon molecules by using bis(trimethylsilyl)trifluoroacetamide (BSTFA) with a known carbon isotopic value. Values reported were determined by two or three replicate analyses, and the results were averaged to obtain a mean value and to evaluate the measurement error.

Radiocarbon analyses were performed at the National Ocean Sciences AMS Facility (NOSAMS), Woods Hole, MA, USA. The isolated compounds were combusted to CO<sub>2</sub> and subsequently reduced to graphite using Cobalt as a catalyst, following the procedure described by *Pearson et al.* [1998]. Stable carbon isotope measurements were also performed on subsamples of the CO<sub>2</sub> gas produced during the graphitization process with a VG PRISM [NOSAMS, 2003]. Stable carbon isotopic compositions are reported in standard delta notation relative to the VPDB standard, with a standard error of 0.4‰ in the case of irm-GC/MS measurement, and 0.1‰ in the case of measurement on CO<sub>2</sub>. <sup>14</sup>C contents are expressed as fraction modern [NOSAMS, 2003].

### 2.2.8. <sup>13</sup>C- and <sup>1</sup>H-NMR

To evaluate the purity of isolated fractions, a representative isolated GDGT-0 (Fig. 2.1, I) fraction was analyzed by high field <sup>13</sup>C-NMR and a representative isolated phytol (Fig. 2.1, V) fraction was subjected to <sup>1</sup>H-NMR. NMR spectrometry was performed on a Bruker ARX400 spectrometer equipped with a dual <sup>1</sup>H-<sup>13</sup>C probe. Spectra were obtained at 300 K in CDCl<sub>3</sub>. Proton and carbon chemical shifts were referenced to internal CDCl<sub>3</sub> (7.24 / 77.0 ppm).

## 2.3. Results and discussion

### 2.3.1. Target lipids

Compound specific radiocarbon analysis can only be performed when the desired compounds can be isolated from sediments in quantities large enough for AMS, i.e. > 30 µg. For the specific purpose of dating, they need to be derived from a marine organism, as terrestrial sourced compounds can be of considerable age before they enter a marine sediment. In contrast, marine derived compounds need only to be corrected for a, generally known, reservoir effect. A good candidate is crenarchaeol (Fig. 2.1, II), which is present in high quantities in globally distributed sediments [Schouten *et al.*, 2000b], and is derived from ubiquitously occurring marine pelagic crenarchaeota [Karner *et al.*, 2001]. Also present in high quantities in almost all sediments is GDGT-0 (Fig. 2.1, I) [Schouten *et al.*, 2000b], a lipid produced by a large number of archaea [De Rosa and Gambacorta, 1988]. A third candidate is the class of 4-methylsterols (Fig. 2.1, IV), which are predominantly produced by dinoflagellates [Boon *et al.*, 1979] and can therefore also possibly be used as marine biomarkers suitable for compound specific radiocarbon dating. As any single 4-methylsterol, isolation of dinosterol (Fig. 2.1, IV b) would not yield enough material, but the isolation of 4-methylsterols as a class would. Pearson *et al.* [Pearson *et al.*, 2000] showed that the entire compound class of sterols could serve as an excellent proxy for the

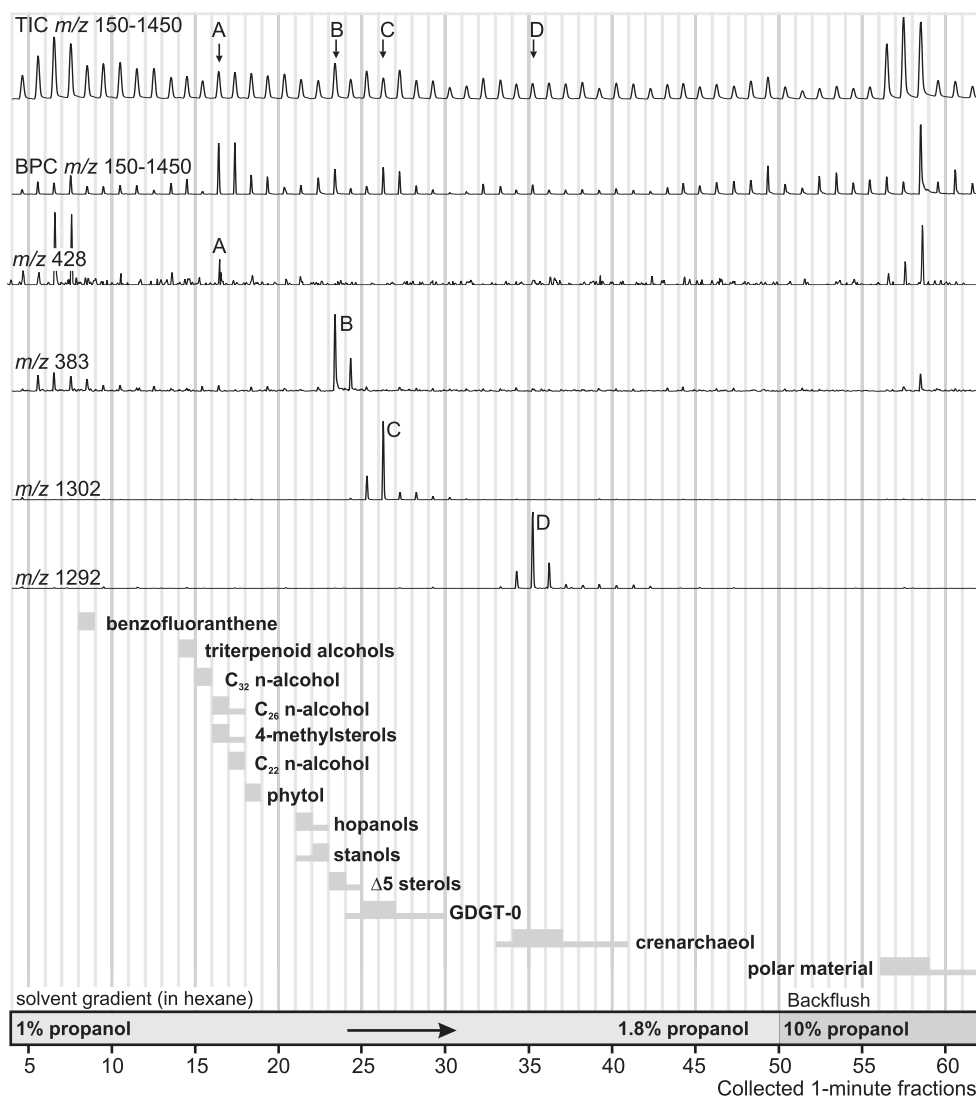


**Figure 2.3** Total ion current (TIC,  $m/z$  150-1450), base peak chromatogram (BPC) and mass chromatograms of a flow injection analysis of 1 minute fractions obtained with semi-preparative HPLC of one of the samples, with an overview of the major lipids present in the collected fractions. Each peak in the TIC corresponds to one collected fraction. The first peak in the chromatograms correspond to the fraction collected between 4 and 5 min. The base peak chromatogram (BPC) indicates in which fractions single compounds are dominantly present.  $m/z$  383 is characteristic for  $\Delta^5$  sterols,  $m/z$  1302 is indicative for GDGT-0,  $m/z$  1292 is indicative for crenarchaeol and  $m/z$  428 indicates the presence of dinosterol and other 4-methylsterols. Below the mass chromatograms, gray areas indicate the presence of major compounds or compound classes in the different fractions, as detected by GC or HPLC-MS. Fractions containing only a small part of the total amount of a compound (class), i.e. collected at the start or end of elution, are indicated by smaller grey areas. Fractions collected during the backflush phase of the followed method are included in the FIA-MS series. Only after several minutes after the backflush started (at 50 min), the polar material that retained on the column started to elute, as can be derived from the high TIC values in the fractions collected between 56 and 59 min. The fractions indicated by the letters A, B, C and D contain the highest amounts of respectively  $\Delta^5$  sterols, GDGT-0, crenarchaeol and 4-methylsterols. The mass spectra of fractions B, C and D are presented in figure 2.4.

$^{14}\text{C}$  concentration of ocean surface waters. This suggests that the isolation of sterols in classes instead of isolation of individual lipids is a valid procedure. Furthermore, all 4-methylsterols are derived from the same source with the same radiocarbon content. For these reasons, it was decided to isolate these compounds as a group.

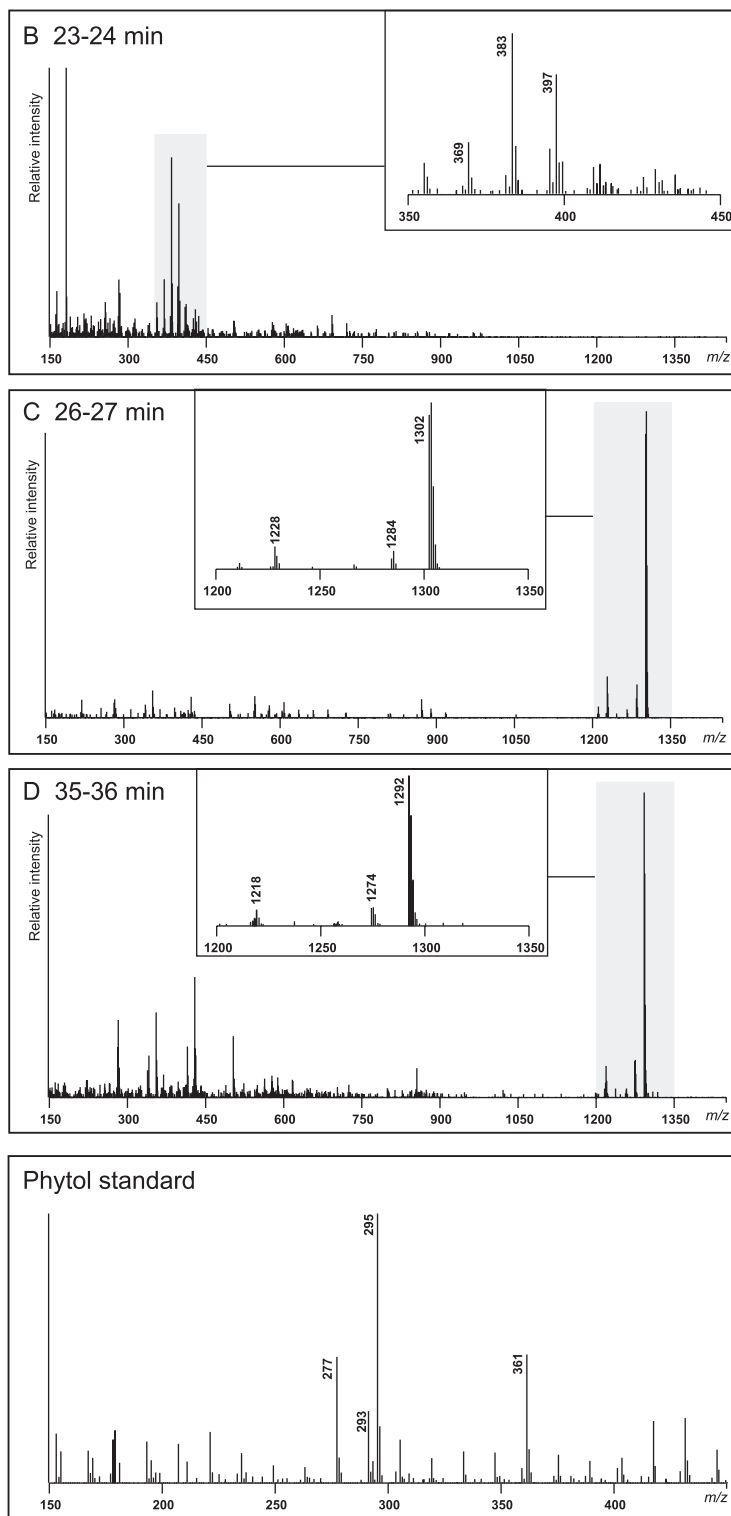
For the same reasons, it was also decided to isolate  $\Delta^5$  sterols (Fig. 2.1, III) as a group. These compounds are produced by nearly all aerobic eukaryotes and virtually absent in prokaryotes, and can therefore be regarded as biomarkers for phototrophic eukaryotes [Coolbear and Threfall, 1989]. Many of them have been attributed to phytoplankton as well as to terrestrial plants [Volkman, 1986], but the most abundant sedimentary  $\Delta^5$  sterols ( $\text{C}_{27}$  and  $\text{C}_{28}$ ) are generally assumed to be of phytoplanktonic origin. Furthermore, the investigated setting of Saanich Inlet is known to be highly productive [Timothy and Soon, 2001] and the sedimentary organic carbon to be of a predominant marine origin [McQuoid, 2001].

A fifth candidate selected for isolation is phytol (Fig. 2.1, V) that is released upon saponification of the residual polar fraction of the total lipid extract (Fig. 2.2). This phytol is derived from non- or hardly degraded chlorophyll and has, like the  $\Delta^5$  sterols, an almost exclusively phytoplanktonic origin [Sun *et al.*, 1998]. Free sedimentary phytol was only present in low amounts while phytol still bound to chlorophyll-moieties was present in quantities sufficient for radiocarbon analysis.

### 2.3.2. Isolation

Compounds had to be isolated in substantial amounts compared to amounts generally handled on current analytical chromatographic equipment. Therefore, it was necessary to start with large amounts of lipid extracts (approximately 20 mg of polar material, derived from 100-150 g of freeze-dried sediment). To increase throughput, the separation was performed in two steps (Fig. 2.2). A first purification of the target compounds was performed by semi-preparative HPLC, where 1-minute fractions were collected. The use of a semi-prep column allowed for a relatively large throughput of polar fractions (ca. 1 mg / injection). After combination of collected fractions containing the same compounds, they were further purified on an analytical size column. In this step smaller time fractions (0.5 min) were collected to preserve the resolution obtained by the column. Free sedimentary phytol, collected after steps A and B (Fig. 2.2) coeluted with other compounds and was only present in low amounts. Therefore this phytol was not used. Phytol released upon saponification of the residual polar fraction of the total lipid extract (step C, Fig. 2.2) was isolated by a second performance of steps A and B. In this second isolation, compounds coeluting with phytol were absent.

A fast detection of target compounds in the collected fractions was performed by FIA-APCI-MS. Lipid detection by UV was not feasible, as the target lipids contain no chromophores. The great advantage of FIA is the (machine) time that can be saved: while

**Figure 2.4**

Mass spectra of the fractions collected at 23-24 min (B), 26-27 min (C) and 35-36 min (D) (see Fig. 2.3), and the mass spectrum of a phytol standard. The upper spectrum (B) clearly shows the  $[M+H]^+ - 18$  ions generated from  $C_{27}$ ,  $C_{28}$  and  $C_{29}$   $\Delta^5$  sterols, namely  $m/z$  369, 383 and 397 respectively. The mass spectra C and D are dominated by the ions  $[M+H]^+$ ,  $[M+H]^+ + 1$ ,  $[M+H]^+ - 18$  (loss of  $H_2O$ ) and  $[M+H]^+ - 74$  (loss of glycerol), indicative for tetraethers. The mass spectrum of phytol is characterised by  $m/z$  277, 293, 295 and 361. Other peaks in the mass spectra are background ions and mainly derived from the septa on the vials used for FIA-MS analysis.

GC or HPLC-MS analyses take more than 1 hour per isolated fraction, FIA only takes 1 minute per sample. To first assess the quality and specificity of the spectra generated by FIA-APCI-MS, the results of the FIA of the first batch of collected fractions were compared with GC, GC-MS and HPLC-MS analyses of these fractions. This made it possible to routinely perform FIA-APCI-MS scanning of collected fractions for target compounds later on. The total ion current (TIC, Fig. 2.3) generated by this method provides hardly any information due to a high background signal. The base peak chromatogram (BPC, Fig. 2.3) indicates, however, in which fractions single compounds are dominantly present. By using specific mass chromatograms and peak apex mass spectra (Figs. 2.3 and 2.4) the different target compounds could rapidly be traced within the collected fractions.

Fractions containing 4-methylsterols (Fig. 2.1, IV) were recognizable by  $m/z$  428 generated by its dominant constituent dinosterol (Fig. 2.1, IV b). They eluted after approximately 17 min during the semi-preparative step (Fig. 2.3), but coeluted with *n*-alkanols. The *n*-alkanols could, however, easily be removed using silicalite, a molecular sieve (Fig 2.5, [West *et al.*, 1990]). The mass spectrum and retention time of phytol (around the 19<sup>th</sup> min) was determined by analysis of a standard, but the generation of detectable positive ions by APCI turned out to be inefficient resulting in low intensities of specific ions (Fig. 2.4;  $m/z$  277, 293, 295 and 361). Only by studying specific mass chromatograms and injection of sufficient amounts of the analyte (100-200 ng, 1% of the total), it was possible to recognize phytol-generated ions above background level during FIA-APCI-MS. Therefore, all fractions which could possibly contain phytol, based on retention time, were also screened by GC analysis. Analysis of the cholesterol standard provided a reference spectrum and retention time for  $\Delta^5$  sterols, which yield base peaks at  $m/z$   $[M+H]^+-18$ , generated by the loss of their hydroxyl-group (Fig. 2.4).  $\Delta^5$ -Sterols (Fig. 2.1, III) eluted at 23-25 min and coeluted partly with GDGT-0 (Fig. 2.1, I), which started to elute after 24 min (Fig. 2.3). GDGTs give very clear and distinctive mass spectra that are easy to recognize, characterized by  $m/z$   $[M+H]^+$ ,  $[M+H]^++1$ ,  $[M+H]^+-18$  and  $[M+H]^+-74$  (Fig. 2.4) [Hopmans *et al.*, 2000]. During the second purification step using the analytical size column and smaller time fractions, the  $\Delta^5$  sterols and GDGT-0 could, however, be collected separately.

The amounts (Table 2.1) and purity of the different fractions were determined by HPLC-MS, GC and GC-MS analysis. The quantities obtained were more than sufficient for  $^{14}\text{C}$  analysis (Table 2.1). More importantly, integration of chromatograms produced by GC and compound identification using GC-MS of the sterol and phytol fractions indicated that they consisted at least for 95% of the desired compounds (Fig. 2.5). HPLC-MS analysis of the isolated GDGT fractions showed that GDGT-0 and crenarchaeol were also >95% pure. However, material non-amenable to APCI-MS or GC, especially column bleed, could still remain undetected. To ascertain that no major undetectable contamination was present, high field  $^{13}\text{C}$ -NMR was performed on a representative isolated GDGT-0 fraction. The spectrum compared favorably with literature data, i.e. all significant resonances could be attributed to carbons from GDGT-0. This strongly suggests that no other compounds were present in

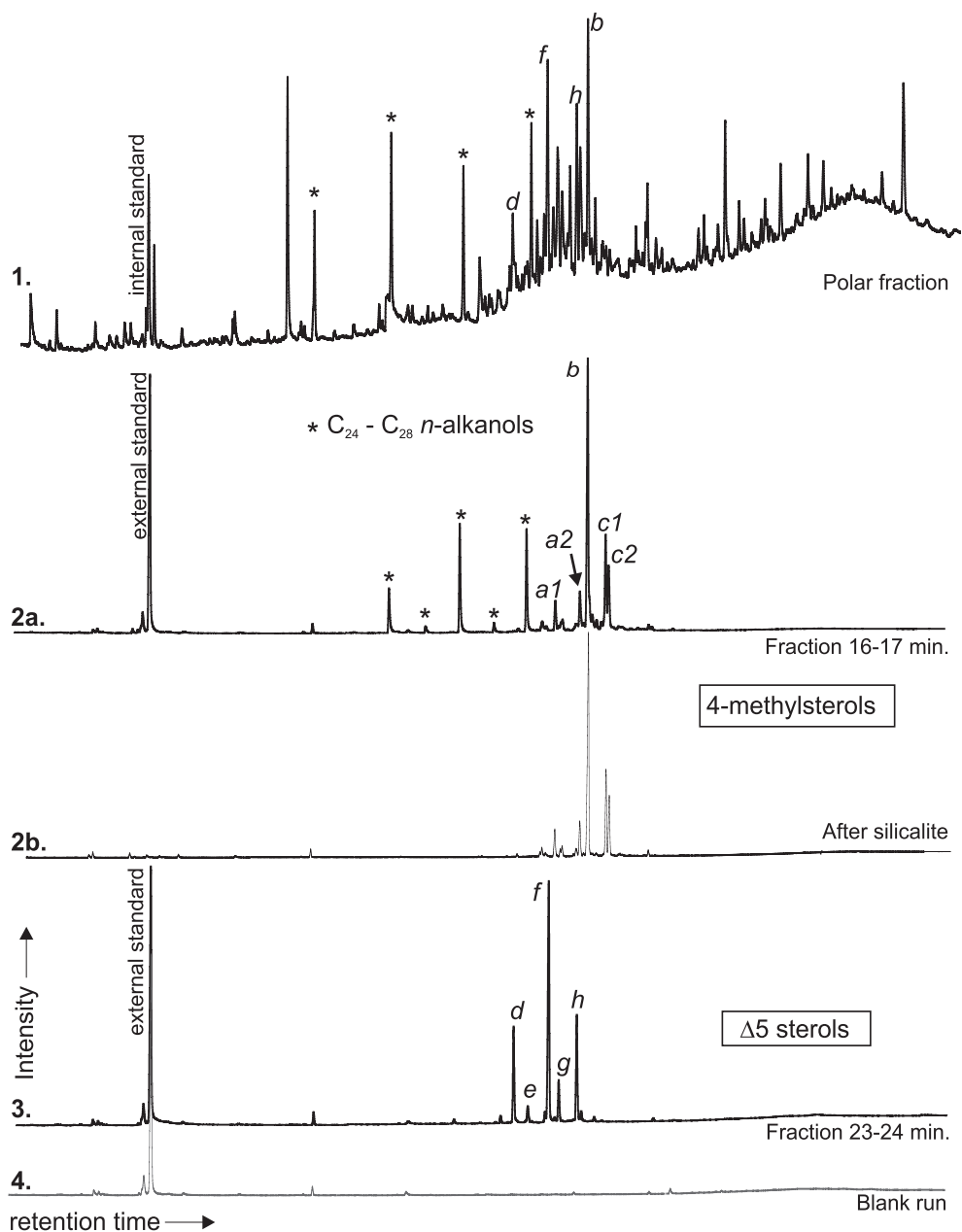


**Figure 2.5** Gas chromatograms of the polar fraction of a total lipid extract and of the fractions containing  $\Delta 5$  sterols and 4-methylsterols at different stages of the isolation procedure. **1.** The polar fraction shows the complexity of the mixture before separation. **2a.** The fraction collected between 16 and 17 min contained a number of straight-chain alkanols, together with 4-methylsterols. **2b.** Silicate treatment removed the straight-chain alkanols quantitatively. **3.** The fraction collected between 23 and 24 min contained  $\Delta 5$  sterols. **4.** A blank run including the external standard is shown as a reference. Indicated peaks *a* to *h* refer to structures given in Fig. 2.1. *a1* and *a2*, and *c1* and *c2* are stereoisomers.



significant amounts. A representative phytol fraction was subjected to  $^1\text{H-NMR}$  analysis and all significant proton signals could be attributed to phytol, indicating >95% purity. Sterol fractions were not subjected to NMR, but because these fractions were isolated under the same conditions as phytol and the GDGTs, and because they had intermediate retention times during HPLC, absence of significant contamination could also be inferred for the sterol fractions. However, these fractions were not totally transparent but exhibited still a faint greenish lush, most likely derived from chlorophyll-derived moieties. Future isolations of sterols using the described method should therefore be performed on fractions pretreated with base hydrolysis, as was performed on the phytol fractions. This will break down and remove chlorophyll-derived moieties to such an extent that they do not coelute with the sterols.

### 2.3.3. Isotopic fractionation during isolation

Chromatographic separation leads to (carbon) isotopic fractionation of the compound within an eluting peak [*Caimi and Brenna, 1997*]. To avoid carbon isotopic fractionation, care was taken to include collected fractions containing the front and tail of eluting peaks into the combined fractions. The  $\delta^{13}\text{C}$  values of the untreated cholesterol standard, of the cholesterol standard subjected to the isolation procedure and of the  $\text{CO}_2$  produced upon combustion of the cholesterol for radiocarbon analysis, were all identical well within the analytical error (Table 2.1), showing that the HPLC procedure did not result in any significant fractionation.

Chlorophyll-derived phytol did not coelute with other compounds during gas chromatography and therefore it was possible to determine the  $\delta^{13}\text{C}$  values of phytol before the isolation procedure and to compare those values with the  $\delta^{13}\text{C}$  values after isolation. This was done for three samples (Table 2.1). The differences in the  $\delta^{13}\text{C}$  values (+0.5‰; +0.7‰ and -0.6‰) are within the measurement error (twice 0.4‰). This points to the absence of a significant carbon isotopic fractionation effect (<0.7‰), and thus the procedure does not affect the radiocarbon age determination. Apparent negative and positive shifts indicate furthermore that even if any fractionation is induced by the isolation procedure, this is not biased towards a certain direction.

Overall, the isolation method did not result in any significant carbon isotopic fractionation.

### 2.3.4. Radiocarbon Contents

The  $^{14}\text{C}$  contents of the modern cholesterol standard before and after the isolation procedure were identical within measurement error (Table 2.1), indicating that no significant contamination of old or fossil carbon was introduced during the isolation

**Table 2.1** Amounts, stable carbon isotopic values and radiocarbon contents and ages of targeted sedimentary compounds

Compound	Sample	Isolated amount (GC / HPLC-MS) µg C (± 5%)	CO <sub>2</sub> -recovery (pressure) µg C (± 1%)	δ <sup>13</sup> C value		δ <sup>13</sup> C value CO <sub>2</sub> ‰ (± 0.1)	<sup>14</sup> C content F modern (± 0.003)	Radiocarbon age Yr. BP (±50)
				before isolation	after			
Cholesterol	direct	1000	937	-25.9		-25.87	1.129	Modern
	'isolated'	1000	986		-25.8	-25.87	1.127	Modern
GDGT-0	Vena del	1100	130			-24.73	0.05 (± 0.01)	23000 (±1400)
Crenarchaeol	Vena del	1200	150			-22.15	0.049	24100 (±450)
TOC *	Saanich Inlet A					-22.22	0.780	1990
GDGT-0	Saanich Inlet A	1015	982			-21.44	0.677	1560
Crenarchaeol	Saanich Inlet A	990	938			-21.68	0.832	1470
Δ5 sterols	Saanich Inlet A	480	431			-21.50	0.787	1920
4-methyl sterols	Saanich Inlet A	400	373			-21.77	0.857	1240
phytol **	Saanich Inlet B	100	95	-21.1	-21.7	-21.80	0.775	2050

\* Total sedimentary organic carbon

\*\* Phytol fraction of Saanich Inlet A lost

procedure. The fossil tetraethers isolated from the 6 million year old Vena del Gesso marl were almost radiocarbon-dead (Table 2.1). The measured values of ca. -950 ‰ indicate a contamination of ca. 5% modern carbon. However, this apparent contamination may also be caused by handling in the last stage of preparation for radiocarbon analysis or by analytical problems in the radiocarbon measurement. For unknown reasons the CO<sub>2</sub> recoveries of these samples were much lower than was expected from the amount measured by HPLC-MS. The eventual small sample size implied a greater error in the <sup>14</sup>C analysis due to the background signal and detection limits. Earlier measurements of small, radiocarbon-dead samples isolated by the established method of preparative capillary gas chromatography produced approximately the same results (data not published). Therefore, we conclude that no significant contamination of modern carbon was introduced during the HPLC isolation procedure. The radiocarbon contents of the different isolated compounds or compound classes, as given for one sediment sample (Table 2.1) are within the range of expected values, when compared to the independently determined sediment age (420 yr calBP) and taken a reservoir effect of 800 yr into account. This indicates that specific compounds and compound classes were indeed successfully and rapidly isolated for radiocarbon dating. The results of these and other <sup>14</sup>C measurements, as well as the implications for research in earth sciences and (palaeo)oceanography will further be discussed in Chapter 3.

## **2.4. Conclusions**

Normal phase HPLC was used successfully to isolate lipid biomarkers with neglectable carbon isotopic fractionation or contamination involved. The application of FIA-APCI-MS greatly increased the speed of scanning the collected fractions for the presence of target compounds. With an average work-up time of 1 week, the followed procedure proved to be a relatively fast and easy way to isolate higher molecular mass (>C<sub>30</sub>) and polar (non-derivitized alcohols) lipid biomarkers for compound-specific <sup>14</sup>C analysis, thereby increasing the number and type of organic lipids for which this is possible.

## **Acknowledgements**

The Ocean Drilling Project is thanked for providing subsamples of core 1034C obtained at ODP leg 169S. Michael Whiticar and Melissa McQuoid of SEOS, Victoria University, BC, Canada are thanked for providing the freeze core taken at Saanich Inlet. The Staff at the National Ocean Sciences Accelerator Mass Spectrometry Facility is thanked for <sup>14</sup>C analysis. J.A.J. Geenevaasen (University of Amsterdam) is thanked for the NMR analyses. A.J. Vos - van Avezaath is thanked for extraction of the Vena del Gesso samples.



## Chapter 3

### Compound-specific radiocarbon dating of the varved Holocene sedimentary record of Saanich Inlet, Canada

*Rienk H. Smittenberg, Ellen C. Hopmans, Stefan Schouten, John M. Hayes,  
Timothy I. Eglinton and Jaap S. Sinninghe Damsté*

Submitted to 'Paleoceanography'

**Abstract** The radiocarbon contents of various biomarkers, extracted from the varve-counted sediment of Saanich Inlet, Canada, were measured in order to assess their applicability for dating purposes. Calibrated ages obtained from the marine planktonic archaeal biomarker crenarchaeol compared favorably with varve-count ages, thus showing for the first time that compound-specific radiocarbon dating can be successfully applied. The same conclusion could be drawn for a more general archaeal biomarker (GDGT-0), although this biomarker proved to be less reliable due to its non-specific origin. The results also lend support to earlier suggestions that marine crenarchaeota use dissolved inorganic carbon (DIC) as their carbon source. The radiocarbon ages of phytoplankton derived biomarkers  $\Delta^5$  sterols, 4-methyl sterols and chlorophyll-derived phytol, were quite variable. This is probably related to highly variable  $^{14}\text{C}$  contents in the upper water layer due to interannual variations in stratification, ocean-atmosphere  $\text{CO}_2$  exchange and fresh water input with related hard-water effects. The average reservoir age offset  $\Delta R$  of 430 yr, determined using the crenarchaeol radiocarbon ages, varied by  $\pm 110$  yr. This may be caused by natural variations in ocean-atmosphere mixing or upwelling at the NE Pacific coast. However, comparison of crenarchaeol radiocarbon ages with a reservoir age-corrected calibration curve that is also shifted in time results in an almost perfect match, indicating that the observed variability may also be due to an inconsistency in the marine calibration curve when used at sites with high reservoir ages. This observation underlines the importance of assessing reservoir ages not only for specific sites, but also through time, and that the currently used calibration model may require adjustment in order to correct for a temporal shift in the marine calibration curve in regions with high reservoir ages.

#### 3.1. Introduction

Radiocarbon analysis has been used since the 1950's for dating purposes, but it is only since the development of accelerated mass spectrometry (AMS) in the 1980's that sample size requirements have been reduced to the extent that compound-specific radiocarbon analysis

(CSRA) has become possible [Eglinton *et al.*, 1996]. Radiocarbon analysis of specific sedimentary organic compounds of known origin (so-called "biomarkers") can in theory be used as an alternative dating method for organic carbon-rich sediments. Dating based on total organic matter is often not possible since this is a complex mixture derived from a multitude of sources varying in radiocarbon age [Eglinton *et al.*, 1997; Pearson *et al.*, 2001]. CSRA may be of particular utility for samples where other dating methods are impractical or to supplement dates on 'traditional' materials (e.g. organic macrofossils or carbonate), in order to increase precision or resolution [Eglinton *et al.*, 1997]. To date, CSRA has almost exclusively been used to address carbon source related questions, by investigating the spread in radiocarbon age between different sedimentary components [Pearson *et al.*, 2001; Petsch *et al.*, 2001; Ohkouchi *et al.*, 2002] in a manner that is comparable to radiocarbon analysis of fractions from the total organic carbon [e.g. Druffel *et al.*, 1996; Wang *et al.*, 1998; Megens *et al.*, 1998; Trumbore, 2000; Raymond and Bauer, 2001b].

Here we evaluate the potential of CSRA as a dating tool for marine sediments by comparing the radiocarbon ages of different biomarkers produced in the marine environment with independently determined ages for sediment deposited over the later Holocene. For this purpose, varve-dated sediments from Saanich Inlet (Fig. 3.1), recovered during leg 169S of the Ocean Drilling Program (ODP) in 1996 [Bornhold *et al.*, 1998] were used. This site was chosen because of its high sedimentation rates and its relatively high organic carbon content, and for its well constrained sediment ages. In addition to the ODP samples, very recent Saanich Inlet sediments deposited before and after above-ground nuclear weapons testing, recovered by freeze coring, were also examined. The increase in atmospheric  $^{14}\text{C}$  resulting from these activities (The so-called 'bomb-spike') provides an effective tracer to follow surface-ocean derived biomarkers [Pearson *et al.*, 2000]. In addition to a correspondence with surface ocean DIC, the validity of compound-specific radiocarbon dating requires that the biomarkers are deposited co-eval with the rest of the sediment. For instance, Ohkouchi *et al.* [2002] found that lateral transport of fine-grained particles greatly affected the radiocarbon ages of haptophyte-derived alkenones, when compared with the ages obtained from planktonic foraminifera that were not displaced after their initial sedimentation. In Saanich Inlet, resuspension of the benthic layer occurs to a small extent while some lateral transport of sill sediment towards the basin is also observed [Sancetta and Calvert, 1988], occurring mainly near the fjord mouth during deep water renewals. However, because of the high accumulation rates and the local scale of these processes, it can be assumed that such effects will not significantly influence biomarker ages.

To fully evaluate the potential of biomarker  $^{14}\text{C}$  dating, the calibration from conventional radiocarbon age to calendar years must also be considered. Calibration of atmospheric  $\text{CO}_2$  derived samples is fairly straightforward [Stuiver *et al.*, 1998a]. However, for marine derived samples the reservoir age, i.e. the greater age of dissolved inorganic carbon (DIC) compared to atmospheric  $\text{CO}_2$ , needs to be taken into account. The marine

calibration curve of *Stuiver et al.* [1998a] is based upon the atmospheric calibration curve, but incorporates a global average reservoir age through time  $R_g(t)$  of around 400  $^{14}\text{C}$  yr. A complicating factor is that the reservoir age varies worldwide between 200 and 1300  $^{14}\text{C}$  yr [*Stuiver et al.*, 1998b and references therein], due to ocean circulation patterns and local upwelling and mixing. Therefore a site specific reservoir age offset  $\Delta R$  needs to be known in order to obtain accurate calibrated ages. In this study, the obtained biomarker radiocarbon ages could be directly compared with sediment calendar ages, as well as with previously measured regional reservoir ages, thus providing the opportunity to evaluate the potential reservoir age variations of Saanich Inlet through time. Regional or local reservoir ages may not always have varied parallel with the global changes [e.g. *Siani et al.*, 2001], especially at coastal sites with varying fresh water input and upwelling [e.g. *Ingram and Southon*, 1996]. Improving the spatial resolution of independently determined reservoir ages will contribute to the development and/or accuracy of regional calibration curves. Furthermore, paleoceanographic studies may also benefit from robust records of regional or local reservoir age variations, as they might reveal past climatic or oceanographic changes.

### 3.2. Setting

The sediment samples used for this research were taken from ODP core 1034C, leg 169S, in Saanich Inlet, British Columbia, Canada (Fig. 3.1). This is a fjord at the south-east coast of Vancouver Island with a maximum depth of 237 m. The deeper part of the basin is isolated from the strait of Georgia by a two-fold sill with depths of 65 and 75 m in the Satellite channel. The near-surface circulation pattern in Saanich Inlet is highly variable, and affects only the waters above sill depth. Surface water is largely derived from the Strait of Georgia, influenced by fresh water from the Fraser River, that has its highest discharge in summer, and by fresh water from the Cowichan River, which has its highest discharge during winter and spring. This causes the salinity of the surface water to vary between 25‰ and 29‰, while below sill depth a salinity of *ca.* 31‰ prevails. The resulting strong pycnocline causes the deeper part of the basin to be isolated [*Anderson and Devol*, 1973; *Takahashi et al.*, 1977]. Together with a relatively

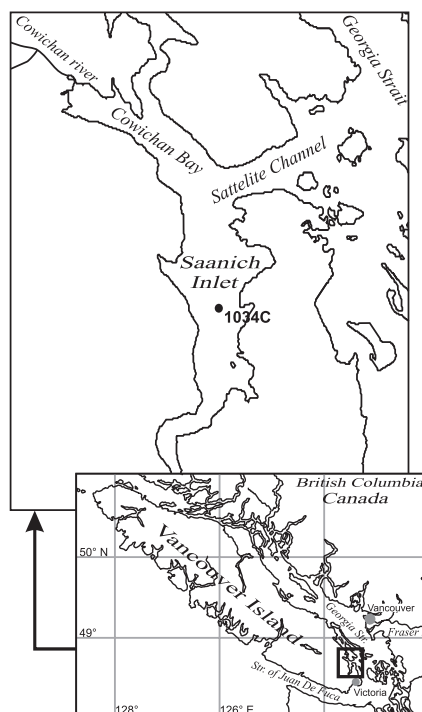


**Figure 3.1** Chart of the Southern Georgia Strait showing Saanich Inlet and the location of ODP hole 1034.

high primary production and subsequent heterotrophic degradation, this isolated setting supports the development of anoxia, which is prevalent below 120 m water depth throughout most of the year, and is virtually permanent below 200 m. [Richards, 1965; Bornhold *et al.*, 1998]. ‘Bolus shaped’ deep water renewals occur annually between August and October to a depth of 100 m, and on average every other year to a depth of 200 m, depending on the density of the introduced water [Anderson and Devol, 1973]. This water comes from Juan de Fuca Strait and is a mixture of warm, well mixed and oxygenated surface water and relatively cold and saline deep water from upwelling at the Pacific coast. During bottom water renewal, the present anoxic water mass is displaced upwards, with relatively minor mixing along the interface between the two water masses [Bornhold *et al.*, 1998 and references herein].

*Gucluer and Gross* [1964] estimated that 65% (wt.) of Saanich Inlet sediment is clay- and silt sized terrigenous material, mainly introduced by the Fraser and Cowichan river. The remaining 35% is of biogenic, mainly silicious phytoplanktonic origin. Part of this planktonic material is produced outside the fjord, mainly in the Satellite Channel [Hobson and McQuoid, 2001]. The terrigenous material causes a dark color in winter, which in summer turns to a lighter color by a sequence of successive diatom blooms. Because of the virtually permanent anoxic bottom water conditions, benthic fauna are absent and the seasonal record of deposition is preserved as fine laminae, resulting in a rhythmical varved sequence spanning approximately the last 6000 years [Bornhold *et al.*, 1998]. Because the varved sequence is virtually complete, the age of the cored sediments can be determined with an annual resolution. *Nederbragt and Thurow* [2001] compiled composite varve records from parallel cores from two locations in the fjord by correlation of massive beds and characteristic features in the varve pattern. This approach reduced the error introduced by missing varves. The obtained floating varve-count age-scale was calibrated with published radiocarbon dates obtained from wood remains.

**Table 3.1** Origin and age of the sediment subsamples used in this study

Core section	Composite core depth (m)	Section depth (cm)	Sediment age
Freeze core	--	0 - 52	1984 – 1998 AD
Freeze core	--	116 -141	1932 – 1950 AD
1034C 1H-5	6.02 – 7.45	0-78 ; 103-150	568 – 465 BP
1034C 2H-3	10.9 – 12.1	0 - 124	1111 – 977 BP
1034C 2H-4		0 - 150	1273 – 1125 BP
1034C 3H-6	26.8 – 28.3	0 - 10 ; 30 - 150	2707 – 2533 BP
1034C 4H-4	34.0 – 35.1	0 - 109	3600 – 3500 BP
1034C 5H-4	43.6 – 44.3	0 - 69	4940 – 4840 BP



### 3.3. Materials and methods

#### 3.3.1. Sediment samples

Sediment subsamples from different depths (Table 3.1) were obtained from advanced hydraulic piston (APC) cores taken in 1996 at Hole 1034C of Ocean Drilling Project leg 169S, Saanich Inlet, Canada [Bornhold *et al.*, 1998] (Fig. 3.1). The calendar ages of the subsamples were determined using the varve-based age model of Nederbragt and Thurow [2001]. In addition to the ODP samples, a 150 cm - long freeze core was taken from the upper sediment of Saanich Inlet in 1998. Dating was performed by a combination of  $^{210}\text{Pb}$  dating and varve counting. A pre-bomb (1932-1950 AD) and a post-bomb (1984-1998 AD) sample were selected for analysis.

#### 3.3.2. Extraction

Sediment samples were freeze dried before lipid extraction, resulting in 100 – 150 g dry sediment. Part of this sediment was reserved for TOC analysis. Extraction was done using an Automated Solvent Extractor (Dionex Corp., Sunnyvale, CA, USA), using a dichloromethane - methanol (DCM - MeOH, 9:1 v/v) mixture, deployed over three static cycles of 5 min of 100°C and 1000 psi. The extracts were washed with double distilled water in a separatory funnel to remove salt. The bulk of the solvent was removed by rotary evaporation after which the extracts were dried over small columns filled with  $\text{Na}_2\text{SO}_4$ . The last solvent was evaporated under a stream of nitrogen.

#### 3.3.3. Isolation of compounds

The extracts were separated into two fractions by column chromatography over activated  $\text{Al}_2\text{O}_3$  with *n*-hexane (hydrocarbon fractions) and DCM - MeOH (1:1 v/v; polar fractions) as eluents. Fractions containing only the  $\text{C}_{27}$ ,  $\text{C}_{29}$  and  $\text{C}_{31}$  *n*-alkanes were isolated from the hydrocarbon fractions by urea adduction and preparative capillary gas chromatography (PCGC). Hexane was removed from the hydrocarbon fractions by rotary evaporation and the residues were subsequently dissolved in a solution of urea in methanol, and evaporated to dryness under a stream of nitrogen. The resulting urea crystals were rinsed with *n*-hexane to remove non-linear hydrocarbons before the crystals were dissolved in double distilled water to liberate straight-chain *n*-alkanes. The latter were recovered by extraction of the water phase with *n*-hexane. The recovered fractions contained almost exclusively a series of *n*-alkanes. The  $\text{C}_{29}$ ,  $\text{C}_{31}$  and  $\text{C}_{33}$  *n*-alkanes were isolated from these fractions by preparative capillary gas chromatography (PCGC) using a low-bleed fused silica capillary column (25 m x 0.32 mm) coated with CP Sil 5 (film thickness 0.52  $\mu\text{m}$ ) mounted on a Hewlett-

Packard 6890 gas chromatograph in conjunction with a Gerstel preparative fraction collector, similar to that described by *Eglinton et al.* [1996].

From the polar fractions the glycerol dialkyl glycerol tetraethers (GDGT's) crenarchaeol and GDGT-0, and the  $\Delta^5$  sterols, 4-methyl sterols and chlorophyll-derived phytol were isolated using the procedure described by *Smittenberg et al.* [2002, Chapter 2]. In short, repeated semi-preparative normal phase HPLC was performed to isolate the selected biomarkers from sediment extracts, while flow injection analysis - mass spectrometry (FIA-MS) was used for rapid analysis of collected fractions to evaluate the separation procedure. Phytol was released from chlorophyll moieties during a saponification step using 1 M aqueous KOH in MeOH. After isolation, the fractions containing 4-methyl sterols were eluted over a column filled with pre-combusted silicalite (PQ Zeolites, The Netherlands) with ethyl acetate, a method similar as described by *West et al.* [1990], to remove *n*-alkanols. A faint green color persisted in most sterol fractions after isolation, probably caused by chlorophyll moieties of similar polarity. These were removed by performing base hydrolysis of the fractions in 3 ml 0.5 M KOH in methanol at 100°C for 2 h in reaction tubes. The sterols were recovered by adding an equal amount of pure water, and rinsing the water - methanol phase three times with hexane - DCM (9:1 v/v). After evaporation of the solvents, the fractions were taken up in DCM and dried over a small column filled with Na<sub>2</sub>SO<sub>4</sub>. In contrast to the other sediments intervals, from the interval corresponding to 1273 - 1125 BP, only a GDGT-0 fraction was isolated. This fraction was subjected to ether bond cleavage using the method described by *Hoefs et al.* [1997], resulting in a fraction containing C<sub>40</sub> biphytanes. Four GDGT fractions were split into two or three sub-fractions to assess reproducibility.

#### 3.3.4. Gas Chromatography and Gas Chromatography - Mass Spectrometry

To evaluate the composition of the lipid extracts and of isolated fractions, gas chromatography (GC) and gas chromatography – mass spectrometry (GC-MS) was performed on aliquots of the extracts. GC was performed using a Fisons 8000 series instrument equipped with an on-column injector and a flame ionisation detector (FID). A fused silica capillary column (25 m x 0.32 mm) coated with CP Sil 5 (film thickness 0.12 µm) was used with helium as carrier gas. Known amounts of deuterated ante-iso C<sub>22</sub>-alkane standard were added to the aliquots for quantification. The fractions were subsequently dissolved in pyridine together with bis(trimethylsilyl)trifluoroacetamide (BSTFA) and this mixture was heated (60°C; 20 min) to convert alcohols into their corresponding trimethylsilyl ethers. The derivatized fractions were dissolved in ethyl acetate and injected at 70°C. The oven was programmed to 130°C at 20°C / min and then at 4°C / min to 320°C at which it was held for 10 min. Quantification of eluted compounds was performed by comparing their integrated peak areas with that of the added standard.

GC-MS was performed using a Hewlett-Packard 5890 gas chromatograph interfaced to

a VG Autospec Ultima mass spectrometer operated at 70 eV with a mass range of  $m/z$  50-800 and a cycle time of 1.7 s (resolution 1000). Gas chromatography was performed as described above. Compounds were identified by comparison of mass spectra and retention times with those reported in literature.

### 3.3.5. High Performance Liquid Chromatography - Mass Spectrometry

Aliquots of polar fractions (see below) were made suitable for injection on an HPLC system following the method as described by *Hopmans et al.* [2000]. High Performance Liquid Chromatography - Mass Spectrometry (HPLC-MS) was performed on a Hewlett-Packard (Palo-Alto, CA, USA) 1100 series HPLC equipped with an autoinjector and Chemstation chromatography manager software, coupled to an HP 1100 MSD mass spectrometer using atmospheric pressure chemical ionization (APCI-MS), operated in positive ion mode. Compounds were identified by comparison of mass spectra and retention times with those reported in literature. Quantification was performed by integration of peaks in the summed mass chromatograms of  $[M+H]^+$  and  $[M+H]^++1$  ions and comparison with a standard curve obtained using a dilution series of a known amount of a GDGT-0 standard, as described by *Smittenberg et al.* [2002, Chapter 2].

### 3.3.6. Stable carbon isotopic analysis

Compound specific stable carbon isotopic compositions of the cholesterol standard and of the  $n$ -alkane, the  $\Delta^5$  sterol, the 4-methyl sterol and phytol fractions were measured. Analyses were performed on a Delta-C or a Delta-plus XL irm-GC/MS-system, both in principal similar to the Delta-S system as described previously by *Merrit et al.* [1995]. The carbon isotopic compositions of derivitized compounds (phytol and sterols) were corrected for added carbon molecules by using bis(trimethylsilyl)trifluoroacetamide (BSTFA) with a known carbon isotopic value. Values reported were determined by two or three replicate analyses, and the results were averaged to obtain a mean value and to evaluate the measurement error. Values are reported in standard delta notation relative to the VPDB standard, with a standard error of 0.3‰. In most cases, the  $\delta^{13}\text{C}$  values of 5% aliquots of the  $\text{CO}_2$  produced upon combustion during preparation for radiocarbon analysis (see below), were determined on a VG PRISM mass spectrometer.

### 3.3.7. Radiocarbon analysis

Freeze-dried and homogenized sediments containing approximately 1 mg total organic carbon (TOC) were prepared for radiocarbon analysis by a warm acid treatment (10% HCl,

60°C, 3 hrs) to remove carbonates. They were subsequently rinsed with distilled water until neutral and filtered on pre-combusted (850°C, 8 h) quartz filters, dried overnight (60°C) and transferred into pre-combusted quartz tubes for AMS sample preparation. Furthermore, leaf remains and a seed were recovered from two sediment samples. These terrestrial macrofossils were also prepared for radiocarbon analysis by an acid-base-acid treatment to remove humic and fulvic acids, following standard procedures.

Preparation for  $^{14}\text{C}$  AMS analysis of isolated fractions was done following the procedure described by *Eglinton et al.* [1996] and *Pearson et al.* [1998]. In short, after isolation the biomarkers were dissolved in a minimal volume of DCM and eluted over a pre-combusted (480°C, 8 h) small column filled with silica to remove any column bleed material. The fractions were collected into pre-combusted (850°C, 8 hr.) quartz tubes and dried under a stream of nitrogen. After the addition of (also pre-combusted) CuO(s) as the oxidizing agent, the tubes were vacuum sealed and combusted (900°C, 5 h) to yield  $\text{CO}_2$ . Of all fractions, except the *n*-alkane fractions, 5% aliquots were used for  $\delta^{13}\text{C}$  analysis. The remaining  $\text{CO}_2$  was reduced to graphite with Co(s) as a catalyst. The sediments for TOC analysis, and the terrestrial macrofossils were also put in pre-combusted quartz tubes and treated in the same way as the biomarker fractions, except that also 1 mg of Ag(s) was added to the quartz tubes, and that Fe(s) was used as a catalyst for graphitization. Radiocarbon analysis was performed on the obtained graphite targets at the National Ocean Sciences AMS facility (NOSAMS) at Woods Hole (MA, USA).

### 3.3.8. Reporting and calibration of radiocarbon ages

Radiocarbon contents were corrected for 0.1  $\mu\text{mol}$  carbon with a fraction modern of 0.25, which is assumed to have been added during the combustion process, based on prior work [*Pearson et al.*, 1998]. The corrected radiocarbon contents are reported as fraction modern ( $f_m$ ).  $f_m$  is also known as  $A_{\text{SN}}/A_{\text{ON}}$  [*Stuiver and Polach*, 1977], or as  $^{14}\text{C}_\text{N}$  [*Mook and Van der Plicht*, 1999] and represents the  $^{14}\text{C}$  activity of a fraction compared to the activity of a 'modern' international standard, both corrected for carbon isotopic fractionation using their respective  $\delta^{13}\text{C}$  values. Furthermore, conventional radiocarbon ages are reported, i.e. the ages calculated from measured radiocarbon contents using the traditional Libby half life of radiocarbon [*Stuiver and Polach*, 1977]. The radiocarbon contents are also reported as initial, or age corrected,  $\Delta^{14}\text{C}$  values. This follows the convention of many studies in cases where the actual (calendar) age of a radiocarbon dated sample is known [*Stuiver and Polach*, 1977]. In the literature, initial  $\Delta^{14}\text{C}$  may also be encountered as  $\Delta$ , or as  $^{14}\delta_\text{N}^i$  [*Mook and Van der Plicht*, 1999].

$$\text{initial } \Delta^{14}\text{C} = (f_m \times e^{(\lambda \times \text{yrBP})} - 1) \times 1000\%$$

$\lambda$  is the decay constant ( $1/8267 \text{ yr}^{-1}$ ) of  $^{14}\text{C}$ , and yrBP the year of deposition, i.e. the

sediment age in calendar year BP, which is the age scale used in age model of Saanich Inlet [Nederbragt and Thurow, 2001]. These values express the radiocarbon contents corrected for decay between deposition and the year of measurement, and thus reflect the initial radiocarbon content at the time of sedimentation. This can be useful for the determination of the carbon source or sources of the various biomarkers, as they can be compared with historic atmospheric and oceanic radiocarbon concentrations.

Radiocarbon ages were calibrated using the atmospheric calibration curve of *Stuiver et al.* [1998a] implementing a moving average over the sedimentary year span. In the same way, marine-derived biomarker ages were calibrated using the marine calibration curve, applying a regional reservoir age offset ( $\Delta R$ ) of 401 yr, in accordance with the reservoir age of 801 yr previously determined for Saanich inlet [Bornhold et al., 1998].

### 3.4. Results

Gas chromatography (GC), gas chromatography – mass spectrometry (GC-MS) and high-performance liquid chromatography – mass spectrometry (HPLC-MS) of the lipid extracts of the various sediment samples revealed very similar biomarker compositions throughout the investigated core samples. Representative chromatograms are shown in figure 3.2. Table 3.2 lists the recovered amounts and  $\delta^{13}\text{C}$  values of the biomarkers used for this study, as well as the radiocarbon contents of the bulk and biomarker fractions. The radiocarbon contents of the  $>300\ \mu\text{g}$  split fractions were the same within the measurement error of  $0.05\ f_m$  (Table 3.2). However, small splits indicated that some machine induced isotopic fractionation occurred towards higher  $f_m$  values when samples  $<100\ \mu\text{g}$  are concerned. This confirms the conclusion of *McNichol et al.* [2001] that great care should be taken in the analysis of very small samples, and that errors will be relatively large. Because most fractions are, however, larger than  $100\ \mu\text{g}$  (Table 3.2), and because the effect seems to be relatively small ( $<0.03\ f_m$ ), this uncertainty associated with small samples is considered not to significantly influence the interpretation of the results.

The conventional radiocarbon ages and the calculated initial  $\Delta^{14}\text{C}$  values are given in table 3.3. Table 3.4 lists the biomarker ages as calibrated with the atmospheric calibration curve, and for marine-derived biomarkers also the calibrated ages obtained with the marine calibration.

**Table 3.2** Amounts, stable- and radiocarbon isotopic compositions of sedimentary total organic carbon (TOC), terrestrial macrofossils and isolated biomarkers originating from differently aged sediment layers. Phytol = Chlorophyll derived phytol. Amounts are determined after combustion to CO<sub>2</sub> by nanometry, with an error of 5 µg. δ<sup>13</sup>C values are expressed relative to VPDB, with an error of 0.3 ‰ for all samples, except *n*-alkanes which have an error of 0.5 ‰. The error of the fraction modern radiocarbon (f<sub>m</sub>) is 0.005 or less. Multiple values are fractions split before combustion. \* Measured on corresponding biphytanes. <sup>s</sup> Small split replicate

Sediment age (Cal. yr)	TOC	Terr. m.fossil	<i>n</i> - alkanes	Cren- archaeol	GDGT-0	Δ5 sterols	4-methyl sterols	Phytol
<b>Amount (µg)</b>								
1984–1998 AD	1242		32	204	211	152	166	335
1932–1950 AD	1117	668	77	569	587	186	212	268
568–465 BP	919		115	317	510	430	373	99
				418	383			
				58 <sup>s</sup>	89 <sup>s</sup>			
1111–977 BP	966	395	140	425	630	284	359	392
1273–1125 BP					358*			
					361*			
					99 <sup>*,s</sup>			
2707–2533 BP	949		146	498	666	385	124	179
				554				
3600–3500 BP	737			550		100	78	157
4940–4840 BP	796		52	372	431		110	68
<b>δ<sup>13</sup>C (‰)</b>								
1984–1998 AD	-22.3		-31.4	-21.6	-22.1	-22.3	-23.7	-20.0
1932–1950 AD	-22.1	-28.2	-31.4	-21.5	-21.6	-22.1	-22.6	-21.7
568–465 BP	-21.6		-31.7	-21.8	-21.6	-21.5	-21.8	-22.0
				-21.6	-21.3			
				-21.3 <sup>s</sup>	-21.6 <sup>s</sup>			
1111–977 BP	-22.0	-27.6	-32.1	-21.3	-21.2	-23.2	-22.0	-20.5
1273–1125 BP					-22.3*			
					-22.8*			
					-21.0 <sup>*,s</sup>			
2707–2533 BP	-22.0		-31.6	-21.4	-21.7	-22.3	-23.0	-20.8
				-21.4				
3600–3500 BP	-22.1		-31.6			-22.8	-24.8	-20.1
4940–4840 BP	-22.3		-31.2	-21.3	-21.8		-24.1	-18.8
<b><sup>14</sup>C (f<sub>m</sub>)</b>								
1984–1998 AD	0.898		0.546	1.059	1.045	1.026	0.957	1.005
1932–1950 AD	0.825	0.987	0.544	1.935	0.910	0.916	0.879	0.921
568–465 BP	0.780		0.590	0.829	0.826	0.789	0.859	0.836
				0.840	0.823			
				0.868 <sup>s</sup>	0.843 <sup>s</sup>			
1111–977 BP	0.670	0.864	0.507	0.788	0.659	0.714	0.770	0.776
1273–1125 BP					0.772*			
					0.763*			
					0.796 <sup>*,s</sup>			
2707–2533 BP	0.584		0.459	0.657	0.658	0.657	0.695	0.658
				0.649				
3600–3500 BP	0.533			0.607		0.668	0.672	0.638
4940–4840 BP	0.456		0.380	0.536	0.549		0.648	0.620

Sediment age (Cal. yr)	TOC	Terr. m.fossils	n-alkanes	Cren- archaeol	GDGT-0	$\Delta 5$ Sterols	4-methyl Sterols	Phytol	Atmosph. $\Delta^{14}\text{C}$	Marine $\Delta^{14}\text{C} - 49\text{‰}$ <sup>E</sup>
Initial $\Delta^{14}\text{C}$ (‰)										
1984–1998 AD	-107 ± 4		-446 ± 9	+54 ± 9	+40 ± 8	+21 ± 7	-48 ± 9	-0 ± 9	+300	+50 ± 25
1932–1950 AD	-174 ± 4	-12 ± 3	-455 ± 5		-89 ± 6	-84 ± 7	-120 ± 9	-79 ± 9	-20	-104
568–465 BP	-170 ± 3		-372 ± 5	-118 ± 6	-121 ± 3	-158 ± 3	-86 ± 4	-111 ± 3	+3	-99
				-106 ± 4	-124 ± 3					
				-76 ± 9 <sup>s</sup>	-102 ± 8 <sup>s</sup>					
1111–977 BP	-240 ± 3	-20 ± 4	-425 ± 5	-106 ± 5	-232 ± 3	-191 ± 5	-126 ± 4	-119 ± 7	-17	-108
1273–1125 BP					-106 ± 3 <sup>*</sup>					
					-116 ± 3 <sup>*</sup>					
					-73 ± 8 <sup>*s</sup>					
2707–2533 BP	-200 ± 3		-370 ± 4	-98 ± 3	-96 ± 3	-100 ± 3	-47 ± 6	-97 ± 5	+8	-84
				-109 ± 3						
3600–3500 BP	-182 ± 3			-68 ± 3		+26 ± 6	+32 ± 7	-21 ± 6	+16	-74
4940–4840 BP	-177 ± 2		-314 ± 6	-32 ± 4	-7 ± 3		+169 ± 5	+121 ± 7	+50	-42
$^{14}\text{C}$ age (yr BP)										
1984–1998 AD	870 ± 35		4710 ± 130	Modern	Modern	Modern	350 ± 75	35 ± 70	modern	modern
1932–1950 AD	1540 ± 35	110 ± 30	4890 ± 75		760 ± 50	710 ± 65	1030 ± 85	660 ± 75	170	870
568–465 BP	1990 ± 30		4240 ± 70	1510 ± 55	1540 ± 30	1900 ± 35	1230 ± 40	1450 ± 30	480	1310
				1400 ± 40	1570 ± 35					
				1130 ± 90 <sup>s</sup>	370 ± 80 <sup>s</sup>					
1111–977 BP	3220 ± 35	1180 ± 40	5460 ± 80	1910 ± 45	3130 ± 40	2710 ± 55	2100 ± 40	2030 ± 75	1150	1900
1273–1125 BP					2060 ± 45 <sup>*</sup>					
					150 ± 40 <sup>*</sup>					
					1770 ± 75 <sup>*s</sup>					
2707–2533 BP	4320 ± 45		6250 ± 80	3370 ± 40	3350 ± 40	3380 ± 35	2920 ± 65	3360 ± 40	2480	3230
				3470 ± 35						
3600–3500 BP	5060 ± 45			4010 ± 40		3250 ± 70	3200 ± 80	3620 ± 75	3320	4050
4940–4840 BP	6310 ± 40		7880 ± 120	5020 ± 60	4810 ± 50		3490 ± 65	3830 ± 90	4360	5090

**Table 3.3** Initial radiocarbon contents and conventional radiocarbon ages of sedimentary total organic carbon (TOC), terrestrial macrofossils (Terr.m.fossils) and isolated biomarkers originating from differently aged sediment layers. Atmospheric and marine radiocarbon contents and ages are values of the calibration curve published by *Stuiver et al.* [1998a], averaged over the sediment age span. See text for the use of a reservoir age offset  $\Delta R$  of 401 yr. Initial  $\Delta^{14}\text{C}$  values are age corrected radiocarbon contents based on the sediment ages, calculated as discussed in the text. Multiple values are from fractions split before combustion. Phytol, <sup>\*</sup>, <sup>s</sup> as table 3.2. <sup>E</sup> -49 ‰ is equivalent with a  $\Delta R$  of 401 ± 25 yr.

<b>A</b> Age (atmospheric calibration)								
Sediment age	TOC	Terr. m.fossil	n-Alkanes	Crenarchaeol	GDGT-0	$\Delta 5$ Sterols	4-methyl Sterols	Phytol
1984 - 1998 AD	877 - 732		5592 - 5307	Modern	Modern	Modern	514 - 319	92 - 0
1932 - 1950 AD	1512 - 1385	139 - 0	5659 - 5586		727 - 663	724 - 656	1057 - 922	671 - 553
568 - 465 BP	1965 - 1899		4846 - 4699	1454 - 1338	1466 - 1375	1898 - 1832	1238 - 1107	1351 - 1306
1111 - 977 BP	3481 - 3401	1171 - 1055	6327 - 6203	1891 - 1803	1510 - 1397	2873 - 2785	2125 - 2032	2084 - 1889
1273-1125 BP					3389 - 3313			
					2082 - 1954 *			
					2172 - 2084 *			
2707 - 2533 BP	4912 - 4859		7249 - 7026	3653 - 3549	3634 - 3526	3637 - 3587	3256 - 3027	3665 - 3511
				3784 - 3672				
3600 - 3500 BP	5889 - 5754			4528 - 4425		3629 - 3454	3595 - 3400	4028 - 3837
4940 - 4840 BP	7280 - 7206		8664 - 8420	5876 - 5677	5610 - 5530		3918 - 3727	4391 - 4100

<b>B</b> Age (marine calibration)							
Sediment age	Cren-archaeol	GDGT-0	$\Delta 5$ Sterols	4-methyl Sterols	Phytol		
1984-1998 AD	Modern	Modern	Modern	> 0	> 0		
1932-1950 AD		> 0	> 0	411 - 249	> 0		
568-465 BP	700 - 624	705 - 668	1117 - 1012	503 - 465	648 - 602		
	623 - 537	734 - 678					
1273-1125 BP		1280 - 1163 *					
		1332 - 1272 *					
1111-977 BP	1113 - 994	2485 - 2353	2014 - 1865	1303 - 1234	1274 - 1101		
2707-2533 BP	2777 - 2701	2760 - 2691	2789 - 2718	2318 - 2151	2786 - 2681		
	2870 - 2782						
3600-3500 BP	3552 - 3444		2745 - 2640	2729 - 2498	3142 - 2903		

**Table 3.4** Calibrated age ranges (yr BP) obtained with **A**) the atmospheric calibration curve and, when applicable, **B**) obtained with the marine calibration curve using a  $\Delta R$  of 401  $\pm$  25 yr, of sedimentary total organic carbon (TOC), terrestrial macrofossils (Terr.m.fossils) and isolated biomarkers originating from differently aged sediment layers. Phytol = Chlorophyll derived phytol. \* Measured on corresponding biphytanes



### 3.5. Discussion

#### 3.5.1. Biomarkers isolated for radiocarbon analysis

##### *Selection criteria*

The main goal of our research was to determine whether the  $^{14}\text{C}$  content of specific biomarkers could be used for sediment dating. To this end these biomarkers have to meet several criteria. First, they need to be present in sufficient amounts in the sediment to be able to isolate them in quantities large enough for AMS (i.e.  $> 30 \mu\text{g C}$  [Pearson *et al.*, 1998], but preferably  $> 300 \mu\text{g C}$ ). Therefore, only the most abundant biomarkers present in the Saanich Inlet sediments were considered. Second, the carbon source used by the organisms producing the biomarker needs to be known in order to determine which calibration curve should be applied for conversion to calendar ages. Ideally, biomarkers derived from organisms using atmospheric  $\text{CO}_2$  as their carbon source, i.e. of terrestrial origin, should be used because then age calibration can be performed without reservoir age corrections and associated uncertainties. However, a third criterion is that biomarkers should be incorporated in the sediment shortly after production. Biomarkers with a terrestrial origin may be retained in the soil carbon pool for a substantial period of time before they are transported to the sediment [Raymond and Bauer, 2001a], and thus have to be disqualified. Biomarkers produced in the marine environment reflecting the  $^{14}\text{C}$  content of a DIC pool that has been reasonably stable through time meet all criteria mentioned above. In that respect they are similar to calcareous macrofossils or planktonic foraminifera, particles that are often used for radiocarbon dating of marine sediments. Planktonic biomarkers can thus be considered as their molecular equivalents. Not all marine biomarkers are, however, suitable for  $^{14}\text{C}$  dating. Biomarkers that are (partly) produced by heterotrophic organisms using DOC and POC as their carbon source, must be disqualified because some of this carbon substrate can be of substantial age due to its refractory nature [Williams and Druffel, 1987; Raymond and Bauer, 2001b]. A final consideration is the spatial context of the samples. Okhouchi *et al.* [2002] showed that alkenones isolated from sediments of the Bermuda rise were up to 7000 yr older than planktonic foraminifera from the same sediment depth, pointing to lateral transport of the alkenones with fine-grained sediments. However, as pointed out in the introduction, the marine part of the sediment and co-occurring marine biomarkers in Saanich Inlet are anticipated to be of local and contemporary origin. Thus, the Saanich Inlet sediment extracts were screened for potential biomarkers that would likely match the above-mentioned criteria, which is discussed below.

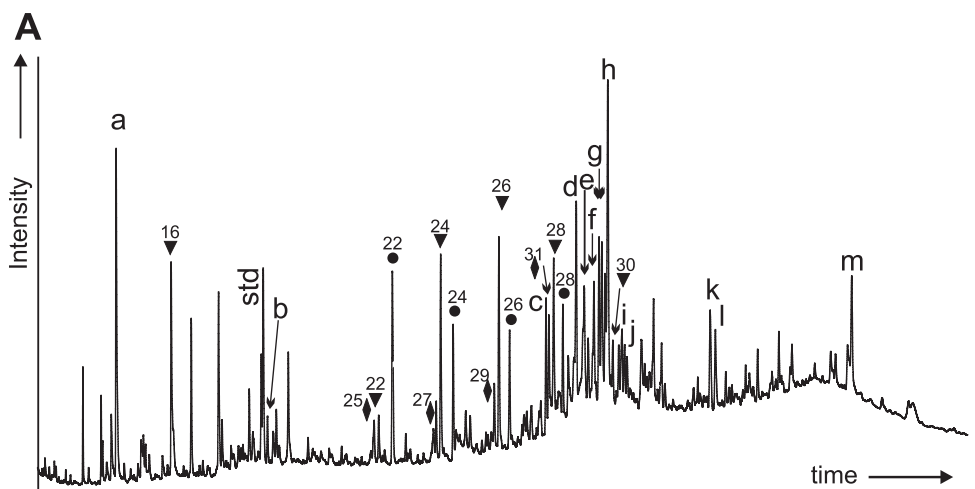
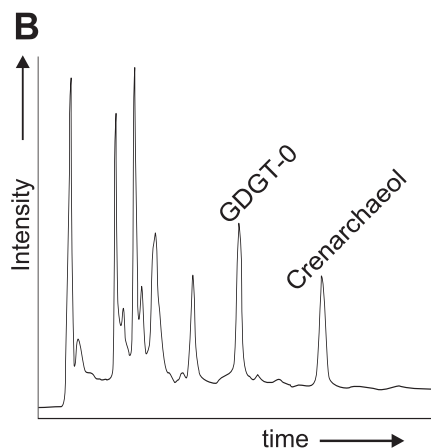


**Figure 3.2** A. Typical gas chromatogram of a total lipid extract of Saanich Inlet sediment. Legend:  $\blacklozenge$  *n*-alkanes.  $\blacktriangledown$  *n*-alkanoic acids.  $\bullet$  *n*-alcohols. Numbers refer to the number of carbon atoms. *a* loliolide. *b*. free extractable phytol. *c*. cholest-5-ene-3 $\beta$ -ol ('cholesterol') *d*. 24-methyl-cholest-5-ene-3 $\beta$ -ol *e*. 24-ethyl-cholest-22-ene-3 $\beta$ -ol *f*. 24-ethyl-cholest-diene-3 $\beta$ -ol *g*. 24-ethyl-cholest-5-ene-3 $\beta$ -ol and 24-ethyl-cholest-3 $\beta$ -ol ('sitosterol' and 'sitostanol') *h*. 4,23,24-trimethyl-5 $\alpha$ (H)-cholest-22-ene-3 $\beta$ -ol ('dinosterol') *i*. and *j*. isomers of 4-methyl, 24-ethyl-5 $\alpha$ (H)-cholest-3 $\beta$ -ol. ('dinostanol'). *k*. 17 $\beta$ , 21 $\beta$ (H) C<sub>32</sub> hopanoic acid *l*. 17 $\beta$ , 21 $\beta$ (H) C<sub>32</sub> hopanol. *m*. tricyclic biphytanediol. std = internal standard.



**B.** Total ion current obtained by HPLC-APCI-MS, mass range  $m/z$  200-1450, of a polar fraction of a representative Saanich Inlet sediment extract. The early eluting peaks are mainly chlorophyll moieties.

### $\Delta^5$ Sterols

Pearson *et al.* [2000] showed that the entire compound class of sterols could serve as an excellent proxy for the  $^{14}\text{C}$  content of ocean surface water DIC. In the open ocean, DIC-assimilating phytoplankton can be assumed to be practically the only sterol source. However, terrestrial higher plants also produce sterols [Volkman, 1986], and in coastal areas this may compromise their possible applicability for sediment dating. The generally most dominant sterol class in recent sediments are the  $\Delta^5$  sterols. This is also the case in the Saanich Inlet (Fig. 3.2), with concentrations of the most abundant  $\Delta^5$  sterol, 24-methyl-cholest-5-ene-3 $\beta$ -ol, ranging between 2 and 8  $\mu\text{g/g}$  sediment, and with decreasing

concentrations with increasing age. The overall  $\delta^{13}\text{C}$  values of the  $\Delta^5$  sterols are  $-22\pm 1\text{‰}$  (Table 3.2), which suggests an almost exclusively marine source for the  $\Delta^5$  sterols [Pancost *et al.*, 1997; Schouten *et al.*, 2000a]. Indeed, Saanich Inlet is known to be highly productive [Timothy and Soon, 2001], and the sedimentary organic carbon to be of a predominantly marine origin [McQuoid, 2001]. Furthermore, sterols produced on land are generally for a large part degraded, transformed or bound before reaching any (marine) sediment [Cranwell, 1981]. For these reasons, the  $\Delta^5$  sterols as group were considered to be a good candidate for compound-specific radiocarbon dating.

#### *4-Methyl sterols*

A second major sterol group are the 4-methyl sterols, which are predominantly produced by dinoflagellates [Boon *et al.*, 1979; Mansour *et al.*, 1999], a widely distributed algal group. The most common 4-methyl sterol, dinosterol, was present in concentrations of 4 - 9  $\mu\text{g/g}$  sediment in the Saanich Inlet (Fig. 3.2). Dinoflagellates are often autotrophic, but heterotrophy is also very common, while mixotrophy is sometimes also observed [Hoek *et al.*, 1995]. However, the carbon isotopic composition of the different dinoflagellate groups will not be very different from each other, as the carbon isotopic composition of heterotrophs generally reflect that of their diet [Grice *et al.*, 1998a], which is mainly of a phytoplanktonic origin [Hoek *et al.*, 1995]. Indeed, the  $\delta^{13}\text{C}$  values of the 4-methyl sterol fraction are  $-22\text{‰}$  to  $-24\text{‰}$ , similar to the  $\Delta^5$  sterols (Table 3.2), also pointing to a marine origin. Therefore, 4-methyl sterols are expected to show the same radiocarbon contents as  $\Delta^5$  sterols. Possibly, they may be superior to the  $\Delta^5$  sterols for compound-specific radiocarbon dating of sediments, because higher terrestrial plants do not produce 4-methyl sterols.

#### *Chlorophyll-derived phytol*

Phytol is the side-chain of most common chlorophylls, and can be regarded as an almost exclusively phytoplankton derived biomarker [Sun *et al.*, 1998 and references herein] for the same reasons as the  $\Delta^5$  sterols. Free phytol concentrations were lower than 1  $\mu\text{g/g}$  sediment (Fig. 3.2). However, saponification of the extracts using aqueous 1 M KOH / MeOH resulted in much larger quantities, up to 30  $\mu\text{g/g}$  sediment. The  $\delta^{13}\text{C}$  values of phytol are  $-20\pm 1\text{‰}$  (Table 3.2). This points towards the same marine planktonic origin as the sterol fractions, as biosynthetic effect generally cause the  $\delta^{13}\text{C}$  value of phytol to be 2 - 4 ‰ higher than the sterols of the same algal species [Schouten *et al.*, 1998b]. Therefore, chlorophyll-derived phytol was also selected for compound-specific radiocarbon dating.

*Glycerol dialkyl glycerol tetraethers*

The glycerol dialkyl glycerol tetraethers (GDGTs) crenarchaeol and GDGT-0 occur ubiquitously in sediments [Schouten *et al.*, 2000b; Sinninghe Damsté *et al.*, 2002a; 2002c]. Crenarchaeol seems to be solely produced by the marine planktonic Crenarchaeota, while GDGT-0 is produced by a suite of archaea, occurring virtually everywhere on Earth [Schouten *et al.*, 2000b]. Crenarchaeol and GDGT-0 were present in the Saanich Inlet in comparable quantities at concentrations as high as 50 – 150 µg/g sediment with invariant  $\delta^{13}\text{C}$  values of  $-21 \pm 0.5\%$  (Table 3.2). This suggests that both GDGTs are from the same source, and thus that GDGT-0 is produced mainly by *Crenarchaeota*, and not, or only to a minor extent, by other archaea (e.g. methanogenic archaea). The  $\delta^{13}\text{C}$  values are consistent with practically all earlier measured  $\delta^{13}\text{C}$  values for present-day crenarchaeol, which are almost invariant [Hoefs *et al.*, 1997; Schouten *et al.*, 1998a; Pearson *et al.*, 2001]. This invariance was partly the basis for the assumption that marine Crenarchaeota are chemototrophs which assimilate DIC independent from the availability of oxygen and light [Pearson *et al.*, 2001; Sinninghe Damsté *et al.*, 2002a], and this was recently confirmed by Wuchter *et al.* [2003]. It is furthermore observed that marine *Crenarchaeota* are most abundant at depths with highest nitrate concentrations below an oxygen minimum zone or chemocline, e.g. in the Black sea (unpublished data), and it is hypothesized that reduction of nitrate may be their energy source [Sinninghe Damsté *et al.*, 2002a; Wuchter *et al.*, 2003]. During most of the year this is at intermediate depths between 30 and 100 m in Saanich Inlet, around the chemocline [Anderson and Devol, 1973; Timothy and Soon, 2001], and it is therefore anticipated that the bulk of crenarchaeol and GDGT-0 is produced from DIC by crenarchaeota residing at these depths. Because both GDGTs occur in abundant quantities, and because they are anticipated to reflect the  $^{14}\text{C}$  contents of DIC, they are also considered as good candidates for compound-specific radiocarbon dating.

*Long-chain n-alkanes*

To substantiate any difference between the radiocarbon contents of marine biomarkers and that of the total organic carbon (TOC), terrestrial derived biomarkers were also selected for radiocarbon analysis. Straight-chain  $\text{C}_{27}$ ,  $\text{C}_{29}$  and  $\text{C}_{31}$  *n*-alkanes were isolated in combined fractions from a series of *n*-alkanes exhibiting a carbon preference index of 3 – 4.5. This carbon preference index suggests that they originate from higher plant waxes [Eglinton and Hamilton, 1967] and thus are almost exclusively of terrestrial origin. In Saanich Inlet, terrestrial derived compounds are assumed to be mainly derived from soils in the catchment areas of the Fraser river and Cowichan river, the major source of sediment for the Saanich Inlet [Gucluer and Gross, 1964; Blais-Stevens *et al.*, 2001], although an aeolian contribution of plant-waxes can not be completely discounted.

### 3.5.2. Radiocarbon contents

#### *Radiocarbon ages of marine and terrestrial biomarkers, macrofossils and TOC*

The calibrated radiocarbon ages of the leaf remains in the pre-bomb sediment (1932-1950 AD) and the seed in the sediment of ~500 BP, matched the sediment ages (Table 3.4), which substantiates the varve-based age model, at least for the most recent sediments. This becomes also clear when measured radiocarbon ages are plotted against the sediment ages, together with the calibration curves of *Stuiver et al.* [1998a] (Fig. 3.3). This plot also shows that the ages of TOC are substantially greater than their parent sediments throughout the investigated cores, and also greater than the marine derived biomarkers (Table 3.4). The ages of the marine biomarkers show on average an offset with the sediment age in reasonable agreement with the proposed reservoir age of *ca.* 800 yr in this area [*Bornhold et al.*, 1998]. However, the spread in age between the different marine biomarkers is sometimes substantial and will be discussed below. The *n*-alkanes, representing terrestrial, vascular plant derived organic carbon, exhibit calibrated ages that are 4000 – 5500 yr older than the sediments (Fig. 3.3), which may partly explain the offset of the TOC ages from the marine biomarker ages and the sediment ages. Thus, as already anticipated, the radiocarbon content of TOC can not be used for dating purposes, due to the admixture of pre-aged terrestrial organic carbon with autochthonous organic carbon. A detailed account on the radiocarbon contents of TOC and the *n*-alkanes, in comparison with the marine derived biomarkers, is discussed in Chapter 4

#### *Pre- and post-bomb radiocarbon contents – a carbon source evaluation*

Comparison of the initial  $\Delta^{14}\text{C}$  values (Fig. 3.4) of the biomarkers sedimented before above-ground nuclear weapon testing in the early 1960's (pre-bomb sample, 1932 – 1950 AD), and those deposited afterwards (post-bomb sample, 1984 – 1998 AD), yields insights into the carbon sources of the various biomarkers used in this study. Due to these tests, the atmospheric radiocarbon concentration increased dramatically [*Nydal and Gislefoss*, 1996] with a subsequent dissemination of this 'spike' into the carbon cycle, including the ocean's DIC-pool [*Guilderson*, 2000; *Levin and Hesshaimer*, 2000]. The *n*-alkane post-bomb  $\Delta^{14}\text{C}$  value shows no influence of bomb- $^{14}\text{C}$  when compared to the pre-bomb value (Table 3.3), indicating that aeolian sources of terrestrial higher plant-derived carbon are insignificant compared to riverine transported terrestrial (soil organic) carbon. In contrast, post-bomb TOC is substantially enriched in  $^{14}\text{C}$  compared to pre-bomb TOC. This must thus primarily be due to the contribution of marine derived carbon that was  $^{14}\text{C}$  enriched due to the bomb-spike. The results of the world ocean circulation experiment [*Key et al.*, 1996] and other investigations [*Druffel et al.*, 1996] indicate that currently DIC- $\Delta^{14}\text{C}$  values in the mixed water layer (0-75 m) along the British Columbian coast are between +25‰ and +75‰, while

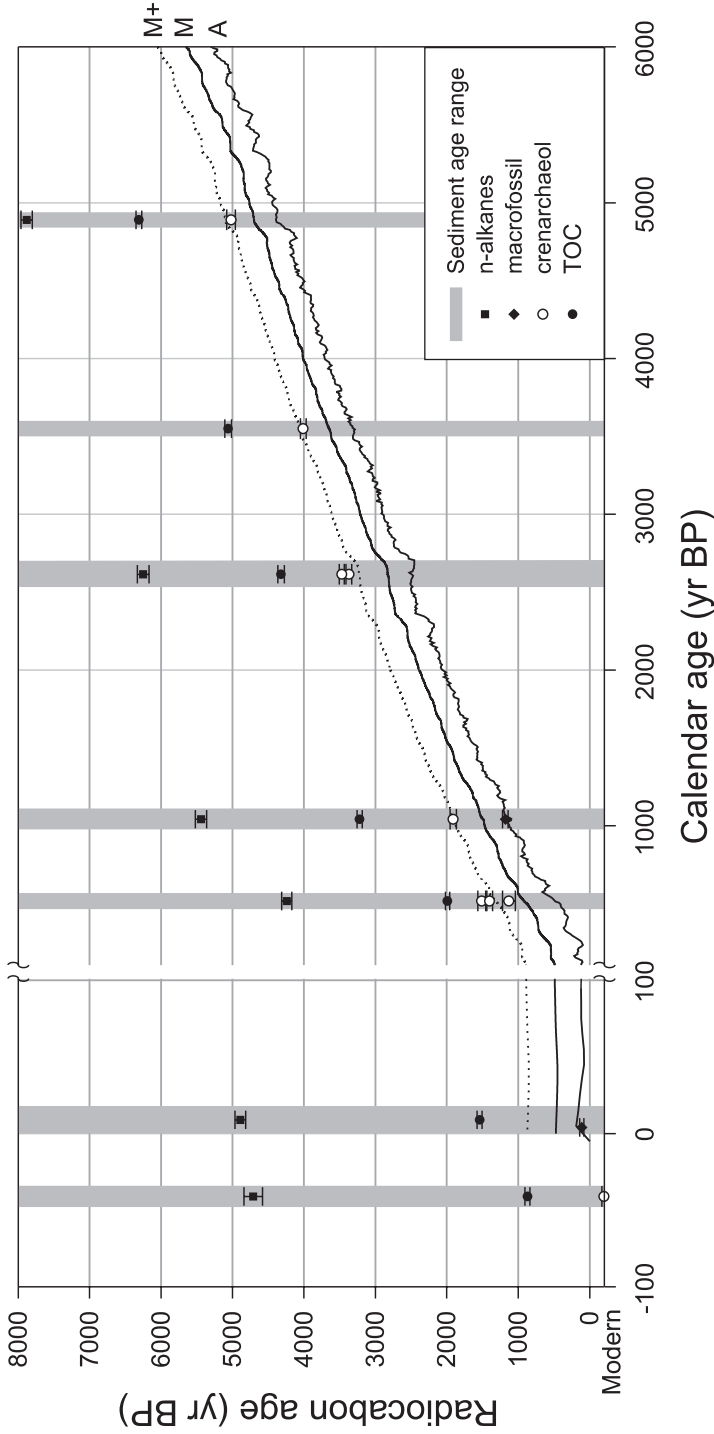


**Figure 3.3** Radiocarbon ages of TOC, *n*-alkanes, macrofossils and crenarchaeol against sediment calendar ages and the calibration curves of *Stuiver et al.* [1998a]. A: Atmospheric calibration curve. M: Marine calibration curve. M+: Marine calibration curve +401 yr ( $\Delta R$ ). Note the change of scale at 100 yr calBP. Because of clarity, the remaining biomarkers are not plotted.

pre-bomb values must have been  $-90 \pm 10$  ‰, according to reservoir ages reported previously for the northeastern Pacific [Southon *et al.*, 1990]. The post-bomb  $\Delta^{14}\text{C}$  values of  $+54$ ‰ and  $+40$ ‰ for crenarchaeol and GDGT-0 respectively, and the pre-bomb GDGT-0 value of  $-89$ ‰ (Table 3.3) are in good agreement with these observations. This strongly suggests that marine planktonic Crenarchaeota make use of DIC that enters the lower parts of the fjord via yearly bottom water renewals. The post-bomb  $\Delta^{14}\text{C}$  values of the phytoplankton-derived biomarkers ( $\Delta^5$ -sterols, 4-methyl sterols and phytol) also supports this conclusion. However, they show relatively lower post-bomb  $^{14}\text{C}$  contents and also show a high variance compared with each other (Fig. 3.3). This points towards different carbon sources for phytoplankton and the marine archaea. Because the  $^{14}\text{C}$  contents of the archaeal biomarkers are most comparable with anticipated DIC- $\Delta^{14}\text{C}$  values, we infer that the radiocarbon content of DIC in the photic zone of Saanich Inlet and the Sattelite Channel, are distinct from, and more variable, than the  $^{14}\text{C}$  concentrations in open ocean waters. In fact, even in the more open ocean setting off the coast of California the  $^{14}\text{C}$  ages of different isolated sterols varied more than desirable [Pearson *et al.*, 2000], although these authors contributed this to relatively poor AMS precision obtained for these samples. The observed variation is furthermore in good agreement with Heier-Nielsen *et al.* [1995], who found that  $^{14}\text{C}$  concentrations in fjord surface waters in Denmark were highly variable due to varying concentrations of dissolved old soil carbonate entrained with fresh water inputs. This so-called 'hard water effect' is regularly observed in fresh water [Goodfriend, 1997; Siani *et al.*, 2000] and may also play a role in the surface water in the Saanich Inlet area. Although there is, to the best of our knowledge, no information available on the  $^{14}\text{C}$  contents of the Cowichan an Fraser river, the main contributors of fresh water to the Saanich Inlet, it is known that two limestone quarries were active near the shores of Saanich Inlet throughout most of the 20<sup>th</sup> century [Kharé *et al.*, 2001], as well as in the Georgia Strait [Stiles, 1995], which may have increased any possible natural hard water effects considerably. Furthermore, the  $^{14}\text{C}$  concentration in coastal surface waters may also vary due to seasonal upwelling events, varying ocean-atmospheric exchange through the year [Goodfriend, 1997] or varying fresh water inputs [Ingram and Southon, 1996]. In Saanich Inlet,

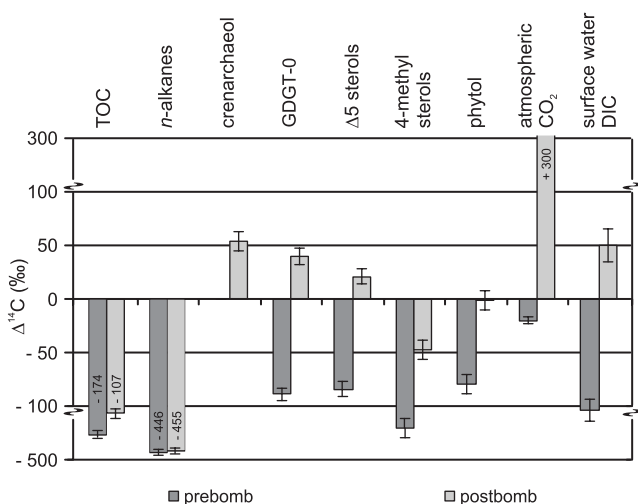


**Figure 3.4** Pre- and post-bomb  $\Delta^{14}\text{C}$  values of TOC and the various biomarkers, together with those of atmospheric  $\text{CO}_2$  and NE Pacific ocean surface water.

surface water characteristics like salinity and nutrient concentrations are indeed considerably influenced by these effects [Takahashi *et al.*, 1977]. It can be assumed that this is also the case for the  $^{14}\text{C}$  concentration, which is reflected in the variable  $^{14}\text{C}$  content of the phytoplankton biomarkers.

As concluded above, the  $\Delta^{14}\text{C}$  values of the archaeal biomarkers indicate a more open ocean mixed-layer DIC source. It is therefore most likely that the bulk of the archaeal lipids is produced at deeper water layers below the chemocline in the Saanich Inlet, where the water properties are primarily influenced by the yearly water renewals. Such a conclusion is in agreement with crenarchaeol maxima observed below the chemocline in e.g. the Black Sea (unpublished data) and with the observation of Pearson *et al.* [2001] that archaeal lipids present in post-bomb sediments of the Santa Barbara basin were produced with old DIC present in the subsurface California current. The renewal water is thought to be derived from intermediate water masses formed in the region of the San Juan Islands by the mixing of warm, low salinity water from the Strait of Georgia with cold, saline water that has upwelled off the coast and moved into the Strait of Juan de Fuca [Anderson and Devol, 1973]. Thus, the  $^{14}\text{C}$  concentration of DIC present below the dynamic surface water layer, possibly already below 10 m during the extended periods of stratification, will be influenced to a much lesser extent by fresh water inputs and by ocean-atmosphere exchange than the upper surface water. Consequently the  $^{14}\text{C}$  contents of the biomarkers produced using this deeper water DIC are much closer to that of the open ocean's mixed layer, and thus also less variable.

#### *Archaeal lipid radiocarbon contents - a reservoir age evaluation*

The marine calibrated ages of crenarchaeol are very comparable with the sediment ages (Table 3.4). However, although the  $1\sigma$  uncertainty of calibrated ages overlap in all cases with the age range of the sediments, the agreement is sometimes marginal. A perfect match of the average calibrated age with the mean sediment age is only obtained for the sample of 1111-977 calBP (Table 3.4), and for the comparison between the post-bomb crenarchaeol with post-bomb ocean surface water, as described above. The remaining samples exhibit on average an offset of  $>100$  yr. Errors in the  $^{14}\text{C}$  analysis can not be excluded, but this is already accounted for in the calibration uncertainty. It is therefore more likely that the offsets these ages from the varve ages are the result of inconsistencies in the calibration procedure, or more specifically, of varying reservoir ages through time.

The marine calibration curve of Stuiver *et al.* [1998a] is based upon the atmospheric calibration curve and a simple box model that incorporates ocean circulation, air-sea exchange and atmosphere / terrestrial biosphere  $\text{CO}_2$  fluxes. It is corrected for a reservoir age,  $R_g(t)$ , of the global ocean relative to the atmosphere.  $R_g(t)$  is determined at 400  $^{14}\text{C}$  yr in pre-industrial times (1850 AD), but varies over time because of the relative inertia of the ocean water  $^{14}\text{C}$  content compared to fluctuations in the atmospheric  $^{14}\text{C}$  production caused



**Table 3.5** Reservoir ages in  $^{14}\text{C}$  yr BP and reservoir age offsets  $\Delta\text{R}$  as calculated with the values given in table 2. The reservoir age is the biomarker age minus the atmospheric age and  $\Delta\text{R}$  is the biomarker age minus the global ocean model age [Stuiver and Braziunas, 1993]. Phytol = Chlorophyll derived phytol. \* Measured on corresponding biphytanes.

Sediment age	Cren-archaeol	GDGT-0	$\Delta 5$ Sterols	4-methyl Sterols	Phytol
<b>Reservoir age</b>					
1932–1950 AD		590	540	860	490
568– 465 BP	920	1060	1420	750	970
1111– 977 BP	760	1980	1560	950	880
1273–1125 BP		850 *			
2707–2533 BP	940	870	900	440	880
3600–3500 BP	690		-70	-120	300
4940–4840 BP	660	450		-870	-530
Average $\pm$ stdev	794 $\pm$ 130				
<b><math>\Delta\text{R}</math></b>					
1932–1950 AD		290	240	560	190
568– 465 BP	490	630	990	320	540
1111– 977 BP	410	1630	1210	600	530
1273–1125 BP		480 *			
2707–2533 BP	590	520	550	90	530
3600–3500 BP	360		-400	-450	-30
4940–4840 BP	330	120		-1200	-860
Average $\pm$ stdev	436 $\pm$ 105				

by heliomagnetic variations. Furthermore, the reservoir age varies geographically [Stuiver and Braziunas, 1993]. A reservoir age at a certain site can be expressed as  $R(t,s)$ , with  $s$ =space, and  $t$ =time, or as  $\Delta\text{R}(s)$  when compared to the marine calibration curve that includes  $R_g(t)$ . Implied in this definition is the notion that the time-dependent changes of a local environment parallel those of the global ocean, thus yielding a time independent  $\Delta\text{R}(s)$ . For northeastern Pacific coastal waters, the reservoir age has been determined at  $788 \pm 33$   $^{14}\text{C}$  year [Southon et al., 1990], mainly based upon shell and wood pairs recovered from approximately the same depth. On a local scale, Bornhold et al. [1998] determined a reservoir age of  $798 \pm 50$   $^{14}\text{C}$  yr for the Saanich Inlet, based upon a wood / shell pair from approximately the same depth, similar to an earlier determined reservoir age of  $801 \pm 23$  yr [Robinson and Thomson, 1981], which may also be read as a  $\Delta\text{R}$  of 401 yr. This local value has been used for the calibration of the various marine biomarkers (Table 3.4). The subtraction of the atmospheric radiocarbon ages from the measured biomarker radiocarbon ages results in the reservoir ages of the different samples (Table 3.5) while the local offset  $\Delta\text{R}(\text{Saanich})$  from the marine calibration curve is determined in the same way by taking the marine calibration curve as a reference (Table 3.5). The reservoir ages show a spread of  $\pm 130$  yr, while the  $\Delta\text{R}$  values exhibit a standard deviation of 105 yr. This indicates that indeed part of the variation in reservoir age results from the variation in the atmospheric

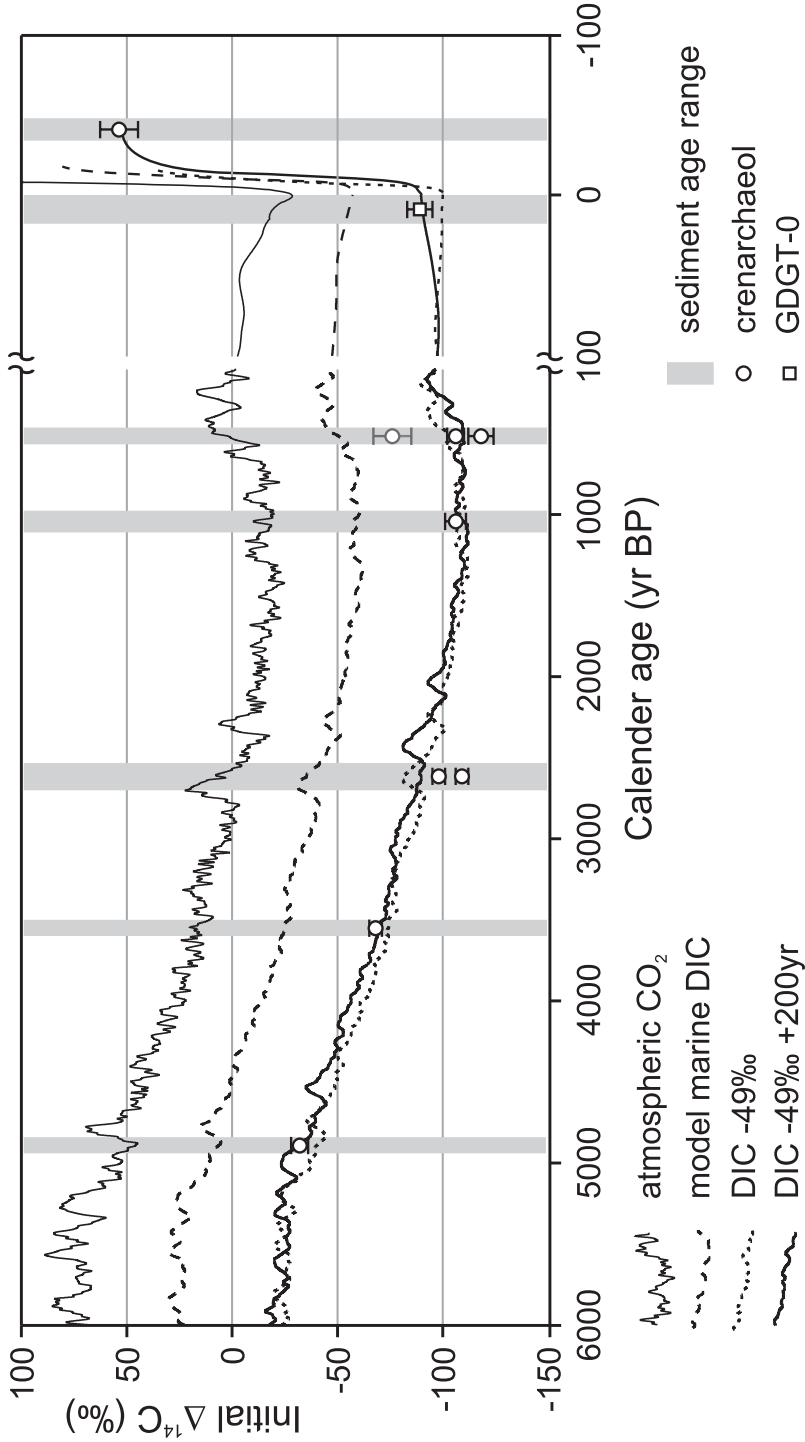


**Figure 3.5** Initial  $\Delta^{14}\text{C}$  values of crenarchaeol, together with various calibration curves. Because the pre-bomb sediment crenarchaeol measurement was corrupted, the GDGT-0 radiocarbon content is plotted as a substitute. The inaccurate (small sized) replicate at ~500 BP is plotted in gray. The atmospheric  $\text{CO}_2$  (upper, continuous) and global marine DIC (upper, dashed) curves are taken from *Suiver et al.* [1998a]. The difference between these two corresponds to the global marine reservoir age  $R_g(t)$ . The DIC -49‰ curve (dotted) displays this curve adjusted for a local reservoir age offset  $\Delta R$  of 401 yr, according to general calibration practice. A perfect calibration is obtained when a crenarchaeol  $\Delta^{14}\text{C}$  value is plotted right on top of this curve. This is not the case for most data, but when the reservoir age-corrected calibration curve is shifted with +200 yr (lower continuous), an almost perfect match is obtained.

radiocarbon concentration through time compared with a relatively inert ocean. This is also apparent when the initial radiocarbon contents of crenarchaeol are contrasted with the sediment ages in the context of both calibration curves (Fig. 3.3). This allows an evaluation of the radiocarbon age of the biomarker in comparison with both calibration curves through time.

The  $\Delta R$  spread of  $>100$  yr may be a naturally occurring effect, and the assumption that the temporal variation of the reservoir effect modeled for the global ocean is practically the same for all regions, may not entirely be true, especially for coastal sites where upwelling or significant fresh water inputs occurs [Stuiver and Braziunas, 1993]. Natural variations in the DIC- $^{14}\text{C}$  concentration on a regional to local scale, like variations in air-sea  $\text{CO}_2$  exchange or upwelling strength can also play an important role. For instance, the (mixed layer) DIC radiocarbon ages of the North Atlantic, the Mediterranean and the Black Sea decreased by some 150 yr between 1900 and 1930 AD. This change was due to a temporary increase of air-sea  $\text{CO}_2$  exchange resulting from a high North Atlantic Oscillation index and related average wind strengths [Siani *et al.*, 2000]. Observations on mollusk shells found in sediments along the British Columbia coast also suggests that coastal surface water DIC- $^{14}\text{C}$  contents can be variable [Southon *et al.*, 1990]. These authors suggest that variations in upwelling or ocean current strength may have played a role, thus affecting the relative contribution of upwelled old oceanic bottom water to the surface. Furthermore the extent and frequency of water renewals, possibly linked with climatic variations, could also be important in the case of Saanich Inlet.

Another factor that may play a role is a delay of the marine calibration curve at sites with high reservoir ages, like the NE Pacific coastal waters. Together with the dissimination of atmospheric  $^{14}\text{C}$  into the oceanic DIC pool, atmospheric  $^{14}\text{C}$  variations are also entrained. At upwelling sites, these 'stored' variations will come to the surface only after considerable time, and will have its influence on the local temporal variation in the reservoir age. Stuiver and Braziunas [1993] included the effect of 'storage' of  $^{14}\text{C}$  variations ocean water only to a minor extent in their model, and they argue that the major part of short-term variations in the marine calibration curve is atmospheric driven. At upwelling sites this effect may however play a more prominent role than is provided in the the model due to the relatively large influence of deep-water DIC to surface water  $^{14}\text{C}$  concentrations. Instead of simply adding a certain reservoir age offset,  $\Delta R$ , to the global reservoir age,  $R_g(t)$ , it may be appropriate to include a temporal shift of the marine calibration curve. Indeed, a shift of 200 yr of the marine calibration curve towards the future results in an almost perfect match for all the crenarchaeol initial  $\Delta^{14}\text{C}$  values (Fig. 3.5). This suggests that that variations in the marine radiocarbon pool may play a more important role on reservoir age variations then the calibration model allows, at least for upwelling areas with high reservoir ages. Obviously, the data provided here are only indicative, and evaluation of larger dataset and thorough modelling needs to be performed before any conclusions can be drawn.

GDGT-0 yields approximately the same results as crenarchaeol, except for one outlier at 1111 – 977 BP, which is considerably older. Possibly some of this GDGT-0 was produced

by methanotrophic or methanogenic archaea assimilating respectively methane or simple organic molecules derived from sedimentary organic matter [Schouten *et al.*, 2000b]. This interpretation is supported by the coincidence with the TOC  $^{14}\text{C}$  age for this interval (Table 3.3). However, the  $\delta^{13}\text{C}$  value of this sample does not differ from the general archaeal value of 21‰ (Table 3.2), and why such a methane-related signal would be absent in the other samples is also not clear. Furthermore, the age of the GDGT-0 derived biphytane fraction of the sediment of 1273 – 1125 BP, directly below, shows an excellent match with the sediment age (Table 3.4). This also suggests that biphytanes derived from GDGTs can be used as an alternative for intact GDGTs, although analysis of the latter is more laborious. Thus, while radiocarbon analysis of GDGT-0 may yield the same results as that of crenarchaeol, its less well constrained origin renders the use of GDGT-0 less reliable.

#### *Phytoplankton biomarker radiocarbon contents - surface water variability*

The calibrated ages and the  $\Delta^{14}\text{C}$  values of phytol,  $\Delta^5$  sterols and 4-methyl sterols isolated from the ODP sediments show considerable variation, both between the different biomarkers isolated from the same sediment layer, as well as in terms of the age difference with the sediments through time (Tables 3.3 and 3.4). As discussed above, relatively young phytoplankton biomarkers ages compared to the archaeal biomarker ages are likely the result of algal growth in well-mixed, stratified surface water with a high contribution of atmospheric  $^{14}\text{C}$ , while old ages may be caused by hard-water effects introduced by run-off and fluvial inputs. Phytol is in general 100 - 150 yr older than the sediment ages for the upper three intervals of the ODP-core (568-465 BP; 1111-977 BP and 2707-2533 BP), and thus quite comparable with crenarchaeol. In contrast, 4-methyl sterols and  $\Delta^5$  sterols show a larger spread of -400 to +900 yr. The phytoplankton biomarkers from the two lowermost sediment intervals (3500-3600 and 4840-4949 BP) show, however, relatively high  $^{14}\text{C}$  contents, especially the phytoplankton biomarkers of the oldest sediment, which appear to be *younger* than the sediments even before a reservoir age correction. This suggests that they have either been synthesized from substantially  $^{14}\text{C}$  enriched carbon, that they are indeed younger than the sediment and mixed downward by some mechanism, or that the samples have been contaminated with modern carbon. Because the sediments show no sign of redistribution (e.g. bioturbation), the second explanation does not seem plausible. Similarly, contamination of all phytoplankton biomarkers with approximately the same amounts of modern carbon also seems unlikely for several reasons: first, carbon abundances based on the  $\text{CO}_2$  yields after combustion of these samples were not larger than estimated abundances determined by gas chromatography, indicating the absence of additional carbon. Second, the phytoplankton biomarkers isolated from the younger sediment intervals do, in contrast, not show unexpected young ages, nor do the archaeal biomarkers, while all samples were isolated and prepared for AMS in exactly the same way. Third, systematic large errors in the  $^{14}\text{C}$  determination of several biomarkers from one sediment layer are also

unlikely, because the biomarkers have not all been analyzed in the same batch. More specifically, the phytol fractions were isolated using a different procedure from the sterols and were analyzed more than 8 months later. We conclude, therefore, that another mechanism(s) must be responsible for the unexpectedly high  $^{14}\text{C}$  concentrations. As discussed above, lesser reservoir ages may stem from higher contributions of atmospheric  $^{14}\text{C}$  in photic zone resulting from a well-mixed stratified surface water layer. Alternatively, errors associated with varve counting for deeper sediment layers may give rise to artificially old ages. This would imply that difference in age between the archaeal biomarker ages and the sediments are even greater than is now estimated, suggesting that reservoir ages were larger at that time. Coincidentally, *Southon et al.* [1990], observed significantly higher reservoir ages around 6000  $^{14}\text{C}$  yr BP. However, the uncertainties in the varve-based sediment age determination allow at most a 200 year shift towards a younger age (i.e. ~4700 BP [*Nederbragt and Thurow*, 2001; *Nederbragt, pers comm.*]). Furthermore, the factors 'sediment age' and 'atmospheric radiocarbon' can not by far account for the observed offset of the phytoplankton biomarkers. The oldest sediment age would need to be around 4000 BP for the initial  $\Delta^{14}\text{C}$  value of 4-methyl sterol to be equal to the atmospheric  $\Delta^{14}\text{C}$  value. To a lesser extent the same is true for phytol. A final but highly speculative hypothesis is that the enigmatic low values may be caused by a flaw in the calibration curve, exhibiting larger 'spikes' of elevated atmospheric  $^{14}\text{C}$  concentrations than is currently thought. However, it seems far more likely that the radiocarbon contents of the oldest phytoplankton biomarkers are 'off' due to some unexplained error. Would future measurements also result in the same young algal biomarkers at the given time-frame, then it would be worthwhile to investigate a scenario which combines a sediment age that is estimated to old with algal growth under conditions with highly elevated  $^{14}\text{C}$  concentrations. Such a scenario would imply that the Saanich Inlet surface water used to be more influenced by stratification and atmospheric-ocean mixing than is nowadays the case, and furthermore that the atmospheric and marine radiocarbon contents experienced substantially larger variations in the past than is currently acknowledged.

### 3.6. Conclusions

Calibrated ages obtained from compound-specific radiocarbon analysis of the marine pelagic archaeal biomarker crenarchaeol, extracted from sediments of Saanich Inlet, Canada, compare favourably with independently determined ages from varve-counting. The same applies for the more generic archaeal biomarker GDGT-0, although the less specific origin of this biomarker renders it slightly less reliable. An average reservoir age offset from the marine calibration curve,  $\Delta R$ , of  $430 \pm 110$  yr is consistent with previous measurements, thus demonstrating for the first time that compound-specific radiocarbon dating can be successfully applied. The results are in good agreement with earlier conclusions in the literature that marine crenarchaeota use DIC as their carbon source.

Although the calibrated crenarchaeol ages match closely with the sediment ages, the reservoir age varies by more than 100 yr. This can either be attributed to a variability of the local or regional reservoir age resulting from natural processes like a variation in upwelling through time, or to inconsistencies in the marine calibration curve for sites such as the Saanich Inlet that exhibit high reservoir ages. Both explanations imply that ideally both spatial and temporal variations in reservoir age should be assessed when radiocarbon dating is performed with marine derived samples.

In contrast to crenarchaeol, the radiocarbon ages of phytoplankton derived biomarkers  $\Delta^5$  sterols, 4-methyl sterols and chlorophyll-derived phytol, were quite variable. This is likely related in part to highly variable  $^{14}\text{C}$  contents in the surface waters of the fjord, resulting from temporal variations in stratification, ocean-atmosphere  $\text{CO}_2$  exchange and fresh water input with associated hard-water effects. The radiocarbon contents of the phytoplankton biomarkers of the oldest sediment exhibited anomalously high values (i.e. young ages). Determining the reason for these discrepancies would require further measurements and error assessment.

While the marine pelagic Crenarchaeota have been shown to be present throughout the water column, it is likely that they are concentrated in the waters immediately below the photic zone, where higher nutrient levels prevail. Correspondingly, they are less sensitive to the variations in surface water  $\text{DIC-}^{14}\text{C}$  that apparently influenced the phytoplankton biomarkers, which resulted in more consistent reservoir ages. However, this also implies that in open ocean settings crenarchaeol may reflect a mixture of surface water and sub-surface water  $\text{DIC-}^{14}\text{C}$  contents. Crenarchaeol is abundant in marine sediments worldwide [Karner *et al.*, 2001], implying that smaller amounts of sediment are needed for radiocarbon dating. For example, while the used subsamples from Saanich Inlet corresponded to ages spanning 100-150 yr, the recovered amounts of crenarchaeol would have allowed a resolution of 10-20 yr. Thus, crenarchaeol may be an ideal biomarker for compound-specific radiocarbon dating of marine sediments. A continuous profile of radiocarbon contents of crenarchaeol, combined with the varve-based age model, would allow for a site-specific marine calibration curve to be obtained.

## Acknowledgements

The Ocean Drilling Project is thanked for providing subsamples of core 1034C obtained at leg 169S. Michael Whitarcar and Melissa McQuoid of SEOS, Victoria University, BC, Canada are thanked for providing the freeze core taken at Saanich Inlet. The staff at the National Ocean Sciences Accelerator Mass Spectrometry Facility is thanked for their help during the preparation procedure for  $^{14}\text{C}$  analysis, and for the final measurements. Ann Pearson, Sandra Nederbragt and Ann McNichol are thanked for useful discussions. Marianne Baas and Michiel Kienhuis are thanked for overall assistance.

## Chapter 4

### Radiocarbon ages of terrestrial n-alkanes from Holocene sediments of a Canadian fjord reveal an increasing 'soil reservoir effect'

*Rienk H. Smittenberg, Stefan Schouten, Timothy I. Eglinton  
and Jaap S. Sinninghe Damsté*

For submission to 'Nature' with additional data

**Abstract** Radiocarbon dating of odd carbon numbered C<sub>27</sub>-C<sub>31</sub> *n*-alkanes present in late Holocene sediments of Saanich Inlet, Canada, predominantly of a vascular plant origin, revealed substantial, but moreover linearly increasing age differences with the varve-dated sediments they were extracted from. This is attributed to an increasing 'soil reservoir effect', caused by the build up and aging of the (refractory) soil organic carbon pool since deglaciation of the area, including *n*-alkanes. The inferred increasing 'soil reservoir effect' is supported by an increasing *n*-alkane flux to the fjord sediment with time. After correction of the *n*-alkane ages for a contribution of 10-20% fossil *n*-alkanes, estimated from the distribution and  $\delta^{13}\text{C}$  values of C<sub>25</sub>-C<sub>33</sub> *n*-alkanes, extrapolation of the observed correlation resulted in an almost exact 'prediction' of deglaciation at 12000 BP and consequent formation of soils in the drainage area. The linearity of the correlation curve indicates that the accumulation of *n*-alkanes is not counterbalanced by degradation and only to a minor degree by erosion. It is concluded that the terrigenous organic carbon pool in the Saanich Inlet region is still increasing as a long-term response to the Pleistocene-Holocene climatic transition, a process that may hold for other temperate regions on earth.

#### 4.1. Introduction

The terrigenous organic carbon pool is the largest active organic carbon pool on the globe [Hedges and Keil, 1995] and consequently the fluxes of organic matter to and from this pool (i.e. production, erosion and degradation) are important for the carbon budgets in the bio- and geosphere [e.g. Killops and Killops, 1993]. The rates of primary production of organic matter, erosion from the continent and degradation are intricately related with climatic parameters such as temperature and precipitation via various feedback mechanisms including the greenhouse effect [e.g. Bertram, 1991; Gleixner *et al.*, 2002]. The drastic climatic change at the Pleistocene - Holocene transition had a large impact on the terrigenous organic carbon pool [Indermuhle *et al.*, 1999]. The increased temperatures caused higher degradation rates of prevalent organic matter, while at the same time areas

that were bare or covered by glaciers during the Pleistocene became vegetated and the terrigenous organic carbon pool expanded towards higher latitudes. Furthermore, well-established ice-core data indicate that the atmospheric CO<sub>2</sub> concentration first decreased until *ca.* 8000 BP with a subsequent increase until the present day [Indermuhle *et al.*, 1999]. These variations in the CO<sub>2</sub> content may be attributed to an initial uptake of terrestrial carbon and a gradual release after 8000 BP. However, the increase of atmospheric CO<sub>2</sub> may also be explained by accounting for a carbonate compensation mechanism in the ocean [Broecker *et al.*, 1993], implying that the terrigenous carbon pool remained relatively constant or increased in the late Holocene [Kaplan *et al.*, 2002]. This demonstrates that it remains difficult to well assess the various causes and effects within the dynamics of the global carbon cycle [Schindler, 2000]. Refractory organic matter makes up most of the terrigenous carbon pool due to its resilience to degradation. The low degradation rates suggest that an approximate steady state between degradation, erosion and accumulation of that refractory organic matter may, in contrast to more labile organic matter, not yet be reached after thousands of years. The assessment whether this is indeed the case requires examination of well-dated, long-term records of the terrigenous organic matter, whereby the ages and relative abundances of its components can be determined. A fully comprehensive study of all material that makes up the organic matter pool is practically impossible. However, analysis of a broad range of selected refractory components may already give sufficient information.

Saanich Inlet, Canada (Fig. 3.1), contains an exquisite sedimentary record spanning the late Holocene. It exhibits high sediment accumulation rates, which is for a large part caused by transport of mineral material from the surrounding continent into the fjord [Gucluer and Gross, 1964]. Due to permanent anoxic bottom water conditions the sedimentary organic matter, including terrigenous material [Cowie *et al.*, 1992], has been well preserved, as well as the sediment structure [Bornhold *et al.*, 1998], which allowed annual dating of the core back to 6000 BP by means of varve counting [Nederbragt and Thurow, 2001]. Here we report calibrated radiocarbon ages of sedimentary long-chain *n*-alkanes, a component of refractory soil organic carbon, and compare them with the varve ages of the sediments. The obtained results provide insight in the development of the refractory terrigenous organic carbon pool over the late Holocene period in the surrounding continent of the fjord, which may be indicative for other temperate regions.

## 4.2. Methods

### 4.2.1. Study site and sampling

The sediments used for this study were obtained from an advanced piston core (APC) taken during ODP leg 169S [Bornhold *et al.*, 1998] (Fig. 3.1). The samples range in age between 500 and 5000 yr BP (Table 4.1), as determined by varve counting [Nederbragt and Thurow,



2001]. Two sub-surface sediment samples were taken from a freeze core taken in 1998 from approximately the same location, representing material that was sedimented either before or after above-ground nuclear weapons-testing in the 1960's. A more detailed account on the setting and the origin of the sub-samples is provided in Chapter 3.

#### *4.2.2. Isolation of n-alkanes*

Solvent extracts were obtained from freeze-dried sediments as described in Chapter 3. Straight-chain hydrocarbon fractions were obtained from the solvent extracts by column chromatography ( $\text{Al}_2\text{O}_3$ ; *n*-hexane), and subsequent urea adduction. From these, fractions containing only the  $\text{C}_{27}$ ,  $\text{C}_{29}$  and  $\text{C}_{31}$  *n*-alkanes were subsequently isolated by preparative capillary gas chromatography (PCGC), in a similar way as described by *Eglinton et al.* [1996].

#### *4.2.3. Gas chromatography and quantification*

Gas chromatography was performed using a Fisons 8000 series instrument equipped with an on-column injector and a flame ionisation detector (FID). A fused silica capillary column (25 m x 0.32 mm) coated with CP Sil 5 (film thickness 0.12  $\mu\text{m}$ ) was used with helium as carrier gas. The samples were dissolved in hexane and injected at 70°C. The oven was programmed to 130°C at 20°C/min and then at 4°C/min to 320°C at which it was held for 25 min. Quantification of *n*-alkanes was performed by gas chromatography by comparing peak areas with that of an added internal standard (deuterated *ante-iso*  $\text{C}_{22}$ -alkane).

#### *4.2.4. Isotope-ratio-monitoring Gas chromatography - Mass spectrometry*

Compound-specific stable carbon isotopic compositions were determined on a ThermoFinnigan DELTA-C irm-GC/MS-system. The gas chromatograph was set up and programmed as described above. Reported stable carbon isotopic compositions values were determined by three replicate analyses, and the results were averaged to obtain a mean value and to evaluate the measurement error. The values are reported in standard delta notation relative to the VPDB standard.

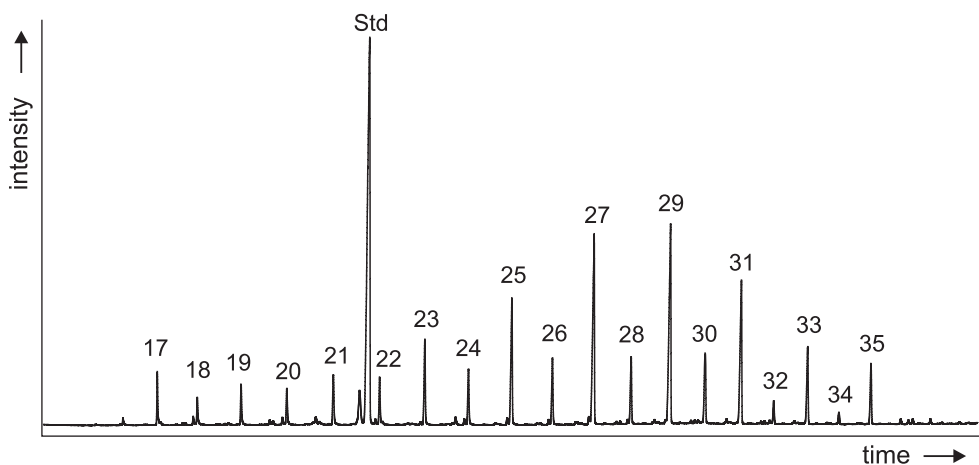


**Figure 4.1** Gas chromatogram of the straight-chain hydrocarbon fraction obtained from the sediment of 568-465 BP, representative for all straight-chain hydrocarbon fractions. The numbers refer to the number of carbon atoms in the homologues. Std = internal standard.

#### 4.2.5. Radiocarbon dating

Radiocarbon content and corresponding radiocarbon age of the various odd  $C_{27}$ - $C_{31}$  *n*-alkanes were determined at the National Ocean Sciences Accelerator Mass Spectrometry Facility at WHOI, MA, as described in Chapter 3. Calibration of radiocarbon ages to calendar ages was performed using the calibration curves of *Stuiver et al.* [1998a].

### 4.3. Results

In all analyzed sediments the *n*-alkanes exhibit a unimodal distribution maximizing at  $C_{29}$  (e.g. Fig. 4.1) and a strong odd-over-even carbon number predominance for the long-chain  $C_{25}$ - $C_{35}$  *n*-alkanes. The carbon preference indices (CPI) for the  $C_{25}$ - $C_{33}$  *n*-alkanes are in the range 4 to 5, except for the post-bomb (1984-1998 AD) sediment, which has a CPI of 2.7 (Table 4.1). In that sediment, a series of  $C_{36}$  -  $C_{46}$  *n*-alkanes is also observed, albeit in relatively low concentration. The stable carbon isotopic compositions of the *n*-alkanes range between  $-28\text{‰}$  and  $-32\text{‰}$  (Fig. 4.2). The odd *n*-alkanes exhibit in general somewhat lower values than their even-numbered counterparts, except for the  $C_{35}$  *n*-alkanes that show a  $\delta^{13}\text{C}$  value of approximately  $-29\text{‰}$ . The combined concentrations of odd  $C_{27}$ - $C_{31}$  *n*-alkanes in the seven examined sediment layers increase upcore from 0.8 to 4.4  $\mu\text{g/g}$  dry sediment (Table 4.1).

The  $\Delta^{14}\text{C}$  values of the seven examined sediment layers decrease, as expected, with increasing varve ages (Table 4.1). The  $\Delta^{14}\text{C}$  values of the odd  $C_{27}$ - $C_{31}$  *n*-alkanes in the post-

**Table 4.1** Radiocarbon content, calibrated age and concentration of sedimentary *n*-alkanes (C<sub>29</sub>, C<sub>31</sub> and C<sub>33</sub>). The Carbon Preference Indices of the C<sub>25</sub>-C<sub>33</sub> *n*-alkanes are also given. <sup>I</sup> The calibrated age ranges are 1σ confidence intervals, the age between brackets has the highest probability. <sup>II</sup> Carbon Preference Index =  $0.5 \times \frac{\{(C_{25}+C_{27}+C_{29}+C_{31})+(C_{27}+C_{29}+C_{31}+C_{33})\}}{\{(C_{26}+C_{28}+C_{30}+C_{32})\}}$

Sediment age (varve-based)	<i>n</i> -alkanes Δ <sup>14</sup> C (±8 ‰)	calibrated age (yr BP) <sup>I</sup>	Concentration (μg/g dry sed.)	CPI <sup>II</sup>
1984 – 1998 AD	-458	5473 (5599) 5730	4.4	2.70
1932 – 1950 AD	-464	5606 (5657) 5844	3.1	4.05
568 – 465 BP	-417	4828 (4854) 4893	2.8	4.25
1111 – 977 BP	-498	6234 (6290) 6354	2.1	4.94
2707 – 2533 BP	-546	7131 (7215) 7285	1.8	4.76
3600 – 3500 BP			1.8	4.13
4940 – 4840 BP	-626	8476 (8617) 8948	0.8	4.82

bomb sediments are identical to those of the pre-bomb sediment. Conversion of the Δ<sup>14</sup>C values to radiocarbon ages and subsequent calibration to calendar ages reveal that all *n*-alkanes ages are 4000 – 5500 yr older than the varve-ages of the sediments (Table 4.1).

#### 4.4. Discussion

##### 4.4.1. *n*-Alkane sources

Both the stable carbon isotopic compositions and the distribution (Figs. 4.1 and 4.2) of the *n*-alkanes suggest that they are predominantly derived from C3 vascular plant material [Eglinton and Hamilton, 1967; Cranwell, 1982; Rieley *et al.*, 1991b]. Bacterial and algal *n*-alkanes generally exhibit carbon-chain lengths <C<sub>24</sub>, maximizing at C<sub>17</sub> [Brassell *et al.*, 1978]. The relatively low abundance of these *n*-alkanes and the absence of a second maximum at C<sub>17</sub> points towards a minimal contribution of such a source. The CPI of 4-5 suggests that, like in many soils and sediments [e.g. Cranwell, 1982; Ternois *et al.*, 2001], the long-chain *n*-alkanes derived from living plants, exhibiting CPI values of 7-20 [Eglinton and Hamilton, 1967; Rieley *et al.*, 1991a], are diluted with *n*-alkanes of fossil origin with a low CPI value, e.g. from weathering organic-rich rocks. The CPI of 2.7 of the post-bomb sample is accompanied by a series of C<sub>36</sub> - C<sub>46</sub> *n*-alkanes (not shown), albeit in relatively low concentration. This suggests that this sediment received an additional contribution of fossil *n*-alkanes, in this case likely derived from petroleum spillage from ships.

The CPI can be used to deconvolute the various sources of *n*-alkanes, especially in conjunction with the δ<sup>13</sup>C values of the individual *n*-alkanes. For instance, Collister *et al.* [1994a] used an iterative mixing model that calculates the relative amounts and δ<sup>13</sup>C values of individual *n*-alkanes from each sediment layer by mixing various sources with different CPI's and δ<sup>13</sup>C contents. This model was applied to estimate the relative contributions of the fossil source and vascular plants to each of the C<sub>25</sub>-C<sub>35</sub> *n*-alkanes present in the Saanich Inlet sediments (Fig. 4.2). The fossil source is likely to have a CPI of 1 [Brassell *et al.*,

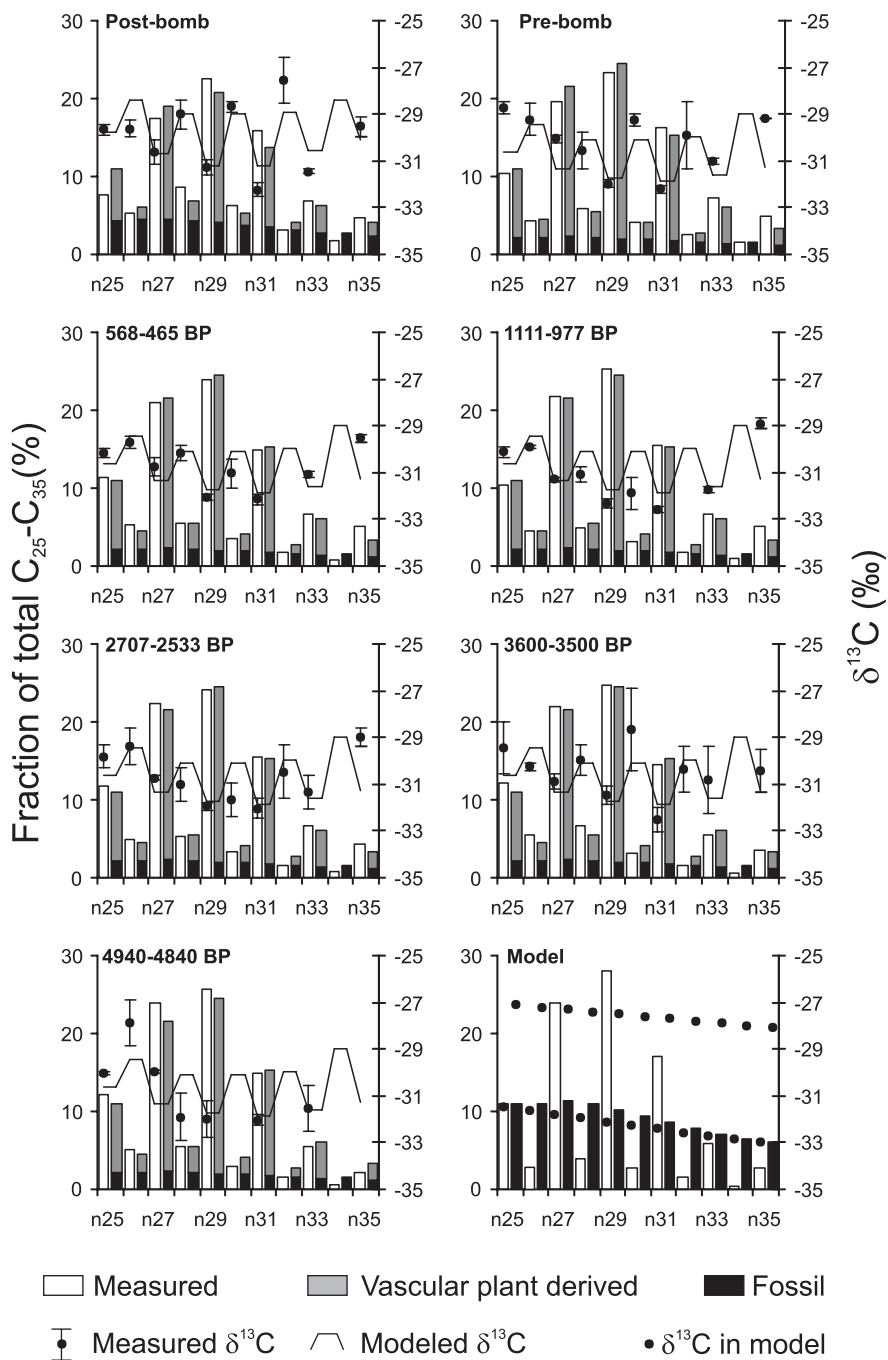


**Figure 4.2** Measured and modeled distribution of  $\text{C}_{25}\text{-C}_{35}$   $n$ -alkanes and their  $\delta^{13}\text{C}$  values. The numbers refer to the carbon chain length. The mixing model uses a fossil and a vascular plant source with the distributions and  $\delta^{13}\text{C}$  values shown in the lower right panel. The model results shown are the ones calculated with a 20% fossil fraction, except for the post-bomb sediment (upper left), for which a 40% fossil fraction was used.

1978; Collister *et al.*, 1994a] and  $\delta^{13}\text{C}$  values between  $-27\text{‰}$  and  $-28\text{‰}$  [Collister *et al.*, 1994a; Pearson and Eglinton, 2000 and references therein]. The vascular plant *n*-alkane source is assumed have a CPI ( $\text{C}_{25}\text{-C}_{33}$ ) of 7 and  $\delta^{13}\text{C}$  values that gradually decrease with increasingly carbon chain length from  $-31.5\text{‰}$  ( $\text{C}_{25}$ ) to  $-33.0\text{‰}$  ( $\text{C}_{35}$ ) [Rieley *et al.*, 1991b; Collister *et al.*, 1994b; Lockheart *et al.*, 1997]. The modeling results in an estimated fossil *n*-alkane fraction of *ca.* 20% for  $\Sigma(\text{C}_{25}\text{-C}_{35})$  for all sediments, except the post-bomb sediment that is estimated to contain approximately 40% fossil *n*-alkanes (Fig. 4.2). However, these estimates should be regarded with some caution: small adjustments in the assumed CPI - and  $\delta^{13}\text{C}$  values of the two sources results in fossil fraction estimates ranging from 10% to 30%. The abundant odd  $\text{C}_{27}\text{-C}_{31}$  *n*-alkanes contain a relatively low fossil contribution when compared to the other homologues due to their relatively high abundance in vascular plant material (Fig. 4.2). According to the above model, the fossil contribution to the  $\text{C}_{27}$ ,  $\text{C}_{29}$  and  $\text{C}_{31}$  *n*-alkanes is only half of that to the  $\Sigma(\text{C}_{25}\text{-C}_{35})$  *n*-alkanes, i.e.  $10\pm 5\%$  for all sediments but the post-bomb sediment. Thus, odd  $\text{C}_{27}\text{-C}_{31}$  *n*-alkanes were anticipated to most reliably represent the original *n*-alkanes of vascular plants and their carbon isotopic composition. Sedimentary *n*-alkanes with a higher plant fingerprint can derive from either aeolian transport of wax lipids of plants or from riverine transported higher plant *n*-alkanes. Since both sources exhibit a similar vascular plant signature, they can not clearly be distinguished from each other by their CPI's or  $\delta^{13}\text{C}$  values. However, aeolian *n*-alkanes derive for a substantial part directly from ablation off living vegetation [e.g. Simoneit *et al.*, 1977; Conte and Weber, 2002], and are thus expected to exhibit high  $^{14}\text{C}$  contents at the time after above-ground nuclear weapons testings, i.e. in post-bomb times. In contrast, riverine transported *n*-alkanes are expected to contain a much lower amount of bomb- $^{14}\text{C}$  in post-bomb times, because most riverine organic carbon is derived from eroded soils, which is expected to contain only a small fraction of very recent material. The relatively low and similar  $^{14}\text{C}$  contents of the odd  $\text{C}_{27}\text{-C}_{31}$  *n*-alkanes in both the pre- and the post-bomb sediments indicates that the long-chain *n*-alkanes in the Saanich Inlet are predominantly derived from fluvial transport of vascular plant material. Indeed, in the temperate rainforest climate of the British Columbian coast rivers are expected to be the major mode of transport of terrigenous organic matter to the marine environment. It is thus most likely that erosion of soils in the hinterland is the main source of the *n*-alkanes in the Saanich Inlet sediments.

#### 4.4.2. The 'soil reservoir effect'

The calibrated ages of the odd  $\text{C}_{27}\text{-C}_{31}$  *n*-alkanes are all substantially higher than the varve-ages of the sediments (Table 4.1). Because only a 10% fossil fraction is estimated for the odd  $\text{C}_{27}\text{-C}_{31}$  *n*-alkanes, it is anticipated that the main cause of these old ages is pre-aging of the *n*-alkanes on the continent before erosion and transportation to the sediment of the fjord. Similar to the 'marine reservoir effect', that reflects the residence time of DIC in the marine

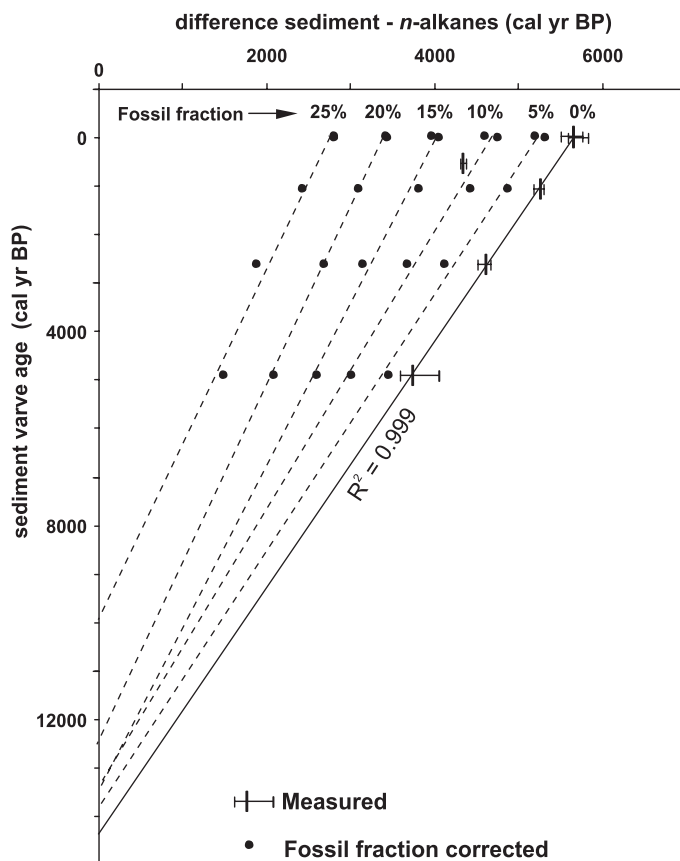


**Figure 4.3** Graph showing the age differences between the varve ages of the sediments and the calibrated ages of the odd  $C_{27}$ - $C_{31}$   $n$ -alkanes (line symbols with error bars). The intersect of the extrapolated regression line represents the age where the  $n$ -alkane age would have been the same as the varve age. The datapoint at  $\sim 500$  BP was not used for the regression line. The increasing age difference is attributed to a 'soil reservoir effect'. The plot furthermore shows age differences (black dots) of the 'Holocene'  $n$ -alkane ages with varve ages, and the accompanying regression lines (dashed), as calculated for various degrees of fossil contribution to the total odd  $C_{27}$ - $C_{31}$   $n$ -alkanes.

environment [Stuiver and Braziunas, 1993], this pre-aging can be referred to as a 'soil reservoir effect'. The somewhat younger  $n$ -alkane age in the sediment of  $\sim 500$  BP (Table 4.1) suggests that at that time period there may have been a relatively higher contribution of more contemporary produced vascular plant material instead of pre-aged material.

When the calibrated ages of the odd  $C_{27}$ - $C_{31}$   $n$ -alkanes are compared with the varve ages of the sediments, it becomes apparent that the difference between these two ages becomes increasingly larger towards recent times (Fig. 4.3). Such an increase with time was not observed for marine derived biomarkers in the same setting (see Chapter 3), indicating that a different terrestrial signal is recorded. Linear regression between the varve age and the difference between the calibrated  $n$ -alkane age and the varve age resulted in a regression

line with an  $R^2$  of 0.68. When the outlying data-point at ~500 BP is neglected, the  $R^2$  increases to 0.99 (Fig. 4.3). The intercept of the linear regression line with the varve age-axis corresponds to the time when the *n*-alkane age would have been equal to the varve age, i.e. exhibiting no 'soil reservoir effect' before entering the sediment. Calculated without the outlier, the intercept lies at  $14400 \pm 500$  BP (Fig. 4.3).

Two striking properties of the regression line can be noticed: First, the correlation is linear, and second, the calculated intercept age is comparable to the time of deglaciation of the area around 12000 BP. Because the areas that are tributary to the Saanich Inlet could only become vegetated after deglaciation [Huntley *et al.*, 2001], terrigenous (soil) organic matter, including vascular plant-derived *n*-alkanes, can not be older than 12000 BP. The intercept age also indicates that from that time onwards accumulation of *n*-alkanes occurred without substantial losses of *n*-alkanes through degradation or erosion, which is the only situation that could have lead to the observed age profile. An alternative situation, a steady state between the in- and output of *n*-alkanes, would have resulted in a constant age difference of the *n*-alkanes with the varve ages, and this is clearly not the case. The inferred low degradation rate is in good agreement with the generally attributed low degradation rate of long-chain *n*-alkanes [e.g. Cowie *et al.*, 1992]. More interestingly, the results also indicate that erosion of soils, directly connected to erosion of *n*-alkanes, does not seem to be very important in the hinterland of Saanich Inlet area. However, because of the low number of data points, that furthermore only cover the late Holocene, the results do not totally exclude that some erosion may occur. In fact, the absence of any erosion would be highly unlikely, and would actually have resulted in the absence of long-chain *n*-alkanes in the Saanich Inlet, which is clearly not the case.

In addition to the above discussed 'soil reservoir effect', the *n*-alkane  $^{14}\text{C}$  ages will also be influenced by the small ( $10 \pm 5\%$ ) contribution of fossil *n*-alkanes. Indeed, the intercept of the regression line with the varve-age-axis as calculated without the outlier lies at 14400 BP (Fig. 4.3), in contrast to the expected 12000 BP. The effect of various fossil fractions on the  $\Delta^{14}\text{C}$  contents is calculated by a simple binary mixing model using the measured  $\Delta^{14}\text{C}$  values and an assumed contribution of radiocarbon-dead fossil *n*-alkanes. Calibration of thus obtained 'Holocene *n*-alkane'  $^{14}\text{C}$  ages results in fossil-corrected *n*-alkane calendar ages, allowing again comparison with the varve ages (Fig. 4.3). Although the same fossil fraction causes the same  $^{14}\text{C}$ -age shift for all odd  $\text{C}_{27}\text{-C}_{31}$  *n*-alkanes, this shift varies for the calendar ages. This is due to the varying atmospheric  $^{14}\text{C}$  content through time [ $+44\%$  to  $+85\%$  in the considered time frame; Stuiver *et al.*, 1998b], which influences the calculated fossil-corrected *n*-alkane ages via the calibration step. The intercepts derived from correlation of the varve ages with the *n*-alkane ages corrected for a 10-15% fossil contribution are approximately 13500 BP (Fig. 4.3), while a 20% fossil contribution results in the anticipated 12000 BP. This is in good agreement with the estimated fossil fraction  $10 \pm 5\%$  made on the basis of the CPI and  $\delta^{13}\text{C}$  values of the long-chain *n*-alkanes. Thus, although a 10% – 20% fossil fraction is responsible for an extra offset of the *n*-alkanes ages

compared to the varve ages, the proposed 'soil reservoir effect' remains the ruling factor for their radiocarbon age.

The accumulation of refractory terrigenous organic matter in soils, including long-chain *n*-alkanes, should not only be reflected by their radiocarbon age but also by an increasing concentration in the soil, and ultimately by an increasing flux to the fjord sediment with time. By using the varve thickness data [Nederbragt and Thurow, 2001] in combination with wet bulk density and porosity data reported elsewhere [Gucluer and Gross, 1964; Bornhold *et al.*, 1998; Nederbragt and Thurow, 2001] sediment accumulation rates were estimated (Fig. 4.4).

Subsequently, the flux of the odd C<sub>27</sub>-C<sub>31</sub> *n*-alkanes to the sediment could be determined using the concentrations listed in Table 4.1. The total fluxes may be split into fossil and Holocene-aged *n*-alkane fluxes, based upon the fossil fractions of 10% (most sediments) and 25% (post-bomb sediment) as estimated earlier. The fluxes all show an increasing trend upcore, while this is not the case for the sediment accumulation rate (Fig. 4.4). This implies that the main cause for the increasing odd C<sub>27</sub>-C<sub>31</sub> *n*-alkane flux must be the increasing *n*-alkane concentration with time (Table 4.1), consistent with a build-up of a soil reservoir in the hinterland.

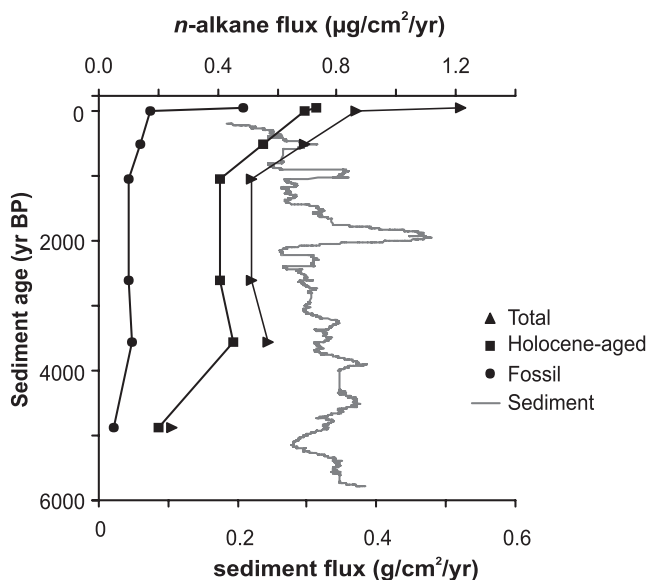


**Figure 4.4** Total, fossil and Holocene-aged (soil) *n*-alkane fluxes (upper axis) together with the sediment flux to the Saanich Inlet (lower axis), that was calculated from varve thickness data [Nederbragt and Thurow, 2001], wet bulk density data [Bornhold *et al.*, 1998] and porosity data and modeling [Gucluer and Gross, 1964; Nederbragt and Thurow, 2001].

#### 4.5. Conclusions

Odd C<sub>27</sub>-C<sub>31</sub> *n*-alkanes present in late Holocene sediments of Saanich Inlet, Canada, are predominantly derived from vascular plants and have a 10±5% contribution of fossil *n*-alkanes. They show linearly increasing ages when compared to sediment ages that were earlier independently determined by varve counting. This is attributed to an increasing 'soil reservoir effect', caused by the build up and aging of the (refractory) soil organic carbon pool since deglaciation of the area. After correction of the *n*-alkane ages for the



contribution of fossil *n*-alkanes, extrapolation of the regression line resulted in a good 'prediction' of the onset of the Holocene at 12000 BP. This indicates that the accumulation of *n*-alkanes is not counterbalanced by degradation and only to a minor degree by erosion. The existence of the proposed 'soil reservoir effect' is supported by an increasing *n*-alkane flux to the fjord sediment with time. Although this study was performed using long-chain *n*-alkanes only, it can be assumed that this mechanism is valid for a large range of terrestrial refractory organic compounds. This suggests that there has been an increasing accumulation of refractory terrigenous organic carbon in the soils of the areas that are tributary to the Saanich Inlet since the end of the last ice age until the present day, and likely in a larger part of the western North-American coast. On a larger scale, this may indicate that the terrigenous organic carbon pool in temperate regions is still increasing as a long-term response to the Pleistocene-Holocene climatic transition.

### **Acknowledgements**

The staff at the National Ocean Sciences Accelerator Mass Spectrometry Facility at Woods Hole, USA, is thanked for their help during the preparation procedure for <sup>14</sup>C analysis, and for the final measurements. Marianne Baas and Michiel Kienhuis are thanked for assistance with the isolation of the *n*-alkanes. The Ocean Drilling Project is thanked for providing subsamples of core 1034C obtained at leg 169S. Dr. M.J. Whiticar of SEOS, Victoria, Canada, is thanked for providing the pre- and post-bomb sediments.



## Chapter 5

### A 400 year record of Holocene environmental changes in an euxinic fjord as revealed by the sedimentary biomarker record

*Rienk H. Smittenberg, Richard D. Pancost, Ellen C. Hopmans, Matthias Paetzel  
and Jaap S. Sinninghe Damsté*

Resubmitted after revision to 'Palaeogeography, Palaeoclimatology, Palaeoecology'

**Abstract** A 400 year sedimentary record of the euxinic Kyllaren Fjord was investigated using organic biogeochemical, geochemical and sedimentological approaches. Accumulation rates of a suite of biomarkers were determined and in some cases their stable carbon isotopic composition. Biomarkers were separated into three different groups: terrestrial derived, general aquatic/marine derived, and aquatic/marine derived but related to high primary productivity. Variations in bulk sediment parameters and biomarker accumulation rates with depth were used to interpret the sedimentary record. We infer that in the first half of the 19<sup>th</sup> century an environmental change occurred, caused by a change in either the precipitation regime, vegetation and/or land use. The data also show that in the last century, and especially in the last decades, a distinct increase in primary productivity occurred. Most likely this is caused by a 'natural' eutrophication due to the transformation of the fjord from an open to a confined system by the building of a partially open dam in 1954, possibly combined with anthropogenic eutrophication. A concurrent shoaling of the fjord chemocline may have had a mediating effect in the change towards a higher productivity by enhancing nutrient and carbon recycling. Enhanced carbon recycling is reflected by decreased  $\delta^{13}\text{C}$  values of several biomarkers.

#### 5.1. Introduction

In the last decades, the concern and debate regarding the magnitude of the anthropogenic impact on the Earth's climate and environment has been growing and has moved upwards on the political and scientific calendar. To correctly evaluate the climate data measured in recent times, and estimate the impact of mankind relative to natural variability, (proxy) palaeoclimatic data is needed [e.g. *Mann et al.*, 1998]. Available records, such as those developed from tree-rings and ice-cores, have already provided much palaeoclimatic information [e.g. *Jones et al.*, 1998; *Petit et al.*, 2000]. Still, a need remains for additional high-resolution records to improve the current understanding, and to assess the impact of climate change on local or regional scales. Like tree-rings and ice-cores, well preserved

laminated sediments can provide high resolution temporal records [Kemp, 1996]. Examples include isolated lakes, peat bogs [e.g. *Leavitt and Carpenter, 1989; Zolitschka and Negendank, 1999*], marine basins [e.g. *Pike and Kemp, 1997*] and anoxic silled fjords [e.g. *Paetzel and Schrader, 1992; Pellatt et al., 2001; Nordberg et al., 2001*]. Silled fjords can be particularly useful repositories of high-resolution palaeoclimatic information, because high sedimentation rates are commonly coupled with bottom water anoxia, precluding benthic macrofauna and resulting in the preservation of laminae.

Here, we report a study of the molecular biogeochemistry, geochemistry and sedimentology of the upper 50 cm of the sediment of the anoxic Kyllaren fjord, Norway, representing approximately the last 400 years. The abundance and, in some cases, stable carbon isotopic compositions of a suite of lipid constituents in sediments taken from the centre of the fjord were investigated. In this way, we traced variations in input and source of organic material to the basin including terrestrial sources, several species of phytoplankton, and microbial communities. Using this information, we reconstructed the climatic influences on the fjord ecosystem and the impact of anthropogenic activity, especially eutrophication.

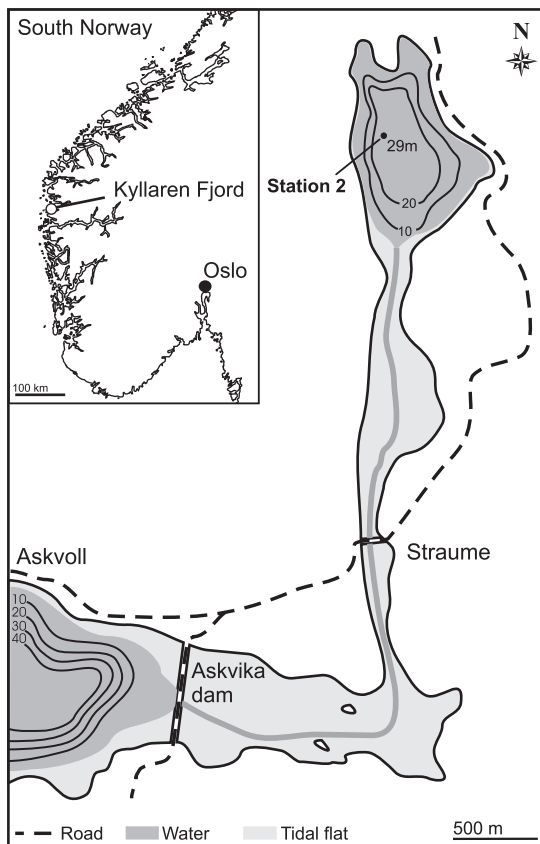


**Figure 5.1** Location map of the Kyllaren fjord. The fjord lies approximately at 61°25' N and 5°10' E

## 5.2. Study area

Kyllaren fjord is 29 m deep in the depocenter, has an area of 0.35 km<sup>2</sup>, and is connected with the open sea through a shallow inlet which consists of a tidal flat and an 1-2 m deep water channel, depending on the tide (Fig. 5.1). Consequently, bottom water exchange is restricted, resulting in a permanent halocline and associated chemocline between 5 and 10 m water depth. The salinity of the bottom water is ca. 25‰. The upper water layer varies in salinity from 5‰ in summer when precipitation is high, to 16‰ in winter when the fresh water supply is lower. The temperature of the bottom water varies between 7 and 9°C, while the temperature in the upper 5 m ranges from 2°C in winter to 14°C in summer. The resulting vertical density gradient results in a stratified water column throughout the year, particularly during the summer.

The area has a temperate sea climate with high precipitation, particularly from September to January. In winter, the prevailing wind direction is SW, i.e. from the open ocean into the fjord, and in summer NW. The last 80 years, local precipitation has been 2000 to 4500 mm/year, and no apparent long term trend has been observed. The mean annual air temperature has risen from around 6°C to 7°C in the last century. The vegetation around the fjord consists primarily of pine and birch, but there is also some grassland for cattle grazing. The area has a peaty soil.

Phytoplankton blooms occur three times a year; a light induced bloom occurs in April, a temperature induced bloom in May/June, and a nutrient induced bloom in September as a consequence of autumn rains. Organic matter remineralisation and consequent oxygen depletion in combination with a lack of circulation results in anoxic bottom water conditions and the prevalence of free sulphide in the water column. Whether the mean depth of the chemocline has been deeper in the past is not known but it appears that it has shoaled in the last decades. In the winters of 1994 and 1996 spontaneous escape of H<sub>2</sub>S(g) was reported for the first time. In February 1994, the chemocline had temporarily shoaled up to 0.5 m depth [*Paetzel*, unpublished results].

In 1954 a dam with a 5 m wide opening was built across Straume (Fig. 5.1) to replace a wooden bridge. This seems to have influenced the fjord hydrology and ecosystem distinctively, as it restricted water exchange with the open sea. In 1988 the Askvika dam (Fig. 5.1) was built across the outlet reducing the opening towards the open fjord from 450 m to 2 x 15 m width, which further restricted water-exchange with the open sea. A second 2 m wide opening was introduced into the dam at Straume in 1993. This event coincided with an increase of the bottom water salinity from 21‰ to 25‰.

### **5.3. Methods**

#### *5.3.1. Sampling*

Seven sediment cores were taken from the depocenter of the Kyllaren in September 1997 (Station 2, Fig. 5.1) using a gravity corer (recovery 42-58 cm) deployed from a raft. Different cores were used for density measurements, carbon analyses, dating, and smear slides for diatom and grain size distribution analyses. For biogeochemical analysis two cores were subdivided into 2.5 cm subsamples, placed in geochemical bags and after transportation stored at -28°C. One core, Kyl 2-D, was slightly disturbed and used for a detailed composite lipid analysis. The other core, Kyl 2-2, was used to develop a depth profile for different biomarkers.

#### *5.3.2. Sedimentological and geochemical analyses and dating*

Grain size distribution estimates and diatom counts were performed using smear slides made with Mountex (Merck) as mounting medium (refraction index 1.67), by transmitted

light microscopy using a Leitz SM-LUX-POL microscope. Total carbon and total sulfur were measured with a LECO SC-144 DR at 1420°C. Total Organic Carbon was measured on a Rock-Eval II analyser. Bulk  $\delta^{13}\text{C}$  values were measured with a Finnigan-MAT mass spectrometer. C/N ratios were determined using a Fisons EA 1108.

$^{210}\text{Pb}$  and fallout- $^{137}\text{Cs}$  dating was performed on bulk sediment ground to  $<63\ \mu\text{m}$ , using a Canberra gamma-spectrometer with a Ge (Li) p-type well-type detector (GCW2022-7500SL-LB). Mass accumulation rates were calculated based on bulk density measurements and  $^{210}\text{Pb}$  and fallout- $^{137}\text{Cs}$  data. Below 15 cm depth (around 1850) dating becomes uncertain because  $^{210}\text{Pb}$  values drop to background level. From that point the depth-age curve is extrapolated using the lowermost calculated mass accumulation rate, factoring changes in laminae thickness.

### 5.3.3. Lipid analysis

#### *Extraction and fractionation*

All samples were freeze-dried before lipid extraction. Subsamples (1-2 g) of core Kyl 2-2 were extracted for 16 h using a Soxhlet-apparatus, with a dichloromethane/methanol (DCM/MeOH, 7.5:1 v/v) mixture. To remove elemental sulfur, excess of activated copper powder was added to the solvent prior to extraction. To remove salts, the extracts were washed with distilled water. The extracts were concentrated by rotary evaporation and dried over magnesium sulphate. Deuterated ante-iso  $\text{C}_{22}$ -alkane was added to the total lipid extracts to serve as an internal standard. For total lipid analysis, an aliquot (1-5 mg) of the extract was methylated with diazomethane ( $\text{CH}_2\text{N}_2$ ) in diethyl ether to convert fatty acids into their corresponding methyl esters. Subsequently, highly polar compounds were removed by column chromatography over silica gel with ethyl acetate as the eluent. The eluate was dried under a stream of nitrogen. The residue was dissolved in 25  $\mu\text{l}$  pyridine and 25  $\mu\text{l}$  bis(trimethylsilyl)trifluoroacetamide (BSTFA) was added. This mixture was heated at 60°C for 20 min to convert alcohols into their corresponding trimethylsilyl ethers. The derivatised extracts were diluted to 1 mg/ml and analysed by gas chromatography (GC) and gas chromatography-mass spectrometry (GC-MS).

To analyze highly unsaturated lipids that would otherwise remain undetected, five extracts originating from different core depths were hydrogenated to produce saturated lipids. Aliquots of these extracts were dissolved in ethyl acetate to which *ca.* 100 mg  $\text{PtO}_2$  and a few droplets of acetic acid were added. These aliquots were subsequently flushed with hydrogen for 1 h and stirred overnight. The hydrogenated extracts were then eluted with DCM over a small column containing magnesium sulphate and calcium carbonate, then separated over a column containing activated  $\text{Al}_2\text{O}_3$ ; First hexane was used as eluent, and subsequently a hexane/DCM (v/v 1:1) mixture. The eluted fractions were analysed with GC, GC-MS and irm-GC-MS.

For detailed identification of lipids and for compound specific carbon-isotope analysis,

two subsamples (7.5-10 cm and 17.5-20 cm depth of core Kyl 2-D) were ultrasonically extracted with a DCM/MeOH (7.5:1 v/v) mixture for 3 min (x3). The extracts were combined, centrifuged, concentrated by rotary evaporation and prepared for GC and GC-MS analyses as described above. An aliquot (~10 mg) of the extract of the 7.5-10 cm sediment sub-sample was fractionated via thin layer chromatography (TLC) following the method of *Skipski et al.* [1965]; First a mixture of isopropyl-ether/acetic acid (96:4 v/v) was used to develop the first half of a kieselgel (silica 60) plate. After drying, a petroleum-ether/ether/acetic acid mixture (89:10:1 v/v/v) was used to develop the whole plate. Ten fractions were scraped off, and these were ultrasonically extracted and derivatised using the methods described above. An aliquot (50 mg) of the total lipid extract of the 17.5-20 cm sediment sub-sample was hydrogenated as described above, and 10 mg of this hydrogenated extract was fractionated into nine fractions using TLC. The TLC fractions were analysed with GC, GC-MS and irm-GC-MS.

#### *Gas Chromatography and Gas Chromatography-Mass Spectrometry*

GC was performed using a Hewlett Packard 6890 instrument equipped with an on-column injector and a flame ionisation detector (FID). A fused silica capillary column (25 m x 0.32 mm) coated with CP Sil 5 (film thickness 0.12 µm) was used with helium as carrier gas. The samples were dissolved in ethyl acetate and on-column injected at 70°C. The oven was programmed at 20°C/min to 130°C and then at 4°C/min to 320°C at which it was held for 25 min.

GC-MS was performed using a Hewlett-Packard 5890 gas chromatograph interfaced to a VG Autospec Ultima mass spectrometer operated at 70 eV with a mass range of  $m/z$  50-800 and a cycle time of 1.7 s (resolution 1000). Compounds were identified by comparison of mass spectra and retention times with those reported in literature. Quantification was performed by comparing integrated peak areas of compounds with that of the internal standard, obtained by gas chromatography, as well as by integrating peak areas of one or more diagnostic mass fragments of the different compounds, obtained by GC-MS, and comparing these with the total ion current of the internal standard.

#### *Isotope-Ratio-Monitoring Gas Chromatography - Mass Spectrometry*

The DELTA-C irm-GCMS-system is in principal similar to the DELTA-S system as described previously by *Merritt et al.* [1995]. The gas chromatograph was equipped with a fused silica capillary column (25m x 0.32mm) coated with CP Sil-5 (film thickness = 0.12 µm). The carrier gas was helium. The samples (dissolved in ethyl acetate or hexane) were on column injected at 70°C and subsequently the oven was programmed at 20°C/min to 130°C and then at 4°C/min to 320°C at which it was held for 20 min. The isotopic composition of alcohols was corrected for the added carbon molecules by using BSTFA

with a known carbon isotopic value. Most values reported were determined by two replicate analyses, and the results were averaged to obtain a mean value and to evaluate measurement error. Both bulk and compound stable carbon isotopic compositions are reported in standard delta notation relative to the VPDB standard, with a standard error of 0.05‰.

### *High Performance Liquid Chromatography - Mass Spectrometry*

For pigment analysis, approximately 20 mg of freeze-dried sediments were three times ultrasonically extracted with acetone for 3 min, under continuous cooling with ice. The combined extracts were then rotary evaporated until a small volume, dried under nitrogen, weighed, and dissolved to a concentration of 1.0 mg/ml. To avoid degradation, extracts were stored at -20°C and measured the same day. Direct light was avoided as much as possible during the work-up procedure and analysis. The pigments were analysed with high performance liquid chromatography – mass spectrometry (HPLC-MS) using an HP 1100 series LC/MS equipped with an auto-injector, photodiode array detector, mass detector, and Chemstation chromatography manager software. 20 µl of sediment extracts, filtered through a 0.45 µm PTFE filter, were injected onto an C<sub>18</sub>-column (HP Eclipse XDB; 2.1 x 150mm, 5µ), maintained at 40°C. Separation was achieved using a linear gradient of 10% to 2% water in methanol in 20 min. Total run time was 50 min. Flow rate was 0.6 ml/min. Detection was achieved by UV-detection at 436 nm and atmospheric pressure positive ion chemical ionisation MS (APCI-MS) of the eluent. Conditions for APCI-MS were as follows: nebulizer pressure was set at 45 psi, the vaporizer temperature at 400°C, drying gas (N<sub>2</sub>) was delivered at 8 L/min, the capillary voltage was -4 kV and the corona needle was set at 6 µA. Compounds were identified from their retention times, UV spectra (200-700 nm) and APCI-mass spectra ( $m/z$  500-600). Relative quantification of the individual carotenoids was achieved by comparing the peak area in the mass chromatograms of the appropriate protonated molecular ion ( $m/z$  [M+1]<sup>+</sup> = 529 and 547 for isorenieratene and okenone, respectively).

Polar fractions of the total lipid extracts of core Kyl2-2 were used to obtain depth-profiles of glycerol dialkyl glycerol tetraethers (GDGTs), following the method as described by *Hopmans et al.* [2000]. Briefly, aliquots of the fractions were dried under a stream of nitrogen, and the residue dissolved by sonication (10 min) in hexane/propanol (99:1 v/v). The resulting suspension was centrifuged (1 min, 3500 rpm) and the supernatant filtered through a 0.45µm, 4 mm diameter FPTE filter prior to injection. Analyses were performed using the same HPLC-MS system as described above. Separation was achieved on an NH<sub>2</sub> column (Econosphere, 4.6 x 250mm, 5 µm; Alltech Associates) maintained at 30°C. Tetraethers were eluted isocratically with 99% hexane and 1 % propanol for 5 min, followed by a linear gradient to 1.8 % propanol in 45 min. Flow rate was 1 ml / min. Detection was achieved using APCI-MS of the eluent under the following conditions: nebulizer pressure 60 psi, vaporizer temperature 300°C, drying gas (N<sub>2</sub>) flow 6 L/min and



temperature 250°C, capillary voltage -3 kV, corona 5  $\mu$ A ( $\sim$ 3.2 kV). Positive ion spectra were generated by scanning  $m/z$  950-1450 in 1.9 s. Individual GDGTs were quantified by integration of peaks in summed mass chromatograms of  $[M+H]^+$  and  $[M+H]^++1$  ions and compared with a standard curve obtained using a dilution series of a known amount of GDGT-0.

## 5.4. Results and discussion

### 5.4.1. Lithology, accumulation rates and bulk measurements

The sediment has a fine texture (clay-silty clay) and is laminated. Small plant remains are present, but these were not analysed. The sediment can be divided into five different units (Fig. 5.2). The upper 5 cm (unit A; 1960-1998 AD) consists of very soft material in which lamination is not yet distinctly visible. The underlying unit is 7 cm thick (B, 5-12 cm; 1900-1960) and characterized by the development of lamination due to compaction. The following unit (C, 12-23 cm; 1780-1900) consists of 1-3 mm thick laminae and has a coarser texture (clay loam). From 23-41 cm depth (unit D; ca. 1650-1780), the laminae are approximately 1 mm thick, and unit E (41-52 cm; ca. 1550-1650) again consists of 1-3 mm thick laminae. The depths of these units vary up to 3 cm amongst the different cores from this site, and this is taken into account when correlating results among different cores.

The thickness of the laminae suggest a relatively stable mass accumulation rate (MAR) in the lower intervals with a slight maximum in unit C (Fig. 5.2). The MAR increased however dramatically in the uppermost part of unit B and unit A. Inorganic carbon (carbonate) contents are low (2-3%, Fig. 5.2) and cannot account for this change, which thus likely reflects an increase in terrestrially derived clastic material. Coinciding with the increase in MAR, the total organic carbon (TOC) content decreases from 11% to 6% (Fig. 5.2), while the sulfur content increases from ca. 1.4% to ca. 1.7% (Fig. 5.2). Because the TOC content is highly influenced by dilution of inorganic material, changes in the contribution of organic material is better represented by the TOC accumulation rate (AR). This shows a maximum in the lower part of unit C, and a minimum at the boundary of unit C and B. After that, it increases substantially in units B and A, reflecting the increase in MAR. The sulphur AR is congruent (Fig. 5.2). These changes must reflect significant variations in either the inflow of terrestrial organic matter or the amount of primary productivity, although a change in the preservation of organic matter may also play a role. Bulk carbon isotopic ratio values ( $\delta^{13}C_{org}$ ) are ca. -26‰ in unit D; in unit C  $\delta^{13}C_{org}$  values start to rise to reach a maximum of -24.5‰ in unit B; in the top 5 cm (unit A),  $\delta^{13}C_{org}$  values decrease again to -25.5‰ (Fig. 5.2). The C/N ratio of the bulk sediment is 50 in units E and D, increases towards 80 in unit C, then drops suddenly to 20 in units B and A (Fig. 5.2).

Microfossil analyses provide further insight into the nature of primary productivity variations during the sampled interval. Diatoms are represented by both benthic and

planktonic species and specific to both marine and fresh water environments, but have a low abundance (data not shown). Benthic species are presumably flushed in, as the bottom water is anoxic. Although the quantities are too low to interpret species variations, the total diatom content clearly increases in the upper 10 cm. Moreover, specific marine diatoms indicative of high productivity environments are the main contributors to this increase.

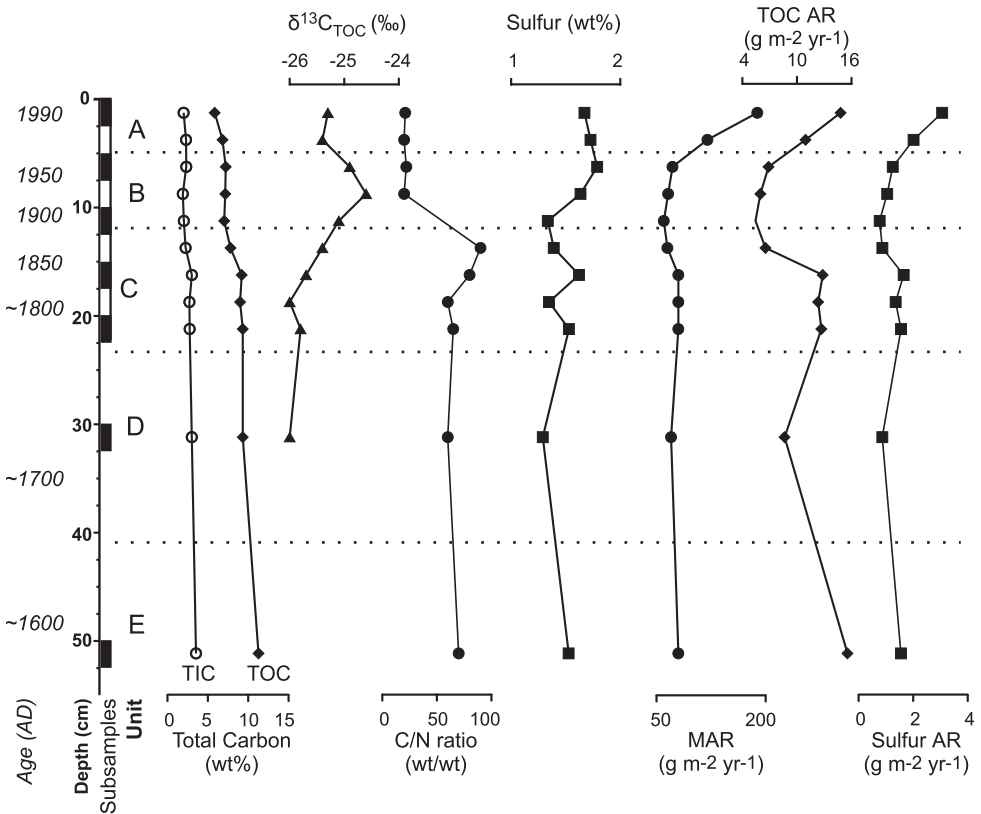


**Figure 5.2** Bulk data of Kyllaren Fjord sediments with depth. The age of the sediments are indicated, as well as the depth of the sub-samples used for analysis. A-E refer to the sedimentary units mentioned in the text. TIC = Total Inorganic Carbon. TOC = Total Organic Carbon. The C/N ratio is based on weight percentages.  $\delta^{13}C$  values are expressed against the VPDB standard. MAR = Mass Accumulation Rate. AR = Accumulation Rate.

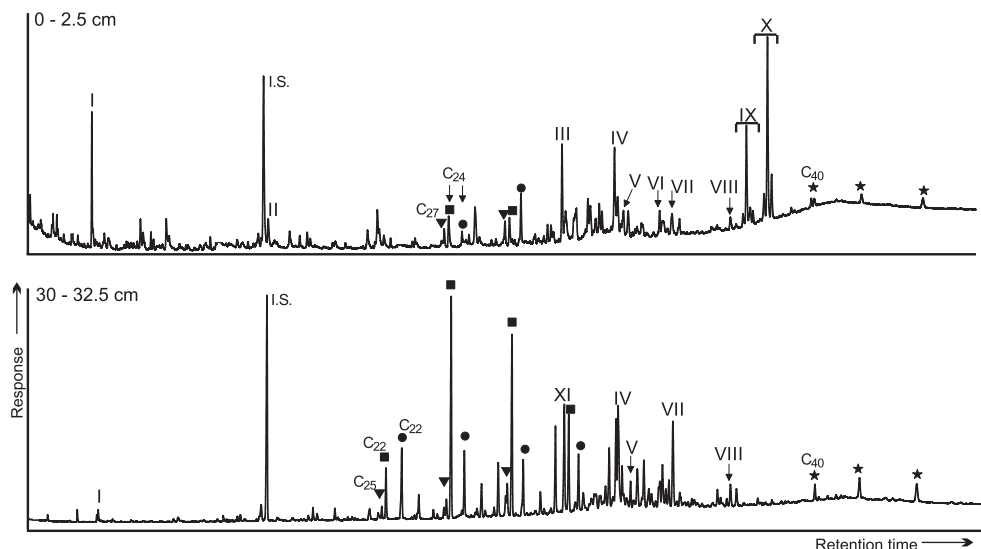


**Figure 5.3** Capillary gas chromatograms of total lipid fractions of a surface (0-2.5 cm) and a deeper sediment (30-32.5 cm) with a number of biomarkers indicated. Key: ▼ *n*-alkanes; ■ *n*-alkanoic acids; ● *n*-alkanols; ★ wax-esters; I.S. Internal Standard; I C<sub>20</sub> HBI; II phytol; III cholesterol; IV sitosterol; V dinosterol; VI tetrahymanol; VII ursolic acid; VIII 17β,21β(H)-bishomohopanoic acid; IX C<sub>37</sub> alkenones; X C<sub>38</sub> alkenones; XI 17α,21β(H)-homohopane (coeluting with C<sub>31</sub> *n*-alkane).

#### 5.4.2. Lipid biomarkers

A variety of marine/aquatic and terrestrially derived compounds were identified in the sediments. Most of these biomarkers, and some of their stable carbon isotopic compositions, are listed in table 5.1. Fig. 5.3 shows gas chromatograms of total lipid fractions obtained from a surface (0 - 2.5 cm) and from a deeper sediment (30 - 32.5 cm). Fig. 5.4 shows accumulation rates of selected biomarkers. Fig. 5.5 shows accumulation rates of glycerol dialkyl glycerol tetra-ethers (GDGTs).

#### Long-chain *n*-alkyl compounds

Long-chain *n*-alkyl compounds comprise a major part of the total lipid fractions, especially in the deeper sediments (Fig. 5.3). Specifically, long-chain *n*-alkanes, *n*-alkanoic acids, and *n*-alkan-1-ols are present in substantial amounts, with lower abundances of alkan-2-ones and wax-esters (see Table 5.1 for chain length distribution and δ<sup>13</sup>C values). Their ARs (Fig. 5.4) increase upcore until a maximum occurs in unit C (~1840 AD) followed by a decrease until 1900 AD. After 1900 AD, the ARs of *n*-alkanes and the C<sub>22</sub> and C<sub>24</sub> *n*-alkanol stay relatively constant, while the C<sub>26</sub> *n*-alkanol AR increases again. The AR profiles of the wax-esters and alkan-2-ones (not shown) are similar.

Compound (class)	O/E Predominance	$\delta^{13}\text{C}$ (‰)	Compound (continued)	$\delta^{13}\text{C}$ (‰)	$\delta^{13}\text{C}$ values:
<b><i>n</i>-Alkyl compounds</b>					
<i>n</i> -alkanes (C <sub>17</sub> – C <sub>35</sub> )		-28 to -32	17 $\beta$ .21 $\beta$ (H)-trishomohopan-32-on	t	a. decreasing values with increasing carbon chain lengths
<i>n</i> -alkanols (C <sub>14</sub> – C <sub>32</sub> )	Odd	-34	17 $\alpha$ .21 $\beta$ (H)-bisnorhopane	t	b. average of C <sub>24</sub> and C <sub>26</sub>
alkan-2-ols (C <sub>21</sub> – C <sub>37</sub> )	Even	n.d.	17 $\alpha$ .21 $\beta$ (H)-homohopane	f	c. C <sub>24</sub> fatty acid
<i>n</i> -alkanoic acids (C <sub>16</sub> – C <sub>32</sub> )	Odd	-28.5	17 $\beta$ .21 $\beta$ (H)-hopane	f	d. average of C <sub>38</sub> , C <sub>40</sub> , C <sub>42</sub> and C <sub>44</sub>
wax-esters (C <sub>38</sub> – C <sub>48</sub> )	Even	-31.8	17 $\beta$ .21 $\beta$ (H)-bishomohopane	f	e. Average of C <sub>27</sub> , C <sub>29</sub> and C <sub>33</sub> measured in hydrogenated fraction
methyl- <i>n</i> -ketones (C <sub>21</sub> – C <sub>35</sub> )	Odd	-33	17 $\beta$ .21 $\beta$ (H)-trishomohopane	f	f. average of oleane and ursane in hydrogenated fraction
17 $\beta$ .21 $\beta$ (H)-C <sub>36</sub> hopane			17 $\beta$ .21 $\beta$ (H)-C <sub>36</sub> hopane	t	g. derivative measured in hydrogenated fraction
<b><i>Long chain alkenones</i></b>					
C <sub>37:2</sub> methyl-alkenone		-25.3	<b>Triterpenoids</b>		h. n.d. not determined
C <sub>37:3</sub> methyl-alkenone			lupeol		t. trace amount
C <sub>37:4</sub> methyl-alkenone			taraxer-14-en-3 $\beta$ -ol		
C <sub>38:2</sub> ethyl-alkenone		-26.3	friedelan-14-en-3-on	t	
C <sub>38:3</sub> ethyl-alkenone			friedelan-3-on		
C <sub>38:4</sub> ethyl-alkenone			$\beta$ -amyrine		
			ursenol		
			ursenolic acid		
			olean-13'(18)-en-3 $\beta$ -ol	g	
			oleanolic acid		
			tetrahymanol		
<b><i>Steroids</i></b>					
cholest-5-en-3 $\beta$ -ol (cholesterol)			<b>Carotenoids</b>		
5 $\alpha$ -cholestan-3 $\beta$ -ol (cholestanol)			isorenieratene	-24.2	
24-methyl-cholest-5, 24(28)-dien-3 $\beta$ -ol			okenone	-39.4	
24-methyl-cholest-5-en-3 $\beta$ -ol (campesterol)					
24-methyl-cholest-5,22-dien-3 $\beta$ -ol					
24-ethyl-5 $\alpha$ -cholest-22-en-3 $\beta$ -ol					
24-ethyl-cholest-5,22-dien-3-ol (stigmasterol)					
24-ethyl-cholest-5-en-3 $\beta$ -ol (sitosterol)		-27.3	<b>Glycerol dialkyl glycerol tetra-ethers</b>		
24-ethyl-5 $\alpha$ -cholestane-3 $\beta$ -ol - 2 isomers (sitostanol)			2x acyclic C <sub>40</sub> isoprenoid chain (A)		
4 $\alpha$ ,23,24-trimethyl-5 $\alpha$ (H)cholestan-3 $\beta$ -ol (dinostanol)			acyclic and monocyclic C <sub>40</sub> isoprenoid chain		
4 $\alpha$ ,23,24-trimethyl-5 $\alpha$ (H)cholestan-3 $\beta$ -ol (dinostanol)			2x monocyclic C <sub>40</sub> isoprenoid chain		
4 $\alpha$ ,23,24-trimethyl-5 $\alpha$ (H)cholest-22-en-3 $\beta$ -ol (dinosterol)			bicyclic and tricyclic C <sub>40</sub> isoprenoid chain (B)		
			2x trimethyl C <sub>40</sub> isoprenoid chain (C)		
			dimethyl and trimethyl C <sub>40</sub> isoprenoid chain (D)		
			2x dimethyl C <sub>40</sub> isoprenoid chain (E)		
<b><i>Hopanooids</i></b>					
17 $\beta$ .21 $\beta$ (H)-hopan-30-ol			<b>Miscellaneous compounds</b>		
17 $\beta$ .21 $\beta$ (H)-hopan-22(29)-ol (diplopterol)			phytol	-26.9	
17 $\beta$ .21 $\beta$ (H)-2-methyl-homohopan-31-ol			farnesol	-23.7	
17 $\beta$ .21 $\beta$ (H)-homohopan-31-ol			C <sub>20</sub> highly branched isoprenoid loliolide	-20.8	
17 $\alpha$ .21 $\beta$ (H)-bishomohopan-31-ol			$\alpha$ -tocopherol		
17 $\alpha$ .21 $\beta$ (H)-bishomohopan-32-ol					
17 $\beta$ .21 $\beta$ (H)-bishomohopan-32-ol					
17 $\beta$ .21 $\beta$ (H)-bishomohopanoic acid					
17 $\alpha$ .21 $\beta$ (H)-bishomohopan-31-on					

**Table 5.1** Compounds identified in the Kyllaren Fjord sediments, with their  $\delta^{13}\text{C}$  values if measured. The even to odd distribution is given for the *n*-alkyl compounds.

Long-chain *n*-alkyl compounds are in most cases derived from surface waxes of leaves [Eglinton and Hamilton, 1967]. Consistent with this are the relatively low  $\delta^{13}\text{C}$  values of the *n*-alkyl compounds (Table 5.1) and their strong odd or even carbon number predominance: The carbon preference index (CPI) for the  $\text{C}_{23}$ - $\text{C}_{33}$  *n*-alkanes is 10, while the CPI of the  $\text{C}_{20}$ - $\text{C}_{28}$  *n*-alkanols is 0.1, indicating higher plant sources [Kolattukudy, 1980; Lockheart *et al.*, 1997]. Similarly, the alkan-2-ones are probably product of microbial oxidation of (terrestrial) alkanes or *n*-alkanoic acids, as they have so far only been found in soils, peat, or sediments rich in terrigenous material [Volkman *et al.*, 1981; Lehtonen and Ketola, 1990; Rieley *et al.*, 1991a].

### Long-chain alkenones

$\text{C}_{37}$  alken-2-ones and  $\text{C}_{38}$  alken-3-ones with 2-4 double bonds are absent in sediments below 10 cm, but at shallower depths their ARs increase substantially (Fig. 5.4). Long-chain alkenones (LCA) are biosynthesized by members of the haptophyte order Isochrydales, of which *Emiliania huxleyi* and *Gephyrocapsa oceanica* are the most widespread members [Brassell, 1993 and references cited therein]. In marine settings both  $\text{C}_{38}$  alken-2-ones (methyl ketones) and  $\text{C}_{38}$  alken-3-ones (ethyl ketones) are normally observed [e.g. Rosell-Melee *et al.*, 1994; Conte *et al.*, 2001]. In Norwegian fjords, this 'marine' pattern has also been reported [Conte *et al.*, 1994; Ficken and Farrimond, 1995], but in the Kyllaren fjord the  $\text{C}_{38}$  methylketones were absent. This pattern is similar to that found in sediments from the fjord phase of the currently isolated lake Pollen, Southern Norway [Innes *et al.*, 1998]. The ratio between the total abundances of the  $\text{C}_{37}$  and the  $\text{C}_{38}$  alkenones ( $\Sigma\text{C}_{37}/\Sigma\text{C}_{38}$ ) is 0.7, again similar to the LCA pattern observed in the lake Pollen sediments [Innes *et al.*, 1998].  $\text{C}_{38}$  alken-2-ones were also absent from the LCA patterns of sediments of the brackish Baltic Sea at salinities  $<7.7$  ‰ [Schulz *et al.*, 2000] and of sediments of some lake sediments of various salinities and geographical regions [Cranwell, 1985; Li *et al.*, 1996; Thiel *et al.*, 1997]. The  $\Sigma\text{C}_{37}/\Sigma\text{C}_{38}$  ratio was in those settings not as low as observed in lake Pollen and in Kyllaren fjord. In general the  $\text{C}_{37}$  alkenones are more abundant than the  $\text{C}_{38}$  alkenones (i.e.  $\Sigma\text{C}_{37}/\Sigma\text{C}_{38} > 1$ ), although in late log and stationary growth phases  $\text{C}_{38}$  alkenones appear to be more predominant than in early growth phases, sometimes resulting in a  $\Sigma\text{C}_{37}/\Sigma\text{C}_{38}$  ratio  $<1$  [Conte *et al.*, 1998]. Rosell Melee *et al.* [1994] reported ratios as low as 0.7, but at higher temperatures at (sub)tropical latitudes. Volkman *et al.* [1995] found that *G. oceanica* produced relatively higher amounts of  $\text{C}_{38}$  alkenones than *E. huxleyi*. It thus appears that the haptophyte species that produces the 'Baltic Sea pattern' (i.e. lacking  $\text{C}_{38}$  methyl ketones), or a related strain, has been present in the Kyllaren fjord over the last decades. The low  $\Sigma\text{C}_{37}/\Sigma\text{C}_{38}$  ratio may be specific for this certain strain, but it may also be determined by the predominant physiological state of the algae living in the fjord, related to relatively low salinities.

Because of the uncommon LCA distribution, likely produced by an unknown strain of haptophytes, the  $U_{37}^{K'}$  index as a palaeotemperature proxy [Brassell *et al.*, 1986; Müller *et*

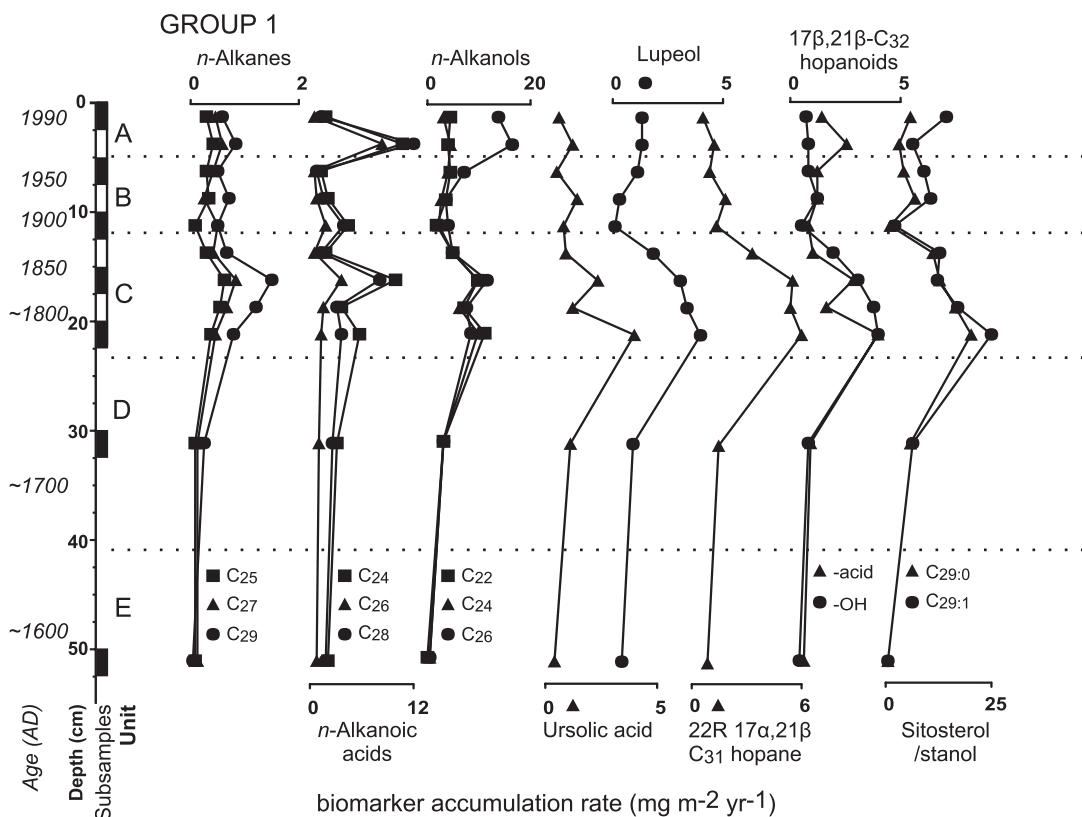
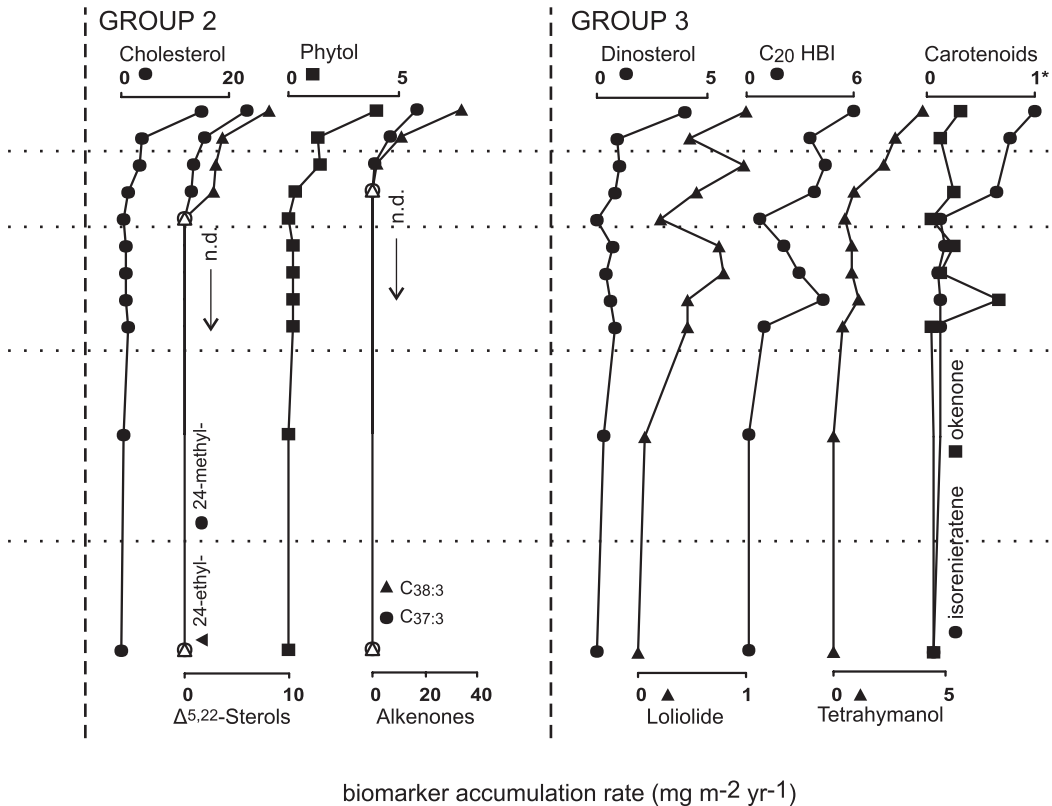


**Figure 5.4** Accumulation rates of a suite of biomarker lipids, divided into three groups according to their inferred origin. The age of the sediments are indicated, as well as the depth of the sub-samples used for analysis. A-E refer to the sedimentary units mentioned in the text. Group 1: Terrigenous biomarkers. Group 2: Aquatic biomarkers produced by organisms strongly favoured by

*al.*, 1998] may not be reliable [e.g. *Freeman and Wakeham*, 1992; *Thiel et al.*, 1997; *Schulz et al.*, 2000; *Versteegh et al.*, 2001]. Still, the calculated temperature of ca. 9 °C from the distribution of the LCA's is consistent with reported water temperatures in spring. Alkenone  $\delta^{13}\text{C}$  values are  $-26 \pm 1\%$  (Table 5.1). This is relatively low compared with values reported from other studies [e.g. *Goericke and Fry*, 1994; *Bidigare et al.*, 1997; *Riebesell et al.*, 2000], but still within the commonly reported range.

### Steroids

Steroids are another important class of biomarkers. The  $\text{C}_{29}$  sterols, sitosterol (24-ethylcholest-5-en-3 $\beta$ -ol) and sitostanol (24-ethyl-5 $\alpha$ -cholestan-3 $\beta$ -ol) dominate the sterol distribution together with cholesterol (cholest-5-en-3 $\beta$ -ol). The ARs of sitosterol and sitostanol increase until ~1800 AD, then decrease within unit C until ~1900 AD and stay



eutrophication. Group 3: Biomarkers derived from aquatic organisms that have been more generally present in the fjord, including the phototrophic green and purple sulfur bacteria. \* Accumulation rates of okenone and isorenieratene are normalized to the maximum abundance of isorenieratene. Open symbols = not detected (n.d.).

relatively constant in the upper part of the core (Fig. 5.4). Generally, C<sub>29</sub> sterols are associated with contributions from higher plants [Huang and Meinschein, 1976], although it has been shown that this relationship is grossly oversimplified [Volkman, 1986], as certain algae can also produce C<sub>29</sub>-sterols. Therefore, inferences drawn from sterol distributions regarding organic matter sources must be made with caution, and should be supported by other lipid data. The δ<sup>13</sup>C value (ca. -28‰; Table 5.1) of sitosterol is also not sufficiently diagnostic to distinguish between a marine or terrestrial source. However, the AR rate profiles for sitosterol and sitostanol are similar to those of the *n*-alkanes, suggesting a common (i.e. terrestrial higher plant) source.

Cholest-5-en-3β-ol (cholesterol), 24-methyl-cholest-5,22 dien-3β-ol and 24-ethyl-cholest-5,22-dien-3β-ol are only present in low abundance or were undetected in the lower part of the core but their ARs increase strongly in the upper 10 cm depth (Fig. 5.4). C<sub>27</sub> and C<sub>28</sub> sterols are generally attributed to algal sources, as these sterols are only found in small amounts in higher plants compared to marine/aquatic organisms. However, as is the case

with sitosterol and -stanol, source assignments cannot be made with certainty on structural grounds alone. Still, we suggest an algal source for these compounds, because their ARs parallel those of alkenones and dinosterol (see below), diagnostic algal biomarkers.

Dinosterol (4 $\alpha$ ,23,24-trimethyl-cholest-5-en-3 $\beta$ -ol) is a specific sterol biomarker for dinoflagellates [Boon *et al.*, 1979; Kokke *et al.*, 1982; Mansour *et al.*, 1999], occurring both in fresh water and marine environments. Therefore, its presence clearly indicates input from aquatic primary producers but cannot be used to distinguish marine vs. freshwater conditions. It is present throughout the core, with an increasing AR towards the top of the core, paralleling those observed for alkenones and C<sub>27</sub> and C<sub>28</sub> sterols (Fig. 5.4).

### Hopanoids

Hopanoids are membrane lipids of aerobic bacteria where they have a regulating and rigidifying function similar to that of sterols in the Eukarya. Hopanoids, often with functional groups, are commonly reported in both marine and freshwater environments, and are supposed to be bacteriohopanepolyol derivatives [Rohmer *et al.*, 1992]. A suite of these derivatives with different functional groups is present in the Kyllaren fjord sediments (Table 5.1). Most hopanoids possess the 17 $\beta$ ,21 $\beta$ (H)-stereochemistry, but some 17 $\alpha$ ,21 $\beta$ (H)-isomers are also present. The AR of the most abundant hopanoids, 17 $\beta$ ,21 $\beta$ (H)-bishomohopanol (C<sub>32</sub>- $\beta\beta$ -hopanol), 17 $\beta$ ,21 $\beta$ (H)-bishomohopanoic acid (C<sub>32</sub>- $\beta\beta$ -hopanoic acid) and 22R 17 $\alpha$ ,21 $\beta$ (H)-homohopane (C<sub>31</sub>-22R- $\alpha\beta$ -hopane), increase upcore until 20 cm depth, and decrease gradually towards shallower depths (Fig. 5.4). The  $\beta\beta$ -stereo-isomers exhibit  $\delta^{13}\text{C}$  values of -32‰ to -34‰. In contrast, C<sub>31</sub>-22R- $\alpha\beta$ -hopane shows a value of ca. -24‰.

Although the  $\alpha\beta$ -isomers are generally assumed to be a result of sedimentary diagenesis of bacterial derived  $\beta\beta$ -isomers, their occurrence has also been reported in contemporary peats, mainly consisting of *Sphagnum*-mosses. Quirk *et al.* [1984] reported C<sub>31</sub>-22R- $\alpha\beta$ -hopane to appear at the earliest stage of decay of *Sphagnum cuspidatum* in Scotch peats, although the exact origin remains unclear. Pancost *et al.* [2000] reported C<sub>31</sub>-22R- $\alpha\beta$ -hopane in recent Dutch and Irish peats, and report carbon isotopic compositions similar to those observed here (-24‰ to -26‰). It was suggested that the reported C<sub>31</sub>-22R- $\alpha\beta$ -hopane was formed by very early diagenetic isomerisation probably resulting from the high acidity in the mire. In any case, a fossil source can be ruled out because of the absence of 22S-isomers. We conclude that it is most likely that the C<sub>31</sub>-22R- $\alpha\beta$ -hopane originates from peats from the surrounding area, and thus has a terrestrial source.

C<sub>32</sub>- $\beta\beta$ -hopanol and C<sub>32</sub>- $\beta\beta$ -hopanoic acid are highly ubiquitous compounds and a specific source assignment is therefore problematic. However, because of the similarity of their ARs with that of the C<sub>31</sub>-22R- $\alpha\beta$ -hopane, as well as with higher plant biomarkers, we tentatively appoint the  $\beta\beta$ -hopanoids also to a predominantly terrestrial origin.



### Other triterpenoids

Triterpenoids with friedelane, oleanane and ursane skeletons are only produced by higher plants [Brassell and Eglinton, 1983], and are present throughout the core. We determined the abundance of lupeol and ursolic acid as representatives of this compound class. The latter compound is the major triterpenoid detected most *Sphagnum* species [Baas *et al.*, 2000]. Their AR profiles are similar to those of the hopanoids, sitosterol, sitostanol and the *n*-alkyl compounds, consistent with the assignment of terrestrial sources to these compounds (Fig. 5.4). Oleanane and ursane, products formed upon hydrogenation of oleanol and ursenol, have an average  $\delta^{13}\text{C}$  value of -30‰, which is also consistent with this source assignment.

An unrelated triterpenoid present in the sediments is tetrahymanol (gammacer-3 $\beta$ -ol). This compound is produced by the photosynthetic purple bacteria *Rhodospseudomonas palustris* and by ciliates of the Tetrahymena-taxus [Kleemann *et al.*, 1990; Harvey and McManus, 1991] when their diet contains no sterols, i.e. when they rely entirely on a prokaryotic food source [Sinninghe Damsté *et al.*, 1995 and references cited therein]. It may therefore be used as a marker for the presence of extensive bacterial activity. Tetrahymanol was detected in the upper 20 cm of the core, where its AR exhibits an increase upcore (Fig. 5.4).

### Glycerol Dialkyl Glycerol Tetraether lipids

A suite of different glycerol dialkyl glycerol tetraethers (GDGTs) were identified in the sediments (Table 5.1). They can be divided into isoprenoidal GDGTs (Fig. 5.5; A & B) and branched GDGTs (C-E). Isoprenoid GDGTs are only known to occur in the membranes of archaea [De Rosa *et al.*, 1986; Schouten *et al.*, 2000b]. GDGT-0 (A) comprises two biphytanyl chains, and occurs ubiquitously in the kingdom Archaea. It is for instance produced by methane oxidising, methanogenic, thermophilic and marine pelagic archaea [De Rosa and Gambacorta, 1988; Schouten *et al.*, 2000a]. Crenarchaeol (B) contains a bicyclic and a diagnostic tricyclic biphytanyl chain (Fig. 5.5), and is attributed to widespread pelagic marine archaea [Schouten *et al.*, 2000b; Sinninghe Damsté *et al.*, 2002c]. Crenarchaeol and GDGT-0 are produced in approximately the same amounts by marine crenarchaeota, and the similarity in the AR profiles of these two tetraethers in the lower part of the investigated core (Fig. 5.5) suggests that until 1900 AD almost all GDGT-0 is derived from marine crenarchaeota. The AR of GDGT-0 increases substantially after 1900 AD, while the crenarchaeol AR increases only slightly during that period (Fig. 5.5), which points towards an additional archaeal source for GDGT-0 after 1900 AD, possibly methanogens. GDGTs C - E have varying combinations of di-methyl and tri-methyl alkyl chains (Fig. 5.5) and have only recently been identified [Sinninghe Damsté *et al.*, 2000]. They are the only known non-isoprenoidal tetraethers and have so far been found only in peats, soils, lacustrine sediments, and marine sediments receiving a large terrestrial input. Their exact origin is not yet elucidated, but their structure points towards the coexistence of

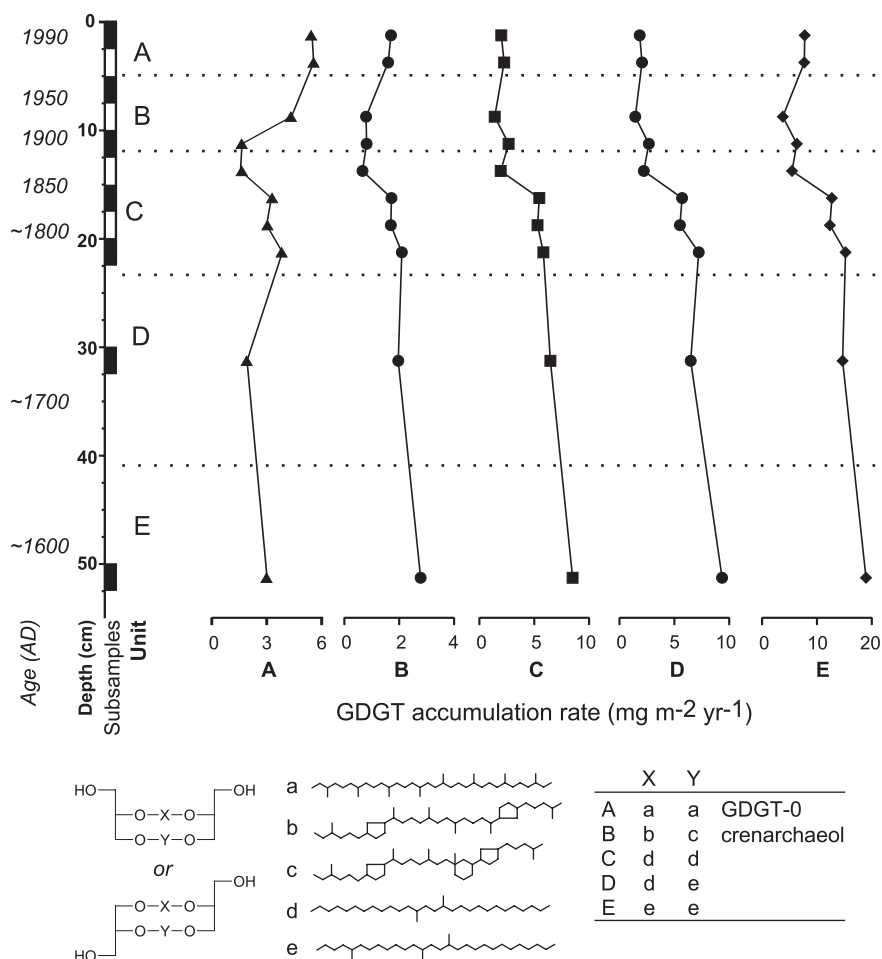


**Figure 5.5** Accumulation rates and structures of Glycerol Dialkyl Glycerol Tetraethers (GDGTs). The age of the sediments are indicated, as well as the depth of the sub-samples used for analysis. GDGT-0 and crenarchaeol belong to biomarker group 3 (see Fig 5.4), C-E to group 1.

typical archaeal and bacterial biosynthetic pathways in a single organism. This suggests that they are biosynthesised by archaea or bacteria thriving in terrestrial environments [Schouten *et al.*, 2000b]. The ARs of GDGTs C-E show a distinct decrease upcore, but stay more or less constant in the upper 10 cm of the core.

### Green and purple sulfur bacterial biomarkers

The carotenoid isorenieratene was detected as isorenieratane in hydrogenated apolar fractions using GC-MS, and directly using HPLC-MS. Isorenieratene is only produced by the brown strain of the green photosynthetic sulfur bacteria (*Chlorobiaceae*) which only live in the photic zone under euxinic circumstances [Hartgers *et al.*, 1993 and references cited therein]. The AR of isorenieratene increases substantially in the upper 10 cm of the core (Fig. 5.4). Another *Chlorobiaceae*-derived biomarker, farnesol, is also present in the investigated sediments. This is the ester-bound side-chain in bacteriochlorophyll-*e*, used by *Chlorobiaceae*. The carbon isotopic compositions of isorenieratane and farnesane, the products formed upon hydrogenation of respectively isorenieratene and farnesol, are both approximately -24‰ (Table 5.1). Another carotenoid present in the studied core interval is okenone, specific for purple photosynthetic sulfur bacteria (*Chromatiaceae*), which also require photic zone euxinia. An okenone derivative was first noticed as an important compound in one TLC fraction of the hydrogenated total lipid extract of 17.5–20 cm of core Kyl-D, and later identified in all samples using HPLC-MS analysis. The okenone AR has a maximum between 20 and 10 cm depth (Fig. 5.4). The  $\delta^{13}\text{C}$  value determined on hydrogenated okenone is -40‰ (Table 5.1).

The  $\delta^{13}\text{C}$  values of these sulfur bacterial biomarkers are lower than normally encountered. *Chlorobiaceae* exhibit minimal carbon isotopic fractionation during carbon assimilation due to their utilisation of the reverse TCA cycle [Sirevåg *et al.*, 1977]. As a result, isorenieratene and farnesol  $\delta^{13}\text{C}$  values are typically -14 to -18‰, i.e. enriched relative to compounds from most co-occurring organisms [Sinninghe Damsté *et al.*, 1993; Goericke and Fry, 1994].

*Chromatiaceae* use the common Calvin cycle during carbon assimilation and their biomarkers are expected to have similar  $\delta^{13}\text{C}$  values as marine phytoplankton [Sirevåg *et al.*, 1977; Goericke *et al.*, 1994], while we measured -40‰. Schaeffer *et al.* [1997] found  $\delta^{13}\text{C}$  values of -27‰ for isorenieratene and farnesol, -33‰ for phytol and -45‰ for hydrogenated okenone in a meromictic lake in Switzerland, a setting similar to the Kyllaren fjord regarding bottom water stagnation and euxinia. The observed values for both *Chromatiaceae* and *Chlorobiaceae* biomarkers suggests that DIC in the stagnant water below the chemocline is depleted in  $^{13}\text{C}$  by approximately 15‰ relative to surface waters.

### Miscellaneous algal biomarkers

Phytol is derived from the side-chain of different types of chlorophyll, and is relatively labile. Because of this, it degrades fast in the terrestrial organic matter pool, and is, therefore, normally ascribed to aquatic photoautotrophic organisms when found in sediments. The AR of phytol decreases rapidly downcore, consistent with those of the long-chain alkenones and dinosterol, defined algal biomarkers. Phytol from the total lipid extracts has a  $\delta^{13}\text{C}$  value of -27‰ (Table 5.1).

Loliolide is present throughout the sediment, with an increasing AR upcore. This compound is an anoxic degradation product of the carotenoid fucoxanthin, which can be synthesised by a variety of algal classes, with diatoms as a major producer [Wahlberg and Eklund, 1998]. Degradation of fucoxanthin to loliolide generally occurs quantitatively and rapidly after sedimentation [Repeta, 1989]. Some other carotenoids may degrade to loliolide via oxidative degradation by enzymes, but fucoxanthin is the only major source recognised in sediments; therefore is regarded as an algal and, tentatively, diatom biomarker.

A C<sub>20</sub> highly branched isoprenoid alkane (2,6,10-trimethyl-7-(3-methylbutyl)dodecane; C<sub>20</sub> HBI) is present throughout the core (Fig. 5.4). The AR of C<sub>20</sub> HBI and loliolide increases upwards through the core. The carbon isotopic composition of the C<sub>20</sub> HBI is *ca.* -21‰ (Table 5.1). According to Rowland and Robson [1990], C<sub>20</sub> HBI has mainly been found in marine, but also in some lacustrine settings, so it can be regarded as an aquatic or algal biomarker. More specifically, it may be a diatom biomarker, given its structural similarity to the C<sub>25</sub> and C<sub>30</sub> HBI's, diagnostic for diatoms [Volkman *et al.*, 1994; Hird and Rowland, 1995] However, a specific source for the C<sub>20</sub> HBI has not yet been found and the investigated core lacks the C<sub>25</sub> and C<sub>30</sub> HBI's.

### *Biomarker groups*

Biomarkers can be separated into three different groups based on trends in ARs and source assignments. Fig. 5.4 defines these three groups.

Group 1 biomarkers have maximum ARs in the 17-25 cm section and consist of long-chain *n*-alkyl compounds, higher plant triterpenoids, sitosterol and sitostanol, and the bacterial derived hopanoids. All of these compounds are consistent with, and many are diagnostic for a terrestrial source, and the composite distribution is particularly similar to biomarkers observed in peats. GDGTs C-E (Fig. 5.5) are also included in this group because they most likely derive from a terrestrial source.

Group 2 consists of biomarkers that are undetected or only present in low abundance below 10 cm depth, but appear and increase drastically above this depth. Most striking members of this group are the long-chain alkenones, which become the dominant compounds in the lipid extract in the surface sediment (Fig. 5.3). The C<sub>27:1</sub>, C<sub>28:2</sub> and C<sub>29:2</sub> sterols and phytol also belong to this group and these biomarkers represent marine/aquatic primary producers.

Biomarkers of group 3 are similar to those of group 2 in that their ARs strongly increase in the upper 10 cm of the core. The difference with group 2 is that they are present throughout the core with a more gradual decrease of ARs downcore. This group comprises dinosterol, loliolide, C<sub>20</sub> HBI, tetrahymanol, the carotenoids okenone and isorenieratene, and GDGT-0 and crenarchaeol. These compounds are attributed to common aquatic organisms, such as dinoflagellates, diatoms, photosynthetic green and purple sulfur bacteria (carotenoids), and to marine pelagic crenarchaea (crenarchaeol and GDGT-0).

### Lipid preservation

In general, excellent preservation is observed in anoxic sediments [Harvey and Macko, 1997; Hartnett *et al.*, 1998], and we expect that also to be true for Kyllaren Fjord sediments. A permanent anoxic condition is indicated by the continuous occurrence of the sulfur bacterial biomarkers isorenieratene, farnesol and okenone. Furthermore, the sediment shows no signs of bioturbation. However, lipid degradation does take place under anoxic conditions, and different lipid classes are known to degrade at different rates [e.g. Cranwell, 1981; Harvey *et al.*, 1989; Sun and Wakeham, 1994]. Lipids of group 2 and 3 exhibit concentration profiles similar to typical degradation profiles where concentrations decrease with age and depth. However, the least reactive compounds in these groups, the long-chain alkenones and dinosterol [Cranwell, 1981; Sun and Wakeham, 1994], are the compounds that most clearly show this decrease with depth, while the opposite is expected. The lipids of group 1 increase in abundance with depth, a trend that is inconsistent with solely diagenetic controls. Therefore, we conclude that although degradation may have decreased biomarker abundances with depth, input variability is the main contributing factor for the observed variations in the biomarker depth profiles.

#### 5.4.3. Sedimentary regime and organic carbon input

The most apparent feature in the MAR is the large increase in the last 50 years (Fig. 5.2). This is likely the result of a significant change in the fjord system, caused by the building of the partially open dam in 1954. This restricted the water exchange between open sea and the fjord, resulting in a silting up of the inlet and trapping of incoming particulate matter. In this way, Kyllaren Fjord suddenly became similar to a meromictic lake, a transformation that also occurs naturally by the isostatic uplift of the Fennoscandinavian continent [15cm/100yr in this area; Pirazzoli, 1991], which decreases fjord and sill depths. Other (euxinic) fjords have been transformed into permanent stratified lakes by such natural processes, e.g. Framvaren fjord [Skei, 1988] or Lake Pollen [Innes *et al.*, 1998].

Although less dramatic, the MAR shows a second maximum between 25 and 17 cm depth. This maximum becomes more apparent if we consider the TOC and the group 1 biomarker ARs, which closely follow the MAR at this depth. More specifically, most biomarkers of group 1 reach their maximum AR at the beginning of this period, and level off to reach pre-1800 AD values again in 1900 AD. Additionally, at these depths the sediment is somewhat coarser and shows thicker laminae. All of this is consistent with an elevated influx of sediment and terrestrial organic matter between 1800 AD and 1850 AD. During this period, a cooling of the Northern Hemisphere took place [Jones *et al.*, 1998], and this probably coincided with a change in precipitation regime and erosive climate in the investigated area, although no specific records exist. Consequently, erosion of the soil around the fjord could have been higher, resulting in the observed higher sediment input and related higher TOC and terrestrial biomarker ARs. C/N ratios also show a maximum during this period. This could be consistent with a positive correlation the C/N ratio with

particle size [Hedges and Oades, 1997 and references cited therein]. Alternatively, a higher content of vascular plant remains can also account for this rise, and this would again be consistent with a greater amount of peat-derived organic matter. Alternatively or additionally, there could have been a change in vegetation or land use during this period, leading to the same sedimentary features. However, as with precipitation regime there are, to the best of our knowledge, no records of this, nor are there any pollen data available.

In contrast, the increase in MAR in the upper 10 cm of the core is associated with a decrease in TOC content. Because the sedimentary organic carbon is predominantly composed of terrestrial derived organic carbon, at least until the upper 10 cm; this must be explained by a gradual decrease of the (average) organic matter content of eroded soil. This could be caused by a gradual change in the relative contribution of two or more different sources: e.g. a 'normal' soil containing relatively low amounts of organic matter, and an organic matter rich peat or a peaty soil. Alternatively, it can be a result of a changing balance between input and decomposition of soil organic matter in favour of the latter. Decomposition is positively correlated with mean annual temperature and dryer conditions. Since the Little Ice Age, Northern Hemisphere temperatures have been rising until this date, albeit with some fluctuations, e.g. a colder spell between 1800 AD and 1850 AD [Jones *et al.*, 1998]. Therefore, decreasing TOC contents may well be a result of a slow equilibration of soil organic matter contents towards values reflecting contemporary mean annual temperatures. A third possibility, however, is that a gradual change of vegetation (also reflecting a climate change) or land-use reduced the soil organic matter content in some way.

#### 5.4.4. Permanent stratification and carbon and nutrient recycling

Okenone (from *Chromatiaceae*, purple sulfur bacteria) and isorenieratene (from *Chlorobiaceae*, green sulfur bacteria) are present throughout the core (Fig. 5.4), indicating that euxinia extended into the photic zone during at least the investigated time frame. The okenone AR maximizes between 20 and 10 cm depth, while the isorenieratene AR increases in the upper 10 cm, coincident with the increase in marine/aquatic biomarker ARs. The tetrahymanol AR, produced either by photosynthetic bacteria or by ciliates grazing on bacteria, exhibits a similar increase upcore (Fig. 5.4). These observations indicate an intensification or extension of euxinic conditions over the investigated period. The differences in abundance of *Chlorobiaceae* and *Chromatiaceae* are likely a result of interactions between these species, and their specific adaptations concerning light and nutrients. For example, *Chlorobiaceae* are better adapted to grow at low irradiances below algal blooms compared to *Chromatiaceae*, and the latter species grow normally just above the former [Montesinos *et al.*, 1983]. The shift of a greater abundance of biomarkers specific for *Chromatiaceae* to those specific for *Chlorobiaceae* could be a reflection of increasing algal productivity during the last 50 years, as discussed in section 4.5, favouring growth conditions for *Chlorobiaceae* over that for *Chromatiaceae*.

The conspicuous depletion in  $^{13}\text{C}$  of the sulfur bacterial biomarkers (okenone,

isorenieratene and farnesol) is possibly caused by carbon recycling in the fjord, a mechanism earlier proposed for ancient settings [e.g. *Küspert, 1982; Schouten et al., 2000c*] and by e.g. *Hartgers et al. [2000]* and *Velinsky and Fogel [1999]* in recent settings. During photosynthesis, primary producers assimilate  $^{12}\text{C}$  in favour over  $^{13}\text{C}$  due to several fractionation effects [*Hayes, 2001*]. As a result, marine derived organic matter is generally depleted in  $^{13}\text{C}$  relative to DIC by 25‰ [*Rau et al., 1996*] and terrigenous organic matter typically exhibits  $\delta^{13}\text{C}$  values of -28‰ to -32‰ [*Tyson, 1995c; Lockheart et al., 1997*]. Heterotrophic degradation of sinking OM leads to  $^{13}\text{C}$  depleted dissolved inorganic carbon (DIC) at depth. In cases where the water column is well mixed, this effect is minimised, especially when one considers that there must be a residual  $^{13}\text{C}$ -enrichment of DIC during aquatic primary production. However, equilibration with atmospheric  $\text{CO}_2$  is also part of the  $^{13}\text{C}$  balance, resulting in a net depletion of  $^{13}\text{C}$  in any aquatic system. In the case of a more or less permanent stratified situation, DIC below the thermo/halo- (and often chemo-) cline can be strongly depleted in  $^{13}\text{C}$  relative to DIC in the upper water column, due to the separation of the location of DIC-assimilation (upper layer) and remineralisation (lower layer). Such a situation exists in the Kyllaren fjord, where water below the halo/chemocline has minimal contact with the atmosphere and stratification prevails to preserve  $^{13}\text{C}$ -depleted DIC in the lower waters.

Stratification also has important consequences for the nutrient budget and nutrient (re)cycling in the fjord. In winter, thermal conditions make the stratification less stable, and wind driven mixing is at its strongest. Nutrient-rich water below the halo/chemocline is (partly) mixed into the upper water layers, replenishing nutrients to the upper water layer. Those nutrients, including  $^{13}\text{C}$ -depleted DIC, are then available for the first bloom to occur in spring. Although the estimated temperatures derived from the  $U_{37}^{K'}$  index (ca. 9°C) were judged not very reliable, they are consistent with spring water temperatures. The  $\delta^{13}\text{C}$  values of long-chain alkenones and phytol (ca. -26‰; Table 5.1) are relatively low but within the range of commonly reported values. However, the low alkenone and phytol  $\delta^{13}\text{C}$  values could also reflect algal growth on DIC that is somewhat depleted in  $^{13}\text{C}$ , although we have also not constrained all of the controls on carbon isotope fractionations. In contrast, the  $\delta^{13}\text{C}$  value of the  $\text{C}_{20}$  HBI, anticipated to be derived from diatoms, is not depleted relative to values found in other modern marine settings [around -20‰, *Fry and Wainright, 1991; Hird and Rowland, 1995*]. Possibly, this indicates that this biomarker is mainly produced in summer, when there is less or no winter-overtuned DIC available, but mainly DIC derived from atmospheric  $\text{CO}_2$ .

Consistent with decreased  $\delta^{13}\text{C}_{\text{DIC}}$  values during algal blooms are the  $\delta^{13}\text{C}_{\text{TOC}}$  values. From the bottom of the core until 10 cm depth,  $\delta^{13}\text{C}_{\text{TOC}}$  values gradually increase, as is to be expected from a decreasing terrestrial derived organic matter input relative to marine sources or alternatively from a faster degradation of marine organic matter relative to terrestrial derived organic matter within the sediment, leading to a relative enrichment of terrigenous derived organic matter with core-depth. However, above 10 cm depth, the  $\delta^{13}\text{C}_{\text{TOC}}$  decreases again, which is apparently inconsistent with a dramatic increase of marine organic matter, which is typically enriched in  $^{13}\text{C}$  relative to terrigenous organic

matter [Tyson, 1995c]. Thus, this marine organic matter appears to be unusually depleted in  $^{13}\text{C}$  relative to that observed in other modern settings. This could be attributed to many factors, but the mixing of  $^{13}\text{C}$ -depleted DIC into the photic zone during blooms is an explanation particularly consistent with the isotopic composition of the biomarkers.

#### 5.4.5. *Strong increase in primary production and shoaling of the chemocline in the last decades*

In the upper 10 cm (1900 AD - present), and especially in the last decades, a substantial increase in the ARs of marine/aquatic biomarker occurs (especially lipids of group 2), while the ARs of terrigenous lipids (group 1) remain more or less constant (Fig. 5.4). Furthermore, C/N ratios indicate a shift towards a greater share of fresh, presumably aquatic, organic matter. Both these observations suggest that in the last century, and especially in the last 50 years, primary productivity in the fjord has increased dramatically. The increase of the AR of the sulfur bacterial biomarkers may, besides a general rise of primary productivity, also be explained by an extension of euxinic conditions, i.e. a shoaling of the chemocline. It is, indeed, likely that the inferred increase in primary productivity resulted in a higher availability of degradable organic matter and subsequent an enhanced consumption of dissolved oxygen in the water column.

One explanation for the increased primary production is anthropogenically induced eutrophication, which is commonly reported for coastal regions [Zimmerman and Canuel, 2000; Struck *et al.*, 2000] and lakes [e.g. Rieley *et al.*, 1991a]. In Norway, eutrophication and a consequent intensification of algal blooms has been recorded in fjords in the last decades, spreading from south Norway to the North along the coast [Johannessen and Dahl, 1996; Dale *et al.*, 1999 and references cited therein]. Although anthropogenically induced eutrophication is a viable explanation for the higher productivity and anoxia, the almost complete cut-off of the fjord from open sea should also be considered. It is likely that the restricted water exchange between open sea and the fjord resulted in an increased efficiency in the trapping of material delivered to the fjord, including nutrients, as reflected by the increasing MAR, thereby causing 'natural' eutrophication of the fjord system. This could have resulted in the same effects on the fjord as would have been caused by anthropogenic eutrophication. The eutrophication of the fjord, be it either anthropogenic or 'natural', may have caused a positive feedback mechanism. Because nutrient levels in anoxic basins and fjords are especially high around the chemocline [e.g. Velinsky and Fogel, 1999; Taylor *et al.*, 2001], (oxic and anoxic) primary production around the chemocline is mostly limited by the amount of light. A shoaling of the chemocline with the related high nutrient levels upward into the photic zone could therefore enhance growth conditions for primary producers, thereby causing a more efficient use and cycling of nutrients.



## **5.5. Conclusions**

Biomarker analysis of Kyllaren fjord sediments, combined with bulk measurements, indicate that during the last centuries the fjord has undergone significant environmental changes. In the first half of the 19<sup>th</sup> century, a change in the precipitation regime is inferred from a higher MAR and terrestrial biomarker ARs. In the last century, and especially in the last decades, a distinct increase in primary productivity is inferred. This was most likely caused by a combination of anthropogenic eutrophication and 'natural' eutrophication from the transformation of the fjord from an open to a confined system by the building of a partially open dam in 1954. Low algal and bacterial biomarker  $\delta^{13}\text{C}$  values suggests active carbon recycling, consistent with a shallow chemocline. It is hypothesized that a side-effect of eutrophication, the shoaling of the fjord chemocline, played a mediating role in the change towards a higher productivity, by enhancing nutrient and carbon recycling.

## **Acknowledgements**

Ir. M. Kok is thanked for collecting the samples and S. Aas and E. Torgersen for providing background data. The Norwegian part of the project was funded by the environmental agencies of the Sogn og Fjordane County and Askvoll Community in Norway. Utrecht University (Netherlands), University of Bergen (Norway), and Risø National Laboratory (Denmark) are acknowledged for the use of some of their instrumentation.



## Chapter 6

### Pre- and post-industrial environmental changes as revealed by the biogeochemical sedimentary record of Drammensfjord, Norway

*Rienk H. Smittenberg, Marianne Baas, Michael J. Green, Ellen C. Hopmans, Stefan Schouten and Jaap S. Sinninghe Damsté*

Submitted to 'Marine Geology'

**Abstract** The biogeochemical sedimentary record of the anoxic Drammensfjord, Norway, was investigated on a decadal to centennial time scale over the last millennium, in order to reconstruct the pre-industrial fjord environment and ecosystem and human-induced environmental changes. The sediments were dated by a combination of  $^{14}\text{C}$ - and  $^{210}\text{Pb}$ -analysis and varve counting. Analysis of the bulk sedimentary parameters and of the biomarker distribution revealed that the sedimentary organic matter of the fjord is primarily of terrigenous origin, indicating that the fjord was oligotrophic or mesotrophic. The fjord's bottom water has been continuously euxinic since at least 1000 AD, but photic zone euxinia occurred only irregularly in the fjord. The organic matter flux and composition remained virtually invariable until the 18<sup>th</sup> century. After that time the flux of material derived from coniferous trees starts to increase, indicated by elevated concentrations of dehydroabietic acid and related compounds, marking the onset of sawmill activities in the hinterland. Slow bacterial degradation of this relatively nutrient-poor organic waste caused a gradual eutrophication trend, which is reflected in increased zooplankton and archaeal biomarker accumulation rates. After the industrial revolution around 1850 AD the flux of organic waste from sawmills and paper mills increased substantially. Together with the growing population of the area with accompanying domestic and agricultural waste, the eutrophication process was accelerated, favouring diatoms to thrive, thereby outcompeting other phytoplankton species.

#### 6.1. Introduction

Coastal areas harbour important and intricate ecosystems representing a large part of the world's biodiversity, due to their fertility and dynamic nature. Not accidentally, coastal areas are also the most heavily populated in the world and they are of high agricultural and economic importance. In the last century, visible environmental deterioration of many coastal areas pressed the need for environmental monitoring, often initiated by governments after public concern [e.g. <http://www.epa.gov>; <http://www.rivm.nl>; <http://www.environment.no>], in order to gain insight into ecosystem dynamics and the effects of human activities. However, continuous and comprehensive monitoring started in general only after natural

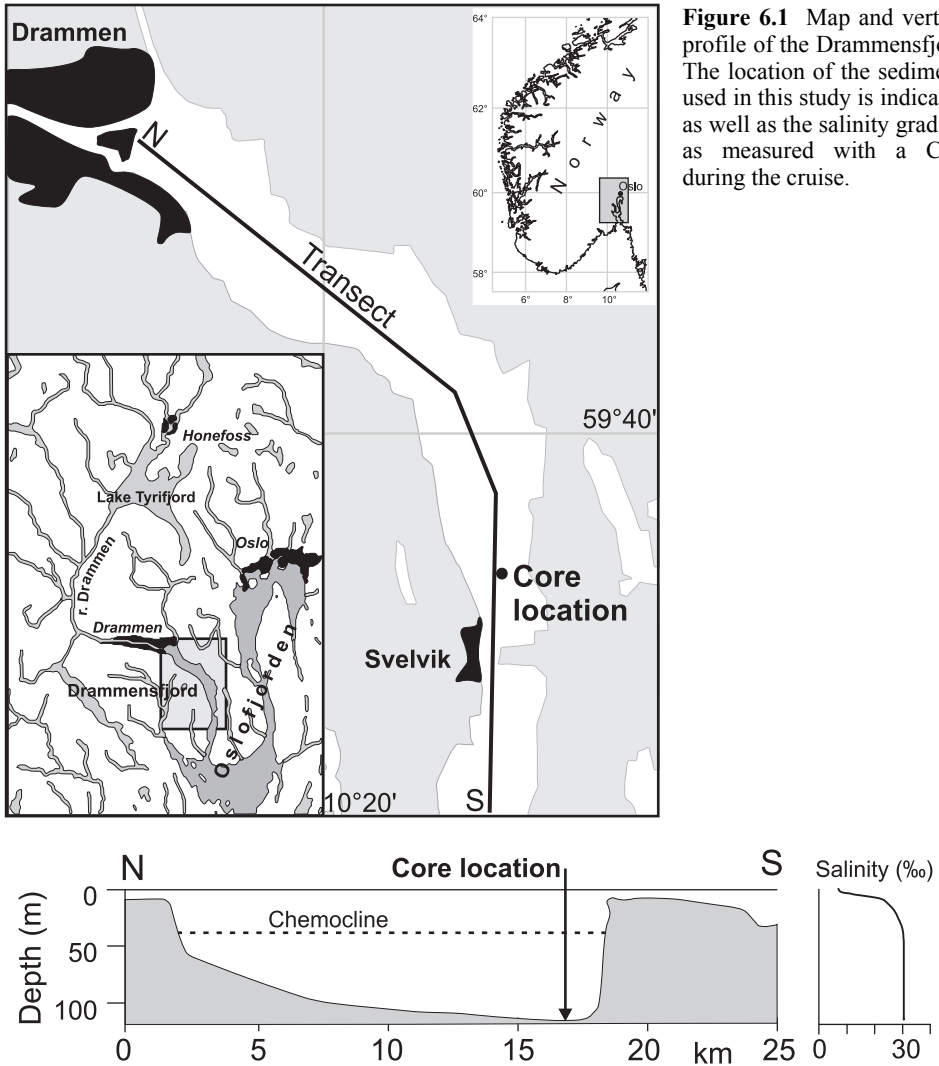


**Figure 6.1** Map and vertical profile of the Drammensfjord. The location of the sediments used in this study is indicated, as well as the salinity gradient as measured with a CTD during the cruise.

ecosystems were severely affected in the last century [Nixon, 1990; Rosenberg *et al.*, 1990; Johannessen and Dahl, 1996; Gowen *et al.*, 1999; Skei *et al.*, 2000] and there is not much information about unaffected coastal environments in populated areas, nor on early anthropogenic effects in pre- and post-industrial times. Furthermore, large-scale factors like climatic variability and variations in oceanic currents may also affect environments [e.g. Broecker, 1995; Hulme *et al.*, 1999; Cullen *et al.*, 2001; Mikalsen *et al.*, 2001; Moy *et al.*, 2002]. Disclosure of sedimentary archives in populated coastal regions may increase knowledge about past environmental change, whether naturally or anthropogenically caused [e.g. Alve, 1991; Zimmerman and Canuel, 2000; Pellatt *et al.*, 2001; St-Onge and Hillaire-Marcel, 2001]. Assemblages of palynomorphs, i.e. of diatoms [Andrén, 1999],

foraminifera [Alve, 1990] or dinoflagellate cysts [Dale *et al.*, 1999] are often used as proxies for recent environmental change. Biogeochemical studies of recent sediments which include biomarkers for the same purpose are less common, although not absent [e.g. Ficken and Farrimond, 1995; Zimmerman and Canuel, 2000; Pinturier-Geiss *et al.*, 2002; Gerdes *et al.*, 2003; Chapter 5], even though this is a widely used methodology in paleoceanographic research [e.g. Brassell *et al.*, 1986]. An advantage of the use of biomarkers is that this allows deconvolution of the various organic matter sources and their variability, thereby revealing information about past physical and chemical conditions, microbial and algal communities and the vegetation of the surrounding area, thus allowing a comprehensive view on the total ecosystem. Determination of the fluxes of various biomarkers gives more insight into the relative importance of various organic matter sources, as well as the response of various organisms to a changing environment.

The sediments of the currently anoxic and polluted Drammensfjord, a side-arm of the greater Oslofjord, Norway (Fig. 6.1) were investigated by Alve [1991] to reconstruct both natural and human-induced environmental alterations over the last 1500 years, for which the author used sediment characteristics, foraminiferal assemblages and pollen grains. In a similar way, eutrophication of the inner Oslofjord was investigated by Dale *et al.* [1999], who used dinoflagellate cyst assemblages to track cultural eutrophication, while Pinturier-Geiss *et al.* [2002] used the abundance of various lipid classes and some biomarkers for the same purpose. These studies concluded that cultural eutrophication started in the area in the first half of the 19<sup>th</sup> century, related with population growth and the industrial development. The study described in this paper aimed to provide more insight into the various organic matter sources and the natural, pre-industrial ecology of the Drammensfjord (Fig. 6.1), and into the early effects of human activities, by analysing the sedimentological archive, focusing on the biomarker distributions and their accumulation rates.

## 6.2. Setting

The Drammensfjord has a length of 20 km and a width of 1.6-3.0 km (Fig. 6.1). It is separated from the greater Oslofjord by a sill at Svelvik, which was dredged around 1900 AD from 6 to 8 m depth, and to 10 m in 1951 AD [Alve, 1990]. Before that time, the ongoing isostatic uplift of Fennoscandia, a result from deglaciation, caused the sill depth to decrease at a rate of 3-4 mm/year in the second half of the Holocene [Pirazzoli, 1991]. Mixing of fresh water of the river Drammen, which enters at the head of the fjord, leads to a brackish surface water layer (salinity 1-10 ‰, depending on the season) that is separated from saline bottom water (30.5 ‰) below 40 m water depth (Fig. 6.1) [Alve, 1990]. River water regulations have smoothed the annual fresh water supply to the fjord in the last 60 years, reducing the effect of spring flooding and increasing the winter supply. This has changed the minimum fresh water supply from winter to late summer, thus increasing the residence time of the surface water during summer. The shallow sill prevents the exchange of bottom waters with the open ocean, and degradation of organic matter, partly by sulphate reducers, leads to euxinic conditions. Oxygen depletion was first detected in 1899 AD, and

the presence of H<sub>2</sub>S in June 1933 [Öztürk, 1995 and references therein]. Ingression of oceanic waters occurs currently once every 3-5 years, mainly between November and May, displacing parts of the euxinic bottom waters upwards [Richards, 1965; Alve, 1995]. The anoxic bottom water conditions prohibit infauna, resulting in the preservation of the laminated sedimentary structure.

It is known from historical records that since at least 1750 AD the fjord has been increasingly affected by sawdust and wood-chips from sawmills along the river Drammen and upstream fresh water bodies [Alve, 1990; 1991 and references therein]. After 1870 AD, a number of paper and pulp mills were established, causing a substantial increase in the amount of fibrous material to the fjord. In the 20<sup>th</sup> century the supply of organic matter to the fjord increased even more, but during the first half of the 1970's most of the paper industry was closed down. During the last century domestic and agricultural waste also increased drastically [Richards and Benson, 1961; Alve, 1991].

### 6.3. Sampling and methods

#### 6.3.1. Sediment collection and sub-sampling

The sediments used for this study were selected from a suite of box, gravity and piston cores that were recovered from the Drammensfjord, Norway, during a cruise in October 1999 with the R/V 'Pelagia' (Fig. 6.1). Several surface sediment cores from the depocenter of the fjord (59°37'99" N, 10°25'39" E) were obtained by taking sub-cores from a box core. From one of these sub-cores, sub-samples of known volume were taken to determine the bulk density. Another sub-core was sliced into 0.5 cm thick slices immediately after recovery for geochemical analysis. The slices were stored on board at -20°C and later freeze-dried in the laboratory. Sections of a piston core (coded D1G), obtained from the same location, were sliced into two halves and stored at 4°C before sub-sampling. The upper part was photographed for grey-scale analysis. One half of the upper section, with a length of 95 cm, was sub-sampled into sections of 0.5 to 7 cm (Fig. 6.2), depending on sediment colour and laminae thickness, and the sub-samples were subsequently freeze-dried. Approximately half of these sub-samples, evenly distributed over the core, were ground to a fine powder and analysed. From the other half of the upper piston core section, sub-samples of known volume were taken for bulk density measurement, as well as for microscopic analysis.

#### 6.3.2. Sedimentological and bulk geochemical analysis

In order to perform varve counting, parts of the piston and gravity cores were photographed with dia-film, which were after development digitised for computerised grey-scale analysis in a similar way as described by *Nederbragt et al.* [2000]. A backscatter electron image (BSEI) was taken from a thin section made from a varved interval at around 190 cm of one

of the piston cores (code D1L), corresponding to the varved interval at around 175 cm depth of core DIG (Fig. 6.2), in order to assess the composition of the varves. A number of smear slides made from sediment sub-samples of the upper 2 m of core DIG were analysed using a normal light microscope. Total organic carbon contents (TOC) and nitrogen (TN) contents were determined on acid-treated (1N HCl, 12 h.) sediment sub-samples using a LECO Element Analyzer. Bulk stable carbon isotopic compositions were determined on a Carlo Erba 1112 series Flash Element Analyzer coupled to a Finnigan DELTA<sup>PLUS</sup> isotope-ratio-monitoring mass-spectrometer and are reported in standard delta notation relative to the VPDB standard, with a standard deviation of 0.1‰. Five freeze-dried 0.5 cm thick box core slices were analysed with Rock-Eval 6 (version 3.02x05) at the University of Utrecht (Netherlands) to obtain hydrogen (HI) and oxygen indices (OI) of the sedimentary organic matter.

### 6.3.3. Dating

For dating purposes, <sup>210</sup>Pb, <sup>137</sup>Cs and <sup>226</sup>Ra radioactivities of a selection of the 0.5 cm thick freeze-dried box core slices were determined, as well as the <sup>210</sup>Pb activities of sediment sub-samples from 0 - 5 cm, 7.5 - 12 cm and 85.5 - 88 cm piston core depth. To determine the <sup>210</sup>Pb activity the sediment samples were spiked with <sup>209</sup>Po and digested with 5 ml concentrated HNO<sub>3</sub> and 5 ml concentrated HF in a microwave oven for 3 h. Subsequently, 2 ml 3.5% HClO<sub>4</sub> was added and the acids were removed by evaporation. The resulting precipitate was re-dissolved in 40 ml 0.5M HCl, followed by spontaneous electrochemical deposition of the Po-isotopes onto silver in 0.5M HCl at 80°C for 4 h. The activity of <sup>210</sup>Pb was measured via its  $\alpha$ -particle emitting granddaughter isotope <sup>210</sup>Po with a Passivated Implanted Planar Silicon detector (Canberra A-600-23-AM). Counting time was 48 h, and the counting error 3-7%. The level of <sup>137</sup>Cs was measured using a high purity germanium  $\gamma$ -ray well-detector (Canberra GCW 2522) with 25% relative efficiency. Counting time was 1 to 3 days, resulting in a counting error of 5-10%. The gamma detector was calibrated with a QCY48 standard mixed with sediment [Zuo *et al.*, 1991; De Haas *et al.*, 1997]. The <sup>226</sup>Ra activity was measured after an equilibrium time of 1 month, using the same detector as used for <sup>137</sup>Cs. The activity was calibrated against a dilution series of the IAEA Uranium RGU-1 standard.

Two pieces of wood remains obtained from the upper part of the piston core sediment were radiocarbon dated following standard procedures. Radiocarbon ages were calibrated towards calendar ages by using the atmospheric calibration curve of *Stuiver et al.* [1998a]. Compound-specific radiocarbon analyses were performed on several isolated glycerol dialkyl glycerol tetraethers (GDGTs), following the procedure described in *Smittenberg et al.* [2002, chapter 2]. The selected GDGTs were isolated from the uppermost (0 - 10 cm) and lowermost (25 - 35 cm) part of the sliced and freeze-dried box core sediment and furthermore from sub-samples from 0 - 7.5 cm and 85 - 92 cm piston core depth. <sup>14</sup>C analysis was performed at Woods Hole Oceanographic Institution (WHOI) as described by *Eglinton et al.* [1996] and in Chapter 3.

### 6.3.4. Biomarker analysis

#### *Extraction and fractionation*

For biomarker analysis, part of the freeze dried sediment subsamples from the studied piston core were extracted with a dichloromethane-methanol (DCM-MeOH, 9:1 v/v) mixture using an Automated Solvent Extractor (Dionex Corp., Sunnyvale, CA, USA), deployed over three static cycles of 5 min of 100°C and 1000 psi. To remove salts, the extracts were washed with double distilled water against DCM in a separatory funnel, and dried over Na<sub>2</sub>SO<sub>4</sub>. The bulk of the solvent was removed by rotary evaporation and the remaining solvent under a stream of nitrogen. The residues were taken up into DCM and stirred overnight with activated Cu(s) to remove elemental sulfur. For quantification, a known amount of deuterated *ante-iso* C<sub>22</sub> alkane was added as an internal standard to weighed aliquots of the total lipid extracts. The aliquots were subsequently methylated with diazomethane (CH<sub>2</sub>N<sub>2</sub>) in diethyl ether to convert fatty acids into their corresponding methyl esters. To remove very polar material, the aliquots were eluted with ethyl acetate over a small column filled with silica. The ethyl acetate was removed under a stream of nitrogen, after which the residues were dissolved in 25 µl pyridine to which 25 µl bis(trimethylsilyl)trifluoroacetamide (BSTFA) was added. This mixture was heated at 60°C for 20 min to convert alcohols into their corresponding trimethylsilyl ethers. The derivatized fractions were diluted to 1 mg/ml in ethyl acetate and analyzed by gas chromatography (GC) and gas chromatography – mass spectrometry (GC-MS).

For analysis of glycerol dialkyl glycerol tetraethers (GDGTs) by high performance liquid chromatography – mass spectrometry (HPLC/MS), aliquots of the total lipid extracts were separated into two fractions by column chromatography over activated Al<sub>2</sub>O<sub>3</sub> with *n*-hexane-DCM (9:1 v/v; 4 column volumes; apolar fraction) and DCM-MeOH (1:1 v/v; 3 column volumes; polar fraction) as eluents. The solvents of the polar fractions were removed as described above, and the residues dissolved by sonication (10 min) in *n*-hexane / iso-propanol (99:1; v/v). The resulting suspensions were centrifuged (1 min, 2300 x *g*) and the supernatants were filtered through a 4-mm-diameter PTFE filter (0.45 µm pore size) to produce fractions suitable for analysis by HPLC.

For carotenoid analysis, *ca.* 5 g. of the freeze-dried sediment sub-samples were three times ultrasonically extracted with acetone for 3 min. under continuous cooling with ice. The combined extracts were then rotary evaporated towards a small volume and dried under nitrogen. The residues were subsequently taken up in DCM and eluted over a small column filled with silica, dried under a stream of nitrogen and dissolved into a known volume of acetone. To avoid degradation, extracts were stored at -20°C and measured the same day. Direct light and heat exposure was avoided as much as possible during the work-up procedure and analysis.



### *Gas chromatography and gas chromatography – mass spectroscopy*

Gas chromatography was performed with a Hewlett-Packard 5890 gas chromatograph equipped with an FID detector and a fused silica column (25 m x 0.32 mm) coated with CP Sil 5 (film thickness = 0.12 µm). The carrier gas was helium. The samples, dissolved in ethyl acetate, were on column injected at 70°C. Subsequently the oven was programmed to 130°C at 20°C/min, then at 4°C/min to 320°C at which it was held for 25 min.

Individual lipids were identified by gas chromatography – mass spectrometry (GC-MS) using a Hewlett-Packard 5890 gas chromatograph interfaced to a VG Autospec Ultima mass spectrometer operated at 70 eV with a mass range of  $m/z$  50-800 and a cycle time of 1.7 s (resolution 1000). The gas chromatograph was equipped and programmed as described above. Compounds were identified by comparison of mass spectra and retention times with those reported in the literature. Quantification of selected compounds was performed by integration of peak areas of one or more diagnostic mass fragments of the different compounds and comparing these with that of the internal standard. The areas of the diagnostic mass fragments were corrected for their relative intensity compared to that of the total ion current using a response factor.

### *High performance liquid chromatography – mass spectrometry (HPLC/MS)*

For GDGT-analysis, high performance liquid chromatography – mass spectrometry (HPLC/MS) was performed using an HP 1100 series HPLC/MS equipped with an auto-injector, single quadrupole mass detector, and Chemstation chromatography manager software, following the method as described by *Hopmans et al.* [2000]. Quantification was performed by integration of peaks in the summed mass chromatograms of  $[M+H]^+$  and  $[M+H]^{+1}$  and comparison with a standard curve obtained using a dilution series of a known amount of a GDGT-0 standard. For carotenoid analysis, the same HPLC system was used as described above, following the method described by *Menzel et al.* [2002], except that only a photo diode array detector was used and no mass detector.

## **6.4. Results and discussion**

### *6.4.1. Sedimentology and varve formation*

The upper part of sediment from the depocenter of the Drammensfjord consists of black, unconsolidated material. Distinctive mm-scale black and grey coloured laminae or varves become increasingly visible down core, and prevail until 92 cm piston core depth (Fig. 6.2). The sediment layers and laminations are often not horizontally oriented (Fig. 6.2). Microscopic analysis of smear slides taken at various depths revealed that the laminated sections were dominated by clay and silt-sized mineral material, though with a substantial contribution of diatoms, other microfossils and structured and amorphous organic matter. In the non-laminated sections the contribution of biogenic material appears to be lower.

The BSEI of the laminated section of core D1L (Fig. 6.3) revealed that the varves are generally composed of four layers: layer 1 is dominated by silt-sized grains of mainly quartz and feldspar, also containing structured and amorphous organic matter and a larger clay content. This layer is interpreted as being deposited during spring floods when larger currents entrain coarser material to the fjord and of a predominantly terrigenous origin. A

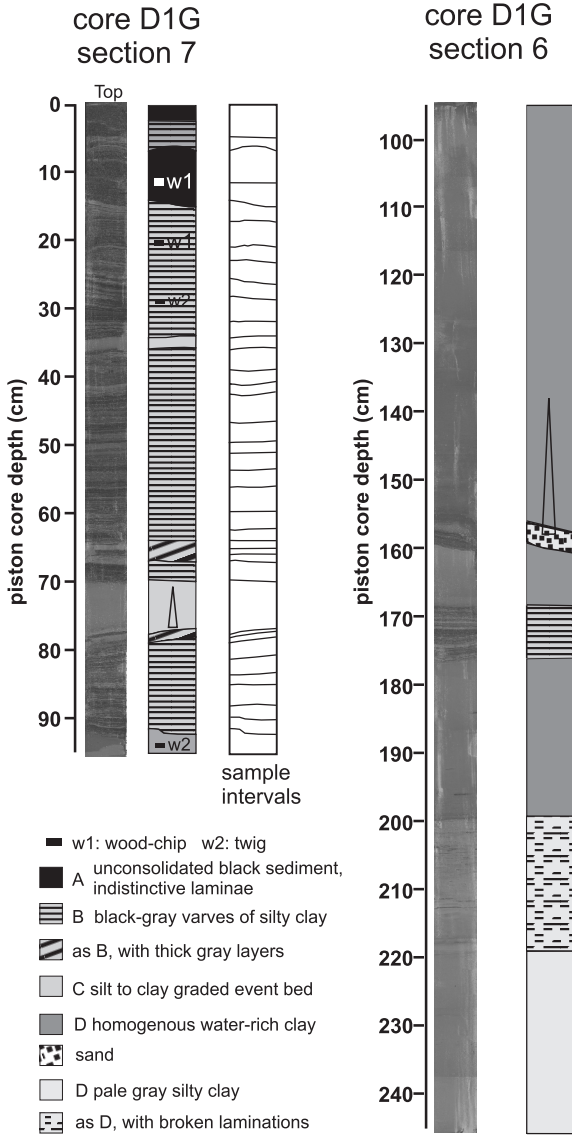


**Figure 6.2** Photograph and sedimentological graphic of the upper 2.5 m of the investigated piston core, divided into two sections (D1G-7 and D1G-6). The sub-sampling intervals used for biogeochemical analysis are indicated.

generally steep gradient occurs towards layer 2 that mainly consists of the same material but with a much smaller silt fraction. This layer probably originates from the slower settling of clay-sized material also introduced to the fjord by spring flooding. Layer 3 has approximately the same matrix as layer 2, but the darker colour indicates a higher contribution of organic matter. This is interpreted as sediment from late spring and summer, when primary productivity is high and organic matter and biogenic inorganic matter are deposited. Layer 4 is then similar to layer 2, and likely to be deposited during autumn and winter when both primary productivity and fresh water input are low.

After recovery of the sediments, exposure to oxygen caused the black colour in the laminated sections (Fig. 6.2) to turn gradually into brown-red and subsequently into the same grey as the neighbouring sediment, leaving the laminated structure hardly visible. This confirms earlier suggestions of *Alve* [1990] that the black colour is caused by iron sulphides formed through reaction of  $H_2S$  and reduced iron. The alternation of black and grey laminae (Fig. 6.3) seems to point to a yearly cycle in the deposition or preservation of

iron sulphides, similar to e.g. the anoxic sediments of Orca basin [Sheu and Presley, 1986], but the black-grey laminations only roughly compare with the annual varves visible on the BSEI (Fig. 6.3). The formation of iron sulphides under euxinic circumstances is influenced by the availability of decomposable organic matter, but more by the reactivity of detrital iron minerals [Bernier, 1984]. This may take place in the water column as well as in the sediment, and is thus relatively independent from sedimentation patterns [Bernier, 1984]. As a reference, the alternation of black and grey laminae in the Orca basin is attributed to a variation between a) a high content of FeS minerals, which are especially responsible for the black colouring of sediments, deposited during times of low mixing; and b) a relatively high content of grey pyrite (FeS<sub>2</sub>) that forms upon reaction of FeS with elemental sulphur [Sheu and Presley, 1986], made available through oxidation of FeS and H<sub>2</sub>S during times of increased mixing. Because it is unlikely that there is a large variation in the supply of reactive iron to the Drammensfjord, it is most likely that the black-grey alternation of the Drammensfjord is caused by the same mechanism as in the Orca Basin. The near absence of grey layers in the upper sediment (Fig. 6.2) may be explained by a larger degree of euxinia in the fjord and a higher production of FeS minerals that are not completely converted to FeS<sub>2</sub> during times of mixing. A yearly variation in the extent of mixing through storms and bottom water renewals will have an effect on the relative thickness of black and grey laminations, and this also suggests that not every black-grey couplet (varve) may represent one year, but could as well be sub-annual or from multiple years.

Microscopic analysis of the grey-coloured layer between 70 and 77 cm piston core depth (Fig. 6.2) revealed a fining upwards sequence from silt to clay with a lower diatomaceous contribution and with a lower TOC content than the surrounding sediment. This indicates that this material is a turbidite, presumably originating from the steep side of the fjord. Below 92 cm piston core depth a different sedimentary unit occurs, consisting of water-rich homogeneous grey clay, which extends down to approximately 135 cm piston core depth, where it meets a fining upwards sequence that starts with coarse sand at 158 cm depth (Fig. 6.2). The latter sequence is certainly an event bed, but it is impossible to determine whether the upper part of homogenous clay is still part of the event, or whether this is sediment slowly deposited under oxic conditions. Below the sand a layer of homogenous water-rich grey clay occurs, which is interrupted by a section of the same fine laminations as observed in the upper meter, between 167 and 176 cm core depth (Fig. 6.2). A distinct transition at 200 cm towards stiff lighter-grey coloured silty clay is encountered, which between 220 and 200 cm depth contains apparently bioturbated relicts of black laminae.

The dry bulk density increases from 0.25 g cm<sup>-3</sup> at 3 cm box-core depth to around 0.7 g cm<sup>-3</sup> at 25 cm (Fig. 6.4), while the dry bulk densities measured on the piston core sediments are 0.8 ± 0.08 g cm<sup>-3</sup>. The clear decrease with depth is attributed to compaction of the sediment.

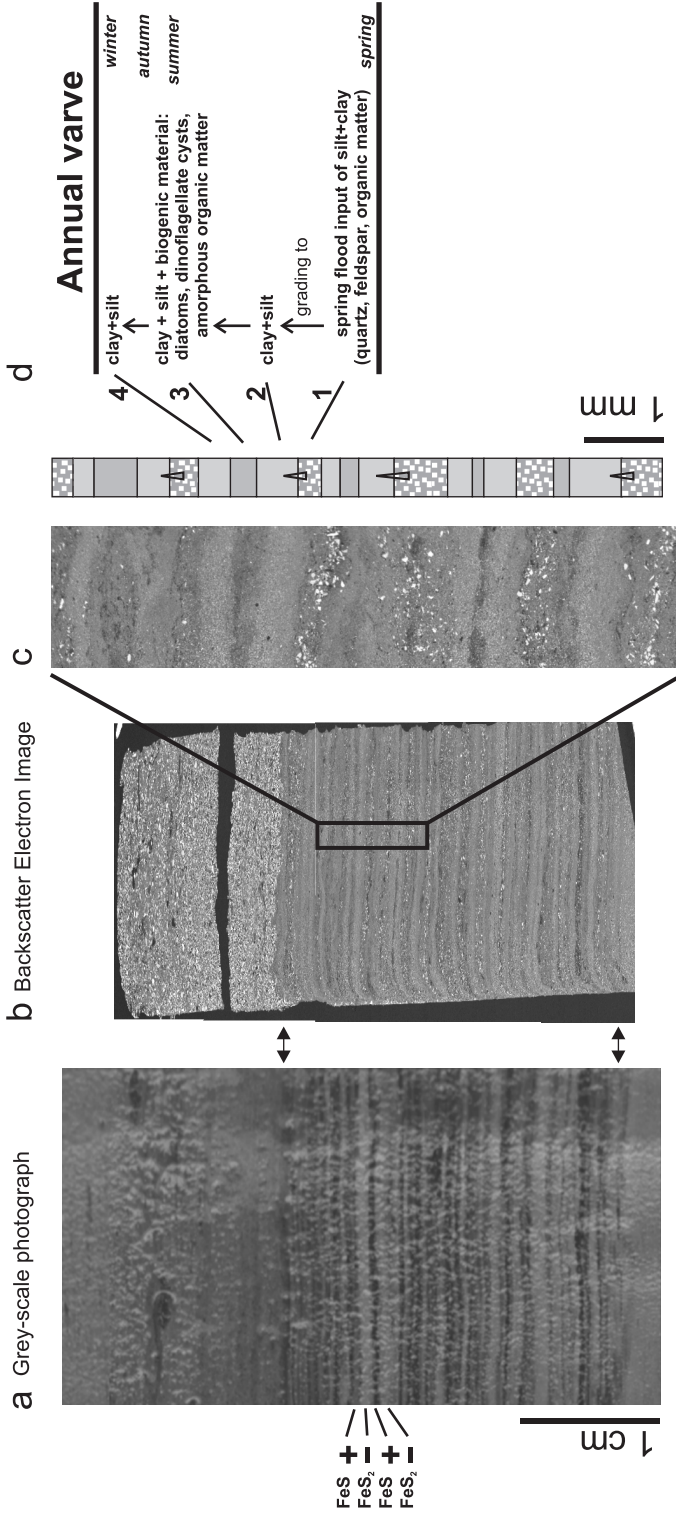


**Figure 6.3** (a) Backscatter Electron Image (BSEI) and (b) photograph of a laminated section from around 190 cm depth of piston core D1L, which can be correlated with the laminated section of 168-177 cm core depth of DIG (Fig. 2). Repetitive sequences (c) of silt to clay-sized layers with a varying contribution of organic matter can clearly be observed on the BSEI, which are interpreted to be annual varves (d). The varves cannot be readily correlated with the black and grey layers on the photograph, which are interpreted as resulting from the presence and absence of iron sulfides. However, the number of sequences is essentially the same for both, indicating that the black and grey layering is also annual.

## 6.4.2. Dating and sediment accumulation rates

The  $^{210}\text{Pb}$  profile obtained from the box core sediment does not reflect a clear exponential decrease (Fig. 6.4) as was observed for another location in the fjord [Zegers *et al.*, 2003], even when plotted against cumulative dry mass (not shown). Possibly the upper box core sediments were somewhat disturbed during sampling. The positive shift of the  $^{210}\text{Pb}$  activity below 15 cm core depth may mark the regime change of fresh water supply due to river water regulations around 1930 AD, which probably also affected the sediment supply. It may also be related to the dredging of the sill from 6 to 10 m depth around the same time, resulting in a decrease in the sedimentation rate. The  $^{226}\text{Ra}$  activity, which determines the background  $^{210}\text{Pb}$  activity, varies between 60 and 70 Bq kg $^{-1}$  (Fig. 6.4), while the  $^{210}\text{Pb}$  activity at 85 cm piston core depth, which should also reflect the background value, is  $70 \pm 5$  Bq kg $^{-1}$ . The maximum in the  $^{137}\text{Cs}$  activity at 7.5 cm box core depth (Fig. 6.4) indicates that at that depth the sediment was deposited in 1986 AD, when the Chernobyl nuclear power plant accident happened. Below 11 cm box core depth no  $^{137}\text{Cs}$  activity is detected, pointing towards sediments from before the first atmospheric nuclear weapons testings in the early 1950's. The  $^{210}\text{Pb}$  activities at 0-5 cm and 7.5-12 cm piston core depth are slightly above background, indicating that at 7.5-12 cm the sediments are from after 1850 AD, while the sediment between 0-5 cm seems to be from after 1900 AD. The radiocarbon age of the wood chip recovered from 11-12 cm is  $240 \pm 45$   $^{14}\text{C}$  yr BP (Table 6.1). Calibration towards calendar age resulted in three possible calendar ages, namely 1940 AD,  $1790 \pm 25$  AD and  $1660 \pm 25$  AD. Taking the  $^{210}\text{Pb}$  results into account, the calibrated  $^{14}\text{C}$  age of 1790 AD for the piece of wood recovered from 11-12 cm piston core depth seems to be the most probable, as the other two possible dates are either regarded too old (1660 AD), or too young (1940 AD). However, 1790 AD also does not correspond well with the  $^{210}\text{Pb}$ -inferred sediment age of *ca.* 1870 AD at 12 cm piston core depth. Possibly, the wood-chip

**Table 6.1**  $\delta^{13}\text{C}$  values and radiocarbon ages of two organic macrofossils and a suite of isolated GDGTs from the depocenter of the Fjord. Core: P = piston core, B = Box core.  $^{\&}$  Sediment ages as derived from the age model described in the text. \* Reservoir age = measured  $^{14}\text{C}$  age minus atmospheric  $^{14}\text{C}$  age.

Compound	Core	depth (cm)	$\delta^{13}\text{C}$ (‰)	$^{14}\text{C}$ age (yr BP)	calibrated age (yr AD $\pm 1\sigma$ )	Sediment age (yr AD) $^{\&}$	Res. age*
wood-chip	P	11-12	-25.3	$240 \pm 45$	1657;1788;1940 $\pm 25$	1870 $\pm 30$	
twig	P	94	-27.5	$1030 \pm 35$	1008 $\pm 20$		
GDGT-0	B	0-10	-24.7	<0	>1950 AD	1998-1990	
Crenarchaeol	B	0-10	-23.9	<0	>1950 AD	1998-1990	
GDGT-0	B	25-35	-25.7	$440 \pm 90$		1880-1820	325
Crenarchaeol	B	25-35	-24.8	$385 \pm 60$		1880-1820	270
GDGT's F+G+H	B	25-35	-28.4	$1610 \pm 35$		1880-1820	1495
GDGT-0	P	0-7.5	-25.2	$520 \pm 75$		1930-1890	420
Crenarchaeol	P	0-7.5	-24.5	$860 \pm 120$		1930-1890	760
Crenarchaeol	P	85-92	-24.5	$1020 \pm 240$		1140-1040	90
GDGT's F+G+H	P	85-92	-28.6	$1050 \pm 80$		1140-1040	120

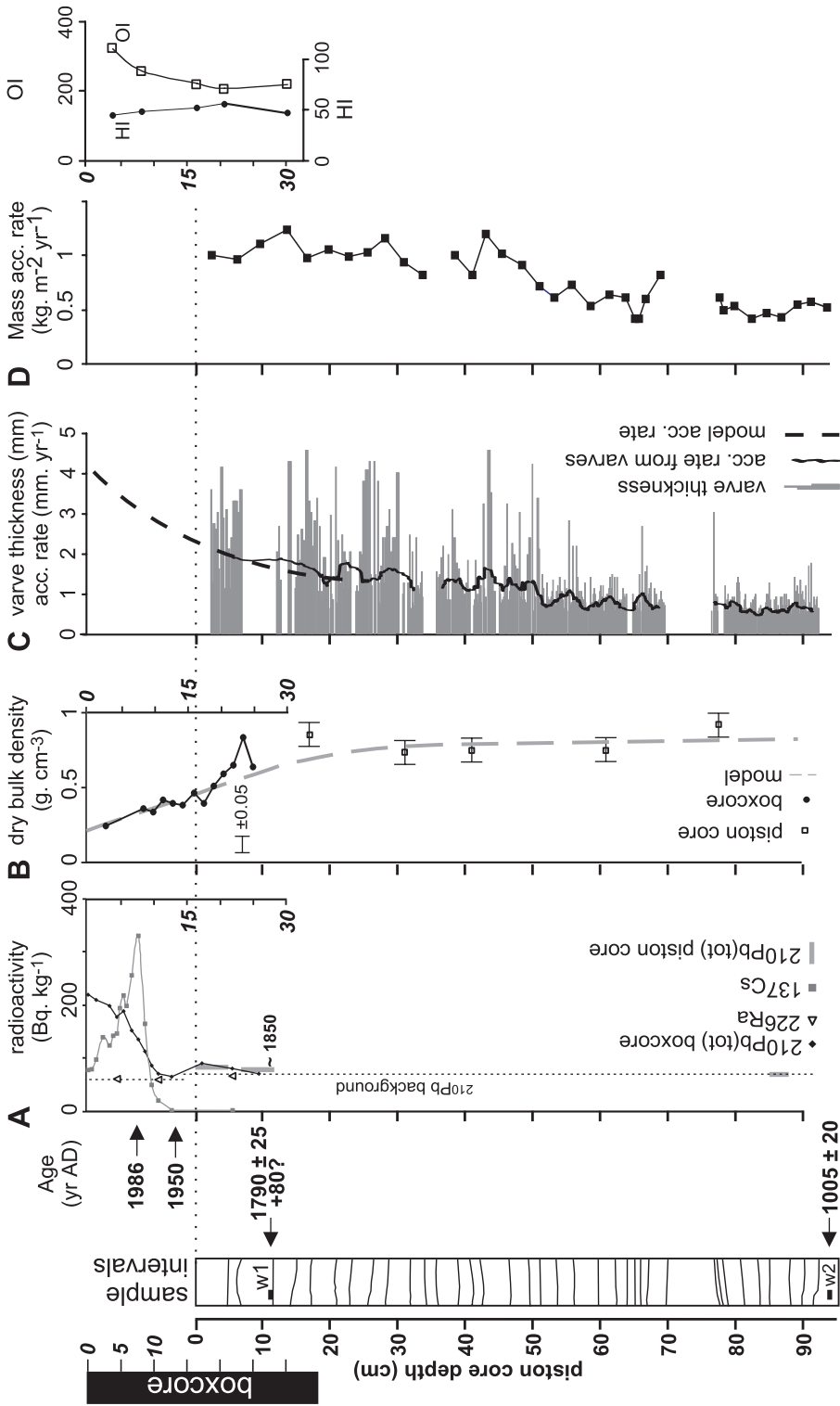


**Figure 6.4** <sup>210</sup>Pb, <sup>137</sup>Cs and <sup>226</sup>Ra data (A), dry bulk density (B), varve-thickness (C) and mass accumulation rate (D) of the sediment of Drammensfjord, as determined on sub-samples of a box-core and the upper meter of a piston core recovered from the depocenter of the fjord. The oxygen indices (OI) and hydrogen indices (HI) measured on box-core material are also shown. The sampling intervals used for geochemical analysis are indicated, as well as ages determined by radiometric analyses. The varve thickness data (C) are the combined thickness of a black and a grey layer (Fig. 6.3). Varves >5mm are considered to be >1yr and are not shown. The accumulation rate (C, black line) is based upon the varve thickness data. The dashed lines in plots B and C represent a fitted model based on the data. Sediment accumulation rates (D) were calculated based upon the fitted bulk density model and the accumulation rates based upon the varve thickness data.

did not directly enter the fjord sediment after its growth, but remained some time on the continent before it was transported to the fjord sediment. For instance, it could be a piece of wood derived from a full-grown and aged tree that was cut for commercial use, as indicated by its angular appearance. The calibrated age of  $1008 \pm 20$  yr of the twig at 94 cm piston core depth ( $^{14}\text{C}$  age  $1030 \pm 35$  yr BP) is considered unambiguous, which means that the laminated sediments above 92 cm piston core depth were deposited after that date.

The number of varves counted between 0 and 94 cm depth by grey-scale analysis was 735. However, in the upper black, relatively unconsolidated part of the sediment no varves could be determined. Furthermore, as described above, the counted varves may in some cases be sub-annual, while other ones may be from more than one year. To correct for this, all unusually thick varves within the sequence were attributed to multiple years. The sediments between 70-77 cm and 35-37 cm depth (Fig. 6.2) were identified as redeposited sediment beds (turbidites), and it is likely that at the bottom of these beds some laminated sediment was eroded. After these corrections, the varve thickness data resulted in an age model that compared favourably with the above sediment ages determined by radiometric analysis. The decreasing varve thickness and accumulation rate with time can be mainly attributed to compaction. Combined with the bulk density data a gradually increasing mass accumulation rate from approximately  $0.5$  towards  $1.0 \text{ kg m}^{-2} \text{ yr}^{-1}$  over the last century is calculated (Fig. 6.4). This may be due to the slow decrease of the sill depth due to the isostatic uplift of the Scandinavian continent at  $3\text{-}4 \text{ mm/year}$  [Pirazzoli, 1991], resulting in a gradually increasing containment of the sediment by the shallow sill.

#### 6.4.3. Pre- and post-industrial biogeochemistry of the fjord system

##### *Bulk organic matter sources*

The accumulation rate (AR) of the total organic carbon (TOC) of the Drammensfjord sediment gradually increases from  $5$  to  $10 \text{ g m}^{-2} \text{ yr}^{-1}$  during the period 1000 - 1800 AD (Fig. 6.5), while the total nitrogen (TN) AR shows approximately the same profile (Fig. 6.5). These ARs closely correlate with the gradual increase in the mass accumulation rate (Fig. 6.5). This suggests that, because the sediment is predominantly of a terrigenous origin, most organic matter is also terrigenous. The  $\delta^{13}\text{C}_{\text{TOC}}$  content increases slightly from  $-27.6\text{‰}$  at 1100 AD to  $-26.7\text{‰}$  around 1850 AD (Fig. 6.5), values which are comparable with the two  $\delta^{13}\text{C}$  values obtained from the two pieces of wood analysed for  $^{14}\text{C}$ ,  $-25.3\text{‰}$  and  $-27.5\text{‰}$  (Table 6.1). This corroborates with the earlier interpretation of a predominantly terrigenous origin of the organic matter. The observed gradual  $\delta^{13}\text{C}_{\text{TOC}}$  increase may stem from a gradual relative increase of marine derived organic matter, as this generally exhibits lower  $\delta^{13}\text{C}$  values than terrigenous organic matter [Deines, 1980; Tyson, 1995c]. However, a gradual change in the composition of the terrigenous organic matter can also not be excluded, taking the different  $\delta^{13}\text{C}$  values of the wood pieces into consideration. The Rock-Eval hydrogen and oxygen indices, respectively *ca.* 50 and 200-300 (Fig. 6.4), obtained for the upper sediments of the fjord, also indicate a predominantly terrestrial origin of the

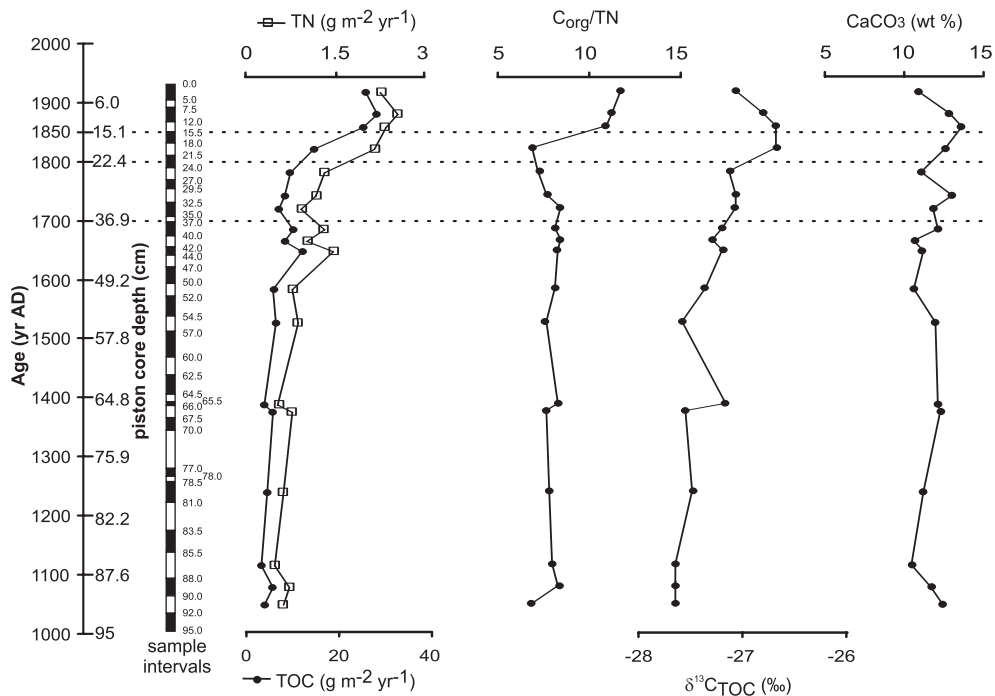


**Figure 6.5** Age/depth profiles of accumulation rates of total organic carbon (TOC) and total nitrogen (TN),  $C_{\text{org}}/\text{TN}$  ratio,  $\delta^{13}\text{C}_{\text{TOC}}$  values and  $\text{CaCO}_3$  contents.

organic matter [type IV, e.g. *Whelan and Thompson-Rizer, 1993*], especially when the anoxic conditions in the fjord are considered. The invariable  $C_{\text{org}}/\text{TN}$  ratio (g/g) of *ca.* 8, until 1800 AD, is similar to many anoxic fjord sediments [*Tyson, 1995a* and references therein], receiving riverine particulate organic matter. In the 18<sup>th</sup> century the accumulation rates of TOC and TN (Fig. 6.5) start to increase substantially to  $30 \text{ g m}^{-2} \text{ yr}^{-1}$  for TOC and  $2.5 \text{ m}^{-2} \text{ yr}^{-1}$  for TN around 1900 AD. This is likely to be related to the increasing sawmill activities in the region of the fjord, resulting in an increased flux of organic waste to the fjord. In the first part of that period the  $C_{\text{org}}/\text{TN}$  ratio decreases gradually from 8 to 7 (Fig. 6.5), with a sudden increase to 12 around 1850 AD. The increase is likely related to industrialisation of the saw- and paper mill industry after 1850 AD, leading to the deposition of large amounts of fibrous organic matter, which generally exhibit high C/N ratio's [*Tyson, 1995a*]. The initial decrease is enigmatic, but may be related to the stimulation of bacterial activity by the initial slow increase of the organic matter load.

### *Terrigenous biomarkers*

The lipid extracts of the sediments are dominated by vascular plant derived long-chain *n*-alkanes, fatty acids and alcohols [*Kolattukudy, 1980*] (Fig. 6.6 and Table 6.2), while



generally less abundant terrigenous biomarkers like alkan-2-ones and wax-esters [e.g. Volkman *et al.*, 1981; chapter 5], are also clearly detectable (Fig. 6.6). This biomarker distribution is in agreement with the dominance of terrigenous organic matter to the fjord as determined by bulk parameters (see above). Besides the very general vascular plant derived *n*-alkyl compounds, dehydroabietic acid (**IV**) was detected throughout the core, except for the lowermost sediments (Fig. 6.6). Its precursor abietic acid (**V**), and product norabietane [Simoneit *et al.*, 1985], and the related compounds pimaric acid (**I**), isopimaric acid (**II**) and their saturated product (**III**) were also found, albeit sometimes in trace amounts. These lipids are a major compound class in the resins of coniferous trees [e.g. Otto and Simoneit, 2002] and have previously been detected in abundance in sediments influenced by paper-mill waste [Simoneit, 1986]. They have also been observed in the sediments of the inner Oslofjord [Pinturier-Geiss *et al.*, 2002].

Another class of compounds indicative of terrigenous input are the branched non-isoprenoidal glycerol dialkyl glycerol tetraethers (GDGTs F+G+H, Fig. 6.7). These compounds have so far only been found in peats, soils and coastal sediments [Sinninghe Damsté *et al.*, 2000], and are currently attributed to a terrigenous prokaryotic source [Schouten *et al.*, 2000b]. The combined non-isoprenoidal GDGTs from 25-35 cm box core depth show a <sup>14</sup>C age of 1610±35 yr BP, pointing towards either extensive pre-ageing of these lipids on the continent [Trumbore, 2000] before transportation to the fjord sediment, or a use of old or fossil carbon derived from e.g. dissolving rock carbonates or slowly degrading organic matter [Heier-Nielsen *et al.*, 1995]. Enigmatically, the combined non-isoprenoidal GDGTs from 85-92 cm piston core depth have an <sup>14</sup>C age of 1050±80 yr BP, which is close to the sediment age, suggesting a carbon source that is in equilibrium with atmospheric CO<sub>2</sub>.

The accumulation rates of the long-chain *n*-alkanes and the fatty acids and alcohols >C<sub>26</sub> (Fig. 6.8) are relatively invariable throughout the core. The same is true for the non-isoprenoidal GDGTs (Fig. 6.9). In contrast, after 1700 AD the distribution of the straight-chain fatty acids and -alcohols, indicated by the average chain lengths (ACL, Fig. 6.8), starts to change towards a dominance of the C<sub>24</sub> homologues, caused by a substantial increase in the accumulation rates of the lower homologues (Fig. 6.6). Furthermore, the coniferous biomarkers dehydroabietic acid and related compounds increase to such extent (Figs. 6.8 and 6.10) that they become dominant lipids in the sediment extracts (Fig. 6.6). This is especially remarkable for the precursor compounds abietic acid and isopimaric acid, which are virtually absent before 1800 AD (Fig. 6.6). These variations in the terrestrial biomarker record indicate that after 1700 AD an ongoing change in the nature of the terrigenously derived organic matter started, with an ever increasing flux of coniferous material to the fjord sediment. Because neither the sediment accumulation rate nor the accumulation rates of the initially dominant terrigenous biomarkers (i.e. the *n*-alkanes, the >C<sub>26</sub> fatty acids and alcohols and the non-isoprenoidal GDGTs) change substantially, an additional input of, and not so much a change to conifer-derived organic matter is inferred.

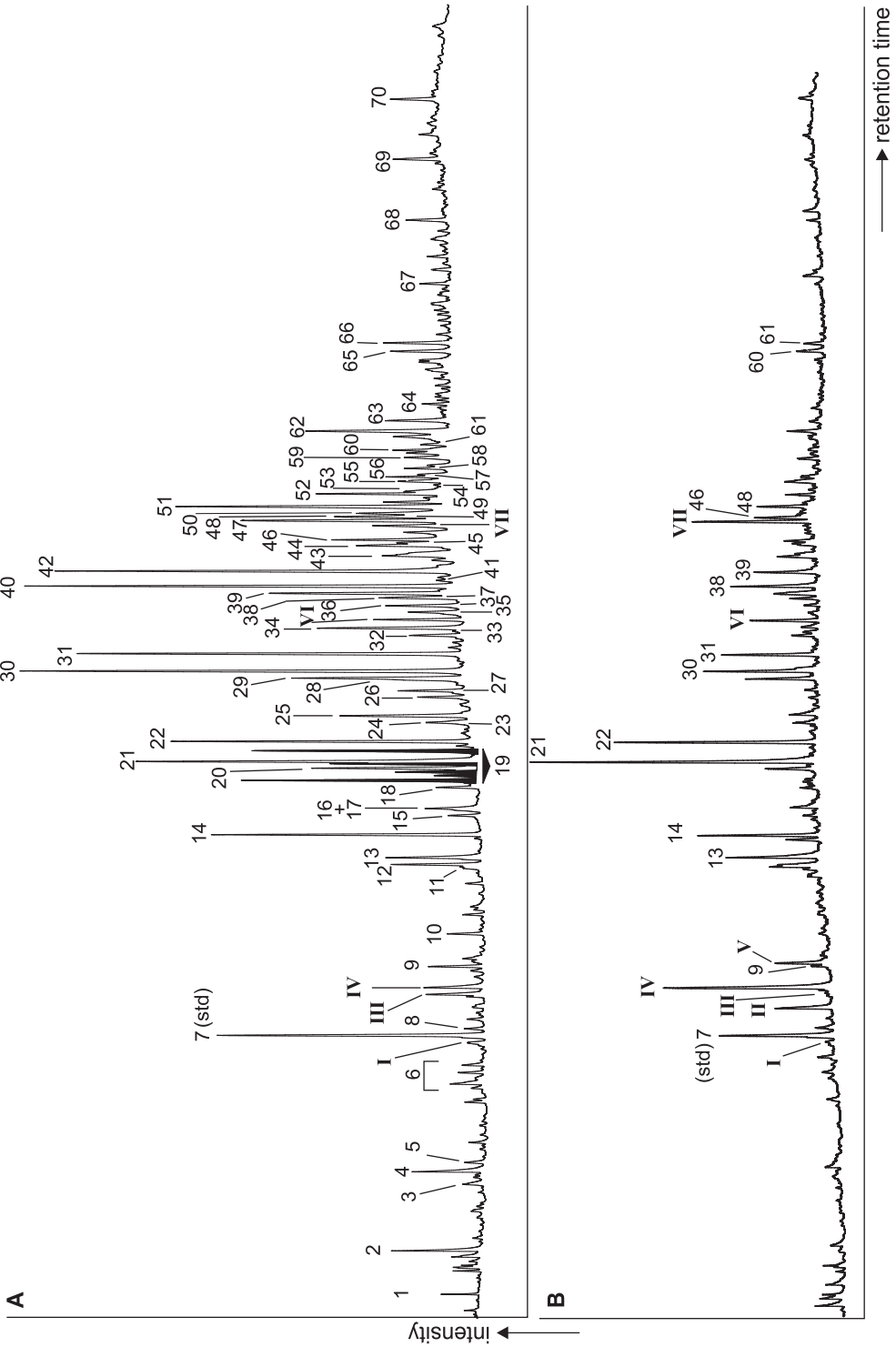


**Table 6.2** List of compounds found in Drammensfjord sediment extracts. The numbering refers to the peak numbers in Fig. 6.6. The structures of the compounds numbered with Roman numerals are given in the appendix. The lettered compounds refer to the compounds shown in Fig. 6.7. FA = fatty acid, OH = alcohol.

1	C <sub>14</sub> FA	41	hop-22(29)-ene
2	Loliolide	42	C <sub>28</sub> OH
3	C <sub>16:1</sub> FA	43	24-methyl-cholest-5-ene-3β-ol
4	C <sub>16</sub> FA	44	24-methyl -cholest-5,22-diene-3β-ol
5	Norabietane	45	(ω-1)-OH C <sub>26</sub> FA
6	C <sub>18:2</sub> + C <sub>18:1</sub> + C <sub>18</sub> FA's	46	C <sub>29</sub> FA
I	pimaric acid	VII	C <sub>26</sub> alkan-2,25-diol
7	dideutero-C <sub>22</sub> ante-iso <i>n</i> -alkane (standard)	47	24-ethyl-cholest-5-ene-3β-ol
8	phytol	48	24-ethyl-cholestan-3β-ol
II	isopimaric acid	49	ω-OH C <sub>26</sub> FA
III	1-phenanthrene carboxylic acid	50	4,23,24-trimethyl-5α(H)-cholest-22-ene-3β-ol
IV	dehydroabietic acid	51	C <sub>30</sub> FA
9	C <sub>23</sub> <i>n</i> -alkane	52	C <sub>30</sub> OH
V	abietic acid	53	4,23,24-trimethyl-5α(H)-cholestan -3β-ol
10	C <sub>20</sub> OH	54	lanosta-9(11),24-dien-3β-ol
11	C <sub>23</sub> alkan-2-one	55	tetrahymanol
12	C <sub>25</sub> <i>n</i> -alkane	56	diplopterol
13	C <sub>22</sub> FA	57	(ω-1)-OH C <sub>28</sub> FA
14	C <sub>22</sub> OH	58	C <sub>31</sub> FA
15	C <sub>26</sub> <i>n</i> -alkane	59	C <sub>28</sub> alkan-2,27-diol
16	C <sub>23</sub> FA	60	C <sub>31</sub> OH
17	C <sub>16</sub> monoglycerol ester	61	ω-OH C <sub>28</sub> FA
18	C <sub>23</sub> OH	62	C <sub>32</sub> FA
19	C <sub>32-34</sub> mono- and bicyclobotyococenes	63	C <sub>32</sub> OH
20	C <sub>27</sub> <i>n</i> -alkane	64	ω-OH C <sub>30</sub> FA
21	C <sub>24</sub> FA	65	17β,21β(H)-bishomohopanoic acid
22	C <sub>24</sub> OH	66	17β,21β(H)-bishomohopanol
23	C <sub>18</sub> monoglycerol ester	67	C <sub>38</sub> wax-esters
24	C <sub>28</sub> <i>n</i> -alkane	68	C <sub>40</sub> wax-esters
25	C <sub>25</sub> FA	69	C <sub>42</sub> wax-esters
26	C <sub>25</sub> OH	70	C <sub>44</sub> wax-esters
27	ω-OH C <sub>22</sub> FA		
28	C <sub>27</sub> alkan-2-one		isorenieratene
29	C <sub>29</sub> <i>n</i> -alkane		β carotene
30	C <sub>26</sub> FA		
31	C <sub>26</sub> OH		<u>isoprenoidal GDGTs</u>
32	C <sub>30</sub> <i>n</i> -alkane	A	GDGT-0
33	(ω-1) C <sub>24</sub> FA	B	GDGT-1
34	C <sub>27</sub> FA	C	GDGT-2
VI	C <sub>24</sub> alkan-2,23-diol	D+E	Crenarchaeol + isomer
35	C <sub>27</sub> OH		<u>non-isoprenoidal GDGTs</u>
36	cholest-5-ene-3β-ol	F	'F'
37	ω-OH C <sub>24</sub> FA	G	'G'
38	C <sub>29</sub> alkan-2-one	H	'H'
39	C <sub>31</sub> <i>n</i> -alkane		
40	C <sub>28</sub> FA		

← **Figure 6.6** Gas chromatograms of total lipid fractions of extracts derived from 50-52 cm core depth (A) and from 5-7.5 cm core depth (B). The peak numbers and lettering refer to compounds listed in Table 6.2. Roman numerals refer to structures shown in the appendix. Note the intensity differences of I-VII compared to the internal standard peaks, which were added in approximately equal amounts to the sediment extracts.

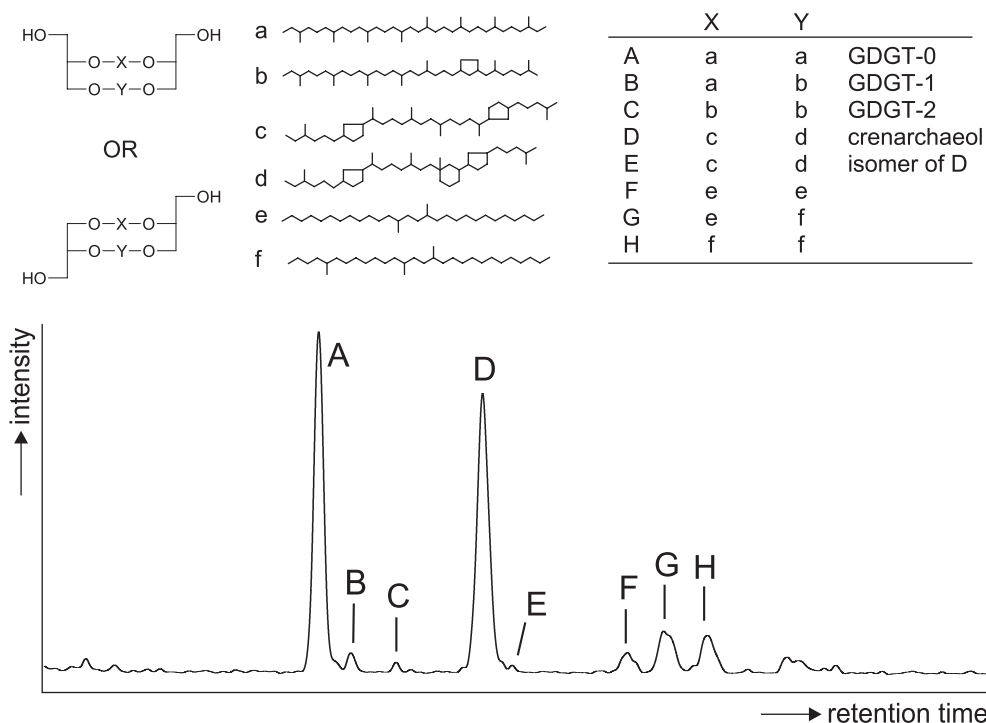


**Figure 6.7** HPLC base peak chromatogram of the polar fraction of the sediment extract from 32.5–35.5 cm piston core depth showing the GDGTs detected in the Drammensfjord.

This is supported by historical reports of sawmills that were present in the middle eighteenth century along the river Drammen [Alve, 1991 and references therein], and with the finding of several wood chips and twigs in the upper part of the sediment (Fig. 6.2). The clear shift in the  $C_{org}/TN$  ratio from 8 to 12 around 1850 AD (Fig. 6.5) and the decreasing  $\delta^{13}C_{TOC}$  values in the upper 20 cm of the piston core (Fig. 6.5) are both as expected from a higher relative contribution of woody tissue to the TOC [Tyson, 1995c and references therein]. This marks the start of industrial sawmill and papermill activities where the flux of fibrous, nitrogen-poor organic matter must have increased substantially, while before that time the organic waste produced from saw mills probably mimicked  $C_{org}/TN$  ratios of naturally occurring terrigenous organic matter.

#### *Bottom water euxinia*

The preservation of varves and the presence of iron sulphides within the Drammensfjord sediments indicate that the present day euxinic conditions in the fjord prevailed over the last millennium. It is, however, not clear whether these circumstances were as extensive as today. Isorenieratene, a carotenoid that is produced by strictly anaerobic photosynthetic

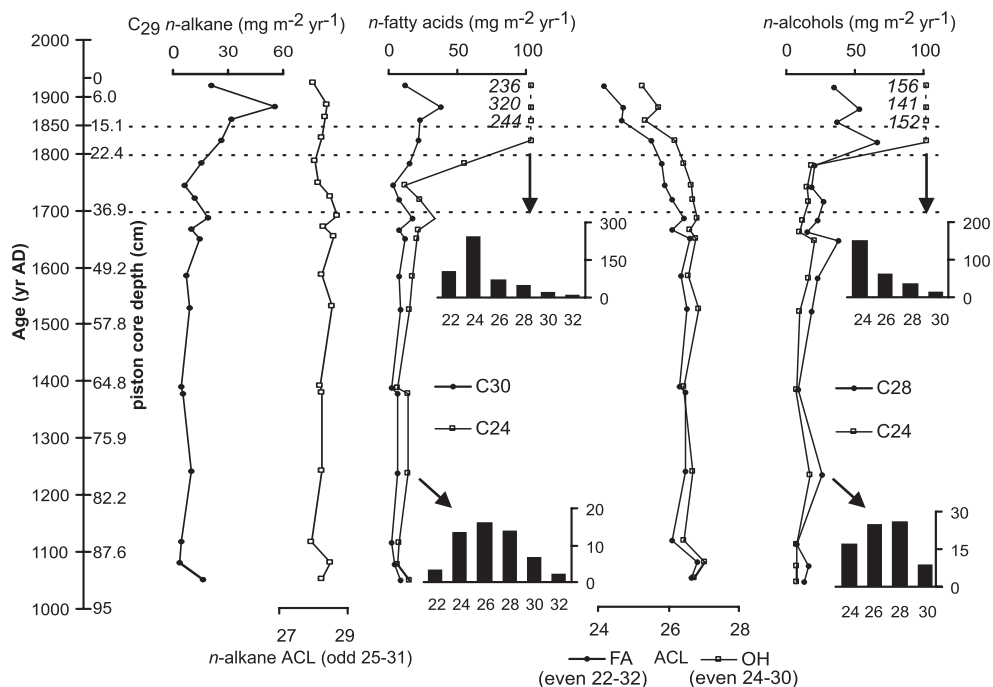


**Figure 6.8** Age/depth profiles of the accumulation rates of long-chain *n*-alkanes, fatty acids and alcohols, their average chain length and distribution.

green sulphur bacteria [Hartgers *et al.*, 1994 and references therein], was detected in trace amounts (*ca.* 10 ng / g sediment) in a number of sediment samples (Fig. 6.10), although in most sediments this carotenoid could not be detected. This indicates that the chemocline was generally situated at considerable depth, occasionally shoaling into the lower part of the photic zone. However, varying turbidity of the water column may also have played a role. The photic zone currently extends only a few meters below the surface, but the chemocline lies at around 30 m water depth. This prevents the growth of photosynthetic green sulphur bacteria, even though they can thrive in very low light conditions [Montesinos *et al.*, 1983]. Another biomarker that points towards anoxic conditions is tetrahymanol (gammacer-3 $\beta$ -ol), which was present throughout the investigated core in quantifiable amounts (Fig. 6.10). Although this compound can be produced by the photosynthetic purple bacteria *Rhodospseudomonas palustris* [Kleemann *et al.*, 1990; Harvey and McManus, 1991], it is also indicative for the presence of extensive grazing by bacterivorous ciliates of the genus *Tetrahymana* [Harvey and McManus, 1991; Sinninghe Damsté *et al.*, 1995 and references therein].

## Eutrophication

A suite of marine or aquatic biomarkers were detected in the Drammensfjord sediments (Fig. 6.6 and Table 6.2), although they were in general much less abundant than the terrigenous derived biomarkers, hampering quantification in many instances. This indicates that the natural state of the Drammensfjord was oligotrophic or mesotrophic, as otherwise a larger contribution of phytoplankton derived biomarkers would have been expected (cf. Saanich Inlet, (Chapter 3), Framvaren fjord [Ficken and Farrimond, 1995], Kyllaren fjord (chapter 5). The most abundant marine biomarkers present in the Drammensfjord sediments are crenarchaeol and GDGT-0 (Fig. 6.7, A and D). Crenarchaeol is produced by marine crenarchaeota [Sinninghe Damsté et al., 2002c] but GDGT-0 is in addition produced by a suite of archaeal groups, e.g. methanogenic archaea, which can thus also be of terrigenous origin [Schouten et al., 2000b and references therein]. However, the similarity in the accumulation rate profiles of GDGT-0 and crenarchaeol suggests that in this case almost all GDGT-0 is derived from marine crenarchaeota. The same argument holds for the much less abundant GDGT-1 and GDGT-2 (Fig. 6.7, B and C) [Schouten et al., 2002]. Loliolide is an anoxic degradation product of fucoxanthine [Repeta, 1989], a carotenoid predominantly found in diatoms [Wahlberg and Eklund, 1998]. This biomarker was also present in quantifiable amounts throughout the core (Fig. 6.10). Its presence agrees with both the presence of diatoms, as already noticed from the presence of their frostules in the sediments, but also with the prevalence of anoxic bottom water conditions over the last millennium. A dominant group of compounds were monocyclo- and bicyclobotryococcenes, which can be attributed to the extant alga *Botryococcus braunii* (Kützing) that often thrives in oligotrophic or slightly brackish conditions. The identification of these compounds and the occurrence of this alga is discussed in Chapter 7. Dinosterol (4,23,24-trimethyl-5 $\alpha$ (H)-cholest-22-ene-3 $\beta$ -ol) and dinostanol (4,23,24-trimethyl-5 $\alpha$ (H)-cholestan-3 $\beta$ -ol) are produced by dinoflagellates [e.g. Boon et al., 1979; Kokke et al., 1982], and may therefore be regarded as aquatic biomarkers. These organisms are also likely to be responsible for the occurrence of lanosta-9(11),24-dien-3 $\beta$ -ol in the sediments [Giner et al., 1991]. Unfortunately, the abundance of these biomarkers was too low for quantification. The only quantifiable sterol was 24-ethyl-cholest-5-ene-3 $\beta$ -ol ( $\Delta^5C_{29:1}$  sterol, Fig. 6.10), but this sterol can be both of terrigenous and marine origin, and is therefore not very indicative

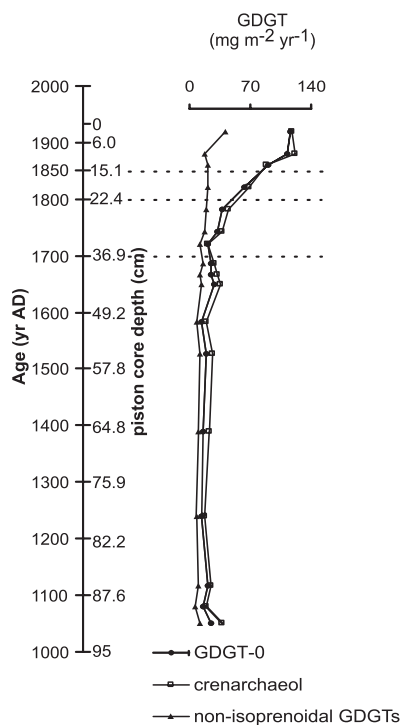


**Figure 6.9** Age/depth profiles of accumulation rates of glycerol dialkyl glycerol tetraethers. For lettering see Fig. 6.7.

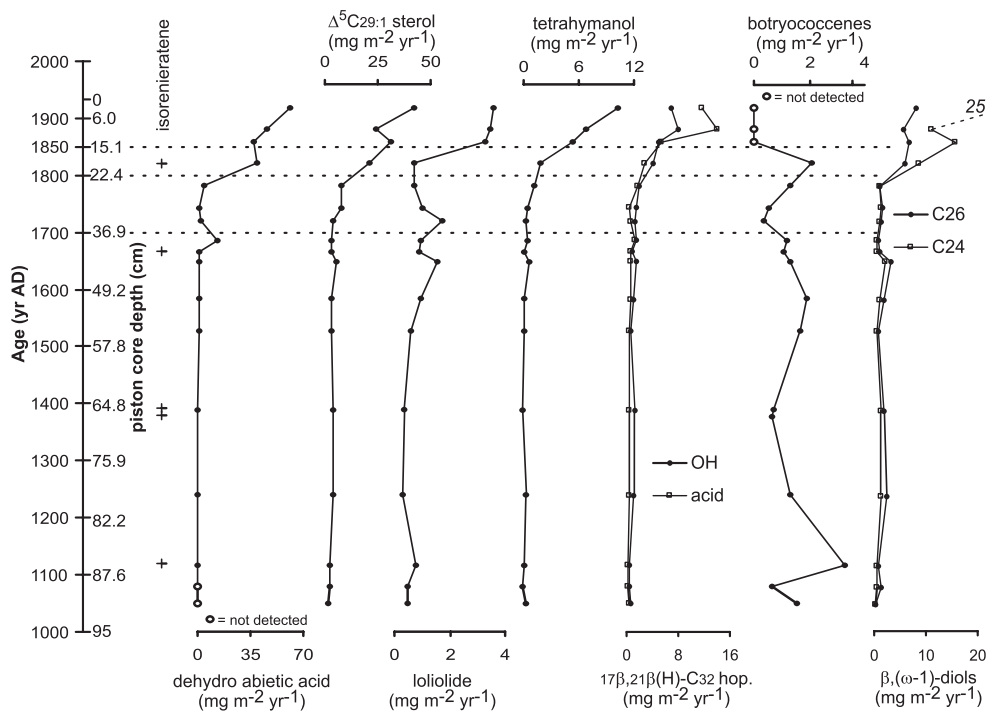


**Figure 6.10** Age/depth profile of accumulation rates of dehydroabietic acid, 24-ethyl-cholest-5-ene- $3\beta$ -ol ( $\Delta^5\text{C}_{29:1}$  sterol), loliolide, tetrahymanol,  $17\beta,21\beta(\text{H})\text{-C}_{32}$  hopanoic acid and -hopenol,  $\Sigma$ (botryococenes), and  $\beta,(\omega-1)\text{-C}_{24}$  and  $\text{C}_{26}$  diols.

[Volkman, 1986]. Cholest-5-ene- $3\beta$ -ol and 24-methyl-cholest-5-ene- $3\beta$ -ol are similarly indistinctive.

The accumulation rates of the general bacterial biomarkers  $17\beta,21\beta(\text{H})\text{-bishomohopanoic}$  acid and -hopenol [Taylor, 1984] increased from the mid-18<sup>th</sup> century onwards (Fig. 6.10), concurrently with those of TOC, TN and the 'coniferous' biomarkers. The accumulation rate of tetrahymanol increases consistently (Fig. 6.10), probably caused by the increasing abundance of bacterial biomass. This confirms the theory of Alve [1991] that the relatively nutrient-poor fibrous organic waste from the early paper mills, represented by the 'coniferous' biomarkers, is slowly degraded by bacteria, in its turn leading to gradually increasing nutrient concentrations in the stagnant fjord waters, favouring foraminiferal abundances and bacterivorous zooplankton. The accumulation rates of crenarchaeol and GDGT-0 (Fig. 6.9) also started to increase from the early 18<sup>th</sup> century onwards, and as the crenarchaeota likely profited as well from the slowly increasing nutrient availability in the fjord waters. In contrast, the accumulation rate of loliolide (Fig. 6.10) remains relatively constant until 1850 AD, while after that date a marked increase occurred in the accumulation rate of this diatom-derived biomarker. Diatoms thrive especially well under eutrophic conditions [Round et al., 1990], and their sudden increase

suggests that before 1850 AD the trophic state of the fjord was not yet sufficient to induce large diatom blooms. However, the industrialisation of the saw- and paper mills must have resulted in such an increase in organic waste, together with increasing domestic and agricultural sewage waste, that the nutrient availability in fjord water reached a critical point for diatoms to become abundant. Under eutrophic conditions extensive diatom blooms may outcompete other organisms and in the Drammensfjord this likely led to the demise of *Botryococcus braunii* within the fjord (Fig. 6.10), as discussed in Chapter 7.

### *Bottom water renewals and carbon recycling*

The stable and radiocarbon isotopic composition of biomarkers may give insight into the extent to which the bottom waters are renewed. The  $\delta^{13}\text{C}$  values of crenarchaeol and GDGT-0 vary between  $-23.9\text{‰}$  and  $-25.2\text{‰}$  (Table 6.1), which is lower than the almost invariably observed  $\delta^{13}\text{C}$  value of around  $-21\text{‰}$  in open ocean settings [Hoefs *et al.*, 1997; Schouten *et al.*, 1998a; Pearson *et al.*, 2001]. This may be related to carbon recycling [Fry *et al.*, 1991; Goericke and Fry, 1994; Hartgers *et al.*, 2000]. Due to stagnant conditions, DIC liberated upon degradation of sinking  $^{13}\text{C}$ -depleted primary produced organic matter is retained in the water column and not exchanged with atmospheric  $\text{CO}_2$ . This  $\delta^{13}\text{C}$ -depleted DIC can, after partial mixing back into the photic zone, be sequestered again by primary producers. This results in lower  $\delta^{13}\text{C}$  values of marine biomass than under normal, well-mixed, open ocean circumstances. Due to the relatively low abundance of marine biomarkers in the fjord sediments, other strictly marine biomarkers were not analysed for their  $\delta^{13}\text{C}$  content, and this hypothesis is not further substantiated in this study. The  $\delta^{13}\text{C}$  values of the various  $\Delta^5$  sterols reported in Chapter 7 are considered ambiguous due to their undefined source.

Crenarchaeol and GDGT-0 from sediments deposited after 1950 AD clearly exhibit  $^{14}\text{C}$  contents influenced by atmospheric nuclear weapons testing (Table 6.1), while those from before 1950 AD both exhibit an  $^{14}\text{C}$  age of around 400 BP. This would imply a marine DIC reservoir age of approximately 300  $^{14}\text{C}$  yr [Stuiver *et al.*, 1998b], which would be in agreement with a mixture of  $\frac{3}{4}$  Eastern North Atlantic ocean water, that exhibited a reservoir age of  $400\pm 50$  yr over the last 2000 yr [Reimer *et al.*, 2002], with  $\frac{1}{4}$  well-mixed  $^{14}\text{C}$ -enriched fresh water from either the Scandinavian coast or from riverine water, i.e. the river Drammen. In contrast, the  $^{14}\text{C}$  ages and calculated reservoir ages of crenarchaeol and GDGT-0 from the upper part of the piston core sediment are somewhat higher (Table 6.1), while the  $^{14}\text{C}$  age of crenarchaeol isolated from 85-92 cm piston core depth shows only a minor difference with the sediment age, resulting in a low reservoir age (Table 6.1). These differences may lie in a varying contribution of fresh water and oceanic water to the fjord, as previously observed in Danish fjords [Heier-Nielsen *et al.*, 1995] where dissolution of mineral, and thus fossil,  $\text{CaCO}_3$  may also play a role. To deconvolute further the varying factors that determine the  $^{14}\text{C}$  content of the GDGTs, which would allow more insight into the source of DIC in the fjord, a larger data set is necessary.



#### 6.4.4. $\beta$ ,( $\omega$ -1)-diols, $\omega$ -hydroxy fatty acids and ( $\omega$ -1)-hydroxy fatty acids

2,23-Dihydroxy- $C_{24}$  alkane (IV) and 2,25-dihydroxy- $C_{26}$  alkane (VII) and to a lesser extent 2,27-dihydroxy- $C_{28}$  alkane (i.e.  $\beta$ ,( $\omega$ -1)-diols), were abundant compounds within the lipid extracts of the Drammensfjord sediments, and their accumulation rate increased substantially concurrently with the conifer-derived biomarkers (e.g. dehydroabietic acid) and marine biomarkers (Fig. 6.10). These diols have only scarcely been reported in the literature [Versteegh *et al.*, 1997], and they have, to the best of our knowledge, never been detected in any identified organism. However, the same diols were detected in the sediments of the anoxic and monomictic Ace Lake, Antarctica [Schouten *et al.*, 2001]. This lake does not receive any vascular plant material, and is dominated by prokaryotic, aquatic organisms [Volkman *et al.*, 1986]. This implies that the  $\beta$ ,( $\omega$ -1)-diols may be attributed to an aquatic source. As Ace Lake and the Drammensfjord are both ecosystems characterised by anoxic conditions, it is anticipated that either an anoxic group of organisms are producing these compounds, or that these compounds are formed upon an anoxygenic alteration of precursor compounds. It is furthermore remarkable that a suite of even carbon numbered  $\omega$ -hydroxy fatty acids ( $C_{22}$ - $C_{30}$ ) and ( $\omega$ -1)-hydroxy fatty acids ( $C_{24}$ - $C_{28}$ ) also occur in the Drammensfjord sediments (Table 6.2). ( $\omega$ -1)-hydroxy fatty acids are produced by methanotrophic bacteria [Skerratt *et al.*, 1992], while they have, to the best of our knowledge, not been detected in higher plants. Long-chain  $\omega$ -hydroxy fatty acids have been reported as minor components in suberin [Kolattukudy *et al.*, 1973]. Aerobic microbial oxidation of long-chain fatty acids may also produce  $\omega$ - and ( $\omega$ -1)-hydroxy fatty acids [Miura and Fulco, 1975], and this has in most instances been assumed to be their most likely source in sediments [e.g. Boon *et al.*, 1977; Goossens *et al.*, 1989; Wakeham, 1999]. However, such sedimentary reports are scarce, and they are, remarkably, only from anoxic or low oxygen-sediments, which makes it unlikely that they derive from aerobic oxidation *in situ*. It is therefore anticipated that the long-chain  $\omega$ -hydroxy fatty acids and ( $\omega$ -1)-hydroxy fatty acids may be derived from methanotrophic bacteria. To further substantiate this hypothesis further research on these compounds is needed, which should include  $\delta^{13}C$  analysis. This was, however, beyond the scope of this study.

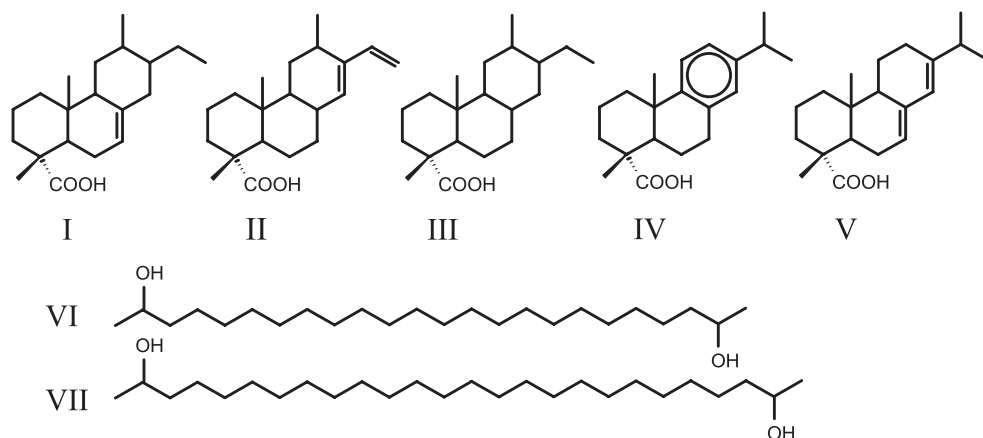
## 6.5. Conclusions

The sedimentological and organic geochemical analyses of the sediments deposited in the depocenter of the presently anoxic Drammensfjord, Norway, revealed a number of environmental changes that occurred over the last millenium. Since 1000 AD euxinic conditions prevailed in the fjord bottom waters, leading to the preservation of annually deposited varves, predominantly composed of terrigenous silt- to clay-sized mineral grains. Due to an oligotrophic or mesotrophic state of the fjord, the sedimentary organic matter is mainly of terrigenous origin. The sediments are furthermore characterised by an annual alternation between the deposition of black iron monosulphides and more colourless iron

disulphides. It is inferred from relatively low  $\delta^{13}\text{C}$  values of crenarchaeotal and algal biomarkers that the  $^{13}\text{C}$  content of DIC is depleted compared to normal oceanic water, due to carbon recycling within the fjord. From 1000 AD to 1700 AD, little change is observed in the fjord's biogeochemistry, except a gradual increase of the contribution of marine organic matter, which is probably caused by the slow shoaling of the sill depth due to the isostatic uplift of Scandinavia. After approximately 1700 AD, the first sign of anthropogenic influence can be traced in the sedimentary record by an initially slow increase in the accumulation rate of 'coniferous' biomarkers, dehydroabietic acid and isomers, and  $\text{C}_{24}$  fatty acids and -alcohols. The accumulation rates of these biomarkers increase substantially after 1850 AD, which is also the case for the accumulation rates of TOC and TN. These changes are attributed to an increasing load of coniferous fibrous material from industrialised sawmills, while the 'background' terrigenous flux to the fjord prevailed. The early sawmill waste of the period after 1700 AD stimulated bacterial activity, which started to liberate increasing amounts of nutrients into the stagnant fjord waters. This favoured the conditions for marine crenarchaeota, zooplankton and foraminifera. After 1850 AD the fjord became ever more eutrophic due to the industrialisation of the saw- and paper mills, favouring the growth of diatoms at the cost of other phytoplankton species.

### Acknowledgements

The authors thank Wim Boer and Rineke Gieles for the  $^{210}\text{Pb}$ ,  $^{137}\text{Cs}$  and  $^{226}\text{Ra}$  analysis. The crew of R/V Pelagia, Matthias Paetzel, Frode Uriansrud and Bart van Dongen are thanked for their assistance in obtaining the sediment cores. The staff at the National Ocean Sciences Accelerator Mass Spectrometry Facility at Woods Hole, USA, are thanked for  $^{14}\text{C}$  analyses. Michiel Kienhuis and Elda Panoto are thanked for their assistance with the GC/MS analysis.



## Chapter 7

### The demise of the alga *Botryococcus braunii* from a Norwegian fjord is due to early eutrophication

Rienk H. Smittenberg, Marianne Baas, Stefan Schouten and Jaap S. Sinninghe Damsté

Submitted to 'The Holocene'

**Abstract** In the sedimentary record of the permanently anoxic Drammensfjord, a suite of lipid biomarkers that are derived from the unicellular alga *Botryococcus braunii*, botryococcenes, is present in varying amounts, but absent in sediments deposited after 1850 AD. The disappearance is concurrent with the industrialization of saw- mills and the introduction of paper and pulp mills along the river Drammen and upstream water bodies, and the related increase of anthropogenic eutrophication. Because of the preference of this alga for oligotrophic conditions, a direct correlation between these two events is inferred. This implies that the disappearance of the botryococcenes can serve as palaeoenvironmental indicator for early eutrophication. This may be a useful tool in the ongoing research to unravel the response of natural systems to climatic, geophysical or anthropogenic changes.

#### 7.1. Introduction

In the last decades, the extent and impact of man-induced eutrophication of coastal waters has been an important issue in environmental research [e.g. *Pätsch and Radach, 1997; Zimmerman and Canuel, 2000*]. However, naturally occurring variations in climate, geophysical setting or other environmental parameters can also influence coastal waters and their trophic state [e.g. *Nordberg et al., 2001; Kalis et al., 2003*]. It is often difficult to separate natural variations from anthropogenically induced effects [e.g. *Hulme et al., 1999; Sullivan et al., 2001; Kalis et al., 2003*]. A recurring problem is that environmental monitoring started only in the second half of the 20<sup>th</sup> century. For instance, eutrophication of the North Sea was only widely recognized in the 1980's [*Pätsch and Radach, 1997*] so that historical records of the natural situation are scarce. However, the ecological history of the coastal environment is reflected in the composition of organic matter in their sediments [e.g. *Struck et al., 2000*]. By tracking the occurrence and amount of compounds (biomarkers) that are specific for organisms sensitive to environmental change, ecological variations through time may be reconstructed [e.g. *Ficken and Farrimond, 1995*]. In this respect, anoxic basins and fjords are especially useful, because these sediments are not affected by bioturbation and organic matter degradation rates are relatively low [e.g. *Degens and Stoffers, 1976; Kemp, 1996; Werne et al., 2000*].

The South Norwegian Drammensfjord (Fig. 6.1) is an anoxic fjord that has suffered from anthropogenic eutrophication [Alve, 1991]. To determine to what extent this influenced the original ecology, the biomarker record of this fjord was investigated. A particularly informative group of biomarkers present is that of the alkylated isoprenoidal hydrocarbons known as botryococcenes derived from the green unicellular algae *Botryococcus braunii* race B [Metzger *et al.*, 1991]. Although the presence of these lipids in sediments have so far been regarded as an indicator for freshwater conditions [e.g. Tyson, 1995b; Kunz-Pirrung, 1999; Matthiesen *et al.*, 2000], this paper discusses its potential wider use as a proxy for oligotrophy.

## 7.2. Setting

The Drammensfjord is a Northwest trending 20 km long and 1.6-3.0 km wide basin separated from the greater Oslo fjord by a 10 m deep sill at Svelvik (Fig. 6.1). The bottom topography is even, with southwards increasing water depths to a maximum of 124 m near the sill. At the head of the fjord, fresh water of the river Drammen enters the basin resulting in a positive water balance. Mixing of this water with the marine fjord waters leads to a brackish surface water layer (salinity 1-10 ‰, depending on the season), which is separated from saline bottom water (30.5 ‰) below 40 m by a transitional layer (Fig. 6.1) [Alve, 1990]. The positive water balance and shallow sill prevents frequent deep water renewals and, combined with the availability of degradable organic matter, this leads to anoxic and sulfide-bearing (euxinic) bottom waters. Bottom water renewals occur once every 3-5 years, mainly between November and May, displacing the euxinic water upwards [Richards, 1965; Alve, 1995]. Depending on the amount of introduced oxygenated water, it takes several weeks to months to restore euxinic bottom water conditions completely. However, because this restoration starts at the bottom of the fjord [Richards, 1965], the fjord sediment is never exposed to oxygen for longer than a few weeks over several years. This implies that benthic life is limited to microorganisms and that the laminated sedimentary structure and biomarker record is well preserved.

Since at least 1750 AD, the fjord has been increasingly affected by sawdust and woodchips from sawmills [Alve, 1990; 1991 and references therein] along the river Drammen and upstream fresh water bodies. After 1870 AD, a number of paper and pulp mills were established, and in the 20<sup>th</sup> century the supply of organic matter to the fjord increased even more. During the first half of the 1970's most of the paper industry was closed down which decreased the fiber supply. However, domestic and agricultural contributions to the organic matter and nutrient load had increased drastically by that time [Richards and Benson, 1961; Alve, 1991]. Regulations of the river water in the last 60 years have smoothed the annual fresh water supply to the fjord by reducing the effect of spring flooding and increasing the winter supply. This replaced the minimum fresh water supply from winter to late summer and increased the residence time of the surface water during summer.

### 7.3. Sampling and methods

#### 7.3.1. Sediment collection and sub-sampling

A suite of box, gravity and piston cores was recovered from three locations in the Drammensfjord during a cruise in October 1999 with the R/V 'Pelagia', of which one piston core taken from the depocenter of the fjord (Fig. 6.1) was selected. The uppermost section of this core, with a length of approximately one meter, was sliced into two halves and photographed for gray-scale analysis. From one half, sub-samples were taken for bulk-density measurements. Depending on sediment color and laminae thickness, the other half was sub-sampled into subsections ranging between 0.5 and 7 cm thickness (Fig. 6.2), which were subsequently freeze-dried. Approximately half of these sub-samples, evenly distributed over the core, were ground for geochemical analysis. Surface sediment samples with a 0.5 cm depth interval were obtained by slicing a box core sediment immediately after recovery, which were subsequently stored on board at  $-20^{\circ}\text{C}$  and later freeze-dried in the laboratory. These samples were used to determine accumulation rates using  $^{210}\text{Pb}$ .

#### 7.3.2. Bulk analyses and dating

Total organic carbon contents (TOC) and nitrogen (TN) contents were determined on acid-treated (1N HCl, 12 h.) sediment sub-samples using a LECO Element Analyzer. For dating purposes, the  $^{210}\text{Pb}$  activities of sub-samples of the piston core at 0 – 5 cm, 7.5 – 12 cm and at 85.5 – 88 cm were determined and compared with the  $^{210}\text{Pb}$  activity profile determined on a box core sediment. The sub-sample at 0 – 5 cm contained a piece of plastic. A wood-chip and a small twig were recovered from the sediment at respectively 11-12 cm and 94 cm depth, and were both radiocarbon dated. Radiocarbon ages were calibrated towards calendar ages by using the atmospheric calibration curve of *Stuiver et al.* [1998a]. A detailed account on the dating methodology is described in Chapter 6.

#### 7.3.3. Biomarker analysis

Sediment subsamples were freeze-dried and extracted with organic solvents as in chapter 6. Aliquots of the total lipid extracts were fractionated into an apolar and a polar fraction by column chromatography over  $\text{Al}_2\text{O}_3$  with respectively a hexane:dichloromethane (9:1 v/v) mixture and a dichloromethane:methanol (1:1 v/v) mixture. The total lipid extract of the 85.5 – 88 cm sediment sample was fractionated into three fractions by first using pure hexane as eluent before applying the other two solvent mixtures, resulting in two apolar fractions (A1 and A2) and a polar fraction (P). For quantification, a known amount of deuterated *ante-iso*  $\text{C}_{22}$  alkane was added as an internal standard to weighed aliquots of the

total lipid extracts. For structural analysis of the carbon skeletons of unsaturated hydrocarbons present in the apolar fractions, an aliquot of the A1 fraction of the 85.5 – 88 cm sediment sample was subjected to hydrogenation in order to obtain saturated products. The fraction was dissolved in ethyl acetate with *ca.* 100 mg PtO<sub>2</sub> and a few droplets of acetic acid, subsequently flushed with H<sub>2</sub>(g) for 1 h. and stirred overnight. The hydrogenated fraction was then eluted with DCM over a small column containing anhydrous MgSO<sub>4</sub>(s) and CaCO<sub>3</sub>(s) and again eluted with hexane over a column containing activated Al<sub>2</sub>O<sub>3</sub>. Quantification and identification of individual compounds was done by respectively gas chromatography (GC) and gas chromatography-mass spectrometry (GC/MS) as described in Chapter 6.

For stable carbon and hydrogen isotopic analysis, aliquots of two representative apolar fractions (A1 from 83.5-85.5 cm and 54.5-57 cm core depth) were eluted with cyclohexane over a small column filled with silicalite (PQ Zeolites, The Netherlands) to remove straight-chain hydrocarbons. To be able to analyze the  $\delta^{13}\text{C}$  contents of sterols, an aliquot of the polar fraction of the 83.5 – 85.5 cm sediment sample was subjected to thin layer chromatography (TLC), using the method of *Skipski et al.* [1965]. Fractions containing only sterols were recovered by sonic extraction (3 x) with DCM of the silica that was scraped off the TLC plate. The recovered sterol fraction was dissolved in 25  $\mu\text{l}$  pyridine to which 25  $\mu\text{l}$  bis(trimethylsilyl)trifluoroacetamide (BSTFA) was added. This mixture was heated at 60°C for 20 min. to convert the sterols into their corresponding trimethylsilyl ethers.

Compound-specific stable carbon and hydrogen isotopic compositions were determined on a ThermoFinnigan DELTA-plus XL isotope-ratio-monitoring GC/MS. The isotopic composition of alcohols was corrected for the added carbon molecules by using BSTFA with a known carbon isotopic value. The stable carbon isotopic compositions were determined by two replicate analyses, and the results were averaged to obtain a mean value and to evaluate measurement error. They are reported in standard delta notation relative to the VPDB standard. The hydrogen isotopic composition was determined on the silicalite non-adducted apolar fraction of 83.5-85.5 cm by three replicate analyses, and is reported in delta notation relative to the SMOW standard.

## 7.4. Results

### 7.4.1. Age model

Comparison of the <sup>210</sup>Pb activity of the upper 5 cm of the piston core with the <sup>210</sup>Pb profile obtained from the box core sediment indicated that the piston core-top is from somewhere between 1900 and 1950 AD, which was supported by the finding of a piece of plastic at the 0-5 cm interval. The calibrated radiocarbon age of the twig recovered at 94 cm core depth is 1000±50 AD. Based on bulk densities and the obtained data the sediment accumulation rate is estimated to decrease from 2 mm yr<sup>-1</sup> at 2.5 cm depth towards approximately 1 mm yr<sup>-1</sup> at

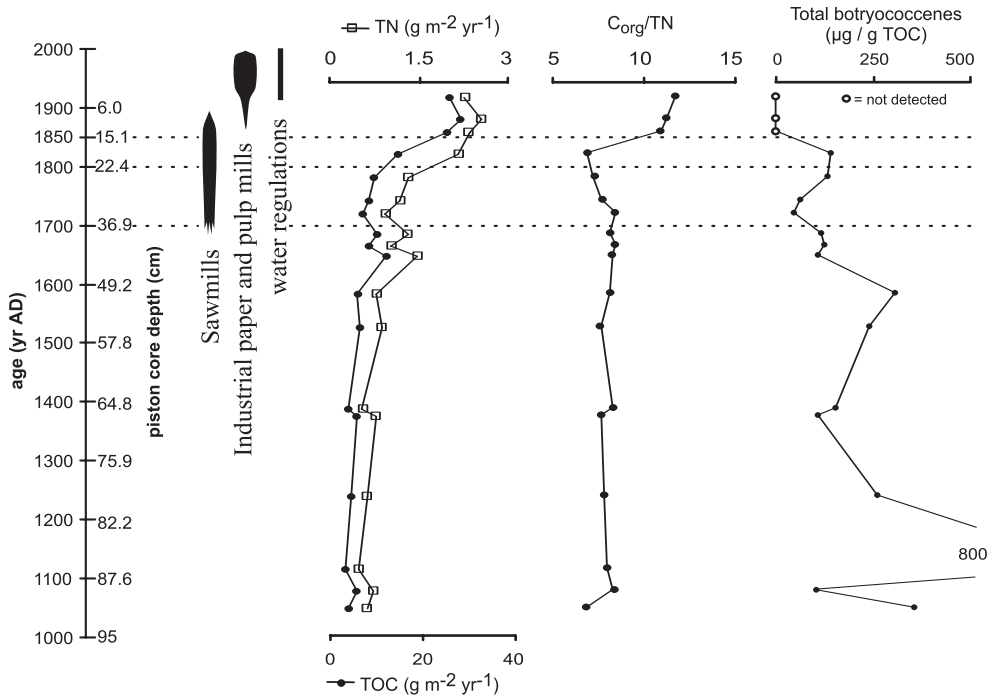


**Figure 7.1** Age/depth profiles of the total organic carbon content (TOC,  $\pm 0.05\%$ ), total nitrogen content (TN,  $\pm 0.01\%$ ), the  $C_{org}/TN$  ratio and the lumped concentration of the botryococcenes on the basis of TOC ( $\pm 30 \mu\text{g/g}$ ). Furthermore the periods of sawmill and paper and pulp mill activity in southern Norway are indicated as well as the period of water regulations in the catchment area of the Drammensfjord.

15 cm core depth, below which only a very gradual decrease occurs (see chapter 6). This implies that the sediment at 11 cm core depth should be from *ca.* 1850 AD. The calibrated radiocarbon age of the wood-chip recovered from 11-12 cm core depth agrees with that age if a correction is made for a growth-age of 40-80 yr, which may be a valid assumption because the appearance of the wood-chip suggests that it is likely derived from a full-grown tree cut for logging (see chapter 6). The thus constructed age model is comparable with the age model of a previously obtained sediment core from the depocenter of the fjord [Alve, 1991].

#### 7.4.2. Bulk sediment geochemistry

Total organic carbon (TOC) and nitrogen (TN) contents are relatively constant throughout the lower part of the core at approximately 1.0 % and 0.1 %, respectively up to 25 cm core depth, i.e. at around 1750 AD (Fig. 7.1). Above that interval the TN content increases towards 0.2%, while the TOC starts to increase until 2.6 % in the upper 10 cm. Furthermore, a clear shift in the  $C_{org}/TN$  ratio from approximately 8 below 18 cm depth

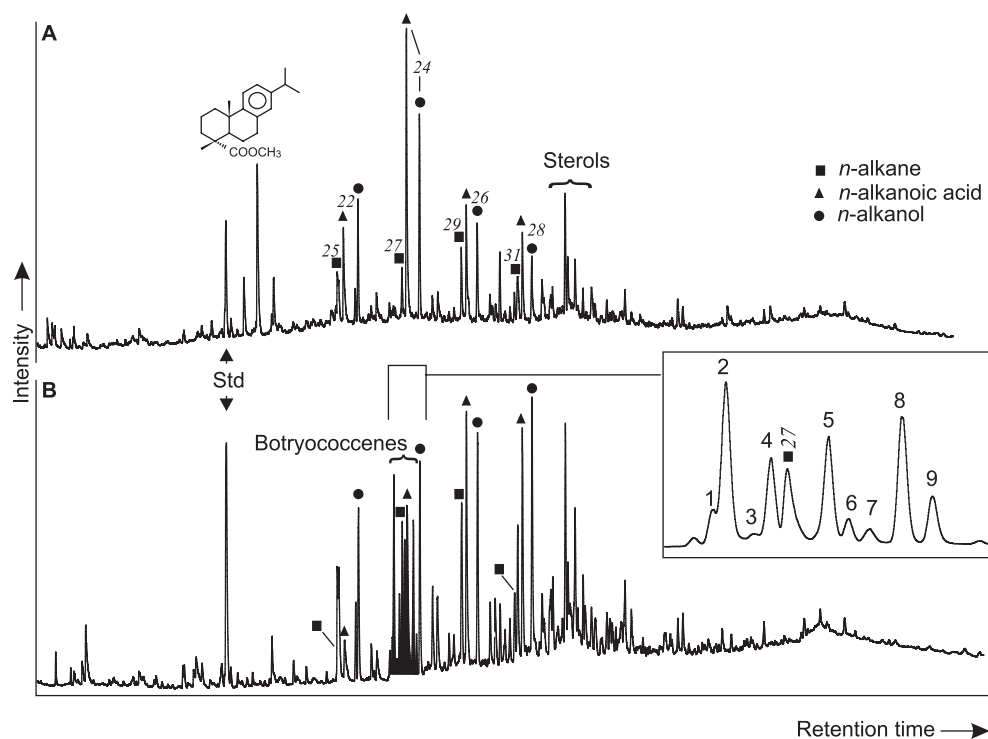


**Figure 7.2** Gas Chromatograms of total lipid extracts obtained from sediment samples of 12-15.5 cm (A) and 85.5-88 cm core depth (B). The number of carbon atoms in the alkyl-compounds is indicated in italics. The black filled area in the lower chromatogram indicates where the suite of isoprenoid hydrocarbons identified as botryococenes eluted. The inset shows a partial gas chromatogram of the apolar (A1) fraction from the same sediment, in which the identified botryococenes are numbered.

**Table 7.1** The elemental composition, pseudo Kováts retention indices and diagnostic MS ions for the botryococenes identified in the Drammensfjord sediments. No. = Compound numbered as in Fig. 7.2; M.F. = Molecular formula; R.I. = pseudo Kováts retention index:  $100n + 100 \times [(R_x - R_n) / (R_{n+1} - R_n)]$  in which  $x$  is the compound of interest;  $n$  = carbon number of the nearest  $n$ -alkane eluting in front of  $x$  on GC;  $R$  denotes retention time. The numbers between brackets behind the diagnostic ions in the mass spectra indicate the relative intensity compared to that of the base peak. \*see also Fig. 7.3.

No.	M.F.	R.I.	Diagnostic ions in mass spectrum ( $m/z$ )
1	C <sub>32</sub> H <sub>54</sub>	2672	438 (2), 273 (2), 217 (4), 177 (14), 137 (47), 123 (50), 81 (100)
2	C <sub>32</sub> H <sub>54</sub>	2677	438 (5), 423 (3), 271 (7), 231 (8), 217 (10), 177 (25), 137 (42), 121 (48), 81 (100)
3	C <sub>32</sub> H <sub>54</sub>	2682	438 (2), 273 (4), 217 (4), 163 (29), 137 (70), 81 (100)
4	C <sub>33</sub> H <sub>56</sub>	2695	452 (3), 273 (3), 231 (3), 177 (16), 149 (21), 123(37), 121 (49), 95 (100)
5	C <sub>33</sub> H <sub>56</sub>	2712	452 (5), 287 (7), 271 (6), 231(10), 217 (10), 177 (33), 123 (73), 81 (100)
6	C <sub>34</sub> H <sub>58</sub>	2723	466 (3), 285 (2), 231 (2), 177 (48), 149 (20), 123 (40), 95 (100)
7	C <sub>33</sub> H <sub>56</sub>	2727	452 (2), 287 (2), 217 (4), 163 (30), 95 (100)
8	C <sub>34</sub> H <sub>56</sub>	2739	466 (5), 287 (4), 231 (9), 177 (83), 149 (32), 123 (85), 95 (100) *
9	C <sub>34</sub> H <sub>58</sub>	2751	466 (3), 177 (44), 149 (22) 123 (44), 95 (100)

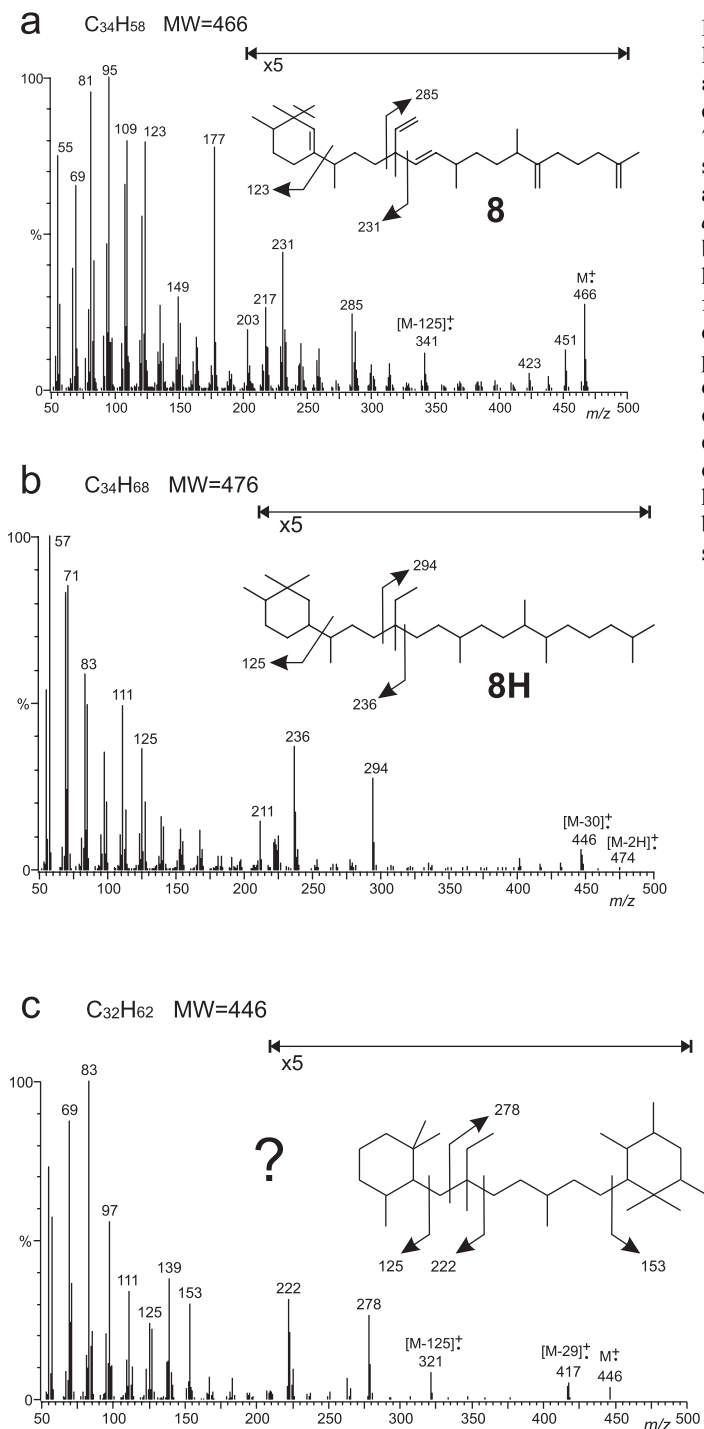


towards 12 above 15.5 cm depth (Fig. 7.1) is observed. The TN content initially increases with the same rate as the TOC content, which causes the increase in the  $C_{org}/TN$  ratio to lag behind the increase in the TOC content.

#### 7.4.3. *Botryococcenes*

Gas chromatography of the total lipid fractions of the extracts of the Drammensfjord sediments revealed a group of nine relatively abundant compounds that were present throughout the lowermost part of the core in varying abundances, but absent in the upper 18 cm (Fig. 7.2). GC/MS analysis of these fractions indicated that these compounds were  $C_{32}$ - $C_{34}$  isoprenoid hydrocarbons with six double bonds or rings (Table 7.1). Comparison of the mass spectra (Table 7.1) with those reported in literature [Maxwell *et al.*, 1968; Metzger *et al.*, 1985; David *et al.*, 1988] indicated that they are likely botryococcenes. Co-injection of an  $C_{34}$  cyclobotryococcene authentic standard [David *et al.*, 1988] with an apolar fraction resulted in co-elution with one of the sedimentary botryococcenes (Fig. 7.2, compound **8**), while the mass spectra (Fig. 7.3a) were identical. A favorable comparison could also be made between the mass spectra (Fig. 7.3b) of the hydrogenated authentic standard [David *et al.*, 1988],  $C_{34}$  cyclobotryococcane (**8H**), and one of the products formed upon hydrogenation of the apolar A1 fraction of 85.5-88 cm core depth, indicating that compound **8** is indeed a  $C_{34}$  cyclobotryococcene. The other compounds present in the hydrogenated A1 fraction exhibited similar mass spectra, although with varying molecular weights (Table 7.1). The  $m/z$  of their molecular ions were not all clearly distinguishable, but characteristic ions at  $m/z > 200$  (i.e.  $222 + 278$ ;  $222 + 294$ ;  $222 + 292$ ;  $236 + 294$ ;  $236 + 292$ ) that are formed through scissions of the alkyl chains around the acyclic quaternary carbon atom, characteristic for all botryococcenes [Metzger *et al.*, 1985], indicated that all formed botryococcenes contained either one or two cyclohexyl rings (e.g. Fig. 7.3c). Thus, all evidence points towards the presence of mono- and bicyclic  $C_{32}$ - $C_{34}$  botryococcenes in the lower part of the investigated core. No trends could be detected in the relative abundance of the various botryococcenes with depth. Compounds **2**, **5** and **8** were generally most abundant. The production of different botryococcene isomers is highly sensitive to growth conditions, while botryococcenes produced by different strains show also marked differences [Metzger *et al.*, 1991]. However, higher molecular weight members are generally produced during later stages of a bloom [Metzger *et al.*, 1991]. For these reasons, all botryococcene isomers were lumped to quantify their abundance (Fig. 7.1).

The stable carbon isotopic signature of the botryococcenes exhibited substantially higher  $\delta^{13}C$  values ( $-14$  to  $-19\%$ ) than those of sterols ( $-24$  to  $-30\%$ ) (Table 7.2), which is in accordance with previous reports of relatively high  $\delta^{13}C$  values for botryococcenes [Huang *et al.*, 1999] and their derivatives [Dowling *et al.*, 1995; Grice *et al.*, 1998b; Summons *et al.*, 2002]. The  $\delta D$  value of the combined botryococcenes from 83.5-85 cm core depth was  $-277 \pm 3\%$ .

**Figure 7.3**

Mass spectra of

**a)** the  $C_{34}$  monocyclobutryococene (compound **8**, Table 7.1) present in Drammensfjord sediments, identical to that of an authentic standard [David *et al.*, 1988].

**b)** The product of **8** after hydrogenation of the apolar A1 fraction from 85.5-88 cm core depth, identical to the saturated product of the authentic standard [David *et al.*, 1988].

**c)** One of the compounds concluded to be bicyclobutryococenes, present in the same hydrogenated apolar fraction as **b**. The proposed molecular structure is tentative.

## 7.5. Discussion

The presence of botryococcenes in the Drammensfjord sediment (Fig. 7.2) can be related to the occurrence of the alga *Botryococcus braunii* race B [Metzger *et al.*, 1991], either in the fjord itself or in the drainage area of the river Drammen (Fig. 6.1). Three races of *B. braunii* are discerned on the basis of their lipid composition [Metzger *et al.*, 1991]. The B race produces botryococcenes. The other two races of *B. braunii* (A and L) produce odd carbon numbered C<sub>23</sub> – C<sub>31</sub> *n*-alkadienes and lycopadiene, respectively [Metzger *et al.*, 1991]. Monocyclobotryococcenes, part of the observed botryococcenes in the Drammensfjord sediments, have previously been detected in *B. braunii* race B cultures originating from Ayama Lake (Ivory coast) and Overjuyo Lake (Bolivia) [David *et al.*, 1988], and in cultures from the Berkeley strain [Metzger *et al.*, 1991]. Furthermore, monocyclobotryococcenes have been reported in sediments of Sacred Lake (Mt. Kenya) [Huang *et al.*, 1999] and in samples collected in the Darwin reservoir, Australia [Metzger *et al.*, 1991]. However, bicyclobotryococcenes have to the best of our knowledge never been detected in *B. braunii* cells and recent sediments, although Grice *et al.* [1998b] suggested their existence based on their detection of sulfur-bound bicyclobotryococcenes in the Sdom formation, Israel. These results suggest that the observed (bi)cyclobotryococcenes have been produced by an unknown strain of *B. braunii* B race. It is, however, also possible that the bicyclobotryococcenes are produced by a strain capable of producing the monocyclic homologues but that environmental conditions caused them to also produce the bicyclic homologues.

*B. braunii* is a widespread occurring alga, and has been reported in ponds, lakes and rivers at arctic, temperate and tropical latitudes. This microalga belongs to the Chlorophytae, and is most characteristic for oligotrophic lakes, although it has also been found in mesotrophic waters [Tyson, 1995b]. Though mainly observed at the top of the photic zone, there have also been reports of *B. braunii* under benthic conditions. The alga has been described as being important or common in humus-rich oligotrophic lakes, ponds and bog-pools in Lapland, Sweden and Finland [Tyson, 1995b]. *B. braunii* not only thrives in fresh water, but also in brackish environments, connected with

**Table 7.2** Compound-specific stable carbon isotopic contents ( $\pm 0.5\%$ ) of various botryococcenes from two sediment core depths, as well as those of a number of sterols from the same sediment. Botryococcenes are numbered as in Fig. 7.2. n.d. = not determined. \* The relatively high value is possibly related with a <sup>13</sup>C enriched *B. braunii* - source.

Compound	$\delta^{13}\text{C}$ (‰)	
	54.5-57 cm	85.5-88 cm
<i>botryococcenes</i>		
2	-15.3	-17.9
3	-14.8	n.d.
4	-14.8	-22.0
5	-18.5	-17.3
6	-17.2	n.d.
7	-17.2	n.d.
8	-15.6	-15.9
9	-14.3	-13.8
<i>sterols</i>		
$\Delta^5\text{C}_{27:1}$	n.d.	-27.1
$\Delta^5\text{C}_{28:0}$	n.d.	-23.8*
$\Delta^5\text{C}_{29:1} + 5\alpha\text{C}_{29:0}$	n.d.	-29.6

the open sea. In culture, no adverse effect was observed for salinities up to that of seawater [Metzger *et al.*, 1991]. In the brackish waters of the Baltic sea area this species is reported regularly, including the environments of the Kattegat between Sweden and Denmark [Woloszynska, 1935; Edler *et al.*, 1994], although only at salinities < 10 ‰. In the last decades *B. braunii* blooms have not been observed [S. Hällfors, pers. comm.]. Because the upper water layer of the Drammensfjord is permanently brackish due to freshwater discharge from the mainland [Alve, 1990], overflowing more saline bottom water (Fig. 6.1), *B. braunii* might be expected to be part of the algal community. *B. braunii* has also been reported in the fresh water bodies in the Oslo region until the early 20<sup>th</sup> century [D. Klaveness, pers. comm.], likely including lake Tyrifjord that drains into the river Drammen (Fig. 6.1). Although lake Tyrifjord, the 5<sup>th</sup> largest lake in Norway, was not included in surveys in the early 20<sup>th</sup> century, *B. braunii* was very common at that time in the largest Norwegian lake, Mjøsa, which lies in the same area [D. Klaveness, pers. comm.]. This suggests that the molecular fossils of *B. braunii* observed in the sediment of the Drammensfjord may be introduced from upstream fresh water bodies. However, the  $\delta D$  value of -277‰ indicates that the botryococenes were biosynthesized in waters with  $\delta D$  values of ca. -7‰. [Wang *et al.*, 2002], and the coupled fractionation of oxygen and hydrogen isotopes within the water cycle [Dansgaard, 1964], combined with  $\delta^{18}O$  data obtained from Norwegian waters [Mikalsen and Sejrup, 2000], suggests that the botryococenes were biosynthesized in saline to brackish waters, i.e. in the Drammensfjord itself. *B. braunii* is indeed known to thrive in environments with intermittently saline conditions [Metzger *et al.*, 1991] and an *in situ* production of botryococenes in the fjord water would also best explain the preservation of these isoprenoidal alkenes, which may be oxidized relatively easily during transport in oxic waters [Sun and Wakeham, 1994; Prahel *et al.*, 2000; Sinninghe Damsté *et al.*, 2002b]. However, it seems uncommon for *B. braunii* to thrive in present-day, unpolluted settings comparable with the Drammensfjord.

According to the constructed age model, the molecular fossils of *B. braunii* disappear from the sedimentary record between 1800 and 1850 AD (Fig. 7.1). This predates the last observation of *B. braunii* in the fresh water bodies in the region [early 20<sup>th</sup> century; D. Klaveness, pers. comm.]. Possibly, *B. Braunii* thrived in the fjord itself before 1800 AD, and only autochthonously produced botryococenes could reach the fjord sediment, while botryococenes produced in the hinterland did not survive transport. It is also possible, however, that before 1800 AD frequent blooms occurred in the Drammensfjord region, resulting in the transport of substantial amounts of botryococenes to the Drammensfjord sediments, while after that time *B. braunii* did only occur as single cells, not capable of producing detectable amounts of botryococenes. The presence of *B. braunii* fossils in sediments is commonly regarded as an indicator for fresh water conditions or for settings with a substantial fresh-water input [e.g. Tyson, 1995b; Kunz-Pirring, 1999; Matthiesen *et al.*, 2000], and their disappearance from the fjord's sedimentary record may thus also be related with a hydrographical change. Water regulations in the drainage area of the Drammensfjord took, however, only place in the 20<sup>th</sup> century [Alve, 1991]. This is

substantially later than the disappearance of *B. braunii* from the Drammensfjord area (Fig. 7.1), which renders this scenario to be unlikely. The gradual decrease in sill depth, due to the isostatic uplift of Scandinavia [Pirazolli, 1991], could also have affected the hydrography of the Drammensfjord. This may have influenced the circumstances for *B. braunii* if the alga was extant in the fjord itself, but not when the *B. braunii* molecular fossils are of allochthonous origin from the hinterland.

It is striking that the disappearance of the botryococenes is concurrent with the increase in the  $C_{\text{org}}/\text{TN}$  ratio, while TOC and TN contents had at that time already started to increase (Fig. 7.1). The first increase of TOC and TN contents can tentatively be connected with the first settlements of sawmills along the river Drammen and upstream water bodies that also took place around that time [Alve, 1991 and references therein]. The settlement of paper and pulp mills in the area led to an increased load of fibrous terrestrial organic matter, exhibiting a high C/N ratio [Aitkenhead and McDowell, 2000]. Degradation of the increasing amount of organic matter must also have led to a higher nutrient concentration in the fjord system, which is reflected in the TN profile (Fig. 7.1). This eutrophication gave then probably rise to a higher primary production, further increasing the TOC accumulation rate. The disappearance of *B. braunii* from the Drammensfjord or its tributaries may well be related with this early anthropogenic eutrophication. Indeed, according to Tyson [1995b], the abundance of *B. braunii* is strongly influenced by its slow rate of growth and blooms of this alga are relatively sporadic due to the time they need to develop. Therefore, they require minimal competition and thus prefer oligotrophic conditions. Because of this, it is very likely that as a result of the increased nutrient availability in the fjord area, *B. braunii* was outcompeted by other, faster growing algae, resulting in their demise. The observed correlation of the disappearance of *B. braunii* with the early eutrophication of the Drammensfjord area suggests that the molecular fossils of *B. braunii* in sediments can be a useful palaeoenvironmental indicator for oligotrophic conditions. Even though in this case it most likely concerns an anthropogenic induced eutrophication effect, the same should be valid for natural occurring eutrophication mechanisms, generally linked to physiochemical parameters like variations in the climate or the oceanographical, hydrographical or geographical setting. Thus, the molecular fossils of *B. braunii* in a coastal marine sedimentary record may be used as an indicator of either a change in the fresh water input to a marine system, but also as an indicator of a change in the trophic state of that fresh water.

## 7.6. Conclusions

In the sedimentary record of the Drammensfjord, Norway, a suite of mono- and bicyclic botryococenes, derived from the unicellular alga *B. braunii* race B, were present before 1800 -1850 AD, but absent thereafter. This can not be related with a change towards less fresh water input to the fjord but coincides with the settlement of pulp and paper mills in the area, which influenced the trophic state of the fresh water bodies in the hinterland of the fjord. Considering the preference of this alga for oligotrophic conditions, it is argued that this early eutrophication first led to the reduction of bloom concentrations to single occurrences, and later to the effective extinction of this alga from the fresh water bodies in the hinterland. It is proposed that molecular fossils of *B. braunii* fossils can be used as an indicator for oligotrophy, in addition to its current use as an indicator for fresh-water input to marine sediments.

## Acknowledgements

The authors thank Wim Boer and Rineke Gieles for  $^{210}\text{Pb}$  analysis. The crew of R/V Pelagia, Matthias Paetzel, Frode Uriansrud and Bart van Dongen are thanked for their assistance in obtaining the sediment cores. The staff at the National Ocean Sciences Accelerator Mass Spectrometry Facility at Woods Hole, USA, is thanked for  $^{14}\text{C}$  analyses. Michiel Kienhuis and Elda Panoto are thanked for their assistance in GC/MS analysis. S. Hällfors, Department of Biological Oceanography Finnish Institute of Marine Research, and Prof. Dr. D. Klaveness, University of Oslo, are thanked for information regarding the current occurrence of *B. braunii* in Scandinavia. Dr. P. Metzger is thanked for providing the botryococcene standard.

## References

- Aitkenhead, J. A. and W. H. McDowell, Soil C:N ratio as predictor of annual riverine DOC flux at local and global scales, *Global Biogeochem. Cy.*, 14, 127-138, 2000.
- Alve, E., Variations in estuarine foraminiferal biofacies with diminishing oxygen conditions in Drammensfjord, SE Norway, in *Palaeoecology, biostratigraphy, palaeoceanography, and taxonomy of agglutinated foraminifera*, edited by C. Hemleben, D. B. Scott, M. Kaminski, and W. Kuhnt, pp. 661-694, Kluwer Academic Publishers, Dordrecht, 1990.
- Alve, E., Foraminifera, climatic change, and pollution: a study of late Holocene sediments in Drammensfjord, southeast Norway, *The Holocene*, 1, 243-261, 1991.
- Alve, E., Benthic foraminiferal distribution and recolonization of formerly anoxic environments in Drammensfjord, southern Norway, *Mar. Micropaleontol.*, 25, 169-186, 1995.
- Anderson, J. J. and A. H. Devol, Deep water renewal in Saanich Inlet, an intermittently anoxic basin, *Estuar. Coast. Mar. Sci.*, 1, 1-10, 1973.
- Anderson, J. J. and A. H. Devol, Extent and intensity of the anoxic zone in basins and fjords, *Deep-Sea Res.*, 34, 927-944, 1987.
- Andr n, E., Changes in the composition of the diatom flora during the last century indicate increased eutrophication of the Oder estuary, South-western Baltic Sea, *Estuar. Coast. Shelf Sci.*, 48, 665-676, 1999.
- Baas, M., R. Pancost, B. Van Geel, and J. S. Sinninghe Damst , A comparative study of lipids in *Sphagnum* species, *Org. Geochem.*, 31, 535-539, 2000.
- Beck, J. W., J. R cy, F. Taylor, R. L. Edwards, and G. Caboich, Abrupt changes in early Holocene tropical sea surface temperature derived from coral records, *Nature*, 385, 705-710, 1997.
- Berner, R. A., Sedimentary pyrite formation: An update, *Geochim. Cosmochim. Acta*, 48, 605-615, 1984.
- Bertram, H.-G., Carbon dioxide and climate: climatic impact of soil-borne CO<sub>2</sub>, in *diversity of environmental biogeochemistry*, edited by J. Berthelin, pp. 391-395, Elsevier Publishers B.V., Amsterdam, 1991.
- Bigdare, R. R., A. Fluegge, K. F. Freeman, K. L. Hanson, J. M. Hayes, D. Hollander, J. P. Jasper, L. L. King, E. A. Laws, J. Milder, F. J. Millero, R. D. Pancost, B. N. Popp, P. A. Steinberg, and S. G. Wakeham, Consistent fractionation of <sup>13</sup>C in nature and in the laboratory: Growth-rate effects in some haptophyte algae, *Global Biogeochem. Cy.*, 11, 279-292, 1997.
- Blais-Stevens, A., B. D. Bornhold, A. E. S. Kemp, J. M. Dean, and A. A. Vaan, Overview of Late Quaternary stratigraphy in Saanich Inlet, British Columbia: results of Ocean Drilling Program Leg 169S, *Mar. Geol.*, 174, 3-26, 2001.
- Boon, J. J., F. De Lange, P. J. W. Schuyf, J. W. De Leeuw, and P. A. Schenck, Organic Geochemistry of Walvis Bay Diatomaceous Ooze. II Occurrence and Significance of the hydroxy fatty acids, in *Advances in Organic Geochemistry*, edited by R. Campos and J. Goni, pp. 255-272, ENADIMSA, Madrid, 1977.
- Boon, J. J., W. I. C. Rijpstra, F. De Lange, J. W. De Leeuw, M. Yoshioka, and Y. Shimizu, Black sea sterol- a molecular fossil for dinoflagellate blooms., *Nature*, 277, 125-127, 1979.
- Bornhold, B. D., J. V. Firth, and et al., Proceedings of the Ocean Drilling Program, Initial Reports, 169S, pp. 5-138, Ocean Drilling Program, College Station, TX, 1998.
- Bradley, R. S. and P. D. Jones, Climate since A.D. 1500, pp. 0-679, Routledge, London, 1992.
- Brassell, S. C., Applications of biomarkers for delineating marine paleoclimatic fluctuations during the Pleistocene, in *Organic Geochemistry. Principles and Applications*, edited by M. H. Engel and S. A. Macko, pp. 699-738, Plenum Press, New York-London, 1993.
- Brassell, S. C. and G. Eglinton, Steroids and triterpenoids in Deep Sea sediments as environmental and diagenetic indicators, in *Advances in Organic Geochemistry 1981*, edited by M. Bjoroy and et al., pp. 684-697, John Wiley & Sons Ltd., Chichester, 1983.
- Brassell, S. C., G. Eglinton, J. R. Maxwell, and R. P. Philip, Natural background of alkanes in the aquatic environment, in *aquatic Pollutants: Transformations and biological effects*, edited by O. Hutzinger, W. H. Van Lelyveld, and B. C. Zoeterman, pp. 69-86, Pergamon Ser. Environ. Sci., Oxford, 1978.
- Brassell, S. C., G. Eglinton, I. T. Marlowe, U. Pflaumann, and M. Sarnthein, Molecular stratigraphy: a new tool for climatic assessment, *Nature*, 320, 129-133, 1986.
- Broecker, W. S., Chaotic climate, *Scientific American*, November 1995, 62-68, 1995.
- Broecker, W. S., Y. Lao, M. Klas, and E. Clarck, A search for an early Holocene CaCO<sub>3</sub> preservation event, *Paleoceanography*, 8, 333-339, 1993.
- Caimi, R. J. and J. T. Brenna, Quantitative evaluation of carbon isotopic fractionation during reversed-phase high-performance liquid chromatography, *J. Chromatogr. A*, 757, 307-310, 1997.
- Collister, J. W.,  . Lichtfouse, G. Hieshima, and J. M. Hayes, Partial resolution of source of *n*-alkanes in the saline portion of the Parachute Creek Member, Green River Formation (Piceance Creek Basin, Colorado), *Org. Geochem.*, 21, 645-659, 1994a.

## References

- Collister, J. W., G. Rieleley, B. Stern, G. Eglinton, and B. Fry, Compound-specific  $\delta^{13}\text{C}$  analyses of leaf lipids from plants with differing carbon dioxide metabolisms, *Org. Geochem.*, 21, 619-627, 1994b.
- Conte, M. H., J. C. Weber, L. L. King, and S. G. Wakeham, The alkenone temperature signal in western North Atlantic surface waters, *Geochim. Cosmochim. Acta*, 65, 4275-4287, 2001.
- Conte, M. H., A. Thompson, and G. Eglinton, Primary production of lipid biomarker compounds by *Emiliana Huxleyi*: Results from an experimental mesocosm study in fjords of southwestern Norway, *Sarsia*, 79, 319-331, 1994.
- Conte, M. H., A. Thompson, D. Lesley, and R. P. Harris, Genetic and physiological influences on the alkenone/alkenoate versus growth temperature relationship in *Emiliana huxleyi* and *Gephyrocapsa oceanica*, *Geochim. Cosmochim. Acta*, 62, 51-68, 1998.
- Conte, M. H. and J. C. Weber, Long-range atmospheric transport of terrestrial biomarkers to the western North Atlantic, *Global Biochemical Cycles*, 16, 89-1-89-17, 2002.
- Cook, E. R., R. D. D'Arrigo, and K. R. Briffa, A reconstruction of the North Atlantic Oscillation using tree-ring chronologies from North America and Europe, *The Holocene*, 8, 9-17, 1998.
- Coolbear, T. and D. R. Threfall, Biosynthesis of terpenoid lipids, in *Microbial Lipids, Vol 2*, edited by C. Ratledge and S. G. Wilkinson, pp. 115-254, Academic press limited, London, 1989.
- Coplen, T. B., New guidelines for reporting stable hydrogen, carbon, and oxygen isotope-ratio data, *Geochim. Cosmochim. Acta*, 60, 3359-3360, 1996.
- Cowie, G. L., J. I. Hedges, and S. E. Calvert, Sources and relative reactivities of amino acids, neutral sugars, and lignin in an intermittently anoxic marine environment, *Geochim. Cosmochim. Acta*, 56, 1963-1978, 1992.
- Cranwell, P. A., Diagenesis of free and bound lipids in terrestrial detritus deposited in a lacustrine sediment, *Org. Geochem.*, 3, 79-89, 1981.
- Cranwell, P. A., Lipids of aquatic sediments and sedimenting particulates, *Prog. Lipid Res.*, 21, 271-308, 1982.
- Cranwell, P. A., Long-chain unsaturated ketones in recent lacustrine sediments, *Geochim. Cosmochim. Acta*, 49, 1545-1551, 1985.
- Crutzen, P. J., Geology of mankind, *Nature*, 415, 23, 2002.
- Cullen, H. M., R. D. D'Arrigo, E. R. Cook, and M. E. Mann, Multiproxy reconstructions of the North Atlantic Oscillation, *Palaeoceanography*, 16, 27-39, 2001.
- Dale, B., T. A. Thorsen, and A. Fjellså, Dinoflagellate cysts as indicators of cultural eutrophication in the Oslofjord, Norway, *Estuar. Coast. Shelf Sci.*, 48, 371-382, 1999.
- Dansgaard, W., Stable isotopes in precipitation, *Tellus*, XVI, 436-468, 1964.
- David, M., P. Metzger, and E. Casadevall, Two cyclobotryococenes from the B race of the green alga *Botryococcus braunii*, *Phytochemistry*, 27, 2863-2867, 1988.
- De Haas, H., W. Boer, and T. C. E. Van Weering, Recent sedimentation and organic carbon burial in a shelf sea: the North Sea, *Mar. Geol.*, 144, 131-146, 1997.
- De Leeuw, J. W. and C. Largeau, A review of macromolecular organic compounds that comprise living organisms and their role in kerogen, coal and petroleum formation., *Org. Geochem.*, 23-63, 1993.
- De Leeuw, J. W., N. L. Frewin, P. F. Bergen, J. S. Sinnighe Damsté, and M. E. Collison, Organic carbon as a palaeoenvironmental indicator in the marine realm, in *Marine Palaeoenvironmental Analysis from Fossils*, edited by D. W. J. Bosence and P. A. Allison, pp. 43-71, Geological Society, London, 1995.
- De Rosa, M. and A. Gambacorta, The lipids of Archaeobacteria, *Prog. Lipid Res.*, 27, 153-175, 1988.
- De Rosa, M., A. Gambacorta, and A. Gliozzi, Structure, biosynthesis, and physicochemical properties of Archaeobacterial lipids, *Microbiol. Rev.*, 70-80, 1986.
- Degens, E. T. and P. Stoffers, Stratified waters as a key to the past, *Nature*, 263, 22-27, 1976.
- Deines, P., The isotopic composition of reduced organic carbon, in *Handbook of environmental isotope geochemistry*, edited by P. Fritz and J. Ch. Fontes, pp. 329-406, Elsevier Scientific Publishing Company, Amsterdam, 1980.
- Dowling, L. M., C. J. Boreham, J. M. Hope, A. P. Murray, and R. E. Summons, Carbon isotopic composition of hydrocarbons in ocean-transported bitumen from the coastline of Australia, *Org. Geochem.*, 23, 729-737, 1995.
- Druffel, E. R. M., J. E. Bauer, P. M. Williams, S. Griffin, and D. Wolgast, Seasonal variability of particulate organic radiocarbon in the northeast Pacific Ocean, *J. Geophys. Res.*, 101, 20,543-20,552, 1996.
- Elder, L., G. Hällfors, and Å. Niemi, A preliminary check-list of the phytoplankton of the Baltic Sea, *Acta Botanica Fennica*, 128, 1-26, 1994.
- Eglinton, G. and R. J. Hamilton, Leaf epicuticular waxes, *Science*, 156, 1322-1335, 1967.
- Eglinton, T. I., L. I. Aluwihare, J. E. Bauer, E. R. M. Druffel, and A. P. McNichol, Gas chromatographic isolation of individual compounds from complex matrices for radiocarbon dating, *Anal. Chem.*, 68, 904-912, 1996.
- Eglinton, T. I., B. C. Benitez-Nelson, A. Pearson, A. P. McNichol, J. E. Bauer, and E. R. M. Druffel, Variability in radiocarbon ages of individual organic compounds from marine sediments, *Science*, 277, 796-799, 1997.
- Ficken, K. J. and P. Farrimond, Sedimentary lipid geochemistry of Framvaren: impacts of a changing environment, *Mar. Chem.*, 51, 31-43, 1995.



- Freeman, K. H., J. M. Hayes, J. M. Trendel, and P. Albrecht, Evidence from carbon isotope measurements for diverse origins of sedimentary hydrocarbons, *Nature*, 343, 254-256, 1990.
- Freeman, K. H. and S. G. Wakeham, Variations in the distributions and isotopic compositions of alkenones in Black Sea particles and sediments, *Org. Geochem.*, 19, 277-285, 1992.
- Fry, B., H. W. Jannasch, S. J. Molyneaux, C. O. Wirsén, J. A. Muramoto, and S. King, Stable isotope studies of carbon, nitrogen and sulfur cycles in the Black Sea and the Cariaco Trench, *Deep-Sea Res.*, 38, 1003-1019, 1991.
- Fry, B. and S. C. Wainright, Diatom sources of  $^{13}\text{C}$ -rich carbon in marine food webs, *Mar. Ecol.-Prog. Ser.*, 76, 149-157, 1991.
- Geel, B. v., O. M. Raspopov, H. Renssen, J. v. d. Plicht, V. A. Dergachev, and H. A. J. Meijer, The role of solar forcing upon climate change, *Quaternary Sci. Rev.*, 18, 331-338, 1999.
- Gerdes, G., B. E. M. Petzelberger, B. M. Scholz-Böttcher, and H. Streif, The record of climate change in the geological archives of shallow marine, coastal, and adjacent lowland areas of Northern Germany, *Quaternary Sci. Rev.*, 22, 101-124, 2003.
- Giner, J.-L., L. Wünsche, R. A. Andersen, and C. Djerassi, Dinoflagellates cyclize squalene oxide to lanosterol, *Biochem. Syst. Ecol.*, 19, 143-145, 1991.
- Gleixner, G., C. I. Czimzik, C. Kramer, B. Lühker, and M. W. I. Schmidt, Plant compounds and their turnover and stabilization as soil organic matter, in *Global Biogeochemical Cycles in the Climate System*, edited by E. D. Schulze, pp. 201-215, Academic Press, San Diego, 2002.
- Goericke, R. and B. Fry, Variations of marine plankton delta  $^{13}\text{C}$  with latitude, temperature and dissolved  $\text{CO}_2$  in the world ocean., *Global Biogeochem. Cy.*, 8, 85-90, 1994.
- Goericke, R., J. P. Montoya, and B. Fry, Physiology of isotopic fractionation in algae and cyanobacteria, in *Stable Isotopes in Ecology and Environmental Science*, edited by K. Lajtha and R. Michener, pp. 187-221, Blackwell Scientific Publications, London, 1994.
- Goodfriend, G. A., Radiocarbon reservoir ages in the Gulf of California: Roles of upwelling and flow from the Colorado River, *Radiocarbon*, 39, 139-148, 1997.
- Goossens, H., R. R. Düren, J. W. De Leeuw, and P. A. Schenck, Lipids and their mode of occurrence in bacteria and sediments - II. Lipids in the sediment of a stratified, freshwater lake., *Org. Geochem.*, 14, 27-41, 1989.
- Gowen, R. J., D. J. Hydes, D. K. Mills, B. M. Stewart, J. Brown, C. E. Gibson, T. M. Shammou, M. Allen, and S. J. Malcolm, Assessing trends in nutrient concentrations in coastal shelf seas: a case study in the Irish Sea, *Estuar. Coast. Shelf Sci.*, 54, 927-939, 1999.
- Grice, K., W. C. M. Klein Breteler, S. Schouten, V. Grossi, J. W. De Leeuw, and J. S. Sinninghe Damsté, Effects of zooplankton herbivory on biomarker proxy records, *Paleoceanography*, 13, 686-693, 1998a.
- Grice, K., S. Schouten, A. Nissenbaum, J. Charrach, and J. S. Sinninghe Damsté, A remarkable paradox: sulfurised freshwater algal (*Botryococcus braunii*) lipids in an ancient hypersaline euxinic ecosystem, *Org. Geochem.*, 28, 195-216, 1998b.
- Gucluer, S. M. and M. G. Gross, Recent Marine Sediments in Saanich Inlet, a Stagnant Marine Basin, *Limnol. Oceanogr.*, 9, 359-376, 1964.
- Guilderson, T. P., Radiocarbon as a diagnostic tracer in ocean and carbon cycle modeling, *Global Biogeochem. Cy.*, 14, 887-902, 2000.
- Gustafsson, M., Thesis, Recent and late Holocene development of the marine environment in three fjords on the Swedish west coast, Earth science centre, Göteborg University, Göteborg, 2000.
- Hartgers, W. A., J. S. Sinninghe Damsté, M. P. Koopmans, and J. W. De Leeuw, Sedimentary evidence for a diaromatic carotenoid with an unprecedented aromatic substitution pattern, *J. Chem. Soc. Chem. Comm.*, 23, 1715-1716, 1993.
- Hartgers, W. A., J. S. Sinninghe Damsté, A. G. Requejo, J. Allan, J. M. Hayes, Y. Ling, T.-M. Xie, J. Primack, and J. W. De Leeuw, A molecular and carbon isotopic study towards the origin and diagenetic fate of diaromatic carotenoids, *Org. Geochem.*, 22, 703-725, 1994.
- Hartgers, W. A., S. Schouten, J. F. Lopez, J. S. Sinninghe Damsté, and J. O. Grimalt,  $^{13}\text{C}$ -contents of sedimentary bacterial lipids in a shallow sulfidic monomictic lake (Lake Cisó, Spain), *Org. Geochem.*, 31, 777-786, 2000.
- Hartnett, H. E., R. G. Keil, J. I. Hedges, and A. H. Devol, Influence of oxygen exposure time on organic carbon preservation in continental margin sediments, *Nature*, 391, 572-574, 1998.
- Harvey, H. R. and S. A. Macko, Kinetics of phytoplankton decay during simulated sedimentation: changes in lipids under oxic and anoxic conditions, *Org. Geochem.*, 27, 129-140, 1997.
- Harvey, H. R. and G. B. McManus, Marine ciliates as a widespread source of tetrahymanol and hopan-3 $\beta$ -ol in sediments, *Geochim. Cosmochim. Acta*, 55, 3387-3390, 1991.
- Harvey, H. R., S. C. M. O'Hara, G. Eglinton, and E. D. S. Corner, The comparative fate of dinosterol and cholesterol in copepod feeding: Implications for a conservative molecular biomarker in the marine water column, *Org. Geochem.*, 14, 635-641, 1989.

## References

- Hayes, J. M., Fractionation of the isotopes of Carbon and Hydrogen in biosynthetic processes, in *Stable Isotope Geochemistry, Reviews in Mineralogy and Geochemistry, Vol 43*, edited by J. W. Valley and D. R. Cole, pp. 225-278, Mineralogical Society of America, Washington, DC, 2001.
- Hedges, J. I. and R. G. Keil, Sedimentary organic matter preservation: an assessment and speculative synthesis, *Mar.Chem.*, 49, 81-115, 1995.
- Hedges, J. I. and J. M. Oades, Comparative organic geochemistries of soils and marine sediments, *Org.Geochem.*, 27, 319-361, 1997.
- Heier-Nielsen, S., J. Heinemeier, H. L. Nielsen, and N. Rud, Recent reservoir ages for Danish fjords and marine waters, *Radiocarbon*, 37, 875-882, 1995.
- Hird, S. J. and S. J. Rowland, An investigation of the sources and seasonal variations of highly branched isoprenoid hydrocarbons in intertidal sediments of the Tamar Estuary, UK, *Mar.Environ.Res.*, 40, 423-437, 1995.
- Hobson, L. A. and M. R. McQuoid, Pelagic diatom assemblages are good indicators of mixed water intrusions into Saanich Inlet, a stratified fjord in Vancouver Island, *Mar.Geol.*, 174, 125-138, 2001.
- Hoefs, M. J. L., S. Schouten, J. W. De Leeuw, L. L. King, S. G. Wakeham, and J. S. Sinninghe Damsté, Ether lipids of planktonic Archaea in the marine water column, *Appl.Environ.Microbiol.*, 63, 3090-3095, 1997.
- Hoek, C. v. d., D. G. Mann, and H. M. Jahns, *Algae*, University Press, Cambridge, UK, 1995.
- Hopmans, E. C., S. Schouten, R. D. Pancost, M. T. J. Van der Meer, and J. S. Sinninghe Damsté, Analysis of intact tetraether lipids in archaeal cell material and sediments by high performance liquid chromatography/atmospheric pressure chemical ionization mass spectrometry, *Rapid.Commun.Mass Spectrom.*, 14, 585-589, 2000.
- Huang, W.-Y. and W. G. Meinschein, Sterols as source indicators of organic materials in sediments, *Geochim.Cosmochim.Acta*, 40, 323-330, 1976.
- Huang, Y., F. A. Street-Perrott, R. A. Perrott, P. Metzger, and G. Eglinton, Glacial-interglacial environmental changes inferred from molecular and compound-specific  $\delta^{13}\text{C}$  analyses of sediments from Sacred Lake, Mt. Kenya, *Geochim.Cosmochim.Acta*, 63, 1383-1404, 1999.
- Hughen, K. A., J. R. Southon, S. J. Lehman, and J. T. Overpeck, Synchronous radiocarbon and climate shifts during the last deglaciation, *Science*, 290, 1951-1954, 2000.
- Hulme, M., E. Barrow, N. W. Arnell, P. A. Harrison, T. C. Johns, and T. E. Downing, Relative impacts of human-induced climate change and natural climate variability, *Nature*, 397, 688-691, 1999.
- Huntley, D. H., P. T. Bobrowsky, and J. J. Clague, Ocean Drilling Program Leg 169S: surficial geology, stratigraphy and geomorphology of the Saanich Inlet area, southeastern Vancouver Island, British Columbia, *Mar.Geol.*, 174, 27-41, 2001.
- Indermuhle, A., T. F. Stocker, F. Joos, H. Fisher, H. J. Smith, M. Wahlen, B. Deck, D. Mastroianni, J. Tschumi, T. Blunier, and B. Stauffer, Holocene carbon-cycle dynamics based on  $\text{CO}_2$  trapped in ice at Taylor Dome, Antarctica, *Nature*, 398, 121-126, 1999.
- Ingram, B. L. and J. R. Southon, Reservoir ages in Eastern Pacific coastal and estuarine waters, *Radiocarbon*, 38, 573-582, 1996.
- Innes, H. E., A. N. Bishop, P. A. Fox, I. M. Head, and P. Farrimond, Early diagenesis of bacteriohopanoids in Recent sediments of Lake Pollen, Norway, *Org.Geochem.*, 29, 1285-1295, 1998.
- Johannessen, T. and E. Dahl, Declines in oxygen concentration along the Norwegian Skagerrak coast, 1927-1993: A signal of ecosystem changes due to eutrophication?, *Limnol.Oceanogr.*, 41, 766-778, 1996.
- Jones, P. D., K. R. Briffa, T. P. Barnett, and S. F. B. Tett, High-resolution, palaeoclimatic records for the last millennium: interpretation, integration and comparison with General Circulation Model control-run temperatures, *The Holocene*, 8, 455-471, 1998.
- Kalis, A. J., J. Merkt, and J. Wunderlich, Environmental changes during the Holocene climatic optimum in central Europe - human impact and natural causes, *Quaternary Sci.Rev.*, 22, 33-79, 2003.
- Kaplan, J. O., I. C. Prentice, W. Knorr, and P. J. Valdes, Modelling the dynamics of terrestrial carbon storage since the Last Glacial Maximum, *Geophys.Res.Lett.*, 29, doi:10.1029/2002GL015230, 2002.
- Karner, M. B., E. F. DeLong, and D. M. Karl, Archaeal dominance in the mesopelagic zone of the Pacific Ocean, *Nature*, 409, 507-510, 2001.
- Kemp, A. E. S., Palaeoclimatology and palaeoceanography from laminated sediments, *Geol.Soc.Spec.Publ. 116*, The Geological Society, Bath, 1996.
- Key, R. M., P. D. Quay, G. A. Jones, A. P. McNichols, K. F. Von Reden, and R. J. Schneider, WOCE AMS radiocarbon I: Pacific Ocean results (P6, P16 and P17), *Radiocarbon*, 38, 425-518, 1996.
- Kharé, P., Kangasniemi, B., and Alder, A. Saanich Inlet Study Synthesis Report Summary, 34 pp., Victoria, BC, Province of British Columbia, 2001.
- Killops, S. D. and V. J. Killops, Production and fate of organic matter, in *An Introduction to Organic Geochemistry*, edited by R. C. O. Gill, pp. 1-21, Longman Group UK Limited, Harlow, 1993.

- Kleemann, G., K. Poralla, G. Englert, H. Kjösen, S. Liaaen-Jensen, S. Neunlist, and M. Rohmer, Tetrahymanol from the phototrophic bacterium *Rhodopseudomonas palustris*: first report of a gammacerane triterpene from a prokaryote, *J.Gen.Microbiol.*, 136, 2551-2553, 1990.
- Kokke, W. C. M. C., L. Bohlin, W. Fenical, and C. Djerassi, Novel dinoflagellate 4 $\alpha$ -methylated sterols from four Caribbean Gorgonians, *Phytochemistry*, 21, 881-887, 1982.
- Kolattukudy, P. E., Cutin, Suberin, and Waxes, in *The Biochemistry of Plants, Vol. 4*, edited by P. K. Stumpf, pp. 571-641, Academic Press, New York, 1980.
- Kolattukudy, P. E., T. J. Walton, and R. P. S. Kushwaha, Biosynthesis of the C<sub>18</sub> family of cutin acids:  $\omega$ -hydroxyoleic acid,  $\omega$ -hydroxy-9,10-epoxystearic acid, 9,10,18-trihydroxystearic acid, and their  $\Delta^{12}$ -unsaturated analogs, *Biochem.*, 12, 4488-4498, 1973.
- Kunz-Pirring, M., Distribution of Aquatic palynomorphs in surface sediments from the Laptev Sea, Eastern Arctic Ocean, in *Land-Ocean systems in the Siberian Arctic: Dynamics and history*, edited by H. Kassens, H. A. Bauch, I. Dmitrenko, H. Eicken, H.-W. Hubberten, M. Melles, J. Thiede, and L. Timokhov, pp. 561-575, Springer Verlag, Berlin, 1999.
- Kuypers, M. M. M., R. Pancost, I. A. Nijenhuis, and J. S. Sinninghe Damsté, Enhanced productivity led to increased organic burial in the euxinic North Atlantic basin during the late Cenomanian oceanic anoxic event, *Paleoceanography*, 17, 1051-1064, 2002.
- Küspert, W., Environmental changes during oil shale deposition as deduced from stable isotope ratios, in *Cyclic and Event Stratification*, edited by G. Einsele and A. Seilacher, pp. 482-501, Springer, Heidelberg, 1982.
- Leavitt, P. R. and S. R. Carpenter, Whole-lake experiments: The annual record of fossil pigments and zooplankton, *Limnol.Oceanogr.*, 34, 700-717, 1989.
- Lehtonen, K. and M. Ketola, Occurrence of long-chain acyclic methyl ketones in *Sphagnum* and *Carex* peats of various degrees of humification, *Org.Geochem.*, 15, 275-280, 1990.
- Levin, I. and V. Heshshaimer, Radiocarbon - a unique tracer of global carbon cycle dynamics, *Radiocarbon*, 42, 69-80, 2000.
- Levitus, S., J. I. Antonov, T. P. Boyer, and C. Stephens, Warming of the world ocean, *Science*, 287, 2225-2229, 2000.
- Li, J., R. P. Philp, F. Pu, and J. Allan, Long-chain alkenones in Qinghai lake sediments, *Geochim.Cosmochim.Acta*, 60, 235-241, 1996.
- Lockheart, M. J., P. F. Bergen, and R. P. Evershed, Variations in the stable carbon isotope compositions of individual lipids from leaves of modern angiosperms: implications for the study of higher land plant-derived sedimentary organic matter, *Org.Geochem.*, 26, 137-153, 1997.
- Mann, M. E., R. S. Bradley, and M. K. Hughes, Global-scale temperature patterns and climate forcing over the past six centuries, *Nature*, 392, 779-787, 1998.
- Mansour, M. P., J. K. Volkman, A. E. Jackson, and S. I. Blackburn, The fatty acid and sterol composition of five marine dinoflagellates, *J.Phycol.*, 35, 710-720, 1999.
- Matthiesen, J., M. Kunz-Pirring, and P. J. Mudie, Freshwater chlorophycean algae in recent marine sediments of the Beaufort, Laptev and Kara Seas (Arctic Ocean) as indicators of river runoff, *Int.J.Earth Sci.*, 89, 470-485, 2000.
- Maxwell, J. R., A. G. Douglas, G. Eglinton, and A. McCormick, The Botryococenes-hydrocarbons of a novel structure from the alga *Botryococcus braunii*, Kützing, *Phytochemistry*, 7, 2157-2171, 1968.
- McNichol, A. P., A. J. T. Jull, and G. S. Burr, Converting AMS data to radiocarbon values: considerations and conventions, *Radiocarbon*, 43, 313-320, 2001.
- McQuoid, M. R., A post-glacial isotope record of primary production and accumulation in the organic sediments of Saanich Inlet, ODP Leg 169S, *Mar.Geol.*, 174, 273-286, 2001.
- Megens, L., J. Van der Plicht, and J. W. De Leeuw, Molecular, radioactive and stable carbon isotope characterization of estuarine particulate organic matter, *Radiocarbon*, 40, 985-990, 1998.
- Menzel, D., E. C. Hopmans, P. F. Van Bergen, J. W. De Leeuw, and J. S. Sinninghe Damsté, Development of photic zone euxinia in the eastern Mediterranean Basin during deposition of pliocene sapropels, *Mar.Geol.*, 189, 215-226, 2002.
- Merritt, D. A., K. H. Freeman, M. P. Ricci, S. A. Studley, and J. M. Hayes, Performance and optimization of a combustion interface for isotope ratio monitoring gas chromatography/mass spectrometry, *Anal.Chem.*, 67, 2461-2473, 1995.
- Metzger, P., E. Casadevall, M. J. Pouet, and Y. Pouet, Structures of some Botryococenes: branched hydrocarbons from the b-race of the green alga *Botryococcus braunii*, *Phytochemistry*, 24, 2995-3002, 1985.
- Metzger, P., C. Largeau, and E. Casadevall, Lipids and Macromolecular Lipids of the Hydrocarbon-rich Microalga *Botryococcus braunii*, in *Progress in the Chemistry of Organic Natural Products*, edited by W. Herz, G. W. Kirby, W. Steglich, and Ch. Tamm, pp. 1-70, Springer Verlag, Wien, 1991.
- Mikalsen, G. and H. P. Sejrup, Oxygen isotope composition of fjord and river water in the Sognefjorden drainage area, Western Norway. Implications for Paleoclimate studies, *Estuar.Coast.Shelf.Sci.*, 50, 441-448, 2000.

## References

- Mikalsen, G., H. P. Sejrup, and I. Aarseth, Late-Holocene changes in ocean circulation and climate: foraminiferal and isotopic evidence from Sulafjord, western Norway, *The Holocene*, 11, 437-446, 2001.
- Miura, Y. and A. J. Fulco,  $\omega-1$ ,  $\omega-2$ , and  $\omega-3$  Hydroxylation of long-chain fatty acids, amides and alcohols by a soluble enzyme system from *Bacillus megatherium*, *Biochim.Biophys.Acta*, 388, 305-317, 1975.
- Montesinos, E., R. Guerrero, C. Abella, and I. Esteve, Ecology and physiology of the competition for light between *Chlorobium limicola* and *Clorobium phaeobacteroides* in natural habitats, *Appl.Environ.Microbiol.*, 46, 1007-1016, 1983.
- Mook, W. G. and J. Van der Plicht, Reporting  $^{14}\text{C}$  activities and concentrations, *Radiocarbon*, 41, 227-239, 1999.
- Moy, C. M., G. O. Seltzer, D. T. Rodbell, and D. M. Anderson, Variability of el Niño/Southern Oscillation activity at millennial timescales during the Holocene epoch, *Nature*, 420, 162-165, 2002.
- Müller, P. J., G. Kirst, G. Ruhland, I. von Storch, and A. Rosell-Melé, Calibration of the alkenone paleotemperature index  $U^k_{37}$  based on core-tops from the eastern South Atlantic and the global ocean (60°N-60°S), *Geochim.Cosmochim.Acta*, 62, 1757-1772, 1998.
- Nederbragt, A. J., J. Thurow, and R. B. Merrill, Data report: Color records from the California Margin: Proxy indicators for sediment composition and climatic change, in *Proceedings of the Ocean Drilling Program, Scientific Results, Vol. 167*, edited by M. Lyle, I. Koizumu, C. Richter, and T. C. Moore, Jr., pp. 319-329, Ocean Drilling Program, College Station, TX, 2000.
- Nederbragt, A. J. and J. W. Thurow, A 6000 year varve record of Holocene climate in Saanich Inlet, British Columbia, from digital sediment colour analysis of ODP leg 169S cores, *Mar.Geol.*, 174, 95-110, 2001.
- Nixon, S. W., Marine eutrophication; a growing international problem, *Ambio*, 19, 101, 1990.
- Nordberg, K., H. L. Filipsson, M. Gustafsson, R. Harland, and P. Roos, Climate, hydrographic variations and marine benthic hypoxia in Koljö Fjord, Sweden, *J.Sea Res.*, 46, 187-200, 2001.
- NOSAMS, <http://www.nosams.who.edu/general/amsgenst.pdf>, 2003.
- Nydal, R. and J. S. Gislefoss, Further application of bomb  $^{14}\text{C}$  as a tracer in the atmosphere and ocean, *Radiocarbon*, 38, 389-406, 1996.
- Ohkouchi, N., T. I. Eglinton, L. D. Keigwin, and J. M. Hayes, Spatial and temporal offsets between proxy records in a sediment drift, *Science*, 298, 1224-1227, 2002.
- Otto, A. and B. R. T. Simoneit, Biomarkers of Holocene buried conifer logs from Bella Coola and north Vancouver, British Columbia, Canada, *Org.Geochem.*, 33, 1241-1251, 2002.
- Öztürk, M., Trends of trace metal (Mn, Fe, Co, Ni, Cu, Zn, Cd and Pb) distributions at the oxic-anoxic interface and in sulfidic water of the Drammensfjord, *Mar.Chem.*, 48, 329-342, 1995.
- Paetzel, M. and H. Schrader, Recent environmental changes recorded in anoxic Barsnesfjord sediments: Western Norway, *Mar.Geol.*, 105, 23-36, 1992.
- Pancost, R. D., K. H. Freeman, S. G. Wakeham, and C. Y. Robertson, Controls on carbon isotope fractionation by diatoms in the Peru upwelling region, *Geochim.Cosmochim.Acta*, 61, 4983-4991, 1997.
- Pancost, R. D., B. Van Geel, M. Baas, and J. S. Sinninghe Damsté,  $\delta^{13}\text{C}$  values and radiocarbon dates of microbial biomarkers as tracers for carbon recycling in peat deposits, *Geology*, 28, 663-666, 2000.
- Pätsch, J. and G. Radach, Long-term simulation of the eutrophication of the North Sea: temporal development of nutrients, chlorophyll and primary production in comparison to observations, *J.Sea Res.*, 38, 275-310, 1997.
- Pearson, A. and T. I. Eglinton, The origin of *n*-alkanes in the Santa Monica Basin surface sediment: a model based on compound-specific  $\Delta^{14}\text{C}$  and  $\delta^{13}\text{C}$  data, *Org.Geochem.*, 31, 1103-1116, 2000.
- Pearson, A., A. P. McNichol, R. J. Schneider, and K. F. Von Reden, Microscale AMS  $^{14}\text{C}$  measurement at NOSAMS, *Radiocarbon*, 40, 61-75, 1998.
- Pearson, A., T. I. Eglinton, and A. P. McNichol, An organic tracer for surface ocean radiocarbon, *Paleoceanography*, 15, 541-550, 2000.
- Pearson, A., A. P. McNichol, B. C. Benitez-Nelson, J. M. Hayes, and T. I. Eglinton, Origins of lipid biomarkers in Santa Monica Basin surface sediment: A case study using compound-specific  $\Delta^{14}\text{C}$  analysis, *Geochim.Cosmochim.Acta*, 65, 3123-3127, 2001.
- Pellatt, M. G., R. J. Hebda, and R. W. Mathewes, High-resolution Holocene vegetation history and climate from Hole 1034B, ODP leg 169S, Saanich Inlet, Canada, *Mar.Geol.*, 174, 211-226, 2001.
- Petit, J. R., J. Jouzel, D. Raynaud, N. I. Barkov, J.-M. Barnola, E. I. Basile, M. Bender, J. Chappellaz, M. Davis, G. Delaygue, M. Delmotte, V. M. Kotlyakov, M. Legrand, V. Y. Lipenkov, C. Lorius, L. Pépin, C. Ritz, E. Salzman, and M. Stievenard, Climate and atmospheric history of the past 420,000 years from the Vostok ice core, Antarctica, *Nature*, 399, 429-436, 2000.
- Petsch, S. T., T. I. Eglinton, and K. J. Edwards,  $^{14}\text{C}$ -dead living biomass: evidence for microbial assimilation of ancient organic carbon during shale weathering, *Science*, 292, 1127-1130, 2001.
- Pike, J. and E. S. Kemp, Early Holocene decadal-scale ocean variability recorded in Gulf of California laminated sediments, *Paleoceanography*, 12, 227-238, 1997.
- Pinturier-Geiss, L., L. Méjanelle, B. Dale, and D. A. Karlsen, Lipids as indicators of eutrophication in marine coastal sediments, *J.Microbiol.Meth.*, 48, 239-257, 2002.

- Pirazzoli, P. A., Fennoscandia: Introduction, in *World atlas of Holocene sea-level changes*, edited by P. A. Pirazzoli and J. Pluett, pp. 35-46, Elsevier Science Publishers B.V., Amsterdam, 1991.
- Prahl, F. G., J. Dymond, and M. A. Sparrow, Annual biomarker record for export production in the central Arabian Sea, *Deep-Sea Res. II*, 47, 1581-1604, 2000.
- Prince, S. D., E. Brown de Colstoun, and L. L. Kravitz, Evidence from rain-use efficiencies does not indicate extensive Sahelian desertification, *Global Change Biology*, 4, 359-374, 1998.
- Quirk, M. M., A. M. K. Wardroper, R. E. Wheatley, and J. R. Maxwell, Extended hopanoids in peat environments, *Chem. Geol.*, 42, 25-43, 1984.
- Rau, G. H., U. Riebesell, and D. A. Wolf-Gladrow, A model of photosynthetic  $^{13}\text{C}$  fractionation by marine phytoplankton based on diffusive molecular  $\text{CO}_2$  uptake, *Mar. Ecol.-Prog. Ser.*, 133, 275-285, 1996.
- Raymond, P. A. and J. E. Bauer, Riverine export of aged terrestrial organic matter to the North Atlantic Ocean, *Nature*, 409, 497-499, 2001a.
- Raymond, P. A. and J. E. Bauer, Use of  $^{14}\text{C}$  and  $^{13}\text{C}$  natural abundances for evaluating riverine, estuarine, and coastal DOC and POC sources and cycling: a review and synthesis, *Org. Geochem.*, 32, 469-485, 2001b.
- Reimer, P. J., F. G. McCormac, F. McCormick, and E. V. Murray, Marine radiocarbon reservoir corrections for the mid- to late Holocene in the eastern subpolar North Atlantic, *The Holocene*, 12, 129-135, 2002.
- Repeta, D. J., Carotenoid diagenesis in recent marine sediments: II. Degradation of fucoxanthin to loliolide, *Geochim. Cosmochim. Acta*, 53, 699-707, 1989.
- Richards, F. A., Anoxic basins and fjords, in *Chemical Oceanography, vol 1*, edited by J. P. Riley and G. Skirrow, pp. 611-643, Academic Press, London, 1965.
- Richards, F. A. and B. B. Benson, Nitrogen/argon and nitrogen isotope ratios in two anaerobic environments, the Cariaco Trench in the Caribbean Sea and Dramsfjord, Norway, *Deep-Sea Res.*, 7, 254-264, 1961.
- Riebesell, U., A. T. Revill, D. G. Holdsworth, and J. K. Volkman, The effects of varying  $\text{CO}_2$  concentration on lipid composition and carbon isotope fractionation in *Emiliania huxleyi*, *Geochim. Cosmochim. Acta*, 64, 4179-4192, 2000.
- Riele, G., R. J. Collier, D. M. Jones, and G. Eglinton, The biogeochemistry of Ellesmere Lake, U.K.-I: source correlation of leaf wax inputs to the sedimentary lipid record, *Org. Geochem.*, 17, 901-912, 1991a.
- Riele, G., R. P. Collier, D. M. Jones, G. Eglinton, P. A. Eakin, and A. E. Fallick, Sources of sedimentary lipids deduced from stable carbon-isotope analyses of individual compounds, *Nature*, 425-427, 1991b.
- Robinson, S. W. and G. Thomson, Radiocarbon corrections for marine shell dates with application to southern Pacific Northwest Coast prehistory, *Syesis*, 14, 45-57, 1981.
- Rohmer, M., P. Bissleret, and S. Neunlist, The hopanoids, prokaryotic triterpenoids and precursors of ubiquitous molecular fossils, in *Biological markers in sediments and petroleum*, edited by J. M. Moldowan, P. Albrecht, and R. P. Philp, pp. 1-17, Englewood Cliffs, Prentice-Hall, 1992.
- Rosell-Melele, A., J. Carter, and G. Eglinton, Distributions of long-chain alkenones and alkyl alkenoates in marine surface sediments from the North East Atlantic, *Org. Geochem.*, 22, 501-509, 1994.
- Rosenberg, R., R. Elmgren, S. Fleischer, P. Jonsson, G. Persson, and H. Dahlin, Marine eutrophication case studies in Sweden, *Ambio*, 19, 102-108, 1990.
- Round, F. E., R. M. Crawford, and D. G. Mann, *The diatoms*, 747pp., University Press, Cambridge, 1990.
- Rowland, S. J. and J. N. Robson, The widespread occurrence of highly branched acyclic  $\text{C}_{20}$ ,  $\text{C}_{25}$  and  $\text{C}_{30}$  hydrocarbons in recent sediments and biota - a review, *Mar. Environ. Res.*, 30, 191-216, 1990.
- Sancetta, C. and S. E. Calvert, The annual cycle of sedimentation in Saanich Inlet, British Columbia: implications for the interpretation of diatom fossil assemblage, *Deep-Sea Res.*, 35, 71-90, 1988.
- Schaeffer, P., Adam, P., Wehrung, P., Bernasconi, S., and Albrecht, P. Molecular and isotopic investigation of free and S-bound lipids from an actual meromictic lake (Lake Cadagno, Switzerland). Proceedings of the 18th int. meeting of organic Geochemistry pp. 57-58, Maastricht, The Netherlands, 1997.
- Schindler, D. W., The mysterious missing sink, *Nature*, 398, 105-107, 2000.
- Schouten, S., M. J. L. Hoefs, M. P. Koopmans, H. J. Bosch, and J. S. Sinninghe Damsté, Structural characterization, occurrence and fate of archaeal etherbound acyclic and cyclic biphytanes and corresponding diols in sediments, *Org. Geochem.*, 29, 1305-1319, 1998a.
- Schouten, S., W. C. M. Klein Breteler, P. Blokker, N. Schogt, W. I. C. Rijpstra, K. Grice, M. Baas, and J. S. Sinninghe Damsté, Biosynthetic effects on the stable carbon isotopic composition of algal lipids: Implications for deciphering the carbon isotopic biomarker record, *Geochim. Cosmochim. Acta*, 62, 1397-1406, 1998b.
- Schouten, S., M. J. L. Hoefs, and J. S. Sinninghe Damsté, A molecular and stable carbon isotopic study of lipids in late Quaternary sediments from the Arabian Sea, *Org. Geochem.*, 31, 509-521, 2000a.
- Schouten, S., E. C. Hopmans, R. D. Pancost, and J. S. Sinninghe Damsté, Widespread occurrence of structurally diverse tetraether membrane lipids: Evidence for the ubiquitous presence of low-temperature relatives of hyperthermophiles, *Proc. Nat. Acad. Sci., USA*, 97, 14421-14426, 2000b.
- Schouten, S., H. M. E. Van Kaam-Peters, W. I. C. Rijpstra, M. Schoell, and J. S. Sinninghe Damsté, Effects of an oceanic anoxic event on the stable carbon isotopic composition of early Toarcian carbon, *Am. J. Sci.*, 300, 1-22, 2000c.

## References

- Schouten, S., W. I. C. Rijpstra, M. D. Kok, E. C. Hopmans, R. E. Summons, J. K. Volkman, and J. S. Sinninghe Damsté, Molecular organic tracers of biogeochemical processes in a saline meromictic lake (Ace Lake), *Geochim.Cosmochim.Acta*, 65, 1629-1640, 2001.
- Schouten, S., E. C. Hopmans, E. Schefuß, and J. S. Sinninghe Damsté, Distributional variations in marine crenarchaeotal membrane lipids: a new tool for reconstructing ancient sea water temperatures, *Earth.Planet.Sci.Lett.*, 204, 265-274, 2002.
- Schulz, H.-M., A. Schöner, and K.-C. Emeis, Long-chain alkenone patterns in the Baltic Sea - an ocean-freshwater transition, *Geochim.Cosmochim.Acta*, 64, 469-477, 2000.
- Sheu, D. D. and B. J. Presley, Variation of calcium carbonate, organic carbon and iron sulfides in anoxic sediment from the Orca Basin, Gulf of Mexico, *Mar.Geol.*, 70, 103-118, 1986.
- Siani, G., M. Paterne, M. Arnold, E. Bard, B. Métivier, N. Tisnerat, and F. Bassinot, Radiocarbon reservoir ages in the Mediterranean Sea and Black Sea, *Radiocarbon*, 42, 271-280, 2000.
- Siani, G., M. Paterne, E. Michel, R. Sulpizio, A. Sbrana, M. Arnold, and G. Haddad, Mediterranean Sea surface radiocarbon reservoir age changes since the Last Glacial Maximum, *Science*, 294, 1917-1920, 2001.
- Simoneit, B. R. T., Cyclic terpenoids of the geosphere, in *Biological markers in the sedimentary record*, edited by R. B. Johns, pp. 43-99, Elsevier, Amsterdam, 1986.
- Simoneit, B. R. T., R. Chester, and G. Eglinton, Biogenic lipids in particulates from the lower atmosphere over the eastern Atlantic, *Nature*, 267, 682-685, 1977.
- Simoneit, B. R. T., J. O. Grimalt, T. G. Wang, R. E. Cox, P. G. Hatcher, and A. Nissenbaum, Cyclic terpenoids of contemporary resinous plant detritus and of fossil woods, ambers and coals, *Org.Geochem.*, 10, 877-889, 1985.
- Sinninghe Damsté, J. S. and J. W. De Leeuw, Analysis, structure and geochemical significance of organically-bound sulphur in the geosphere: State of the art and future research, in *Advances in Organic Geochemistry, 1989*, edited by B. Durand and F. Behar, pp. 1077-1101, 1990.
- Sinninghe Damsté, J. S., S. G. Wakeham, M. E. L. Kohlen, J. M. Hayes, and J. W. De Leeuw, A 6,000-year sedimentary molecular record of chemocline excursions in the Black Sea, *Nature*, 362, 827-829, 1993.
- Sinninghe Damsté, J. S., F. Kenig, M. P. Koopmans, J. Köster, S. Schouten, J. M. Hayes, and J. W. De Leeuw, Evidence for gammacerane as an indicator of water column stratification, *Geochim.Cosmochim.Acta*, 59, 1885-1900, 1995.
- Sinninghe Damsté, J. S., E. C. Hopmans, R. D. Pancost, S. Schouten, and J. A. J. Geenevasen, Newly discovered non-isoprenoid glycerol dialkyl glycerol tetraether lipids in sediments, *Chem.Comm.*, 1683-1684, 2000.
- Sinninghe Damsté, J. S., W. I. C. Rijpstra, E. C. Hopmans, F. Prahl, S. G. Wakeham, and S. Schouten, Distribution of membrane lipids of planktonic *Crenarchaeota* in the Arabian Sea, *Appl.Environ.Microbiol.*, 68, 2997-3002, 2002a.
- Sinninghe Damsté, J. S., W. I. C. Rijpstra, and G.-J. Reichart, The influence of oxic degradation on the sedimentary biomarker record II. Evidence from Arabian Sea sediments, *Geochim.Cosmochim.Acta*, 66, 2737-2754, 2002b.
- Sinninghe Damsté, J. S., S. Schouten, E. C. Hopmans, A. C. T. Duin, and J. A. J. Geenevasen, Crenarchaeol: the characteristic core glycerol dibiphytanyl glycerol tetraether membrane lipid of cosmopolitan pelagic crenarchaeota, *J.Lipid Res.*, 43, 1641-1651, 2002c.
- Sirevåg, R., B. B. Buchanan, J. A. Berry, and J. H. Troughton, Mechanism of CO<sub>2</sub> fixation in bacterial photosynthesis studied by the carbon isotope fractionation technique., *Arch.Microbiol.*, 112, 35-38, 1977.
- Skei, J., T. Bakke, and J. Molvaer, The Norwegian Coast, in *Seas at The Millennium: An Environmental Evaluation*, edited by C. Sheppard, pp. 17-30, Elsevier Science Ltd., Amsterdam, 2000.
- Skei, J. M., Framvaren- environmental setting, *Mar.Chem.*, 23, 209-218, 1988.
- Skerratt, J. H., P. D. Nichols, J. P. Bowman, and I. S. Lindsay, Occurrence and significance of long-chain ( $\omega$ -1)-hydroxy fatty acids in methane-utilizing bacteria, *Org.Geochem.*, 18, 189-194, 1992.
- Skipski, V. P., A. F. Smolowne, R. C. Sullivan, and M. Barclay, Separation of lipid classes by thin-layer chromatography, *Biochim.Biophys.Acta*, 106, 386-396, 1965.
- Smittenberg, R. H., Hopmans, E. C., Eglinton, T. I., Hayes, J. M., Whiticar, M. J., Schouten, S., and Sinninghe Damsté, J. S. Validation of compound-specific <sup>14</sup>C dating, using the varved sedimentary record of Saanich Inlet, Canada, Proceedings of the 20<sup>th</sup> International Meeting on Organic Geochemistry, Nancy, France, p.193, 2001; Chapter 2, This Thesis.
- Smittenberg, R. H., E. C. Hopmans, S. Schouten, and J. S. Sinninghe Damsté, Rapid isolation of biomarkers for compound specific radiocarbon dating using high-performance liquid chromatography and flow injection analysis-atmospheric pressure chemical ionisation mass spectrometry, *J.Chromatogr.A*, 978, 129-140, 2002.
- Southon, J. R., D. E. Nelson, and J. S. Vogel, A record of past ocean-atmosphere radiocarbon differences from the Northeast Pacific, *Paleoceanography*, 5, 197-206, 1990.
- St-Onge, G. and C. Hillaire-Marcel, Isotopic constraints of sedimentary inputs and organic carbon burial rates in the Saguenay Fjord, Quebec, *Mar.Geol.*, 176, 1-22, 2001.

- Stiles, P. M. Holnam West Material Ltd. Limestone Quarry - Texada Island. Focus on British Columbia Industrial Minerals. Proceedings British Columbia Geological Survey, pp.159-162, British Columbia Geological Survey, Vancouver, BC, Canada, 1995.
- Struck, U., K.-C. Emeis, M. Voss, C. Christiansen, and H. Kunzendorf, Records of southern and central Baltic Sea eutrophication in  $\delta^{15}\text{N}$  of sedimentary organic matter, *Mar. Geol.*, 164, 157-171, 2000.
- Stuiver, M. and T. F. Braziunas, Modelling atmospheric  $^{14}\text{C}$  influences and  $^{14}\text{C}$  ages of marine samples to 10,000 BC, *Radiocarbon*, 35, 137-189, 1993.
- Stuiver, M. and H. A. Polach, Discussion: reporting of  $^{14}\text{C}$  data, *Radiocarbon*, 19, 355-363, 1977.
- Stuiver, M., P. J. Reimer, E. Bard, J. W. Beck, G. S. Burr, K. A. Hughen, B. Kromer, G. McCormac, H. Van der Plicht, and M. Spurk, Intcal98 radiocarbon age calibration, 24,000-0 BP, *Radiocarbon*, 40, 1041-1083, 1998a.
- Stuiver, M., P. J. Reimer, and T. F. Braziunas, High-precision radiocarbon age calibration for terrestrial and marine samples, *Radiocarbon*, 40, 1127-1151, 1998b.
- Sullivan, B. E., F. G. Prahl, L. F. Small, and P. A. Covert, Seasonality of phytoplankton production in the Columbia River: A natural or anthropogenic pattern?, *Geochim.Cosmochim.Acta*, 65, 1125-1139, 2001.
- Summons, R. E., P. Metzger, C. Largeau, A. P. Murray, and J. M. Hope, Polymethylsqualanes from *Botryococcus braunii* in lacustrine sediments and crude oils, *Org.Geochem.*, 33, 99-109, 2002.
- Sun, M.-Y. and S. G. Wakeham, Molecular evidence for degradation and preservation of organic matter in the anoxic Black Sea Basin, *Geochim.Cosmochim.Acta*, 58, 3395-3406, 1994.
- Sun, M.-Y., S. G. Wakeham, R. C. Aller, and C. Lee, Impact of seasonal hypoxia on diagenesis of phytol and its derivatives in long Island Sound, *Mar.Chem.*, 62, 157-173, 1998.
- Takahashi, M., D. L. Seibert, and W. H. Thomas, Occasional blooms of phytoplankton during summer in Saanich Inlet, B.C., Canada, *Deep-Sea Res.*, 24, 775-780, 1977.
- Taylor, G. T., M. Iabichella, T.-Y. Ho, M. I. Scranton, R. C. Thunell, F. Muller-Karger, and R. Varela, Chemoautotrophy in the redox transition zone of the Cariaco Basin: A significant midwater source of organic carbon production, *Limnol.Oceanogr.*, 461, 148-163, 2001.
- Taylor, R. F., Bacterial triterpenoids, *Microbiol.Rev.*, 48, 181-198, 1984.
- Ternois, Y., J. Kawanami, L. D. Keigwin, N. Ohkouchi, and T. Takatsuka, A biomarker approach for assessing marine and terrigenous inputs to the sediments of Sea of Okhotsk for the last 27,000 years, *Geochim.Cosmochim.Acta*, 65, 791-802, 2001.
- Thiel, V., A. Jenisch, G. Landmann, A. Reimer, and W. Michaelis, Unusual distributions of long-chain alkenones and tetrahymanol from the highly alkaline Lake Van, Turkey, *Geochim.Cosmochim.Acta*, 61, 2053-2064, 1997.
- Timothy, D. A. and M. Y. S. Soon, Primary production and deep-water oxygen content of two British Columbian fjords, *Mar.Chem.*, 73, 37-51, 2001.
- Trumbore, S., Age of soil organic matter and soil respiration: radiocarbon constraints on belowground C dynamics, *Ecol.Appl.*, 10, 339-411, 2000.
- Tyson, R. V., Carbon:Nitrogen weight ratios of organic matter and some recent and ancient sediments, in *Sedimentary organic matter - organic facies and palynofacies*, edited by R. V. Tyson, pp. 477-485, Chapman & Hall, London, 1995a.
- Tyson, R. V., Distribution of the palynomorph group: phytoplankton subgroup, chlorococcale algae, in *Sedimentary organic matter - organic facies and palynofacies*, edited by R. V. Tyson, pp. 309-317, Chapman & Hall, London, 1995b.
- Tyson, R. V., Isotopic composition ( $\delta^{13}\text{C}$ ) of organic matter and the organic fraction of some recent and ancient sediments, in *Sedimentary organic matter - organic facies and palynofacies*, edited by R. V. Tyson, pp. 467-475, Chapman & Hall, London, 1995c.
- Tyson, R. V., The nature of organic matter in sediments, in *Sedimentary organic matter - organic facies and palynofacies*, edited by R. V. Tyson, pp. 467-475, Chapman & Hall, London, 1995d.
- Velinsky, D. J. and M. L. Fogel, Cycling of dissolved and particulate nitrogen and carbon in the Framvaren Fjord, Norway: stable isotopic variations, *Mar.Chem.*, 67, 161-180, 1999.
- Versteegh, G. J. M., H. J. Bosch, and J. W. De Leeuw, Potential palaeoenvironmental information of  $\text{C}_{24}$  to  $\text{C}_{36}$  mid-chain diols, keto-ols and mid-chain hydroxy fatty acids: a critical review, *Org.Geochem.*, 27, 1-13, 1997.
- Versteegh, G. J. M., R. Riegman, J. W. De Leeuw, and J. H. F. Jansen,  $U^k_{37}$  values for *Isochrysis galbana* as a function of culture temperature, light intensity and nutrient concentrations, *Org.Geochem.*, 32, 785-794, 2001.
- Volkman, J. K., A review of sterol markers for marine and terrigenous organic matter, *Org.Geochem.*, 9, 83-99, 1986.
- Volkman, J. K., F. T. Gillan, and R. B. Johns, Sources of neutral lipids in a temperate intertidal sediment, *Geochim.Cosmochim.Acta*, 45, 1817-1828, 1981.
- Volkman, J. K., D. I. Allen, P. L. Stevenson, and H. R. Burton, Bacterial and algal hydrocarbons in sediments from a saline antarctic lake, Ace Lake, *Org.Geochem.*, 10, 671-681, 1986.
- Volkman, J. K., S. M. Barrett, and G. A. Dunstan,  $\text{C}_{25}$  and  $\text{C}_{30}$  highly branched isoprenoid alkenes in laboratory cultures of two marine diatoms, *Org.Geochem.*, 21, 407-413, 1994.

## References

- Volkman, J. K., S. M. Barrett, S. I. Blackburn, and E. L. Sikes, Alkenones in *Gephyrocapsa oceanica*: Implications for studies of paleoclimate, *Geochim.Cosmochim.Acta*, 59, 513-520, 1995.
- Wahlberg, I. and A.-M. Eklund, Degraded Carotenoids, in *Carotenoids. Vol.3: Biosynthesis and Metabolism*, edited by G. Britton, S. Liaanen-Jensen, and H. Pfander, pp. 195-216, Birkhäuser Verlag, Basel, 1998.
- Wakeham, S. G., Monocarboxylic, dicarboxylic and hydroxy acids released by sequential treatments of suspended particles and sediments of the Black Sea, *Org.Geochem.*, 30, 1059-1074, 1999.
- Wang, X.-C., E. R. M. Druffel, S. Griffin, C. Lee, and M. Kashgarian, Radiocarbon studies of organic compound classes in plankton and sediment of the northeastern Pacific Ocean, *Geochim.Cosmochim.Acta*, 62, 1365-1378, 1998.
- Wang, Y., Huang, Y., and Metzger, P. Molecular hydrogen isotope fractionation by freshwater green alga *Botryococcus braunii* under laboratory-growth conditions. Abstracts of the 223th ACS national meeting, geochemistry division, Orlando, Florida, American Chemical Society.,2002.
- Wefer, G., W. H. Berger, J. Bijma, and G. Fisher, Clues to ocean history: a brief overview of proxies, in *The use of proxies in palaeoceanography: Examples from the South Atlantic*, edited by G. Fisher and G. Wefer, pp. 1-68, Springer-verlag, Berlin, 1999.
- Werne, J. P., D. J. Hollander, T. W. Lyons, and L. C. Peterson, Climate-induced variation in productivity and planktonic ecosystem structure from the Younger Dryas to Holocene in the Cariaco Basin, Venezuela, *Palaeoceanography*, 15, 19-29, 2000.
- West, N., R. Alexander, and R. I. Kagi, The use of silicalite for rapid isolation of branched and cyclic alkane fractions of petroleum, *Org.Geochem.*, 15, 499-501, 1990.
- Whelan, J. K. and C. L. Thompson-Rizer, Chemical methods for assessing kerogen and protokerogen types and maturity, in *Organic Geochemistry. Principles and Applications*, edited by M. H. Engel and S. A. Macko, pp. 289-331, Plenum Press, New York, 1993.
- Williams, P. M. and E. R. M. Druffel, Radiocarbon in dissolved organic matter in the central North Pacific Ocean, *Nature*, 330, 246-248, 1987.
- Woloszynska, J., Über eine Wasserblüte von Cyanophyceen in der Danziger Bucht und eine Wucherung der Diatomee Chaetoceros Eibenii Grun, *Bulletin International de l'Academie Polonaise des Sciences et des Lettres, Classe des Sciences Mathematiques et Naturelles Serie B.Scie*, 101-114, 1935.
- Wuchter, C., S. Schouten, H. T. S. Boschker, and J. S. Sinninghe Damsté, Bicarbonate uptake by marine Crenarchaeota, *FEMS Microbiol.Lett.*, 219, 203-207, 2003.
- Zegers, B. N., W. E. Lewis, K. Boojj, R. H. Smittenberg, W. Boer, and J. P. Boon, Levels of polybrominated diphenyl ether (PBDE) flame retardants in sediment cores from Western Europe, *Environ.Sci.Technol.*, in press, 2003.
- Zimmerman, A. R. and E. A. Canuel, A geochemical record of eutrophication and anoxia in Chesapeake Bay sediments: anthropogenic influence on organic matter composition, *Mar.Chem.*, 69, 117-137, 2000.
- Zolitschka, B. and J. F. W. Negendank, High-resolution records from European Lakes, *Quatern.Sci.Rev.*, 18, 885-888, 1999.
- Zuo, Z., D. Eisma, and G. W. Berger, Determination of sediment accumulation and mixing rates in the Gulf of Lions, Mediterranean Sea, *Oceanol.Acta*, 14, 253-262, 1991.



## Summary

The investigations described in this thesis were conducted to gain more knowledge about the natural environmental and climatic variability in the Holocene on a decadal to centennial time scale, and to assess the impact of mankind in the last centuries. To this end, sedimentary biomarker records of three different anoxic fjords were investigated. The laminated structure and the biogeochemical record of these fjord sediments were well preserved due to high sedimentation rates of 1-10 mm/yr and anoxic bottom water conditions causing low organic matter degradation rates and inhibition of infauna. Records of molecular fossils, or biomarkers, contain in principle signals of terrigenous vegetation and marine biota, which are closely linked with climatic and oceanographic parameters, and with anthropogenic influences. A large part of this thesis is also dedicated to compound-specific radiocarbon analysis. This relatively new technique added a new dimension to the use of biomarkers in paleoceanographic and -environmental research, as it may reveal additional information about the source of organic compounds, as well as about the timing and transport of various organic matter sources. It also opened the possibility to perform dating of sediments using molecular fossils in cases where carbonaceous or organic microfossils are absent or scarce.

To evaluate the power and validity of compound-specific radiocarbon dating, well-dated sediments cored during ODP leg 169S in Saanich Inlet, British Columbia, were selected. Seven sections were taken in age ranging from recent to 5000 yr BP. Several compounds, characteristic of higher plants, phytoplankton and archaea, were isolated from total lipid extracts by preparative GC and semi-preparative HPLC. For preparative HPLC a new method was designed (Chapter 2), to be able to rapidly isolate relatively polar and high molecular weight biomarkers. After radiocarbon analysis, compound specific radiocarbon ages were calibrated to produce calendar ages, for comparison with the sediment ages and the age of the total organic carbon (TOC) (Chapter 3). Refractory organic lipids from higher plants clearly biased the TOC-ages, while the phytoplanktonic and archaeal lipids showed on average age differences with the sediment of approximately 800 years, reasonably consistent with previously published DIC reservoir ages in the region of in the fjord. Because the sediment ages were known, specific reservoir ages could be determined and compared with model reservoir ages. Plankton-derived biomarkers showed considerable variation, while archaeal lipids, especially crenarchaeol, derived from ubiquitously occurring marine pelagic archaea, showed minor variations in reservoir age. The crenarchaeota are assumed to mainly sequester intermediate fjord water DIC, originating from the open ocean, while the plankton uses surface water DIC that is influenced by fresh water. The results furthermore indicate that the Holocene northeastern Pacific Ocean, and with that the reservoir age, may have been subject to larger variations than is currently assumed. In any case, compound specific  $^{14}\text{C}$  dating of crenarchaeol

## Summary

proved to be a promising new dating method for marine, carbonate-poor sediments, because it was relatively easy to isolate in sufficient amounts and consistent regarding reservoir effects. In the future, this method may prove to be useful as an alternative or extension of currently used dating methods for (marine) sediments.

An increasing relative age of the terrestrial biomarker towards recent times pointed towards an ongoing aging of the soil in the fjord environs, due to the ongoing accumulation of the refractory soil organic carbon after deglaciation of the area (Chapter 4). The results suggest that the terrigenous organic carbon pool in temperate regions may still be increasing as a long-term response to the end of the last ice-age.

A 400 year sedimentary record of the shallow, euxinic Kyllaren Fjord (West Norway) was investigated using organic geochemical, geochemical and sedimentological approaches in order to reconstruct environmental changes (Chapter 5). The results of this study show that in the first half of the 19<sup>th</sup> century an environmental change occurred, caused by a change in either the precipitation regime, vegetation and/or land use. The data also show that in the last century, and especially in the last decades, a distinct increase in primary productivity occurred. Most likely this was caused by a 'natural' eutrophication due to the transformation of the fjord from an open to a confined system by the building of a partially open dam in 1954, possibly combined with anthropogenic eutrophication. Decreased  $\delta^{13}\text{C}$  values of several biomarkers point towards enhanced carbon recycling in the fjord over the last century. It is inferred that a shoaling of the fjord chemocline had likely a mediating effect in the change towards a higher productivity by enhancing nutrient and carbon recycling.

The results of a similar biogeochemical study of the sedimentary record of the permanently anoxic South Norwegian Drammensfjord, covering the last millenium, show that eutrophication already started halfway the 19<sup>th</sup> century (Chapter 6). This was concurrent with the industrialization of sawmills and papermills along the river Drammen and upstream water bodies, which could be traced by 'coniferous' biomarkers in the sediment. The concurrent disappearance of a suite of (bi)cyclobotryococenes from the upper fjord sediments also revealed that eutrophication likely caused the demise and eventual disappearance of the alga *Botryococcus braunii* from the fjord (Chapter 7). Because of the preference of this alga for oligotrophic and slightly brackish conditions, and the possibility to easily trace these specific biomarkers, it is argued that the disappearance of this alga from a sedimentary record can serve as palaeoenvironmental indicator for early eutrophication. This may be a useful tool in the ongoing research to unravel the response of natural systems to climatic, geophysical or anthropogenic changes. This also implicates that the current use of *B. braunii* as an indicator for freshwater input in marine systems is not as unambiguous as may be thought and should be used with some care.

## Samenvatting

Het onderzoek beschreven in dit proefschrift is uitgevoerd om meer inzicht te krijgen in de natuurlijke variabiliteit van milieu en klimaat gedurende het Holoceen, op een tijdsschaal van 10-100 jaar, en om de invloed te bepalen die de mens hierop heeft gehad gedurende de laatste eeuwen. Met dit doel voor ogen werden biomarkers onderzocht uit de sedimentaire archieven van drie anoxische fjorden. De gelamineerde structuur en de biogeochemie van deze fjord sedimenten worden goed gepreserveerd, doordat hoge accumulatiesnelheden van sediment (1-10 mm/jr) samen met anoxische bodemwatercondities voorkomen dat organische stof wordt afgebroken, en het bodemleven beperken. Archieven van moleculaire fossielen, of biomarkers, bevatten in principe informatie over de terrestrische vegetatie en mariene biota, welke sterk gerelateerd zijn aan klimatologische en oceanografische parameters, en aan antropogene invloeden. Een groot deel van dit proefschrift is ook gewijd aan component-specifieke koolstof-14 analyse. Deze relatief nieuwe techniek geeft een nieuwe dimensie aan het gebruik van biomarkers in paleoceanografisch en paleo-milieu onderzoek, omdat het additionele informatie herbergt over de oorsprong van verbindingen, evenals over de timing en transport van verschillende bronnen van organische stof. Deze techniek opende ook de mogelijkheid om sedimenten te dateren met moleculaire fossielen, wat bijvoorbeeld nuttig is wanneer kalkskeletjes of grotere organische fossielen schaars of afwezig zijn.

Om de kracht en geldigheid van component-specifieke koolstof-14 datering te onderzoeken, werden goed gedateerde sedimenten geselecteerd, afkomstig uit de Saanich Inlet, een fjord in British Columbia, Canada. Zeven secties werden onderzocht, welke in ouderdom varieerden tussen recent en 5000 jaar oud. Verschillende biomarkers, karakteristiek voor hogere planten, fytoplankton en archaea, werden geïsoleerd uit totaal-extracten middels preparatieve GC en semi-preparatieve HPLC. Voor prep-HPLC werd een nieuwe methode ontwikkeld (Hoofdstuk 2), om in staat te zijn snel relatief polaire en hoog-moleculaire biomarkers te isoleren. Koolstof-14 leeftijden werden gecalibreerd naar kalender-leeftijden, om een vergelijking te kunnen maken met de leeftijden van het sediment en met die van totaal organisch koolstof (TOC) (Hoofdstuk 3). Refractieve biomarkers afkomstig van hogere planten beïnvloedden duidelijk de leeftijd van TOC, terwijl de biomarkers afkomstig van fytoplankton en archaea gemiddeld 800 jaar ouder waren dan het sediment, wat consistent is met eerdere metingen aan de reservoir-leeftijd van opgelost CO<sub>2</sub> (DIC) in de wateren in de regio. Omdat de sediment leeftijden bekend waren konden specifieke reservoir-leeftijden worden bepaald en vergeleken met model reservoir leeftijden. Dit varieerde nogal voor fytoplankton-biomarkers, maar crenarchaeol, afkomstig van veel voorkomende mariene crenarchaeota, liet slechts een klein beetje variatie zien in de reservoir-leeftijd. Dit leidde tot de aanname dat de crenarchaeota vooral leven van DIC in fjord water van intermediaire diepte, wat afkomstig is van de open ocean, terwijl fytoplankton DIC uit het oppervlaktewater betreft, hetwelk is beïnvloed door zoet water. De resultaten geven verder aan dat de NO Pacifische Oceaan in het Holoceen

misschien onderwerp is geweest van grotere variaties dan tegenwoordig wordt aangenomen. In ieder geval is gebleken dat koolstof-14 datering met crenarchaeol een veelbelovende nieuwe manier van dateren is voor mariene, kalkarme sedimenten, omdat deze biomarker relatief gemakkelijk en in voldoende mate is te isoleren, en omdat ze een consistente reservoir-leeftijd vertoont.

Uit de koolstof-14 metingen aan de terrestrische biomarker blijkt dat deze een toenemende relatieve ouderdom vertoont naarmate de tijd vordert (Hoofdstuk 4). Dit duidt er op dat de bodem organische stof in de omgeving van het fjord gemiddeld steeds ouder is geworden. Dit is hoogstwaarschijnlijk veroorzaakt door een voortdurende ophoping van organische stof in de bodem na het verdwijnen van gletsjers uit het gebied, 12.000 jaar geleden. De resultaten suggereren dat de voorraad terrestrisch organisch koolstof op gematigde breedtes nog steeds aan het toenemen is als een langzame reactie op het einde van de ijstijden.

Het sedimentaire archief van het euxinische (H<sub>2</sub>S bevattend) Kyllaren fjord (west Noorwegen), is voor de laatste 400 jaar onderzocht met organisch geochemische, geochemische en sedimentologische technieken, met als doel milieuveranderingen te reconstrueren (Hoofdstuk 5). De resultaten laten zien dat in de eerste helft van de 19<sup>e</sup> eeuw een verandering optrad, veroorzaakt door een verandering in de neerslag, de vegetatie, en/of landgebruik. De resultaten laten verder zien dat in de laatste eeuw, speciaal in de afgelopen decennia, een duidelijke toename in de primaire productie optrad. Dit is waarschijnlijk veroorzaakt door 'natuurlijke' eutrofiëring, doordat het fjord van een open systeem naar een enigszins afgesloten systeem werd veranderd door de bouw van een half open dam in 1954, hoewel antropogene eutrofiëring ook een rol kan hebben gespeeld. Verder kon worden afgeleid dat recycling van koolstof in het fjord toenam in de laatste eeuw. Het ondieper worden van de chemocline in het fjord kan hierbij een rol kan hebben gespeeld, doordat dit een stimulerend effect kan hebben gehad op de produktiviteit door een efficiënter gebruik van aanwezige nutriënten mogelijk te maken.

De resultaten van een vergelijkbare biogeochemische studie aan het sediment van het permanent anoxische Drammensfjord (zuid Noorwegen), het laatste millennium bestrijkend, laten zien dat eutrofiëring al halverwege de 19<sup>e</sup> eeuw startte (Hoofdstuk 6). Dit gebeurde tegelijkertijd met de industrialisatie van zaag- en papiermolens in het stroomgebied van de rivier de Drammen. Dit kon worden gereconstueerd aan de hand van de aanwezigheid van 'conifere' biomarkers in het sediment. Het tegelijkertijd verdwijnen van een groep biomarkers genaamd (bi)cyclybotryococcenen uit het sedimentaire archief gaf ook aan dat eutrofiëring waarschijnlijk de oorzaak is van het verdwijnen van de alg *Botryococcus braunii* uit het fjord (Hoofdstuk 7). Omdat deze alg goed gedijt in oligotrofe en ietwat brakke milieus, en omdat deze groep biomarkers gemakkelijk te herkennen is, wordt verondersteld dat de verdwijning van deze alg uit sedimentaire archieven in de toekomst zou kunnen worden gebruikt als paleo-indicator voor vroege eutrofiëring. Deze resultaten impliceren ook dat het huidige gebruik van *B. braunii* als indicator voor zoetwater-invloeden in mariene systemen niet zonder meer toepasbaar is.

## Dankwoord

*Deze pagina is bijna te kort om iedereen te bedanken die heeft bijgedragen aan de totstandkoming van dit proefschrift. Zonder school en opleiding had ik dit natuurlijk niet kunnen doen: wat dat betreft moet ik mijn leraren op de lagere en middelbare school, de Universitaire docenten, professoren en andere begeleiders in Wageningen en mijn begeleiders op het NIOZ bedanken. Echter, met alleen een opleiding kom je er niet: er zijn daarnaast ook vele anderen die een rol hebben gespeeld in mijn ontwikkeling, dus niet alleen tot onderzoeker, maar ook tot de mens die ik ben.*

*In de eerste plaats zijn dat natuurlijk mijn ouders: zonder jullie liefde en steun zou dit boekwerkje nooit tot stand zijn gekomen.*

*Daarnaast hebben allerlei anderen om mij heen, ieder op weer een andere manier, bijgedragen aan mijn bredere ontwikkeling: familie, vrienden, burens, trainers van de STG 'Pinguins', mensen op zeilschool 'Pean', Gudsekoppers, Argonauten.*

*Maar de jaren gedurende het promotie-onderzoek op het NIOZ zijn natuurlijk het belangrijkste geweest, en hiervoor wil ik toch een aantal mensen specifiek bedanken:*

*Mijn promotor, Jan de Leeuw, en mijn copromotor Jaap Sinninghe Damsté: bedankt voor het in mij geschonken vertrouwen door mij een promotie-plaats aan te bieden, en voor de begeleiding de afgelopen jaren. Naast Jaap, ook Stefan bedankt voor de dagelijkse begeleiding: jullie stonden altijd open voor vragen (en hadden meestal ook een antwoord) en hadden mijn manuscripten altijd binnen no-time van commentaar voorzien, wat erg prettig werkte. Ellen, zonder jouw hulp met het HPLC-werk had dit proefschrift er zeker anders uitgezien. Marianne, niet alleen bedankt voor het doen van een aantal metingen, maar vooral voor je praktische tips en voor het goed draaiende houden van het lab.*

*Rich, Joe and Alina, my consecutive roommates, thank you for answering all these small questions, and for your company, chitchat and good conversations.*

*I also need to thank the people at WHOI/NOSAMS, especially John Hayes, Tim Eglinton, and Dana from the prep-lab, for their help in obtaining biomarker <sup>14</sup>C data.*

*Daarnaast wil ik al mijn (vroegere) collega's bij de afdeling MBT: Enno, Bart, Marcel, Marcel, Peter, Arnoud, Ingeborg, Irene, Michiel, Sebastiaan, Jort, Astrid, Marco, Cornelia, Yvonne, Margot, Wim, Marlèn, Patty, Elda, Ronald, Anhelique, Kees, Jan, Cato, Arne, Hanno, Gerard, bedanken voor de goede atmosfeer, de gezelligheid, en soms ook raad en daad. Dit geldt ook voor al die andere NIOZers, met name collega-OIO's, wat teveel wordt om op te noemen. Ik heb een erg leuke tijd gehad op het NIOZ en ging elke dag met plezier naar het werk.*

*Verder wil ik mijn buurvrouw Elly bedanken voor het passen op mijn huis en het verzorgen van de planten, als ik weer eens een week of langer weg was. En bedankt alle medewerkers bij filmhuis 7Skoop, waar ik de afgelopen jaren de nodige ontspanning en relativering vandaan kon halen. Speciaal mijn ploeggenoten Hans en Netty, en later ook Alex en Maarten: ik zal de gezellige uurtjes en goede gesprekken na de film missen.*



## Curriculum Vitae

Rienk Hajo Smittenberg werd geboren op 23 Maart 1973 te Eck en Wiel, gemeente Maurik. Hij groeide evenwel op in Jirnsum, in het hart van Friesland, waar hij zijn eerste onderricht kreeg op de lagere school 'It Tredde Sté'. In 1991 behaalde hij het VWO diploma aan de RSG Heerenveen. In 1992 begon hij aan de studie 'Bodem, Water en Atmosfeer' aan de Landbouw Universiteit Wageningen, waarin hij zich specialiseerde in de richting 'procesbodembodemkunde'. In September 1998 ontving hij zijn bul, en op dat moment was hij net begonnen als Onderzoeker In Opleiding aan de afdeling Mariene Biogeochemie en Toxicologie (MBT) binnen het, tegenwoordig Koninklijk, Nederlands Instituut voor Onderzoek der Zee (NIOZ), wat heeft geresulteerd in dit proefschrift. Vanaf 1 Augustus 2003 is hij werkzaam als postdoc onderzoeker op de Massachusetts Institute for Technology (MIT), Cambridge, USA, op de afdeling Earth, Atmospheric and Planetary Sciences.

